APPLICATION OF ARTIFICIAL NEURAL NETWORK FOR THE STRUCTURAL INTEGRITY ASSESSMENT OF DENT IN PIPELINES

By

MICHAEL OLUWADAMILARE DUROWOJU

A thesis submitted for the degree of Doctor of Philosophy

School of Marine Science and Technology

NEWCASTLE UNIVERSITY

June, 2017

ABSTRACT

Dent in a pipelines have been of major concern to pipeline operators for years because its severity cannot be easily determined. For many years dent severity was based on dent depth alone. This has led to unnecessary repairs and removal from service incurring considerable loss in revenue. Studies by researchers have indicated that other factors like pipe geometry, pipe material, dent geometry and pressure cycling could influence the severity of the dent in terms of the fatigue life reduction.

Dent severity has been studied using dent depth based assessment, strain based assessment and fatigue assessment . The dent depth over the years has been the major determinant of dent severity. Recent studies have shown that the strain in the pipeline could be a better indicator of dent severity using the static approach. The most common fatigue approach is the stress life S-N approach. This involves extracting stress data either through experimental procedure or finite element analysis and using it with an appropriate S-N curve to determine the fatigue life

One of the major challenges faced in S-N fatigue approach today is determining the stress concentration factors (SCF) associated with the dents. These SCFs are used with an appropriate SN curve to calculate the fatigue life. This, over the years and currently is calculated empirically or using finite element (FE) analysis. The cost of running experimental program can be very expensive and numerical analysis can be time-consuming. It is not sustainable to keep using finite element analysis to calculate the SCF associated with every dent. An algorithm is needed to be able to predict strain and SCF without running an expensive experimental program or running an extensive finite element study

This Research presents an alternative and a sustainable method for calculating the SCF, the maximum strain and the rerounding depth in pipelines with dent. The method involves gathering a large database of SCFs, strains and rerounding depths through a finite element study on a parametric range of industry standard pipes . These parametric datasets focuses on the effects of pipe geometry, dent geometry, material properties and pressure range on the prediction of the strain and stresses which were not systematically considered by other researchers. These parametric datasets are then used to train an artificial neural network (ANN) that predicts the rerounding depth,

maximum strain and the SCF. The ANN presents an accurate and sustainable alternative to the current method used for dent assessment. It's application would reduce the cost and time taken in assessing dent severity. The accuracy of the ANN is dependent on the amount of training data. In order to create the large database of results, a parametric design language (APDL) was created for easy creation and recreation of models. This parametric design language helped in the creation of 256 FE models which was sufficient enough to create the large database of SCF and other data needed to train the ANN

Two types of indenters (Dome and Bar) are used to simulate circumferentially and longitudinally aligned dents. Four different dent depths ranging from 2% d/D to 10% d/D are also simulated to investigate the effect of dent geometry. Four different pipe grades (X46, X65, X80, and X100) are analysed to investigate the effect of pipe materials. Similarly, eight pipes with a different diameter to thickness ratio (D/t) ranging from 18-96 are analysed to investigate the effect of pipe geometry. The pipe is pressured up to 50% and 72% SMYS to investigate the effect of pressure range.

The results from this study show that all the investigated parameters influence the results in various ways. Results show that longitudinally aligned dents have higher stress concentrations factors compared to circumferential dents of similar dent depth. Similarly, pipes with higher diameter to thickness ratios D/t have higher stress concentration factor compared to pipes with lower D/t .The FE result was validated with experimental and analytical results and a good correlation was seen with minimal percentage error. The FE results from the parametric study was fed into an ANN model to train the network. The network was trained with different numbers of the processing element and activation function to find the model with the best performance. The ANN prediction gave a good correlation with the FE results

Keywords:

Finite Element Analysis; Fatigue life; Stress Concentration Factor; Strain-based assessment; Spring back; Rerounding; Artificial neural network

ACKNOWLEDGEMENTS

I thank the Almighty God for the Grace and strength given to me in order to complete this research.

I am very grateful to my supervisor, Dr Yongchang Pu for his time, guidance and intellectual resource to making this research a success. I am also thankful to Dr Simon Benson and Dr Julia Race for their support and advice particularly on the published papers which is key to this research. My sincere gratitude goes to the entire staff of School of Marine science and technology for creating an enabling platform and environment to conducting this research. I also acknowledge the suggestions of my examiners, Prof Purnendu Das and Dr Nianzhong Chen which helped me to better highlight the contribution of this thesis.

I am eternally grateful to my parents Chief and Chief Mrs MAO Durowoju for their prayers, monetary and moral support in making this research a success. Without them, this dream would have been unachievable

I am very grateful to my wife and son Oluwakemi and Oluwadarasimi for their patience and understanding. I particular thank my wife for her moral support and fuelling my drive to achieving this goal

I am also thankful to my brothers Dr Olasunkanmi Durowoju and Dr Olatunde Durowoju who have set the pace and standard to follow. I am thankful for your monetary and moral support. You guys are my role models. I am also thankful to younger brother Oluwatobi Durowoju for his support and prayers. Many thanks to my sisters-in-law, Tosin, Pretti and Omolola, my nieces, Oyindamola, Zoe and Anika and my nephew Boluwatife. You guys rock! Many thanks to the entire Durowoju and Olaitan Family for their prayers

Lastly, I want to thank my friends and colleagues Deji, Ibezimakor, Wale, Charles, Seun, Dapo, Wunmi, Sammy, Toyosi, Lawunmi, Mary,Tunde and so on for your support and your kind words of encouragement

TABLE OF CONTENTS

LIST OF FIGURES

LIST OF TABLES

LIST OF EQUATIONS

NOMENCLATURE

ε_1	Bending strain in circumferential direction
ε_2	Bending strain in longitudinal direction
ε_3	Membrane strain in longitudinal direction
ε_i	Total combined strain inside pipe surface
ε_{max}	Overall strain
ε_o	Total combined strain outside pipe surface
σ_f	Fatigue strength coefficient
σ_A	Equivalent nominal fatigue stress amplitude
σ_y	Yield strength
$\Delta\varepsilon$	Strain range
$\Delta\sigma$	Stress range
Δk	Strength intensity factor
ΔP	Pressure range
a	Crack length
API	American petroleum institute
ANN	Artificial neural network
ASME	American society of mechanical engineers
b_p	Bias
CVN	Charpy V notch
d	Dent Depth
d_a	Increase in crack length
d_i	Initial dent depth after spring back
d_f	Final dent depth after pressurization
dN	Applied load cycle
d/w	Depth to width ratio
D	External diameter
DOE	Department of energy

D/t	Diameter to thickness ratio
E	Young’s modulus
EPRG	European Pipeline Research Group
f()	Activation function
FEA	Finite element analysis
H_o	Dent depth at zero pressure also known as spring back depth
H_r	Reround dent depth
ILI	In-line inspection
K_s	Stress concentration factor
K_d	Stress enhancement factor of the dent
l/w	Length width ratio
L	Length of dent
L/D	Length to diameter ratio
MAOP	Maximum allowable operating pressure
n_h	Number of processing elements in hidden layer
n_i	Number of inputs
n_o	Number of outputs
N	Number of cycles to failure
NPS	Nominal pipe size
OD	Outer diameter
P	Pressure
PDAM	Pipeline defect assessment manual
PE	Processing elements
R_o	Radius of curvature of deformed pipe surface
R_1	Radius of curvature measured in transverse direction
R_2	Radius of curvature in longitudinal direction
SCF	Stress concentration factor
S_L	Desired factor of safety on fatigue life

SMYS	Specified minimum yield stress
t	Pipe thickness
UTS	Ultimate tensile stress
w	Width of dent
w_{nj}	weights
x_y	inputs of a single processing element
y_p	output of a single processing element

CHAPTER 1

INTRODUCTION

1.1 General overview

For over 50 years, considerable amount of research has been carried out to determine the severity of dents and mechanical damages to the integrity of pipelines. Most of the mechanical damage cannot be avoided as they occur through regular day to day activities like excavation and dropped objects. Some of this mechanical damages include dents, gouges, corrosion, girth welds and so on.

A dent in a pipeline by definition is a permanent plastic deformation of circular cross section of the pipe[1]. A plain dent, however, is the damage which causes a smooth change in the curvature of pipe without a reduction in pipe wall thickness. A dent can either be a constrained dent or an unconstrained dent. A constrained dent is one which is not able to re-round due to some constraint stopping it from regaining its original position while unconstrained dent is one which is able to re-round during changes in pressure[1].

For many years, pipeline operators have been faced with the question of whether or not to repair a pipeline with dents or remove from service because the severity of the dent could not be easily determined. Till date, there is no uniformly acceptable method for assessing dents in the pipeline[2]. Different codes and organisations have a different method for assessing dents in the pipeline. For example ASME B31.8 allows up to 6%OD dent depth for constrained and unconstrained[3] depth while PDAM allows up to 10%OD dent depth for constrained and up to 7%OD for the unconstrained dent. This has led to unnecessary maintenance that might lead to high-cost pigging operations, excavation or repairs.

There has been no significant report of failure from plain dent in the past. In the USA, the department of transports website reports failures in liquid and natural gas transmission pipeline. A recent statistic indicates that less than 0.2% of failure incidents on the liquid pipeline are related to dents and less than 0.1% of failure incidents on the gas pipeline are dent related[2,58,69,71,77,80]. Liquid pipeline operators are

considerably more fatigue concerned than the gas pipeline operators. Studies show that while a gas pipeline experience 60 cycles per year with a pressure differential of 200psi, a liquid pipeline can experience up to 1800 times at same pressure differential. Conclusion from that study indicates that failures from dents do not form a significant portion of the total number of failure incidents.

From previous research, it is seen that plain dent does not affect the burst strength of pipelines; however, it can reduce the fatigue life of the pipeline under cyclic pressure loading. Dents generally increase stress in pipeline thereby increasing the pipeline's susceptibility to fatigue damage caused by cyclic pressure loading. Many of the transmission pipelines are old and fatigue failure at dents are now being reported. These reports have raised technical concerns with regulators as regards the current approach and methodology for assessing dents.

1.2 Statement of problem

Dents are the most common defects in pipeline which can affect the structural integrity of pipelines. Over the years, dent depth alone has been used to measure the severity of dents. Recent studies have shown that dent depth is not enough to measure the severity of the dents[5]. New studies suggest that the strain in the pipe could be a better measurement of the severity. When pipes are pressure cycled, they are subjected to fatigue. The most common method for measuring fatigue is the S-N method. This involves measuring the stress concentration in the dent and using it with a published SN curve to calculate the fatigue life. This stress concentration factor can either be measured experimentally or using finite element analysis. Experiments can be very expensive and finite element study can be time-consuming so there is a need to develop an appropriate method for calculating the stress concentration factor (SCF) and strain without running expensive experimental program or an extensive finite element study. Studies have shown that some basic parameters influence the stress concentration and strain in the dent. These parameters include dent geometry, pipe geometry, pipe material and pressure cycling. This study uses finite element analysis to analyse a practical range of pipelines with different dent scenarios. It studies the effects of the parameters that was not systematically considered by other researchers on the SCF and strain. The dataset generated from the finite element study is used as training data for an artificial neural network (ANN) in order to create an ANN-based

formula to predict the SCF and maximum strain. The ANN uses these parameters as input variables to predict the SCF and strain. The predicted SCF can then be used with an appropriate SN curve to determine the fatigue life. Strains will be used in strain-based assessment.

The accuracy of the ANN based formula is greatly dependent on the accuracy of the FE models and the range of training data. It is essential to have an accurate FE analysis by making sure each step of the modelling process is done correctly. A larger range of FE dataset is essential in determining the accuracy of the ANN model. In order to achieve this, a parametric study involving a wider range of industry pipes, grades and dent sizes is needed. This involves creating many FE models which can be time-consuming .

1.3 Aims and Objectives

The main aim of this research is to develop an efficient procedure to predict fatigue life of plain dent of pipelines. The objectives of this research include the following:

1. Creating a parametric design language that will help in the easy creation of FE models.
2. Improving the understanding of the spring-back and re-rounding phenomenon and also improving the understanding of stress distribution and strain in pipelines with dent
3. Identifying the most important parameters, which influences spring-back, re-rounding, SCF and strain in pipelines with dent
4. Creating database for the application of ANN-based formulae for the prediction of the rerounding depth, SCF and the maximum strain in pipeline dents
5. Providing guidance on how to apply the additional knowledge
6. Applying the ANN-based formulae for predicting rerounding depth, SCF and strain using the database generated in the above steps. The identified important parameters will be used as input parameters
7. Providing guidance on how to apply the ANN-based formula for the prediction of reround depth, SCF and maximum strain.

1.4 Organisation of the thesis

These thesis is organised into eight chapters. The first chapter is the introduction which gives a general overview and objectives of the research. Chapter 2 is the literature review which discusses past literature and the current methods available for determining dent severity. It also discusses the various dent research and methods for calculating dent fatigue. Included also in the literature are the current dent management strategy. The theory of artificial neural network (ANN) is also discussed in chapter 2. Chapter 3 studies the general behaviour of a dent when and when not subjected to internal pressure. The spring back and rerounding behaviour is studied in this chapter. Chapter 4 studies the effects of parameters like dent geometry, pipe geometry, pipe material and pressure variation on the stress concentration in dents. It also studies the location and magnitude of the stresses when subjected to different loading conditions. An algorithm for calculating fatigue is also discussed in this chapter. Chapter 5 studies the strains in the dent. It studies the effects of the above parameters on the strain distribution in the pipeline. Chapter 6 uses an artificial neural network to train the dataset obtained the various analysis to predict the rerounding, SCF and strain in the pipe. Chapter 7 discusses the proposed methods for assessing dent severity and gives guidance on how to apply the ANN-based formula. The last chapter is the summary, conclusion, and recommendation for further studies.

CHAPTER 2

LITERATURE REVIEW

2.1 Introduction

This chapter presents a comprehensive review of the past and current practices for assessing dent in pipelines. It gives a brief history of dent assessment and the various research approaches employed in assessing dent severity. This chapter gives an insight of what to expect in the main chapters. Table 2-1 below shows each sections of the literature review and the chapter it relates to. It helps the reader navigate through and understand the thesis

Section	Subsection	Chapter(s)
2.2	2.2.1	1
	2.2.2	1
2.3	2.3.1	3,5
	2.3.2	4
	2.3.3	4
	2.3.4	4
	2.3.5	4
	2.3.6	3,4,5,7
	2.3.7	3,4,5,7
2.4	2.4.1	3,4,5,7
2.5	2.5.1	6,7
	2.5.2	6,7

Table 2-1 Table to help reader navigate through the thesis

2.2 History of dent assessment

The study of dent have been ongoing for many years. Dents are generally classified as a plain dent or dent with associated mechanical damages. This damages include gouges, girth welds and any damage that causes reduction in the pipe's thickness. The history of dent research has been based on these two categories of dents

2.2.1 History of plain dent assessment

Belonos and Ryan[4] were one of the first people in the 1950's to report studies on plain dents. Their test considered the effect of internal pressure, residual stress and static internal pressure at failure on dented pipelines. The residual stresses were obtained by strain gauging the dented pipe and recording the strain changes as the pipe was cut shorter.

Two pipes, NPS26, X52 and NPS20, X42 were used. The NPS 26 pipe has an outer dimeter of 660mm with a 3% oval dent and a length to width ratio (l/w) of 0.7. The NPS 20, X42 pipe has an outer diameter of 508mm with 2% continuous dents . The NPS 26, X52 pipe showed that the external residual stresses were -45300 psi transverse and -20700 psi longitudinal. The NPS 20, X42 pipe showed transverse residual stress in various portions of the dents as approximately 24,694psi and -23,938psi and maximum longitudinal stress of 23,053psi were noted at the centre of the dent. The stresses reported at a pressure of 1000psi and 1200psi and 5 test results showed that the pipe burst away from the dents at pressures between 1580 and 1725psi . They concluded that even though dents have high residual stresses, they do not significantly affect the service performance of a pipe unless there is a notch or scratch within the dents.

CANMET also in 1980s[5] did a series of test to study the behaviour of dents under typical pipeline loading conditions. The study was conducted in two parts. The first study included 8 tests where 4 different round indenters were used to hydraulically form plain dents to a depth of 6% of the pipe outer diameter. The dents either simulated construction damage or in-service damage(i.e. formed after the hydrotest and the then fatigue tested up to 12,000 cycles at a pressure corresponding to hoop stresses as

high as 80% SMYS. The diameters and wall thickness of the pipes ranged from 8 to 20 in and 5.59 to 9.65 mm respectively. The result from the first study provided information on the strains on the inside and outside surface of the pipe wall in the dented region during pressurisation and fatigue testing. An equation was also developed relating the hoop strain in the dent depth at 110% of yield(i.e. during the initial pressure test). The final part of the study involved pressurizing the pipe to 110%SMYS. In the process, cracks were observed in only one specimen near the end of the long dents where re-rounding was restricted.

2.2.2 History of the assessment of dents associated with mechanical damages

Tyson and Wang[7] summarised the work done by CANMET by considering dents, gouges, and gouges in dents. The indenting process was done using 4 types of indenters and was done on 4 different pipe specimens. They came up with a formula to calculate failure pressure of various forms of damage comparing them to experimental results. The results of this test indicate that there was no reduction in failure pressure for plain dents, however, there was one recorded failure due to fatigue when the pipe was cycled to 3000 at the curved end of a long dent. Results from this experiment also confirm that the failure pressure of gouges in the dent is reduced compared to failure pressure dents and gouges alone.

Ong et al[8] also studied the effect of a dent on pressurised pipeline considering the effect on a plain dent and plain dent with a reduction in wall thickness. Results from burst test showed that pipe failure was insensitive to the existence of a local dent; however pipe failure was found to be due to loss of thickness defect.

Bjourney et al[9] also did 5 full-scale plain dent tests on an X52 pipe and 99 full-scale gouge test on an X65 pipe with various repairs made to the gouges. The parameters investigated include the dent depth, load used to produce dent including spring-back and depth of grinding repairs. The result of this test also confirms that the burst pressure is lower for a dent –gouge combination. It was also shown that the full load carrying capacity of a pipe can be achieved by grinding below the depth of any crack.

Maxey[10] summarised the work done by British gas and Battelle. British gas tested rings cut from damaged pipe both before and after pressurisation. The parameters investigated include gouge depth, dent depth, pipe size, pipe toughness, failure

pressure and pipe yield strength. Battelle[11] did a full-scale burst test of pipes that was damaged before and after pressurisation. The parameters investigated are same as that of British gas. It also investigated the effect of gouge length which was not investigated by British gas. He further expanded on the work by considering the effect of temperature on the failure characteristics of pipes with dents and gouges as well as the crack growth that occur with different hold pressure. He further described a method to determine the significance of dents/gouge combination by calculating the expected failure pressure using a parameter Q given as

$$Q = \frac{CVN}{\left(\frac{D}{2R}\right)\left(\frac{d}{t}\right)(2c)} \quad \textbf{(2-1)}$$

Where CVN is the Charpy V-Notch pipe toughness, D/2R is dent depth /pipe diameter ratio, d/t is the gouge depth/pipe thickness ratio and 2c is the gouge length.

Lancaster and Palmer[12] also did an experiment modelling steel pipes using the aluminium pipe. They created short smooth dents to a nominal depth of 13% in an un-pressurised pipe. The dents were strain gauged and pressurised to as high as 110% SMYS. The maximum strain was observed to occur along the pipe axis at the ends of the dents at intermediate pressure p/p_y of 0.35, where p is the internal pressure in the pipe and p_y is calculated pressure to cause yielding of an undamaged pipe. They compared the result of the experiment to a full-scale test performed by CANMET, Battelle and British gas. The result of the experiment showed that dent depth had little or no influence on the burst pressure of pipes and the burst pressure was mainly influenced by the gouge depth. However, the gouge depth had no influence on the rerounding behaviour. It was also noted that the failure pressure were approximately 50% of the pressures calculated by the Battelle model when the gouge intersected the regions of high strain.

Battelle memorial institute studied the failure of defects in line pipe steel through theoretical work and full-scale testing. These researchers noted that line pipe tends to fail in a ductile manner. It has two basic distinctions which include toughness

dependent failures and flow stress dependent failures[13] . This work by Battelle led to the popularly known through-wall and part-wall NG-18 equation[14].

2.3 Dent Research

Dent research has been going on for years. For many years, dent assessment was based on the dent depth only. However, recent studies indicate that the burst strength and fatigue life of dents are affected not only by dent depth but also by other parameters like pipe geometry, material properties, restraint conditions and pressure cycling range [17,18]. Plain dents generally are not of major concern under static loading as confirmed by various experiments, however, it can be of major concern when cyclic pressure loading is applied. This has led to the classification of dent research as static and fatigue research.

2.3.1 Static dent research

Early research recognises that dent depth was one of the important variables of interest. It was the major criteria for assessing the severity of dents. It has been suggested that strain in dents can also be an indicator of dent severity. Dents created initially changes as a function of applied pressure. Codified acceptability limits for plain dents have been empirically derived on the basis of dent depth from full-scale test result since there is no analytical method available for calculating failure pressure.

2.3.1.1 Dent depth based research

B31.8 [19] described dent depth as the gap between the lowest point of the dent and the prolongation of the original contour of the pipe in any direction. Ovality of dents makes it difficult in measuring dent depth. Figure 2-1 illustrate the dent depth as a percentage of the original nominal diameter of the pipe

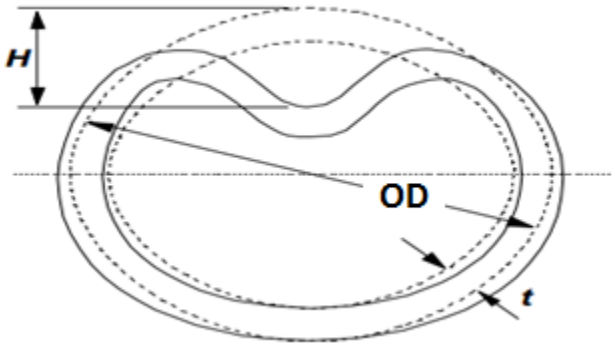

Figure 2-1 Dimensions of a dent [1]

The depth at which a dent is acceptable varies from researcher to researcher. ASME 31.8 [19] allows a dent depth of up to 6% OD for constrained and unconstrained plain dent. PDAM, however, allows up to 10%OD for constrained dents and 7%OD for unconstrained dents. Below is a table showing the depth acceptance criteria of various research organisations

	Plain Dents	
	Constrained	**Unconstrained**
ASME 31.8	Up to 6%OD or strain level up to 6%	
ASME 31.4	Up to 6% OD in pipe diameters > *NPS 4 Up to 6mm in pipe diameters < *NPS 4	
API 1156	Up to 6%OD, >2% OD requires a fatigue assessment	
EPRG	≤ 7%OD at hoop stress of 72% SMYS	
PDAM	Up to 10% OD	Up to 7%OD
Z662	Up to 6mm for ≤ 101.6mm OD <6%OD for > 101.6mm	

*NPS mean nominal pipe size which is an indication of the pipe diameter in inches.

Table 2-2 A static dent assessment for plain dents

2.3.1.2 Spring back and rerounding

Pipeline materials usually exhibit elastic-plastic behaviour. Unconstrained dents tend to spring back slightly once the indenter is removed because a part of the deformation is the elastic deformation. Further application of internal pressure tends to reduce the dent depth. This phenomenon is known as re-rounding. The re-rounding phenomenon is dependent on the pipe properties and the magnitude of the applied pressure [11]. In trying to determine dent acceptance criteria, many full-scale test dents are introduced at zero pressure which is a typical real life scenario for construction dents. But in practice, dents could be introduced during operation when pipelines are under internal pressure. In such cases, the effect of spring back and rerounding have to be considered in determining the dent acceptance criteria. In practice, this is achieved by the use of a spring back correction factor. A spring back correction factor is used to show the relationship between dent depth at 0 pressure and dent depth at rerounding. Various researchers have published a spring back correction factor. Most of these factors were empirically derived and many do not take into account the factors affecting the rerounding process like dents shape, pipe thickness and internal pressure. Cosham and Hopkins[1] reviewed the various spring back correction factors in the pipeline defect assessment manual and recommended the revised EPRG correction factor given as

$$H_o = 1.43H_r \qquad \textbf{(2-2)}$$

Where H_o is the dent depth at zero pressure and H_r is the rerounded dent depth. They pointed out that one of the limitations of this factor is that it does not include the influence of internal pressure. In order to further understand the factor, Gaz de France [20] revisited the correction factor by employing finite element analysis and further test study and they came up with the following factor

$$H_o = \pi . H_r \left[\frac{1}{\pi - 2. \propto . arctan\left(\frac{L}{H_r}\right) . arctan\left(0.1 \frac{D}{t} \frac{P}{\sigma_Y}\right)} \right] \quad \textbf{(2-3)}$$

Where α is the correction factor. This equation addresses the effect of dent shape and internal pressure at the point of denting.

2.3.1.3 Strain-based assessment

In the past, dent assessment was done using dent depth assessment. Recently, it is discovered that dent depth alone is not enough in assessing the severity of dents. More recently ASME B31.8 [19] gives an alternative to the dent depth approach by introducing the strain-based criteria. It states that plain dents and dents on ductile welds of any depth are acceptable provided the strain level associated with it does not exceed 6% for plain dents and 4% for dents on ductile welds. Strain in a dent can be estimated using data from ILI tools or from direct measurement of deformation contour [21]. Strain act on both the longitudinal and circumferential axis of a pipe and each axis further have two types of strain acting namely the bending and membrane strain as seen in figure 2-2 .

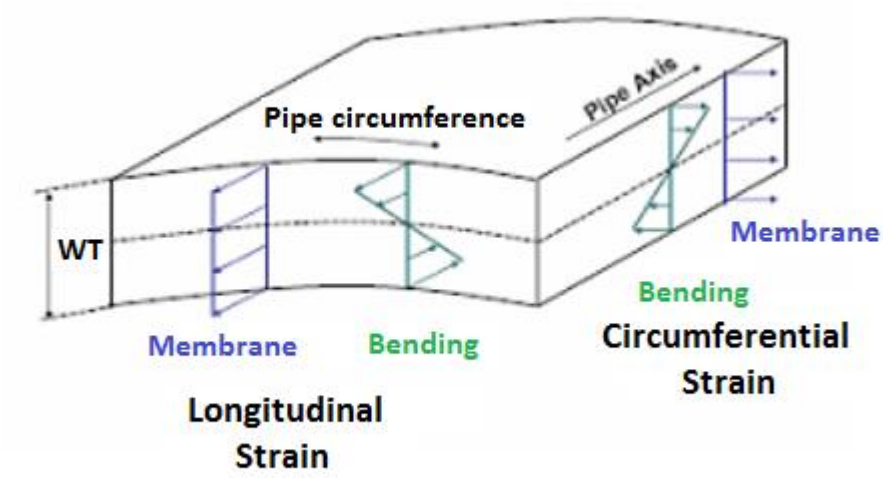

Figure 2-2 Strain components in pipe wall[2]

According to the ASME B31.8 document, the maximum strain in the dent is estimated by first evaluating each strain component separately then assuming each component occur coincidentally at the dent apex, the components are accordingly combined to give the total strain. As seen in figure 2-2 , the membrane strain is constant throughout the pipe wall but the circumferential strain varies through the pipe wall about the neutral axis. The value of the radius of curvature in the longitudinal and circumferential planes is essential in the use of the ASME equations. They are calculated from dent geometry data. However, the ASME code [19] does not give guidance on how to calculate the radius of curvature. There are several mathematical methods available for calculating the radius of curvature. Noronha et al [22] used a B-spline method to calculate the radius of curvature . Rosenfeld et al [11] also used high-resolution calliper tool data to derive the local cold strain associated with indentation. Dawson et al [23] derived the radius of curvature in two stages. The first stage involved fitting a series of polynomial equations around the dent profile and the second stage involves calculating the radius of curvature from the equation throughout the dent profile. The radius of curvature by this method is given by

$$R = \frac{1}{k} = \frac{\left(1 + \left(\frac{dy}{dx}\right)^2\right)^{\frac{3}{2}}}{\frac{d^2y}{dx^2}} \qquad \textbf{(2-4)}$$

Once strains are calculated, they can be compared to an allowable strain limit. ASME B31.8 recommends an allowable strain in plain dent at 6%. This value was chosen as it is lying between 3% strain limit for field bends and 12% material strain level at which likelihood of cracks and deformation is set to appear [23]

2.3.2 Dent fatigue research

both experimental and numerical studies have demonstrated that plain dent does not significantly affect the burst strength of pipelines; however, the fatigue life of the pipeline is reduced [1]. This is so because when pipes are dented, there is an increase in the stress and strain around the dented area due to incremental rounding and re-rounding under cyclic pressure loading. During this process, crack initiates, propagates and eventually fail due to fatigue. Hence the effect of fatigue cannot be overlooked in pipeline integrity assessment.

There are three basic methods of assessing fatigue life in pipeline:

- Empirical or semi-empirical method using SN curve and
- Strain-life (e-N) method
- Fracture mechanics method

2.3.3 S-N Approach

This method is the most common method and it has been used by various researchers [17,25,26,27,29,30,31,32] to calculate the fatigue life. Several empirical and semi-empirical models have been developed to estimate the fatigue life of dented pipelines, some of which are developed for plain dent and some for plain dents associated with mechanical damage. The methodology involves using published fatigue S-N curves from an appropriate design code and accounting for stress concentration in the dents by the use of stress concentration factors (SCF) [1, 23]. The impact of a plain dent on fatigue life is related to two factors one of which is the dent geometry in terms of shape and depth and the other being the range of applied pressure. Dents that are deeper and possess greater levels of local curvature tend to have reduced fatigue life as compared to dents with shallow and relatively smooth contours. In the same manner, fatigue life of plain dents is reduced to a greater degree when increased pressure differentials are assumed [24] . Research efforts conducted by EPRG and PRCI also indicate that if the fatigue life of plain dent is in the order of 10^5 cycles, the presence of a mechanical damage like gouge reduces the value to be of order 10^3.Some of these approaches are further explained below. The general equation relating the applied stress range and the fatigue is given in equation 2-5

$$NS^m = K \qquad \textbf{(2-5)}$$

where N is the fatigue life , S is the applied stress range, m is the slope and K is a constant depending on the joint. This equation is the base equation upon which every other fatigue life equation is derived

2.3.3.1 Cyclic pressure fatigue life of pipelines with plain dents, dent with gouges and dents with welds. J.R Fowler, et al [25]

This document combines experimental and numerical projects in determining the fatigue life of dented pipelines subjected to cyclic internal pressure. This fatigue assessment approach is S-N based and uses either the API RP2A curve 'X' or the DOE curve B. efforts were initially focused on unrestrained plain dents but was subsequently expanded to include a study on dents with gouges and welds. The SCFs are presented in the form of tables as a function of d/D (dent depth over outer diameter), D/t, mean internal pressure and pipe grade. The NPS12 pipe specimen was mostly utilised for the experimental program ranging from 18 to 64 in D/t. However, an NPS24 specimen was also used with a D/t of 94.1. The experimental program involved indenting the specimen with a long bar and flat plate indenters where numerous dents with different depths were formed in each experimental specimen. The numerical part of this project employed the use of finite element analysis to further investigate the stress level of the specimens and predict the fatigue life of the specimen. A 3D elastic and 2D elastic-plastic analysis was carried out. The 3D elastic analysis was performed using the indented shape as the starting point of the analysis (i.e. ignoring the stress state at the end of the indentation process) where the internal pressure was cycled. The 2D elastic-plastic analysis, however, was used to accurately estimate the ($\Delta\sigma/\Delta P$) transfer functions in the dents vicinity and to give a better understanding of the re-rounding behaviour of the dents.

The 2D analysis utilised a 3D shell element and elastic-plastic material properties with an isotropic hardening. The analysis resulted in a set transfer functions which were used in the fatigue life assessment.

From the comparison of the experimental and predicted result, it is revealed that the API 'X' curve is extremely conservative and the DOE curve is less conservative

2.3.3.2 The EPRG model

The EPRG model is based on S-N curves for longitudinal submerged arc welded pipe published in DIN2413 [26]. The S-N curves given by the DIN codes are dependent on the mean stress and ultimate tensile strength. The stress concentration factor (SCF)

used in this method was empirically derived and is a function of the dent depth and pipe geometry. The equation proposed by EPRG based on the DIN curves is given as

$$Nc = exp\{4.292[ln(UTS - 50) - ln(2\sigma A \times Ks) + ln100\} \quad \textbf{(2-6)}$$

Where Nc = predicted number of cycles to failure

UTS = ultimate tensile strength in N/mm^2

$2\sigma_A$ = equivalent cyclic stress at R = 0

R = minimum stress/maximum stress on fatigue cycle

K_s = stress concentration factor given as 2.871 $\sqrt{\mathrm{Kd}}$, where

$$\mathrm{Kd} = \mathrm{Ho}\,\frac{t}{D} \quad \textbf{(2-7)}$$

t = pipe wall thickness

H_o = dent depth measured at zero pressure

It should be noted that the dent depth used in this model is depth at zero pressure and dent depth measured at pressure should be corrected for spring back. The recommended spring back correction factor, in this case, is $H_o = 1.43H_r$. Experience from industry shows that the EPRG model is overly conservative in estimating fatigue life of dents and predicts fatigue life much lower than the service life of the dent[23]. Figure 2-3 depicts the EPRG method for predicting fatigue life.

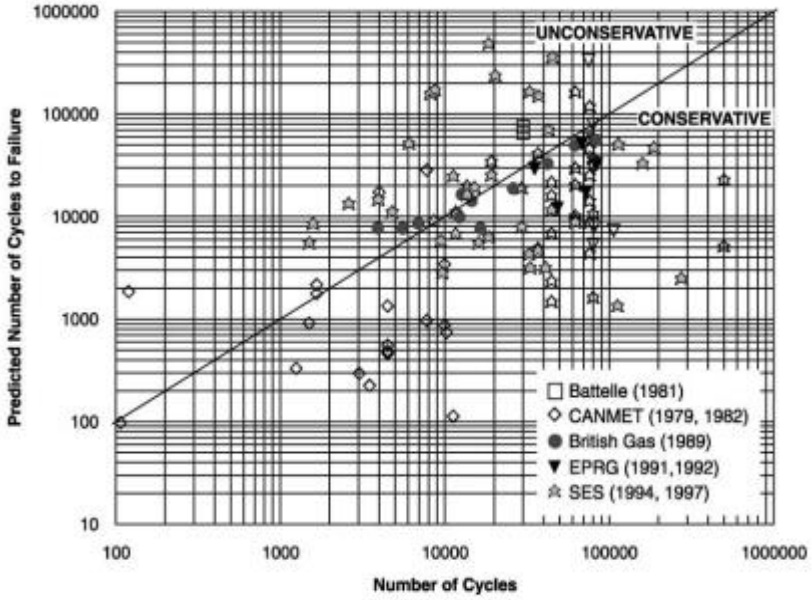

Figure 2-3 EPRG method of predicting fatigue life [1]

2.3.3.3 EPRG method for assessing the tolerance and resistance of pipelines to external damage part 1 and 2, R.J. Bood, et al [27]

This is another semi-empirical stress life S-N based approach developed by EPRG applicable to smooth dents, sharp dents and dent/gouge combinations in the pipe body only. It was developed from the DIN2413 part 1 S-N curve where the dent is assumed to be unrestrained. Here, the fatigue life is calculated with the following equation

$$N = \frac{5622}{S_L}\left(\frac{UTS}{2\sigma_A K_d K_g}\right)^{5.26} \quad \textbf{(2-8)}$$

Where N = predicted number of cycles to failure

S_L = desired factor of safety on fatigue life

UTS = ultimate tensile strength of the pipeline material in N/mm^2

σ_A = equivalent nominal fatigue stress amplitude

K_d = stress enhancement factor of the dent

K_g = stress enhancement factor of the gouge

$$\sigma_A = \frac{\sigma_a}{1-\left(\frac{\sigma_{max}-\sigma_a}{UTS}\right)^2} \quad \textbf{(2-9)}$$

$$K_d = 1 + C_{s,p}\sqrt{\frac{H_o^{1.5}t}{D}} \quad \textbf{(2-10)}$$

Where H_o = dent depth measured after damage at zero internal pressure (mm) = 1.43H

H = measured dent depth at pressure

C_p = 2 for smooth dents with radius > 5t

C_s = 1 for sharp dents with radius < 5t

$$K_g = 1 + 9\frac{d}{t} \quad \textbf{(2-11)}$$

Where d is the gouge depth

2.3.3.4 PRCI- Cyclic pressure fatigue life of plain dents

This is another stress life S-N based method intended for use with offshore pipelines but has found its way to onshore pipelines. It makes use of the DOE-B S-N curve[28] which has been shown to give better correlation to experimental data than curve X in API-RP2A[29]. The fatigue life calculation is done using equation (2-12)

$$N_c = 4.424 \times 10^{23}(SCF.\Delta p)^{-4} \quad \textbf{(2-12)}$$

Where N_c is the predicted number of cycles to failure, SCF is the stress concentration factor which is derived from finite element modelling for a discrete combination of mean pressure, material strength, D/t ratio and d/D ratio. In order to use this model, the SCF is read from tables and then applied in equation (2-12)

2.3.3.5 Effect of smooth and rock dents on liquid petroleum pipeline (API 1156), C.R. Alexander, J.F. Kiefner [17]

This is a stress-life (S-N) based fatigue life methodology. This was developed based on the results of a 3D elastic-plastic finite element analysis combined with the ASME BPVC Div 2 fatigue life curve intended for constrained or unconstrained dents from the dent depth and pressure level. The FEA made use of elastic plastic shell elements with

an isotropic hardening model to develop the Δσ/Δp for various dents configuration. The fatigue life is estimated by equation (2-13).

$$N = exp\left[43.944 - 2.9711ln\left(\frac{1}{2}SCF.\Delta p\right)\right] \quad \textbf{(2-13)}$$

Where N = predicted fatigue in number of cycles

Δσ = stress range = SCF x ∆p

SCF = stress concentration factor from tables based on indenter shape, D/t, d/D and mean pressure

The stress concentration factor SCF were developed using finite element analysis for a range of pipe diameters, dent depth, dent shapes, constraint and pressure cycling conditions. The application of this method to two experimental specimens from the same project indicated that it overly predicted the fatigue life for one specimen and under predicted it for the other[17].

2.3.3.6 Development of a model for fatigue rating for shallow unrestrained dents, M.J Rosenfeld [30]

This project was primarily designed to investigate the re-rounding behaviour of an unconstrained dent in the pipeline. In the course of the project, an equation was developed to estimate the fatigue life of the dent. This is an S-N based approach that utilised fatigue life curve from ASME B31 code for pressure piping[30]. The fatigue life equation is given by

$$N = \left(\frac{6S_{CF}}{\Delta\sigma}\right)^5 \quad \textbf{(2-14)}$$

where

Δσ = stress range

S_{CF} = the cyclic flow strength of the material = $0.5(0.667S_Y + S_U)$

S_Y = yield strength

S_U = tensile strength

From the equation above the cyclic stress range is derived from the following equation developed to estimates stress range at the peak of the dent

$$\Delta\boldsymbol{\sigma} = \left(\frac{\Delta \boldsymbol{p_a D}}{\boldsymbol{2t}}\right)\left(\boldsymbol{2} + \frac{\boldsymbol{6}\left(\Delta \boldsymbol{d^+} + \Delta \boldsymbol{d^-}\right)}{\boldsymbol{t}}\right) \quad \textbf{(2-15)}$$

where Δp_a = applied cyclic pressure range

D = outer diameter

t = wall thickness

Δd^+ = outward dent displacement

Δd^- = inward dent displacement

2.3.3.7 PRCI- Model for fatigue shallow unrestrained dents

This project was aimed at enabling pipeline operators to assess the severity of dents on the basis of their fatigue life in service. It is a stress life S-N approach that estimates the bending stresses in the dent and analyses how they change with variation in pressure in order to be able to calculate the fatigue life. This procedure was simplified into a set of design curves that can be used to give a basic fatigue rating based on the pipe and dent geometry, material properties and the frequency of full operating pressure cycles. The fatigue life is determined from the modified ASME B31 code for pressure piping. The cyclic flow stress σ_{CF} replaces the yield stress in the equation as given by the equation

$$\sigma_{CF} = \frac{1}{2}\left(\frac{2}{3}\sigma_Y + \sigma_U\right) \quad \textbf{(2-16)}$$

However, one of the disadvantages of this approach is that the design curves are only published for discrete values of the pipe and dent geometry and requires interpolation of the curves for intermediate values. Another disadvantage is that the curves are based on initial dent geometries[31].

2.3.3.8 Guidelines for the assessment of dents on welds, M.J Rosenfeld [32]

This stress-life S-N based fatigue life model was designed to estimate the fatigue life of unrestrained dents on either long seam or girth welds. It considers the effect of dent

size, weld quality and the applied pressure spectrum on the fatigue life of a dented pipeline. It employs finite element analysis in calculating the stress concentration factors as a function of the applied pressure range, the initial dent depth d, outer diameter D, D/t and the mean pressure[32]. The initial dent depth (spring back depth) is calculated as

$$d_i = \frac{d_r}{fg} \quad \textbf{(2-17)}$$

where d_r = rebound dent shape

$$f = \frac{1.04}{1+0.0875x^{\frac{-3}{2}}} - 0.052 \quad \textbf{(2-18)}$$

$$x = \frac{(D/w)^{0.3}}{(D/t)^{0.7}\,(p/E)^{0.2}} \quad \textbf{(2-19)}$$

$$g = \frac{0.88(\frac{D}{w})}{1+0.59\left(\frac{D}{t}\right)+0.041(\frac{D}{t})^2} \quad \textbf{(2-20)}$$

Here, w represents the width of dent measured between half depth points, p represents the internal pressure and E represents the elastic modulus. The fatigue life is calculated using the equation below

$$N = 7970\left(\frac{Q}{\Delta\sigma}\right)^{2.865} \quad \textbf{(2-21)}$$

Where N is the number of cycles of failure and Q is a weld quality category and is a function of the allowable weld imperfection according to API 1104.

2.3.4 Strain-life Approach

The strain-life approach is another approach to estimating the fatigue life of dented pipelines. The fatigue life is obtained by superposition of the curve representing the elastic (governing high cycle fatigue) strain portion and plastic strain portion (low cycle fatigue).

One of the most common strain life relationships is derived using the Coffin-Manson equation as shown below

$$\frac{\Delta\varepsilon}{2} = (\sigma_{f'}/E)(2N_f)^b + \varepsilon_{f'}(2N_f)^c \quad \textbf{(2-22)}$$

where $\Delta\varepsilon$ represents the strain range, $\sigma_{f'}$ represents fatigue strength coefficient, E represents modulus of elasticity, b represent fatigue strength component, $\varepsilon_{f'}$ represent fatigue ductility coefficient, c represents fatigue ductility exponent and N_f representing cycles to failure[5].

In equation (2-22), the first term on the right-hand side of the equation represents the elastic strain life portion while the second term on the right-hand side of the equation represents the plastic strain life portion. The schematic representation of the Coffin-Mason strain life is shown in figure (2-4).

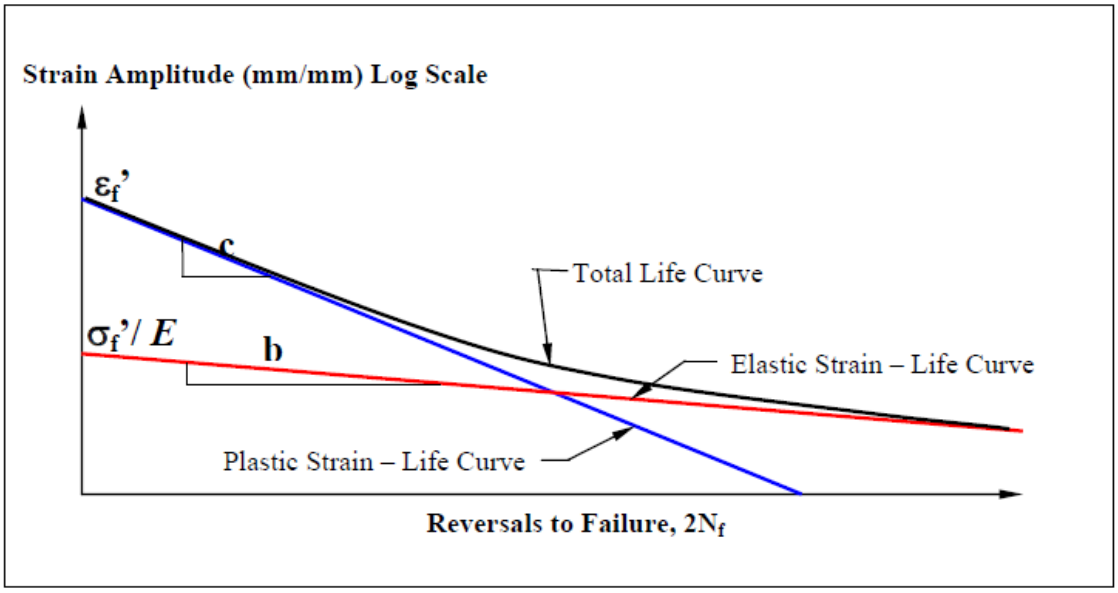

Figure 2-4 Coffin mason strain-life curve [5]

A particular area of interest using this equation is accounting for the effect of mean stress. Different researchers have come up with various ways of accounting for the mean stress some of which include Morrow, Manson and Halford and Smith Watson and Topper.

Morrow was the first to modify the coffin mason equation accounted for the mean stress by modifying the elastic strain life portion of the Coffin-Masson equation (2-22) by proposing a correction factor for mean stress σ_o.

In this equation, tensile mean stresses are positive (i.e. $\sigma_0 > 0$) while compressive mean stresses are negative (i.e. $\sigma_0 < 0$).

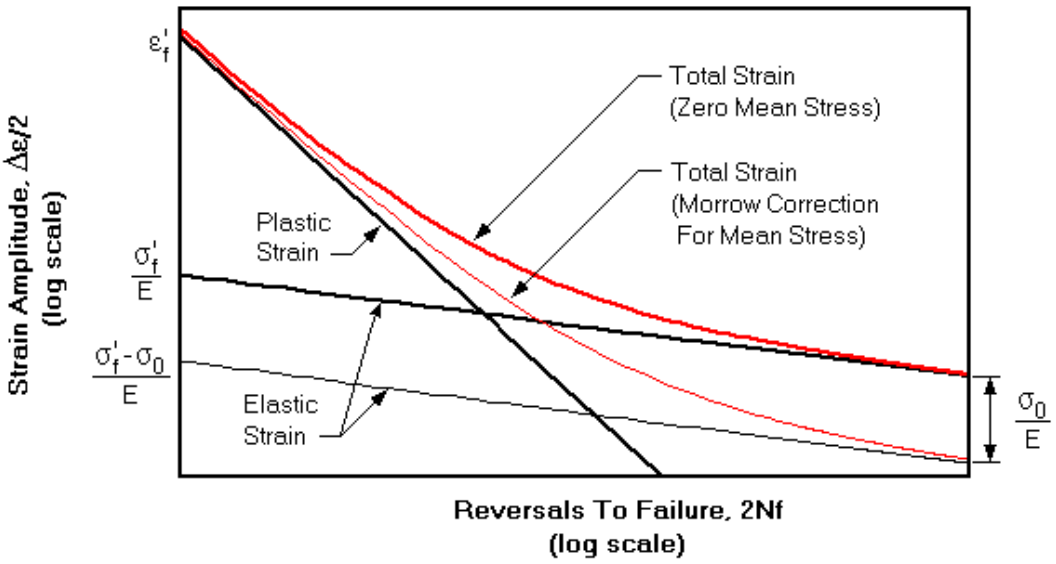

Figure 2-5 Effect of mean stress on the strain life curve (Morrow's correction) [33]

Manson and Halford accounted for the mean stress by modifying both the elastic and plastic strain life portion of the Coffin-Masson equation as shown in equation (2-23)

$$\frac{\Delta\varepsilon}{2} = \left(\frac{\sigma_{f'} - \sigma_o}{E}\right)(2N_f)^b + \varepsilon_{f'}\left(\left(\frac{\sigma_{f'} - \sigma_o}{\sigma_{f'}}\right)\right)^{\frac{c}{b}}(2N_f)^c \quad \textbf{(2-23)}$$

Smith, Watson and Topper also proposed equation (2-24) & (2-25) to account for the effect of the mean stress. Their approach made use of the Basquin relation relating the maximum stress σ_{max} of a fully reversed cycle to fatigue

$$\sigma_{max}\frac{\Delta\varepsilon}{2} = \left(\frac{(\sigma_{f'})^2}{E}\right)(2N_f)^{2b} + (\sigma_{f'}\varepsilon_{f'})(2N_f)^{b+c} \quad \textbf{(2-24)}$$

$$\sigma_{max} = \frac{\Delta\sigma}{2} + \sigma_o \quad \textbf{(2-25)}$$

2.3.5 Fracture Mechanics Approach

Fracture mechanics is one of the three basic approaches to fatigue life estimation. It is based on a fatigue crack growth theory. Unlike the S-N approach which involves crack initiation, propagation and failure, the fracture mechanics approach involves only propagation and failure, it assumes an initial crack. It is characterised by the Paris crack growth equation as follows:

$$\frac{da}{dN} = C(\Delta K)^m \quad \textbf{(2-26)}$$

Where da is the increase in crack length, dN is the applied load cycle, ∆K is the range of strength intensity factor and C and m are constants. However, the stress intensity factor range is a function of the applied stress range ∆σ, the geometry and crack length a , and are calculated by equation (2-27)

$$\Delta K = Y(\Delta\sigma)\sqrt{\pi a} \quad \textbf{(2-27)}$$

The fatigue life is estimated as the number of cycles required to grow a crack from an initial crack size a_i to a critical crack size a_{crit} under cyclic stress range $\Delta\sigma$.When using fracture mechanics for estimating fatigue life of pipeline with dents, parameters like crack growth rate data and initial flaw size to use must be established that governs the crack growth.

BMT fleet [5] gave a summary of the algorithm used to develop a fracture mechanics approach to estimating the fatigue of pipeline dent as shown below:

1. Select appropriate crack growth rate parameters(representative of typical pipeline steel)
2. For each of experimental specimens, use crack growth calculations to determine a calibrated initial flaw size that results in a fatigue life estimate similar to the experimental fatigue life.

3. Based on the results of steps 2, develop a single initial flaw size that is suitably representative of the experimental data
4. Calculate the fatigue lives of all the experimental specimen using the initial flaw size determined in step 3 and the material properties selected in step 1.

2.3.6 Factors affecting fatigue life assessment of dents

There are many factors that affect the accurate prediction of fatigue life of pipeline with a dent. From past research, it is seen that plain dents do not significantly affect the burst strength of pipelines. However, the fatigue life reduces with increase in the dent depth. Dent depth is one of the dent geometric properties that affect the fatigue life estimation of dents. Other properties, such as pipe material properties, pipe geometric properties, restraint conditions, could be also strongly correlated to the fatigue life of dents. They are discussed as follows.

2.3.6.1 Dent geometry factor

As discussed as above, the dent depth plays a very important role in the fatigue life estimation of dents, however, research also indicates that the dent geometry, dent restraint and rerounding stiffness also play an important role in the fatigue estimation of dents. Beller et al[34] in a study found that the point of maximum stress concentration for a semi-spherical dent was at the rim of the dent. They pointed out that as the dent was elongated, the maximum stress moved to the root of the dent. This observation indicates that there is a critical ratio of length to width where the location of fatigue cracking would move from the rim to the centre of the dent. Rosenfeld[30] also concluded in a study that the ability of a dent to reround is related to the depth to width ratio. It found out that the fatigue life also increases with increase in depth to width d/W ratio. The width of the dent, however, was reported to be difficult to measure due to bulging around the shoulders of the dents and is there the distance between the points on the dents where the depth is half the maximum depth. Rinehart and keating[35] also developed a geometric expression which is inversely proportional to the fatigue life by combining dent depth (d/D), dent length (L/D) and rerounding stiffness. The equation is given below.

$$fatigue\ life \propto \frac{1}{\frac{LdW}{D^2t}} \quad \textbf{(2-28)}$$

2.3.6.2 Dent Constraint factor

Dent constraint plays a very important role in the fatigue life assessment of dents. The ability of a dent to spring back or reround depends on whether or not there is a constraint. Fatigue assessment comes into play when cyclic pressure is applied to the dent. An unconstrained dent spring back upon removal of the indenter and rerounds as pressure is applied. From research, it is seen that the fatigue life of restrained dents is higher than equivalent unrestrained dents because of its ability to stop the dent from rerounding due to pressure loading. Experimental work by Alexander and Kiefner [17], keating and hoffman[36] and SES[25] have confirmed this. These tests also show that the mode of failure in both cases are different. The tests conducted by Alexander and Kiefner show that cracking was oriented in the circumferential direction beyond the indenter for a restrained dent. However, in an unrestrained dent, the cracking was axially oriented located within the dented region. Figure 2-6 below shows a comparison between the fatigue life of unrestrained and restrained dent.

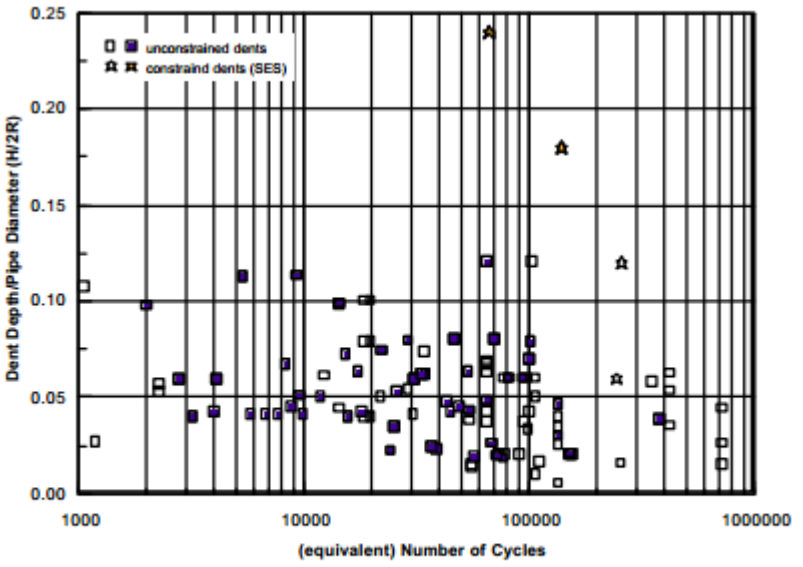

Note: In this figure, open symbols (e.g. ○) denote tests that did not fail during the test (the test was terminated prior to failure) and closed symbols (e.g. ●) denote tests that did fail during the test.

Figure 2-6 Fatigue life of unrestrained and restrained dents[1]

2.3.6.3 Pipe geometry factor

Pipe geometry is also an important factor that affects the fatigue life of dents in the pipeline. Research have shown that D/t ratio affect the fatigue life of pipes. De Carvalho Pinhiero et al[37] shows that the D/t ratio is directly proportional to the stress concentration factor and inversely proportional to the fatigue life. However, there is a counter claim by Dinovitzer et al [38] that showed using FEA model that the fatigue life of dents increases with increasing D/t ratio. Fowler et al [105] undertook finite element analysis to determine the importance of dent features. The results were used to calculate the stress concentration factor (SCF), which was then used to calculate the fatigue life of dented pipe. The SCF varied from 3 to 5 with different D/t ratios. Results indicated that D/t ratio had little role to play in failure beyond a D/t of 40. FE analysis also shows that the SCF increased rapidly from a D/t ratio of 20. It showed that the SCF is at its peak at D/t of 50.

2.3.6.4 Pipe material factor

The pipe material property also affects the fatigue behaviour of dented pipe. Different pipe grades are used in the pipeline industry ranging from X42 to X120. Research confirms that fatigue life of a dented pipe decreases with increasing SMYS. Numerical Work by Rosenfeld[30] and Dinovitzer[38] confirm this. This could be attributed to the fact that dents can reround due to decreasing plasticity of the material.

2.3.6.5 Effect of pressure cycle

Pipeline pressure cycling plays an important role in the estimation of fatigue of pipeline with dents. Liquid and gas pipeline can experience pressure cycling throughout the year. For example, demand for gas is increased in winter compared to summer thereby necessitating change in pressure. Generally, the fatigue life of pipeline with dents decreases with increase in pressure cycling. Work by Kiefner[39] and Rosenfeld[30] have confirmed this. The liquid pipeline tends to be more pressure cycled than the gas pipeline as it can experience up to 1800 times the pressure cycling at the same pressure of an equivalent gas pipeline. Kiefner[39] characterised typical pressure cycling regime for a pipeline based on the benchmarking scheme as seen in table 2.2. This is based on observed pressure pattern that failed as a result of fatigue. The percentage SMYS in the table represent the hoop stress cycle. As an example, a very

aggressively cycled pipeline may experience 20 cycles from 72%SMYS to zero and back to 72%SMYS

Percent SMYS	**Very Aggressive**	**Aggressive**	**Moderate**	**Light**
72	20	4	1	0
65	40	8	2	0
55	100	25	10	0
45	500	125	50	25
35	1000	250	100	50
25	2000	500	200	100
Total	3660	912	363	175

Table 2-3 benchmarked annual cycle count [39]

2.3.7 Dent measurement

Dent can be measured and detected in many ways. It can be measured by direct visual inspection and by using various In-line inspection (ILI) tools which include magnetic flux leakage tool, ultrasonic inspection tool and geometry tools. When measuring dents, certain information like dent depth and shape is required and it's associated with weld, gouges and corrosion. Most of the ILI tools cannot measure all these information at once and might require a combination of two or more ILI tools. Table 2-3 summarises the capabilities of ILI tools for providing required dent information

Dent attribute	**Geometry tool**	**High-resolution geometry tool**	**Metal loss tool**	**Crack detection tool**

Location along pipeline	✓	✓	✓	✓
Orientation	✓	✓	✓	✓
Size(%OD)	✓	✓		
Size and shape of dents		✓		
Detects dents on welds	✓	✓	✓	✓
Detects metal loss in dents			✓	
Detects cracks in dents				✓
Detect rock dents				

Table 2-4 capabilities of in-line inspection tools for dent information culled from API 1156 [18]

2.4 Finite element methodology

Finite element method (FEA) sometimes called finite element analysis (FEA) is a numerical method for solving simple and complex engineering problems. It involves breaking down structures into smaller (finite) elements. The equations associated with these finite elements are then assembled into a larger system of equations that models the entire problem. One of the common methods of dent assessment is using finite element analysis. It can be used in place of theoretical and experimental methods. In the past, values for peak stress, strains and SCF have been generated empirically but nowadays, these values can be generated using finite element method. There are various steps and techniques to follow when using finite element. These steps are categorised into 3 groups such as pre-processing, solution and post processing. There are several FE software packages such as Ansys, Abaqus, Nastran , Patran and so on. Though the software interfaces are different, they all follow the same procedure in solving problems.

2.4.1 Previous work done using finite element analysis

Various researchers have used finite element method. The results are validated against experimental data. They check if it is in reasonable agreement with the experimental data.

Leis et al [60] investigated dent on a pressurised pipe with a quarter symmetry model using 8-node shell elements with a very refined mesh in the region of contact . The indenter and the pipe support were modelled as rigid bodies. The results obtained from the analysis were in reasonable agreement with the experiment data.

Ong et al [8] also studied the effect of a dent on pressurised pipeline using experimental measurement and finite element analysis considering the effect on a plain dent and plain dent with a reduction in wall thickness. The finite element model consisted of quarter pipe symmetry and utilised eight node shell elements. Results from burst test showed that pipe failure was insensitive to the existence of a local dent; however pipe failure was found to be due to loss of thickness defect.

Zarea et al [15] proposed the use of static and dynamic FE models to estimate the residual life of indented damaged pipes. This was done using thin triangular shell elements for the static analysis and quadrilateral shell elements for the dynamic analysis. They established the relationship between the depth and force, dent depth and residual dent depth and calculated the residual stress under cyclic pressure loading. The residual stress was then used to calculate the residual life.

Brooker [16] used a technique similar to leis et al to model denting of pressurised pipeline under localised radial loading. The model included an 8-node full integration solid elements in the dent region with five layers through the wall thickness of the pipe and 8-noded shell elements away from the dent region. Contact between the pipeline and the indenter was modelled with the assumption that the surface was frictionless. It was observed that the indenter shape and size was imperative to pipeline puncture. He also observed that the puncture load can be taken as proportional to the pipe thickness and linearly related to the material ultimate stress. Brooker [16] proposed an equation after the numerical study for lateral indentation showing the influence of pipe diameter and thickness, pipe length and residual depth on the indenting force.

BMT fleet[5] in a study compared five methodologies employed by researchers in fatigue life assessment in order to determine what the cause of conservatism in the approach. They came to the following conclusions

- All the methods studied utilise the S-N approach which is as a result of a wide range of S-N curves available for use
- Isotropic hardening model was used by four methods to idealise the cyclic material behaviour of the pipe
- The stress concentration factor for all the methods was calculated as a function the dent depth (d/D) and the pipe geometry(D/t). Three of the methods accounted for the effect of mean pressure
- Two of the methods accounted for the dent shape

2.5 Artificial neural network

The term neural network derived its origin from the human brain or the human nervous system which consist of a large parallel interconnection of a large number of neurones. The human brain has a highly complex non-linear parallel computer and can organise its structural constituents known as neurones. Neurones interact with each other through a host of structures called dentrites[49]. These neurones are interconnected in a very complex way between each other to create a network. The artificial neural network mimics a small part of the human brain to perform some specific task such as data classification or pattern recognition through a learning process. It has an inter-connection of non-linear neurones that are distributed throughout. When using it for non-numeric values, It is called classification. However using it for numerical values is called regression.

An artificial neural network consists of a set of neurons or processing element (PE) that are connected by links of certain numeric weights. Each neuron has

- a set of input links from other neurons
- a set of output links from other neurons
- a current activation function

- and an activation function to compute the activation level in the next time step

A typical neuron is illustrated in figure 2-7

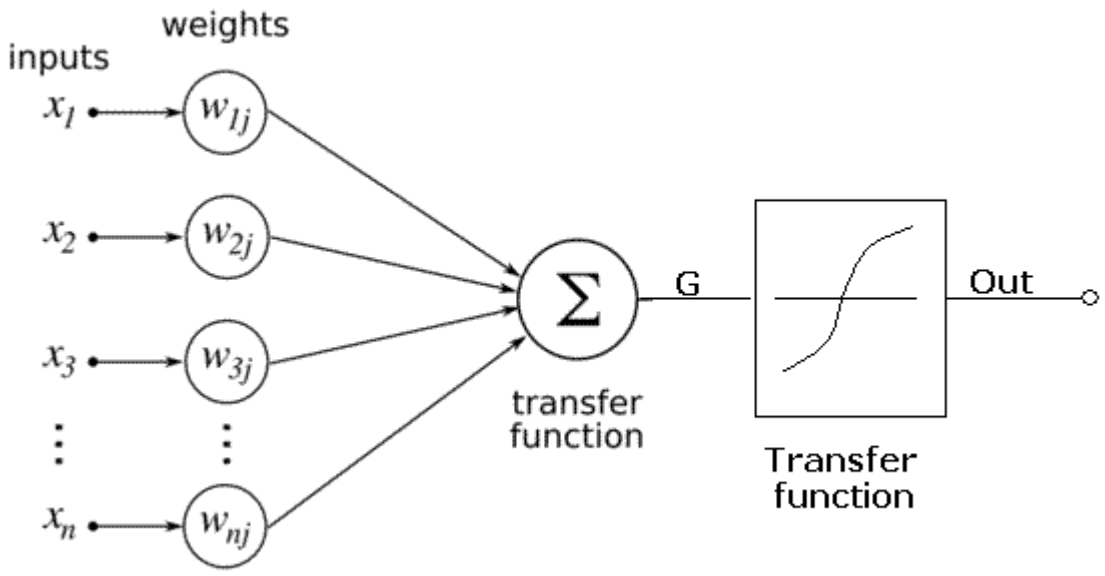

Figure 2-7 A typical neuron in a neural network [50]

In figure 2-12, x_1, x_2…x_n are the inputs, w_{1j}, w_{2j}….w_{nj} are the weights. The total weighted input is the sum of the input activation multiplied by their respective weights

Neural networks have the capacity to derive meaning from loose information, can be utilized to detect trends and identify patterns that are too intricate to ever be seen by either people or other PC procedures. A trained neural network can be considered as a "specialist" in the class of data it has been given to examine.

Other advantages include:

1. Adaptive learning: A capacity to figure out how to do assignments in view of the information given for training

2. Self-Organization: An ANN can make its own particular association or representation of the data it gets amid learning time.

3. Ongoing Operation: ANN calculations might be completed in parallel, and exceptional equipment gadgets are being designed and fabricated which exploit this capacity.

2.5.1 Neural network architecture

A typical neural network architecture will consist of an input layer, one or more hidden layer, and an output layer. The input layer represents the information that is being fed into the system. The hidden layer is dictated by the activities of the input units and the weights between the input and hidden layer. The output layer likewise relies on the action of the hidden layer and weights between the input and output layer

The architecture can be further categorised into

- single layer architecture
- multiple layer architectures

The single-layer association, in which all units are associated with each other, constitutes the broadest case and is of more potential computational force than progressively organized multi-layer associations. In multi-layer systems, units are regularly numbered by layer, rather than taking after a global numbering.

2.5.1.1 Feedforward network

A feed forward network which is shown in figure 2-8 permits signal in one direction only (i.e. from input to output).There is no form of feedback within the system and is usually used in pattern recognition

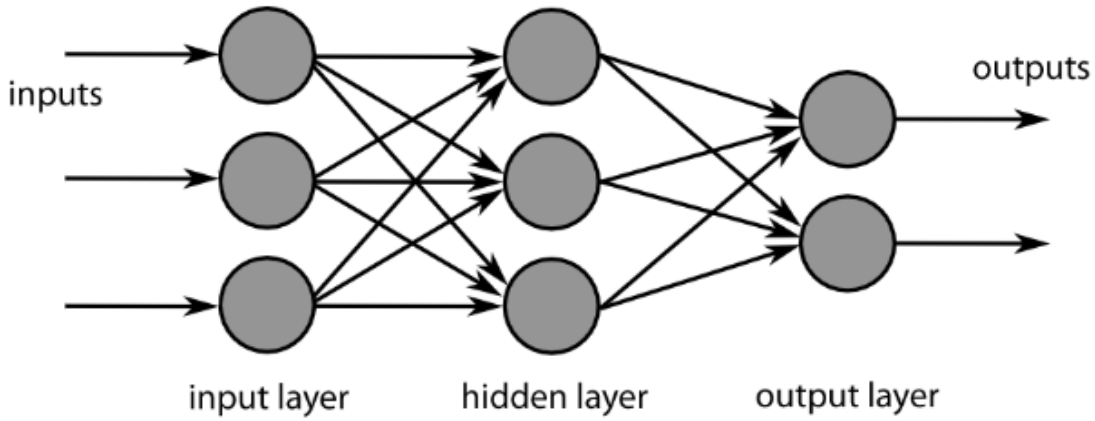

Figure 2-8 A feed forward network [51]

The typical characteristic of a feed forward system include:

1 .perceptron are arranged in layers, the input being the first layer and the output being the last layer. In-between the input and the output layer, there is a hidden layer that has no connection with the external world

2. Each perceptron within one layer is connected to every perceptron in the next layer and information is constantly fed forward from one layer to the next

3 perceptrons within a layer are not connected in any way

The number of neurons in the input layer is equal to the number of input variables, similarly, the number of the output layer is equal to the number of output variables. The accuracy of the model is determined by the number of neurons in the hidden layer.

There are several algorithms that can be used to train a neural network. Some of them include back-propagation, genetic algorithm, and particle swam optimisation. For this study, the back propagation algorithm is used as it is the fastest and the most common technique. It also gives insight on how the weights and biases can affect the behaviour of the network

2.5.2 Activation functions

The behaviour of an ANN greatly depends on the activation function, weights, and biases. There are different types of activation functions. The most common ones are the logistic sigmoid and the hyperbolic tangent transfer functions. Both functions are compared to determine the one that best predicts the SCF. Neural network learning

One of the unique characteristics of an artificial neural network is its ability to learn and recognise pattern. ANN models its learning process by adjusting the weighted connections between neurons in a network. There are several learning algorithms that can be used when training an artificial neural network. The objective of the learning algorithm is to find a set of weight matrices which if applied to the network would map any input to a correct output

2.5.2.1 Supervised learning

This is the type of learning algorithm that provides the desired output and input while training the network. An error can be calculated based on the target output and actual output by providing the network with a pair of input and output. Through the errors, the network can make corrections by adjusting the weight matrix. There are several supervised learning algorithms and the most common are the back-propagation algorithm

2.5.2.2 Backpropagation

The back-propagation algorithm computes each error derivative of the weights (EW) by first computing the rate at which the error change as the activity level of a unit is changed (EA).For the output, The EA is the difference between the actual and the desired output. The EA of the hidden unit is calculated by first identifying all the weights between the hidden units and the output units to which it is connected. The weights are then multiplied by the EAs of the output units, the products are then added. The sum equal the EA for the chosen hidden unit. The EAs for other layers are calculated in similar fashion moving from layer to layer in a direction opposite the way activities propagate through the network. The EW is the product of the EA and the activity through the incoming connection [49]

2.5.2.3 Unsupervised learning

The learning algorithm for an unsupervised learning involves feeding the network with given set of inputs. The neural network then finds a pattern within the input provided without no external aid to create an output.

CHAPTER 3

ELASTIC SPRING BACK AND REROUNDING IN DENTED PIPELINE

3.1 Introduction

This chapter focuses on the response of the pipe during the denting and the pressurisation process. The pipe's response to denting is dependent on some key parameters. These parameters include pipe geometry, dent geometry, pipe material and applied pressure range. When a pipe is dented, the elastic response of the pipe is dependent on these variables. Steel pipes have both elastic and plastic properties. When a pipe is dented, the elastic property comes into effect allowing some spring back in the dents when the cause of denting is released. However, the pipe does not fully gain its original position leaving some plastic deformation. Upon application of pressure, the dent depth is reduced further but does not fully regain its original position. In most experimental data, dent depths are measured after spring back at zero operating pressure and this represents the scenario when a dent is formed during construction. However, in practice dents are introduced in service under internal pressure and the dent depth measured are the rerounding dent depths . The responses of the pipe to the denting process are different and the stress level associated with these scenarios are also different. This led to the introduction of spring back correction factor and triggered the debate about which dent depth should be used in assessment. Cosham and Hopkins have reviewed a number of correction factors and have come to the conclusion that most spring back correction factors are empirically derived and do not account for some parameters including, pipe geometry, dent geometry, and pipe materials. Available test data have a lot of scatters in relation to the rerounding, making the prediction increasingly difficult.

The objectives of this chapter is to

- improve the understanding of the spring-back and re-rounding phenomenon
- Identify the most important parameters, which influences spring-back and re-rounding

- create database for the application of ANN-based formulae in chapter 6
- provide guidance in how to apply the additional knowledge

3.2 Spring back and rerounding mechanism

The process of denting produces both elastic and plastic responses in the material. When an indenter is applied to the pipe to create dent and removed, the elastic component of the deformation is recovered and the dent will naturally move outwards reducing the dent depth. This recovery is referred to as ‘spring back’. At this point the dent does not fully move out, leaving some plastic deformation. When internal pressure is introduced to the pipe, the dent further pushes out. This phenomenon is called ‘rerounding’. The extent to which the dent is pushed out is dependent on the magnitude of internal pressure. As the internal pressure is increased, the dent is further pushed out which consequently reduces the dent depth. Rosenfeld[11] postulated that the process of rerounding includes an initial plastic recovery of the dent depth which is dependent on the pipe properties and internal pressure. Whether further rerounding is plastic or elastic is determined by the magnitude of the stress cycles. It postulates that the dent will eventually shakedown to stable elastic behaviour when the dent depth cycles about a mean depth, which is a function of the geometry and the amplitude of the pressure fluctuations.

3.3 Finite element model

The finite element model is a critical part of this research. The results obtained from this study is used to train the artificial neural network (ANN). It is essential to get an accurate result from this study and the accuracy is dependent on the model itself. BMT fleet[5] compared some methodologies as discussed in chapter 2 and suggested some factors that might be the cause of conservatism in FE results. Included in these factors are the material model used in characterising the cyclic behaviour of the model and the type of analysis itself. This section carefully studies these factors and how it can affect the results in general. There are several steps involved in the modelling such as material assignment, geometry creation, meshing, contact pair creation, boundary conditions and loading. Each of these steps needs to be done correctly in order to obtain an accurate result. In order to create a wider range of data, a total of 256 models are created. These models have varying diameter to thickness ratio (D/t), dent

depths(%d/D), pipe grades, dent orientation and pressure range. Creating 256 models can be difficult and time consuming. In order to achieve this, an Ansys parametric design language (APDL) was created(as seen in appendix E). The APDL allows a first time user to create models without having a prior knowledge of ANSYS. With the APDL, the parameters can be changed and copied to create a new model. This will help to ease the difficult task of creating each model separately. The language as seen in appendix E shows comments on the different steps that helps the user to identify the particular task.

3.3.1 Geometry creation

The pipe and the indenter are modelled using Ansys Mechanical APDL. It is a commercial software that can be used to solve many complex engineering problems including structural, electrical and CFD Problems. For the purpose of the parametric study, eight different pipes are modelled with two types of indenters each to simulate longitudinal and circumferential dent. The pipe geometry ranges from a diameter to thickness ratio (D/t) of 18.6 to 96.These are standard industry pipes that are used both offshore and onshore. All pipes share similar diameter but varying thicknesses. The selected thickness are similar to the one used in API 5L line pipes [53]. A list of the pipe and their thickness are shown in table 3-1.

MODEL	Diameter	Thickness	D/t
A	323.62	17.399	18.6
B	323.62	12.944	25
C	323.62	10.1131	32
D	323.62	8.0905	40
E	323.62	6.4724	50
F	323.62	5.2196	62
G	323.62	4.04525	80

H	323.62	3.371	96

Table 3-1 pipe models and dimensions

The indenter used includes a longitudinal bar indenter with dimensions 609.6mm x 304.5mm x 50.8mm and a dome indenter with diameter 219.07mm. The shapes and sizes of these indenters were selected in order to vary the sizes (particularly the length of the dent) and the dent orientation and to ultimately see their effects on the result.

A Quarter model of both the pipe and the indenter are modelled taking advantage of the symmetry of the pipes and indenters. A sufficient length of pipe is used to avoid interaction with the boundaries. Figure 3-1 shows the model for a longitudinal and circumferential dent.

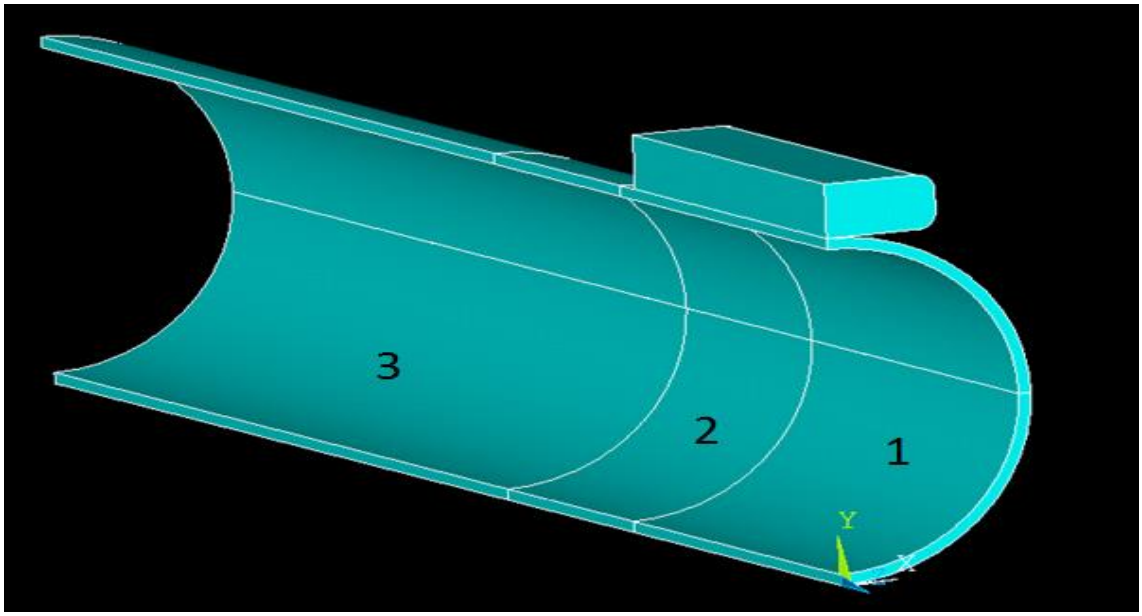

(a)

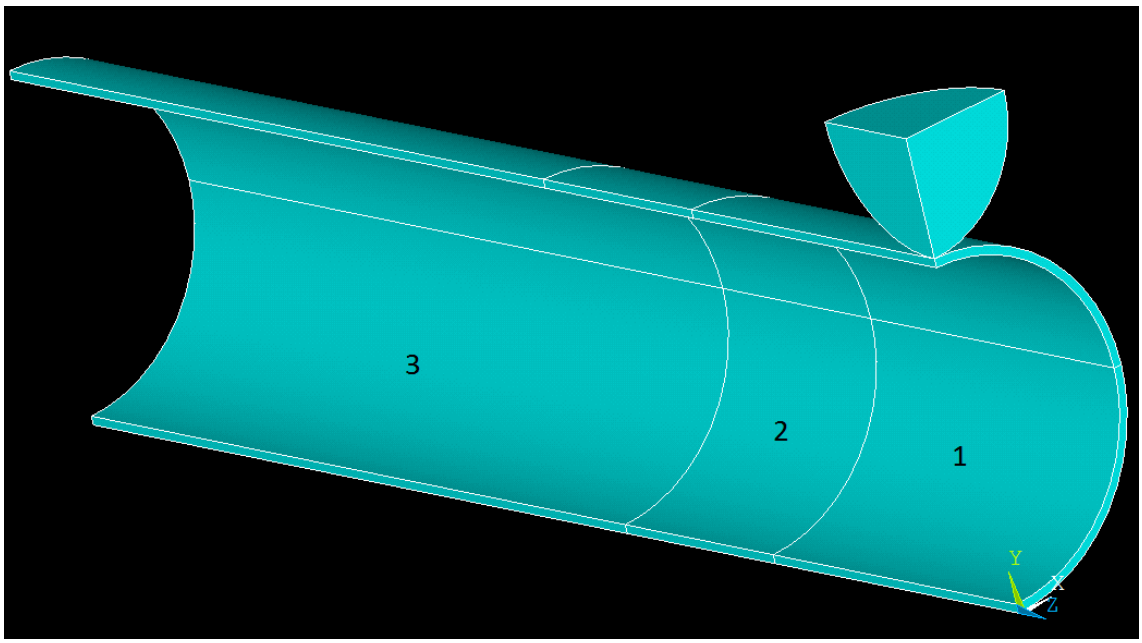

(b)

Figure 3-1 Longitudinal (a) and circumferential (b) dent models

The entire model has two major volumes which consist of the quarter symmetry of the pipe and quarter symmetry of the indenter. The pipe is further divided into 3 regions as seen in the figure above. The advantage of this is that it helps to easily mesh the model and the region of interest can be easily separated from the entire model. Region 1 represents the region of interest as this is the region where the high-stress concentration takes place. It also represents the region of high mesh density. Region 2 is the transition region. It represents the region where the mesh transitions from a higher density to a lower density. The third region represented as 3 is the region of lower mesh density.

3.3.2 Materials

Four different pipes grades are considered in the parametric study. They include X46, X65, X80, and X100. The response of the material to denting depends majorly on the material model so it is important to get the material modelling right. For this study, a multi-linear kinematic model is used to adequately simulate the response of the material during denting, rerounding and pressure cycling. This model is a rate independent version of the kinematic hardening model and is very useful in modelling cyclic plastic behaviour. It assumes that yield surface remains constant in size but

allows translation due to plasticity. It also accounts for the Baushinger effect in that material's stress/strain characteristics change as a result of the microscopic stress distribution of the material. The stress-strain curve for each of the materials is seen in figure 3-2, 3-3, 3-4 and 3-5. Table 3-2 also shows the mechanical properties of each material model. Each material has a young's modulus of 210000Mpa and a Poisson's ratio of 0.3.

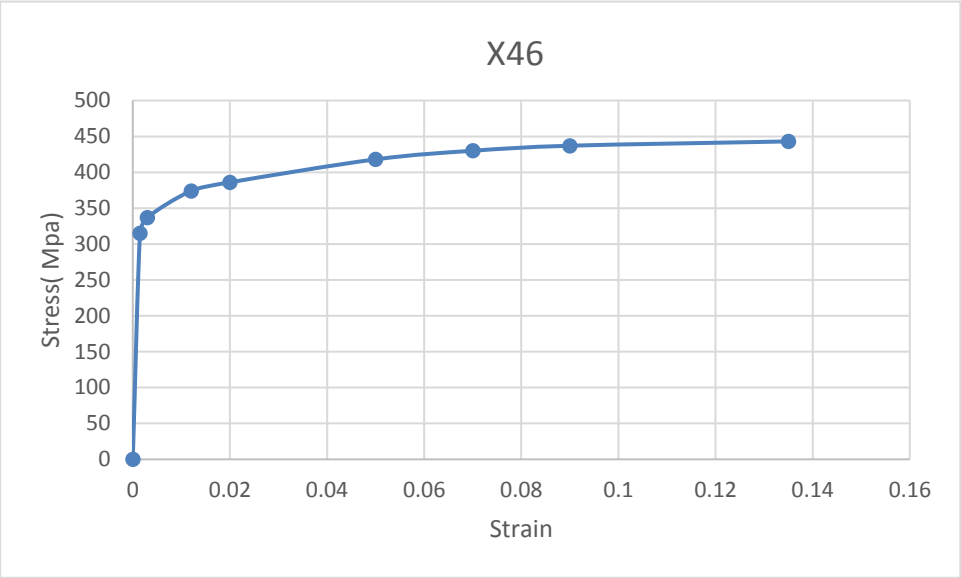

Figure 3-2 Stress-strain curve for X46

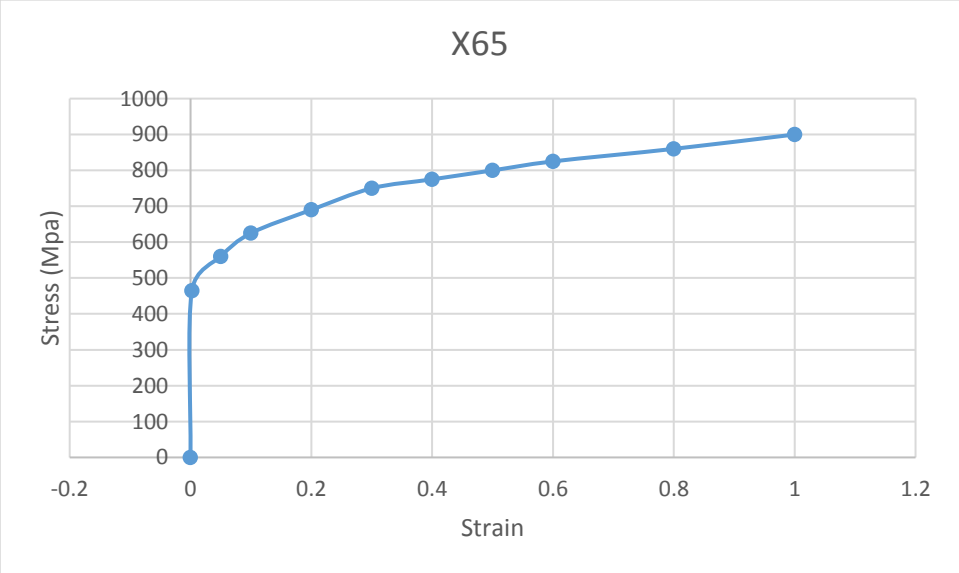

Figure 3-3 Stress-strain curve for X65

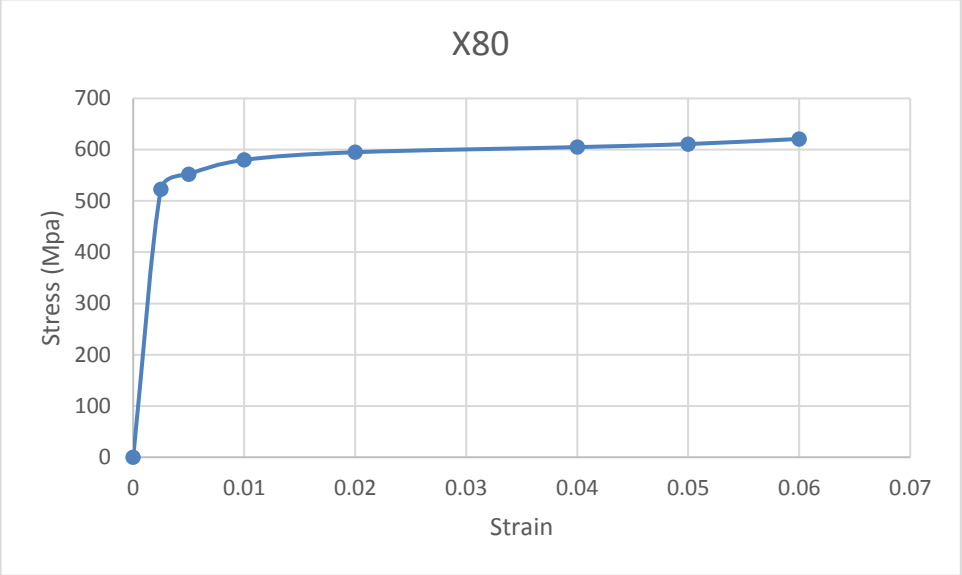

Figure 3-4 Stress-strain curve for X80

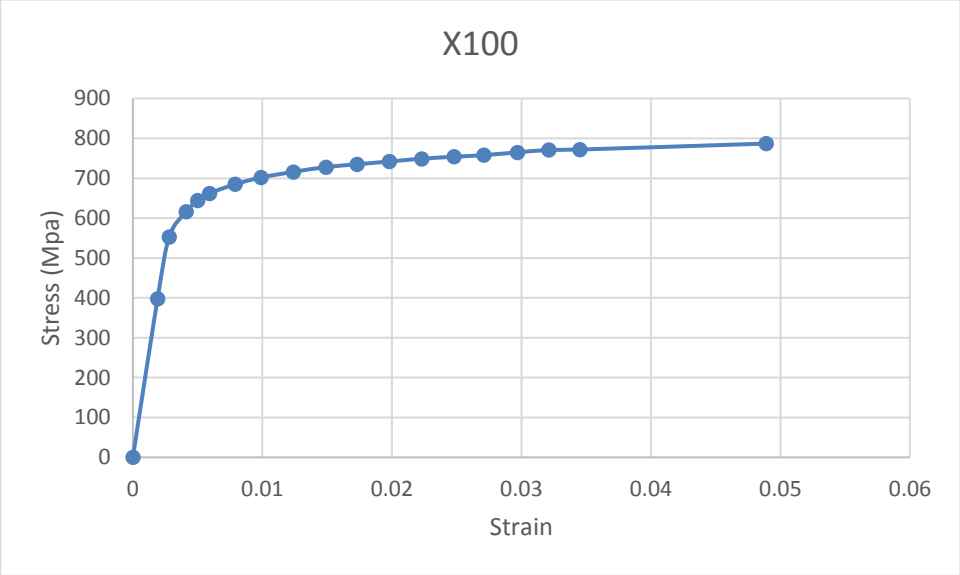

Figure 3-5 Stress-strain curve for X100

API 5L grade	Yield strength (Mpa)	Ultimate tensile strength (Mpa)
X46	317	434
X65	448	530
X80	551	620
X100	690	760

Table 3-2 mechanical properties of pipe models

3.3.3 Elements

It is essential to choose the right element type for the model as it determines the behaviour of the model and its responses to external loads. A solid 186 element is used to model both the pipe and indenter. Contact and target elements CONTA 174 and TARGE 170 are used in modelling the contact pair.

3.3.3.1 Solid 186

The solid186 is a higher order 3D 20 node solid element having three degrees of freedom per node that exhibits quadratic displacement behaviour. This element supports hyper-elasticity, plasticity, large deflection, stress stiffening and large strain capabilities. It can also be used for modelling deformations of nearly incompressible elastoplastic materials and fully incompressible hyperelastic materials. The solid 186 elements are usually available in two forms which include

- The homogeneous structural solid
- Layered structural solid

The homogenous structural solid is usually useful for modelling irregular meshes while the layered structural solid is usually used to model layered thick shells or solid a typical diagram of a homogeneous and a layered structural solid element is given in figures 3-6 and 3-7.

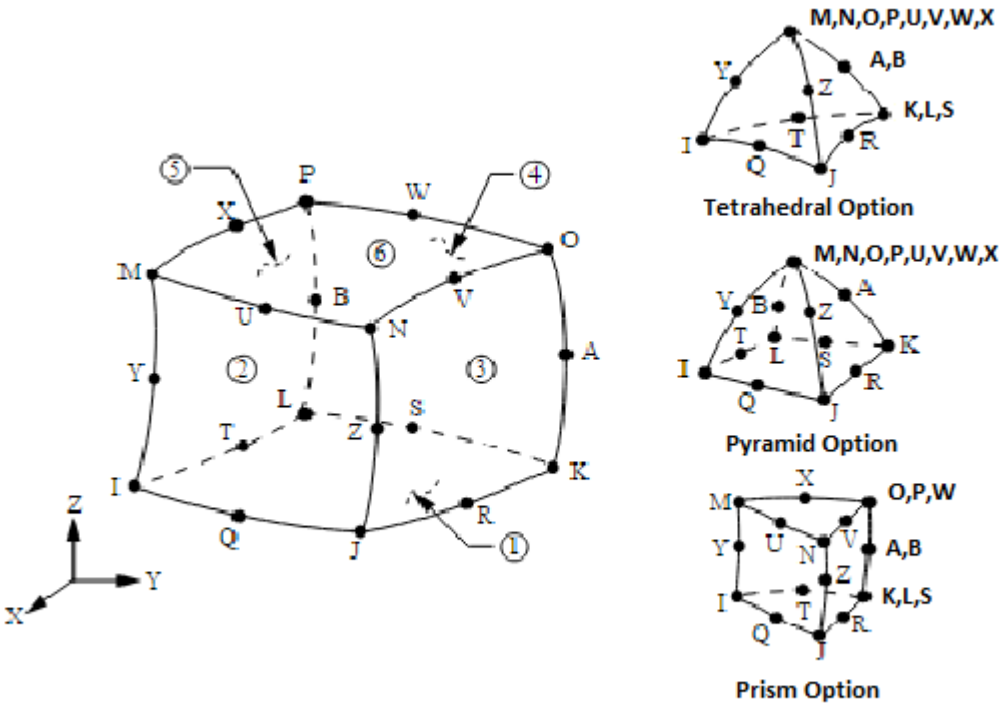

Figure 3-6 Homogeneous structural solid element[52]

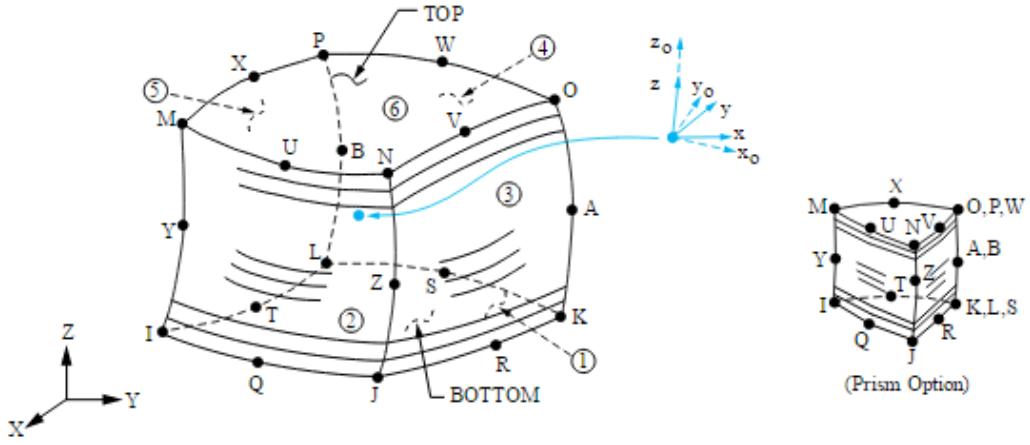

x_o = Element x-axis if ESYS is not supplied.

x = Element x-axis if ESYS is supplied.

Figure 3-7 Layered structural solid elements[52]

For this study, the homogeneous structural solid element is used. Pressures may be input as surface loads on the element faces as shown by the circled numbers on figure 3-6 above. Positive pressure acts on the elements.

3.3.3.2 Conta 174

This element can be applied to a 3D structural contact analysis and is used to represent contact and sliding between 3D target surfaces and the deformable surface defined by this element. It can be used as either a pair based contact or general contact. In the case of a pair based contact which is used in this study, the target surface is determined by the 3D target element TARGE170.The element is found on the surfaces of the solid element with mid-side nodes such as SOLID186 used in this study. It has the same geometric characteristics as the SOLID186 element face with which it is connected. A typical diagram of a CONTA174 element is shown in figure 3-8.

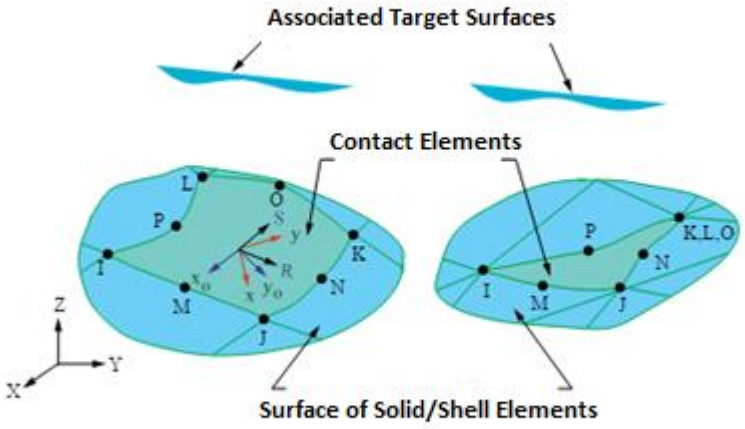

Figure 3-8 Conta174 element

3.3.3.3 Targe170

The targe170 element is usually combined with a contact element. In this study, it is combined with the Conta174 element. It is used to represent the various 3-D target surface for the associated contact element. Target surfaces can either be rigid or flexible. Rigid surface must be represented by a target surface for a rigid-flexible

contact. In the case of a flexible-flexible contact, one of the deformable surfaces must be overlaid by a target surface Complex target shapes can be easily modelled with this element for rigid target surface. In the case of a flexible target, solid, shell or line elements describing the boundary of the deformable target body will be overlaid by the element. In order to create a contact pair. The 3-D contact element (CONTA174) is associated with the target element via a shared real constant set. Ansys only finds contact interaction between surfaces with the same real constant ID. The material ID associated with the contact element is used to specify the interaction properties such as the frictional coefficient. Figure 3-9 shows the geometry of a Targe170 element.

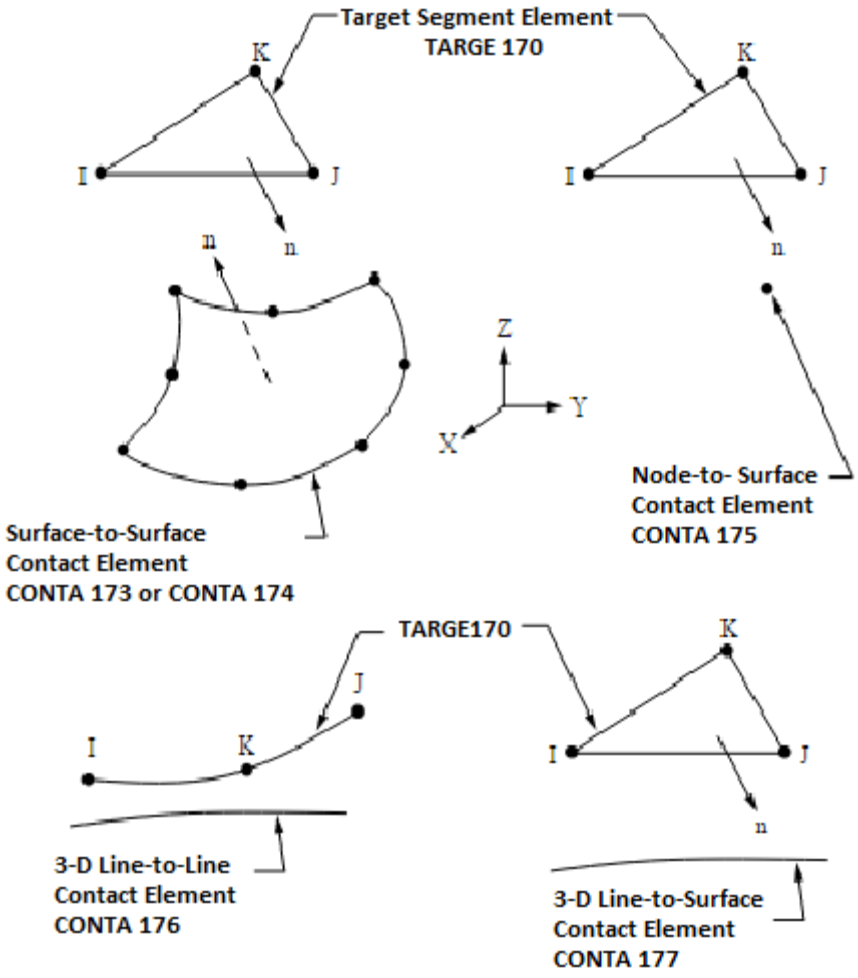

Figure 3-9 Geometry of Targe170 element

3.3.4 Meshing

Meshing is very important as it influences the accurate prediction of the deformation, stresses, and strains in the pipes. In theory, the denser the mesh, the more accurate the result. However, a highly dense mesh can result in a longer computational time and vice-versa. There should be a balance between the mesh density and the computational time. The goal is to find an appropriate mesh with the least computational time, hence, the need for a mesh sensitivity study.

As discussed earlier, all pipe models are subdivided into three regions. Region1 is the region of high mesh density. This is the region of interest as it is the region where the dent is located. The highest stress concentration and strain are also found in this region. There is a need to accurately predict the stresses and strain, hence the need for a high mesh density. The second region (Region 2) is the transition region.it is mediumly dense. There is a need to move from a region of high mesh density to a region of lower density. Region 2 helps to transit from the area of higher mesh density to a lower one. Region 3 has lower mesh density as it is a region of less interest. Although all the eight pipes are subdivided into 3 regions, the density of mesh in each pipe model differs as they have varying pipe thickness. Table 3-3 and 3-4 show the mesh density applied to each pipe model. Before choosing the appropriate mesh density, a mesh sensitivity study was done. The mesh density for the indenters are the same throughout the models as the dimensions for the indenters is constant throughout the models, hence no need to change element size. When meshing, there is a need for a good aspect ratio for the element in order to have good element shape. An element size of 10mm is used to mesh both the dome and bar indenter as this is sufficient enough to mesh them. Table 3-3 and 3-4 also show the element size applied to region 1. For the dome models, region 1 has a division between 80 and 90 with a bias factor of 3. Similarly, for region 2 and 3, the number of divisions varies between 4-10 and 12-26 divisions respectively with no bias. For the bar models, the number of divisions for region 1 is 90 throughout all the models with no bias factor. Region 2 and 3 also have between 5 -13 and 17-34 number of divisions respectively with no bias.

Model	Thickness (mm)	No of division across thickness	No of divisions across region1	Element size at region 1(mm)	No of divisions across region 2	No of divisions across region 3	No of divisions across half circumfer ence	Total number of elements
A	17.399	6	80	3	4	12	50	32016
B	12.944	6	90	2.5	5	17	50	36216
C	10.1131	4	80	3	5	17	50	23316
D	8.0905	4	80	2.5	5	18	50	23516
E	6.4724	3	80	3	5	17	50	18216
F	5.2196	3	80	2.5	6	21	50	18966
G	4.0452	3	80	2	10	27	50	20466
H	3.371	2	80	2	9	26	50	14616

Table 3-3 Meshing for dome models

Model	Thickness (mm)	No of division across thickness	No of divisions across region1	Element size at region 1	No of divisions across region 2	No of divisions across region 3	No of divisions across half circumference	Total number of elements
A	17.399	6	90	3	5	17	50	35346
B	12.944	6	90	2.5	5	17	50	35346
C	10.1131	5	90	2.5	6	18	50	30296
D	8.0905	4	90	2.5	6	17	50	24446
E	6.4724	3	90	3	5	17	50	18696
F	5.2196	3	90	2.5	7	20	50	19446
G	4.0452	3	90	2	8	29	50	20946
H	3.371	3	90	1.5	13	34	50	22446

Table 3-4 meshing for bar models

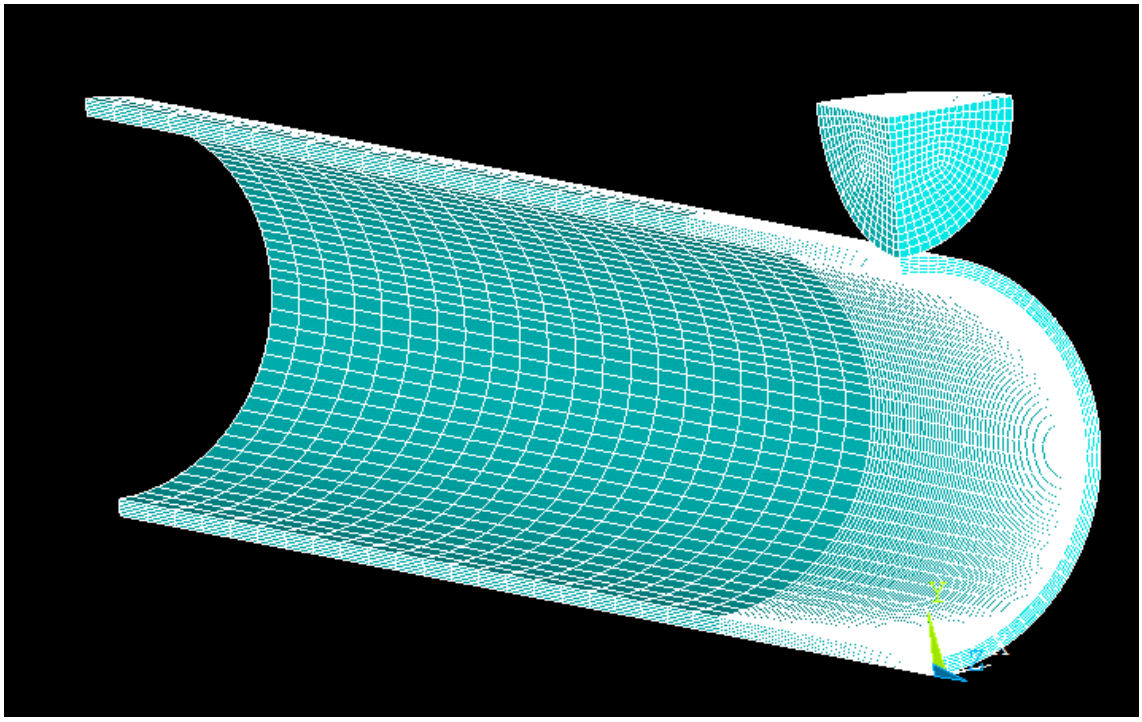

(a)

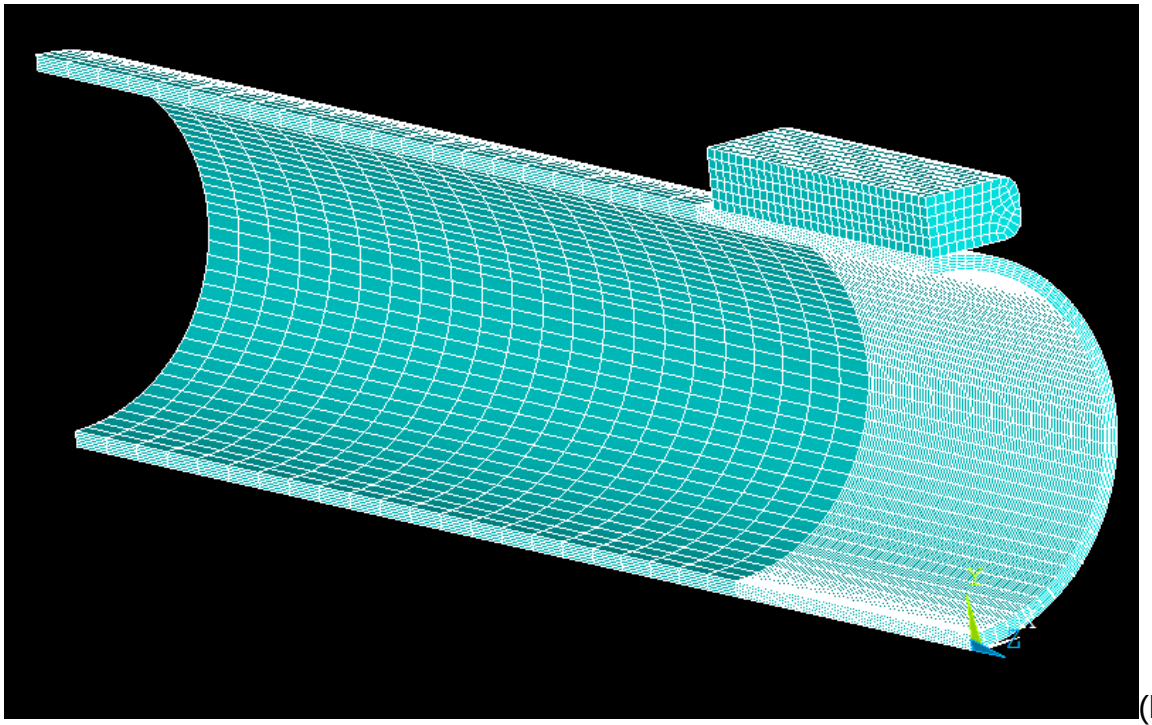

(b)

Figure 3-10 Mesh models for Dome (a) and Bar (b) indenters

3.3.5 Boundary conditions

Getting the boundary conditions right is very important as it affects the calculated result. The boundary conditions are set in a way that it represents how they are constrained and loaded in a real life scenario. The model is constrained on both the side and bottom of the pipe. A remote displacement is applied on the end face of the pipe as indicated by the green arrow in figure 3-11. Here, the X and Y components are free and the Z component is set at zero. This allows the pipe to expand in radial direction when pressurised. Similarly, remote displacement is applied to the bottom line of the pipe, The X and Z components are free but the Y component is set at zero in order not to allow movement in the Y direction during the denting process.

As discussed earlier, a quarter pipe and indenter are modelled considering the symmetry of the pipe and indenter to reduce the computation time. Symmetry boundary condition is put on the sectional faces of the pipe as shown in figure 3-12. The symmetry boundary constraint mirrors all loading and boundary conditions from the quarter pipe to the other parts of the pipe.

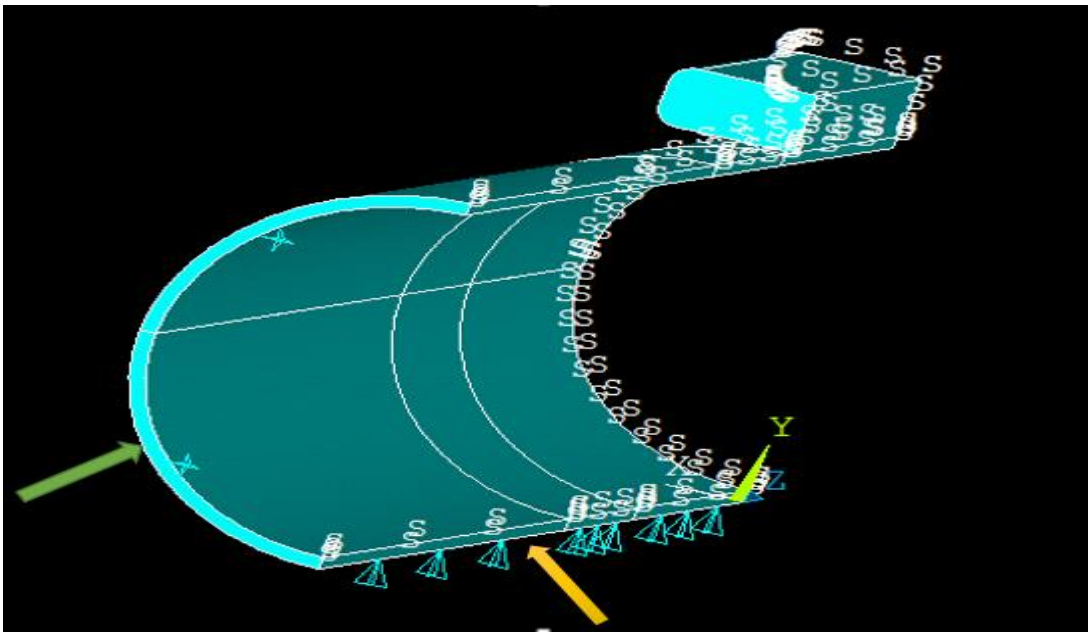

Figure 3-11 Model constraint

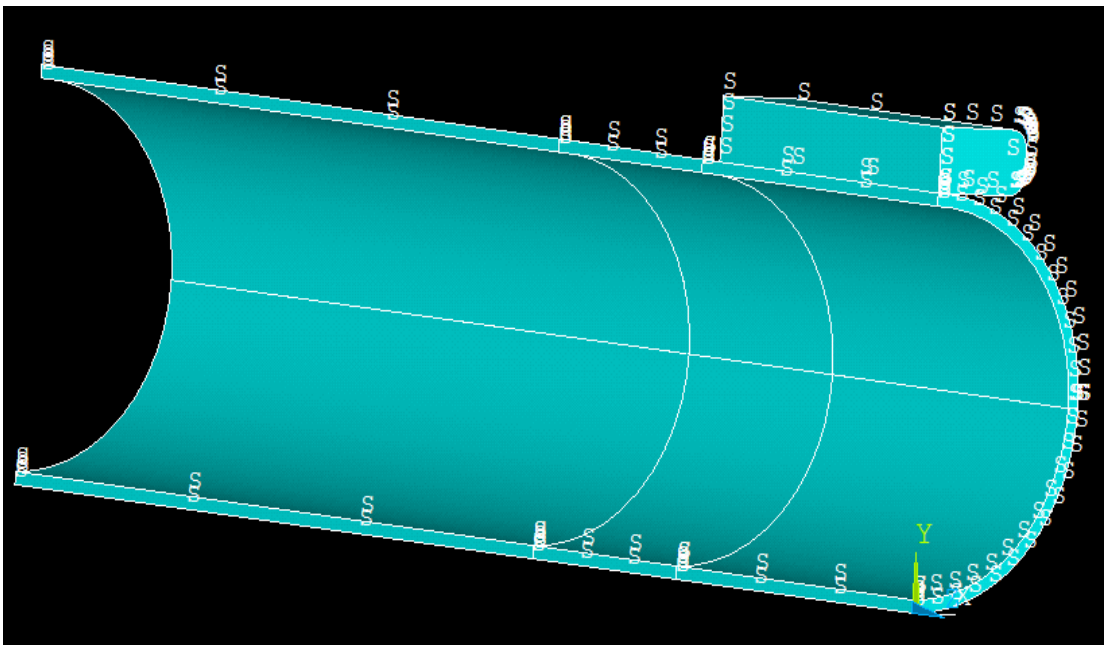

Figure 3-12 Symmetry boundary condition

3.3.6 Contact pair creation

In order to simulate the denting process, a contact pair is created between the indenters and outer pipe surface. Before creation, contact and target nodes are created from the indenter and pipe. The models represent a rigid-flexible contact, therefore the indenter surface represents the target surface and target nodes are shown in Figure 3-13a. Figure 3-13b represents the contact nodes and the contact pair is shown in figure 3-14. The properties of the contact pair include a frictional surface with a coefficient of friction of 0.2, reduced penetration and a symmetric stiffness matrix.

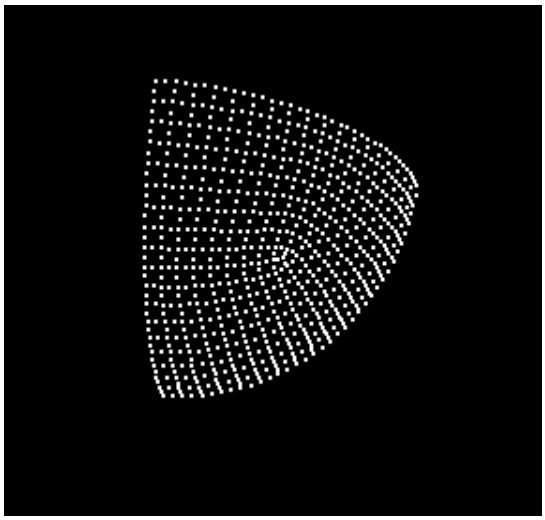

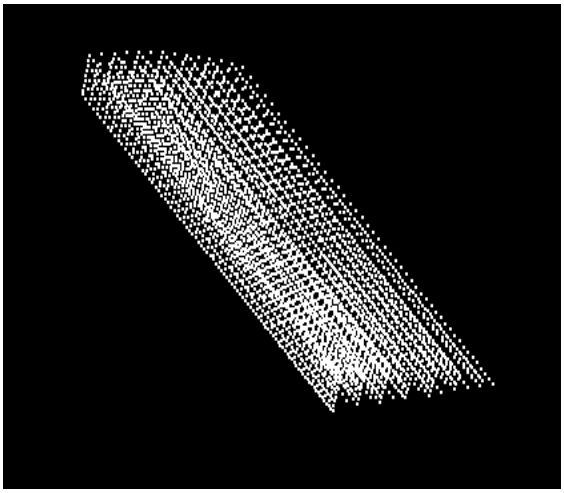

Figure 3-13 Contact and target nodes

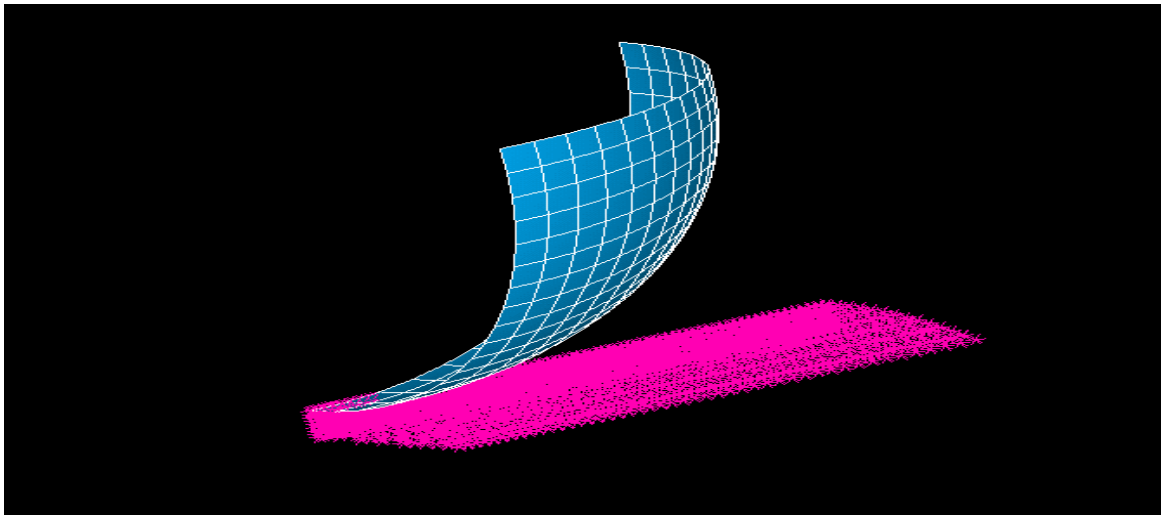

Figure 3-14 Contact pair

3.3.7 Loading

The loading sequence is similar to that of experimental procedures. The aim is to measure the spring back and reround depth after indentation and pressurisation respectively. The model involves several load steps. The first load step is the indentation process, the second load step is the removal of the indenter to allow spring back. Other load steps include pressurising the pipe up to 72%SMYS which is the maximum allowable operating pressure (MAOP). The last load step involves removing the internal pressure to measure the reround depth.

The pipe has both elastic and plastic properties and as a result, a displacement greater than the expected dent depth is applied on the indenter. This is so because, after indentation, the elastic portion of the pipe comes into effect by trying to regain its original position leaving a plastic deformation. This effect is called spring back. The indentation process is done at zero applied pressure which represents construction dents. Figure 3-15 shows a graphical representation of the indentation process (a) and the indenter removal (b)

After the removal of the indenter, an initial pressure of up to 80%MAOP is applied to the inner pipe wall.10 cycles of pressure ranging from 10% to72% SMYS is the then applied afterwards. Finally, the pressure is removed to measure the residual dent depth.

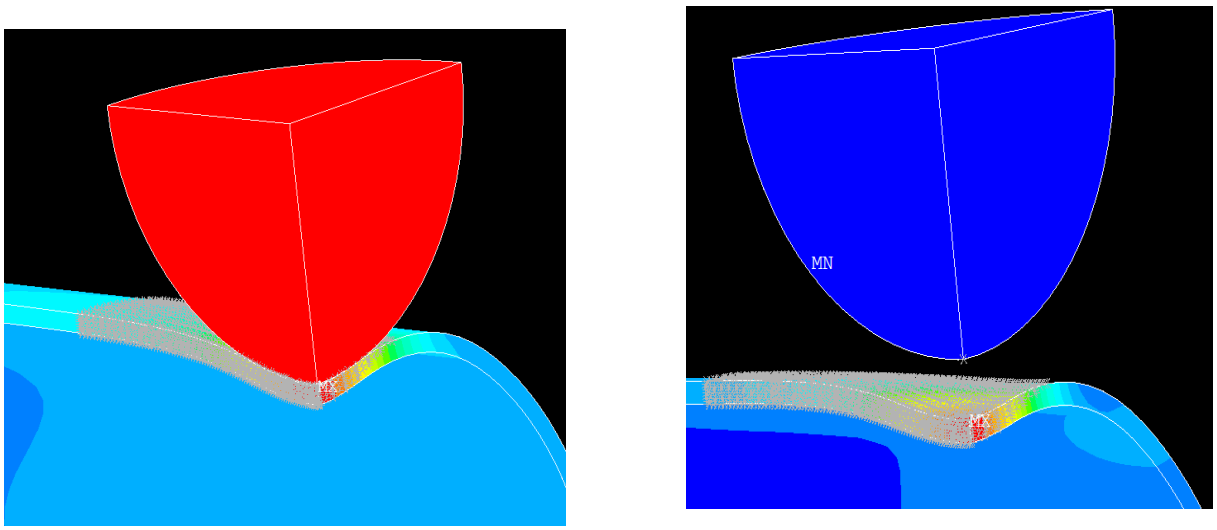

(a) (b)

Figure 3-15 Denting process (a) and indenter removal (b)

3.4 Spring back results

The result from this study has indicated that spring back of the pipe is dependent on some parameters. These parameters can be seen to greatly influence the elastic spring back of the dent. These parameters include pipe geometry, dent geometry, and the material strength.

3.4.1 Effect of pipe geometry on spring back

The graph below shows the effect of pipe geometry on the spring back of dents for an X46 pipe grade. The ratio of the initial depth H_i to the spring back depth H_o(measured depth) is plotted against the different diameter to thickness ratios of the pipes of the same dent depth category. This is done for all the dent depth categories i.e. 2% to 10%. From the graph, it is seen that the ratio of the initial dent depth(H_i) to the spring back depth(H_o) increases as D/t increases. This was also done with other pipe grades and the results are indicating similar trend. The results clearly shows that the diameter to thickness ratio of the pipe is critical in determining the spring back depth of the pipe

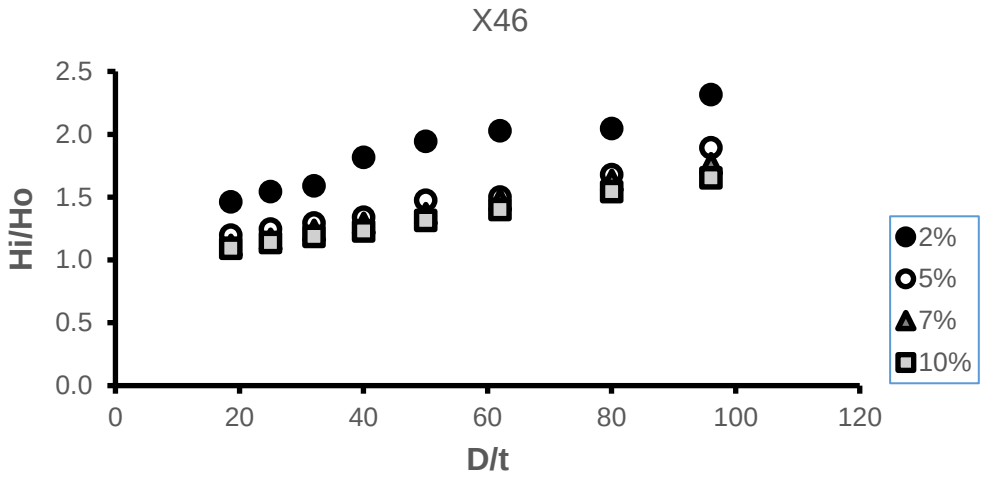

(a)

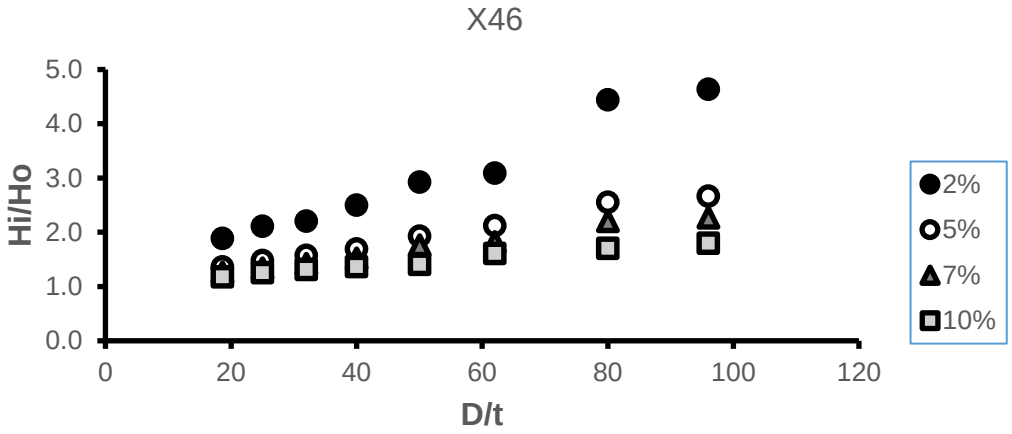

(b)

Figure 3-16 effects of pipe geometry on spring back for a dome (a) and bar (b) X46 pipe grade

3.4.2 Effect of dent geometry on spring back

Figure 3-17 shows the effect of dent geometry on the spring back of the dent. An X100 pipe grade is chosen to illustrate the results. The ratio of the initial dent depth H_i to the spring back depth H_o is plotted against the diameter to thickness ratio (D/t). The two dent types (dome and bar) are compared for the four dent depth categories. From the graph, it is clearly seen that the ratio of the initial to measured dent depths (H_i/H_o) is higher for a bar indenter compared to a dome indenter for the same dent category.

This shows that elastic recovery is higher in shorter dent lengths than the longer dent length. Results also show that the ratio decreases as the dent depth increase. As the dent depths increases further, the ratio of the initial to the measured depths becomes more stable. However smaller dent depths (2% d/D) exhibits the highest ratio. This equally shows that the elastic recovery in pipeline dents is higher in deeper dents compared to shallow dents. The same result was reflected on all of the other pipe grades as seen in appendix A2.

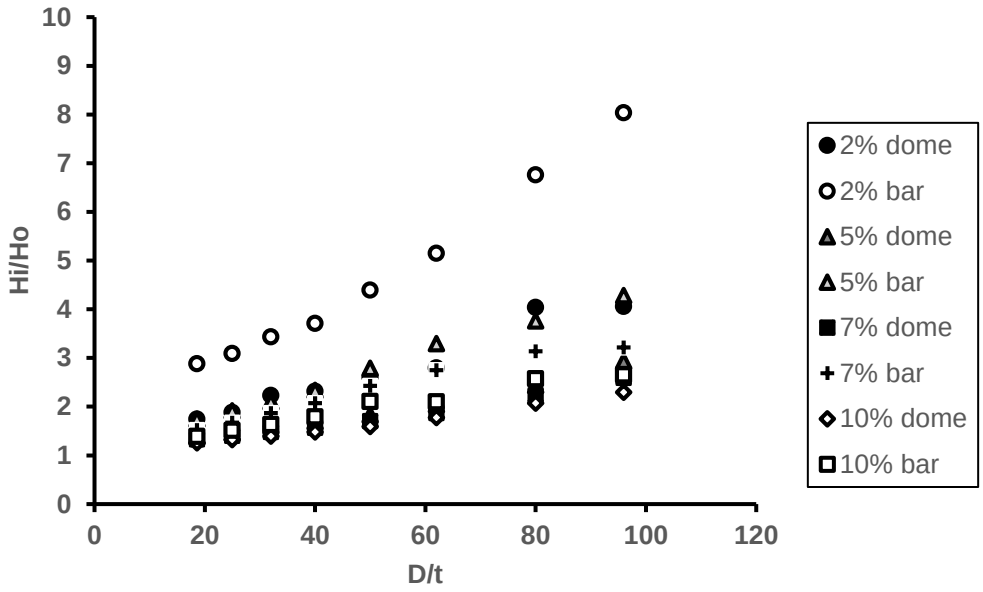

Figure 3-17 effects of dent geometry on spring back for an X100 pipe grade

3.4.3 Effect of pipe grade on spring back

Figure 3-18 illustrates the effect of pipe grade on the spring back of dent for a 10% d/D for both dome and bar models for the four different pipe grades. Both graphs show that the ratio of the initial H_i to the measured H_o increases as the pipe yield strength increases. The lower ratios indicates less elastic recovery, hence, there is a more elastic recovery in higher pipe grades compared to lower pipe grades . This could be attributed to the yield strength of the pipe and the material stiffness. The result is same for both the dome and the bar indenter. Other models are analysed with different dent depths and the result show that they all exhibit similar behaviour as seen in appendix A3.

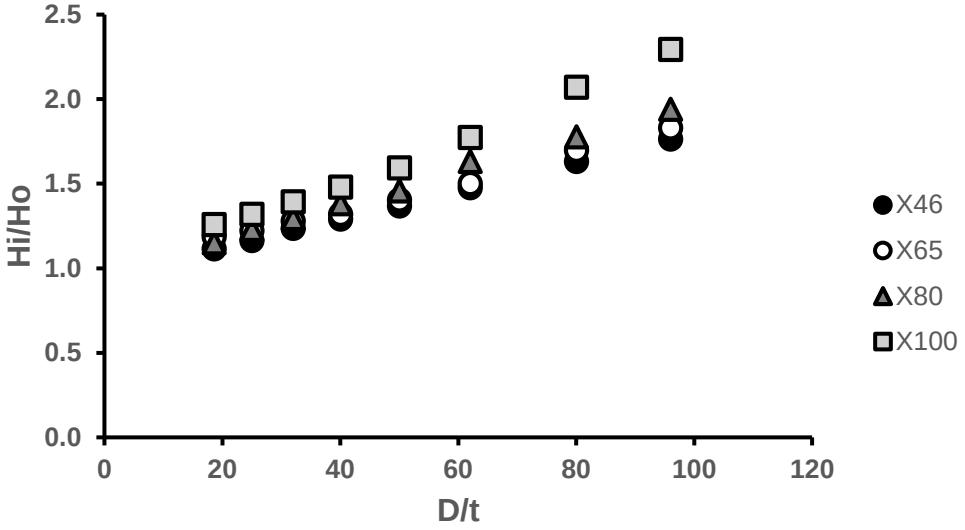

(a)

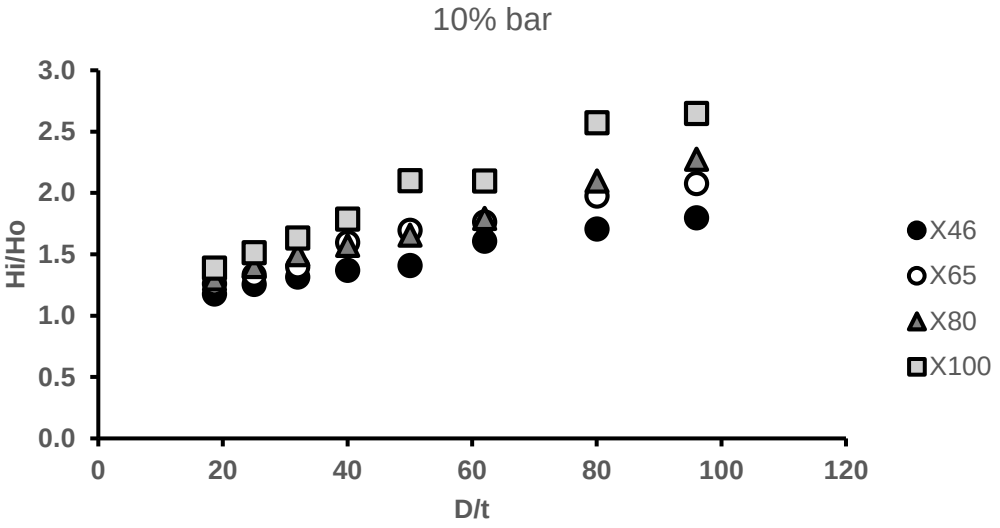

(b)

Figure 3-18 effect of pipe material on spring back for a 10% dome(a) and bar(b) X100 pipe grade

3.5 Result for rerounding

The above results show the responses of the pipe dent during and after indentation. However, when the internal pressure is introduced, rerounding occurs. The dent is further pushed out and the dent depth decreases as the pressure is increased.

3.5.1 Effect of pipe geometry on rerounding

Figure 3-19 shows the influence of pipe geometry on the rerounding of dents for an X46 pipe grade models. It compares the eight different pipe geometries with the four level of dent depth. Results clearly show that the ratio of the measured (H_o) to final dent depth (H_r) increases as the D/t increases for both the dome and bar models. The lower ratios indicates less rerounding and higher ratios indicates more rerounding. This shows that rerounding is higher in pipes with higher D/t and pipes with lower D/t exhibit lesser rerounding. For the dome dent, a linear trend can be seen in the graph. However, for a bar dent, the trend appears linear up to a D/t of 50. From there, the ratio appears to be more stable for all dent depths. This is done for the 3 other pipe grades and the results and trends appear the same for all grades as seen in appendix B1.These results clearly show that rerounding stiffness is higher in pipes with lower D/t compared to pipes with higher D/t.

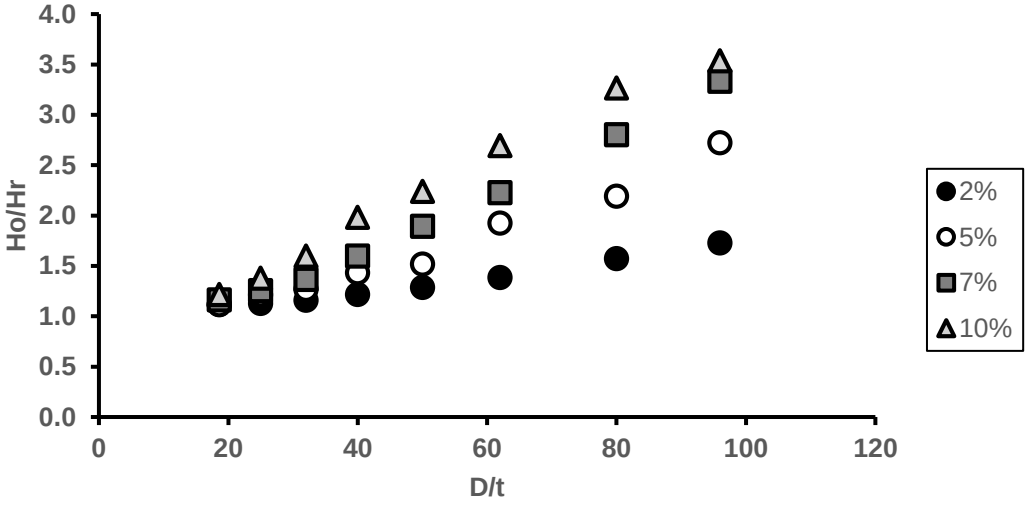

(a)

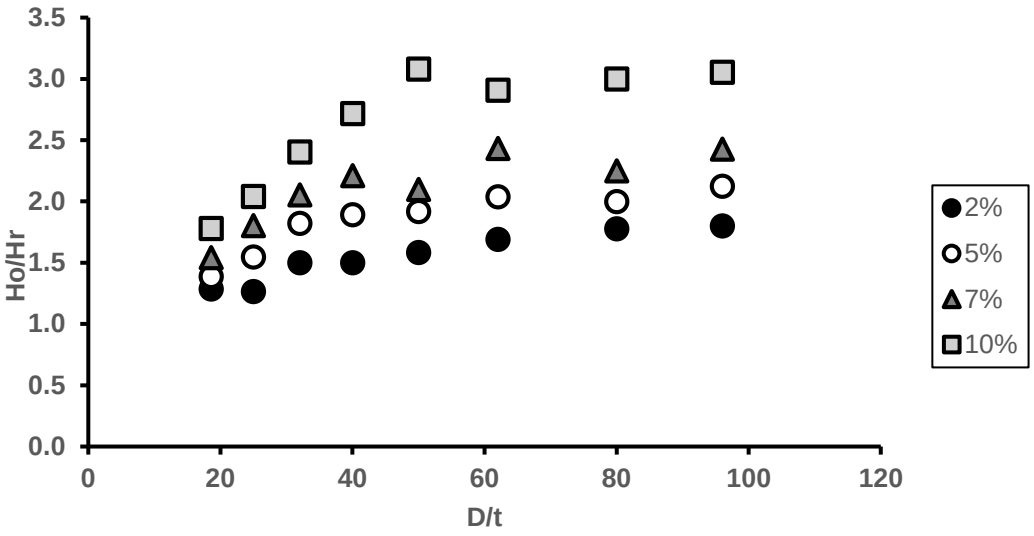

(b)

Figure 3-19 effect of pipe geometry on rerounding for a X46 dome (a) and bar(b) dent

3.5.2 Effect of dent geometry on rerounding

Figure 3-20 shows the result for effect of dent geometry for an X46 pipe grade. Four dent depths are simulated for each of the dent type. This was done on all the pipe geometries. From figure 3-20, it can be seen that the ratio of the measured to the final dent depth H_o/H_r increases as the dent depth increases. Similarly, it can be seen that the ratio is higher for a longitudinal type dent compared to a circumferential type dent up to a D/t of 50, However, as the D/t increases further, the ratio becomes higher in circumferential dent compared to the longitudinal dent. This is so because the circumferential models show a linear pattern as opposed the longitudinal models that exhibit a non-linear pattern. It can also be seen from the results that the margins between the ratios of the measured to the final dent depths are closer in value for smaller D/t. However, as the D/t increases further, the margin between the ratios of each depth increase further.

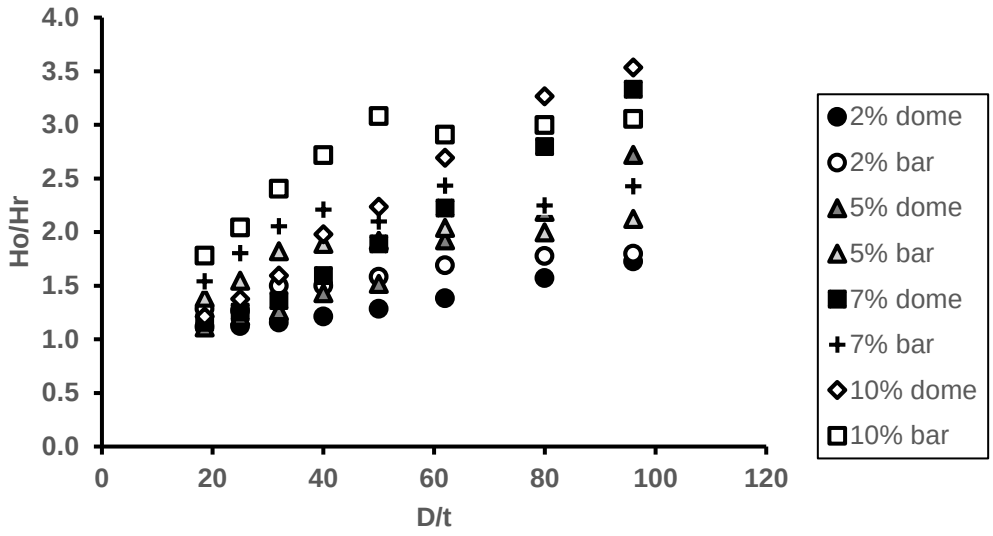

Figure 3-20 effects of dent geometry on rerounding for an X46 pipe grade

3.5.3 Effect of pipe material on rerounding

The result has shown that the pipe grades can influence the reround depth of dent. Figure 3-21 illustrate the effect of pipe material on a 10% dome and an equivalent bar dent for all the pipe grades. It can be seen from the graph that the ratio of the measured to the final dent depth increases as the pipe grade increases for an equivalent D/t. Results show that higher pipe grades experience more rerounding compared to a lower pipe grade for a dome dent. However, the margin between ratios appears very close in the bar dents, though it is clear in some cases that the higher pipe grades have a higher ratio of the measured to final dent depths. Other dent depths (i.e. 2%, 5% and 7%) are analysed and results show similar pattern and trend as seen in appendix B3.

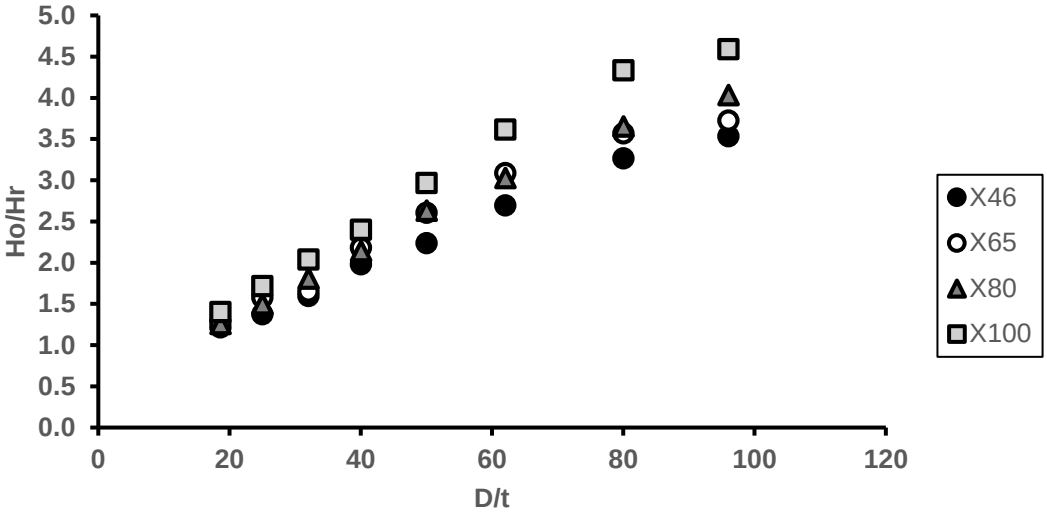

(a)

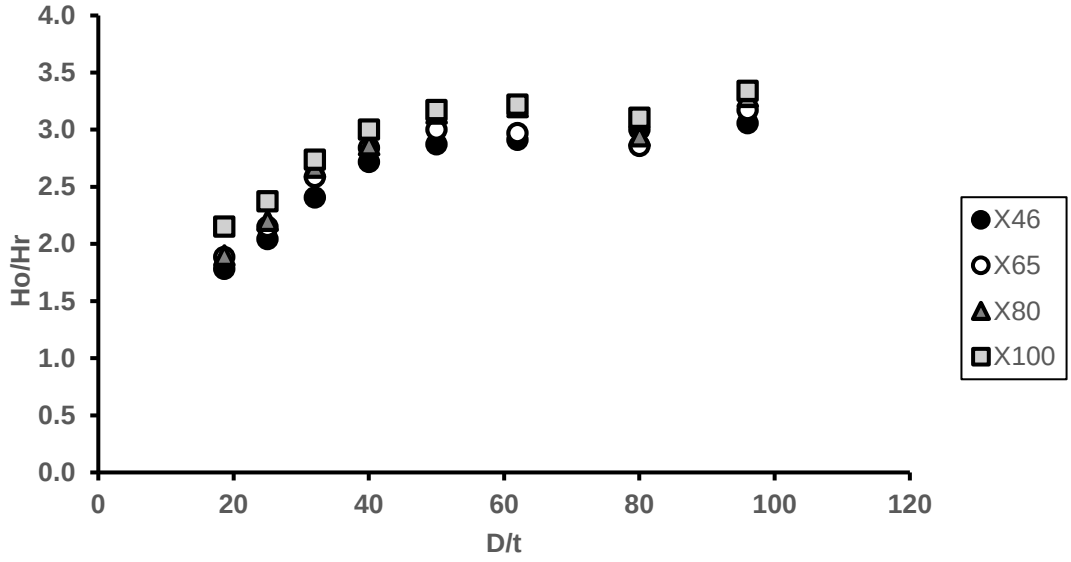

(b)

Figure 3-21 effects of pipe material on rerounding for a 10% dome (a) and bar (b) dent

3.6 Comparison of experimental and finite element model

The finite element models are validated against experiment data. The experimental data used in this study is the experimental project sponsored by American petroleum institute to study the effect of smooth and rock dents on liquid petroleum pipelines [17]. The experiment uses a dome and a bar indenter with pipes of varying diameter and thicknesses. With limited data, plots of the initial dent depth (H_i) versus spring back (H_o) depth and reround depth (H_r) are used to validate the dome model.

3.6.1 Spring back validation

Table 3-5 shows a comparison between experimental results and FEA results. The initial dent depth H_i and spring back depth H_o for a dome indenter are compared for the experimental and FEA result. Though the data are limited, the finite element model gave a good correlation to the experimental model with a maximum percentage error of 17% as seen in table 3-5

Serial No	Experimental[17]			FEA			% error
	H_i(mm)	H_o(mm)	H_i/H_o	H_i(mm)	H_o(mm)	H_i/H_o	
1	6	4.55	1.31	6.2	4	1.55	15
2	12	6.8	1.76	12.2	8	1.52	14
3	18	10.7	1.68	18.1	13	1.39	17
4	18	11.3	1.59	18.1	13.1	1.38	13

Table 3-5 comparison between experimental[17] and FEA results for spring back

3.6.2 Rerounding validation

Table 3-6 similarly shows a comparison between experimental[17] and FEA results. It compares the initial dent depth H_i and reround H_r depth of some selected dataset of the experimental result with FEA results. The table shows a good correlation between the experimental model and finite element model with a maximum percentage error of 16%.

Serial No	Experimental[17]			FEA			% error
	H_o(mm)	H_r(mm)	H_o/H_r	H_o(mm)	H_r(mm)	H_o/H_r	
1	6	1.55	3.8	6.2	1.8	3.4	10.5
2	12	3.8	3.2	12.2	3.2	3.8	16
3	18	3	6	18.1	3	6	0

Table 3-6 comparison between experimental[17] and FEA results for rerounding

3.7 Summary of result and conclusion

The above results have shown how parameters like pipe geometry, dent geometry, and pipe material affect the spring back response and rerounding of the pipe to denting. These parameters are significant in predicting the spring back response and rerounding of the dents. The various conclusions drawn from this study are as follows:

1. The pipe geometry influences both the spring back and reounding of the dent. The ratio of the initial dent depth to the elastic spring back increases with increasing D/t. Similarly, the ratio of the measured dent depth to final dent depth (after pressurisation) increases with increase in the D/t
2. The dent geometry is another critical factor influencing spring back and rerounding. The ratio of the initial dent to the measured dent is higher for longer dents compared to shorter dents. This is an indication that elastic recovery is higher in longer dents compared to shorter dents. However, the ratio of the measured depth to the final depth reduces as the dent depth increases. This clearly shows that deeper dents have less elastic recovery than shallow dents. The ratio of the measured depth to the final depth is equally higher for longer dents compared to short dents. On the contrary, for rerounding, the ratio of the measured to final depths increases as the dent depth increases.
3. Pipe material also influences the spring back and rerounding, results have shown that both the ratio of the initial to the measured depth and the ratio of the measured depth to the final depth increases with increasing pipe grades. This

indicates that pipes with lesser strength exhibit less elastic spring back and rerounding compared to pipes with higher material strength.

CHAPTER 4

FATIGUE ANALYSIS OF PLAIN DENTS USING SN APPROACH

4.1 Introduction

The S-N approach is the most common approach in determining the fatigue life of pipes with dents. The method involves using a published fatigue S-N curve from appropriate design code and accounting for stress concentration in the dents by the use of stress concentration factors (SCF).The cycles to failure can be determined from the curve to determine the fatigue life. The common S-N curves used in dent assessment today are the API RP2A curve 'X' [29], DOE curve B[28], DIN2413 [26] and ASME BPVC Div 2 fatigue life curve.

Many researchers have used the S-N approach to determine the fatigue life of dents in the pipeline. Fowler et al [25] combined experimental and numerical projects by using the API RP2A curve 'X' and the DOE curve B to determine the fatigue life of dented pipelines subjected to cyclic pressure. EPRG also used the S-N approach to calculating the fatigue life of dented pipelines. They made use of the DIN curve as published in DIN 2413 for longitudinally submerged arc welded pipe. The stress concentration factor used in this method was empirically derived. Other research that used the SN approach include, MJ Rosenfeld [3], Alexander and Kiefner [17] and Bood et al [27].

There are many factors that affect the accurate prediction of fatigue life of pipeline with the dents. Fatigue life can be greatly influenced by the presence of some factors which include pipe geometry, dent geometry, pipe material, and the mean pressure. Not all of these parameters were systematically considered in past research. These factors each have their various effects on the accurate prediction of fatigue in pipeline dents. The objectives of this chapter includes

- Improving the understanding of stress distribution in pipelines with dent
- Identifying the most important parameters that influence the distribution and magnitude of stress in the pipeline

- Creating an SCF database for developing ANN based formula in chapter 6

4.2 Current procedure of SN approach

The core of this chapter involves determining the stress concentration factor SCF which is key in determining the fatigue life of dents in the pipeline. As discussed above there are several SN curves that can be used so the question remains which SN curve is most appropriate. Some researchers [1,5] have compared some of these curves with experimental data. Some under-predicted the fatigue lives while some over-predicted it. There is currently no agreement in literature in regards to the most appropriate SN curve to use for application to dent fatigue. Fowler et al [25] in a study concluded that curve X' in the API-RP2A is too conservative for this application and the DOE-B curve gave better correlation.

For the purpose of this study, the DOE-B curve[25] is used. The general equation for this curve is :

$$N = 4.424\ X\ 10^{23}\left(\left[\frac{\Delta\sigma}{\Delta P}\right]\Delta P\right)^{-4} \qquad \textbf{(4-1)}$$

Where ($\Delta\sigma/\Delta p$) is the stress concentration factor based on the finite element work. The SCF values are determined based on the material strength of the pipe, mean pressure, diameter to thickness ratio (D/t) and the spring back depth (H_o). Particular care is taken in determining the type of stress used in the SCF calculation. DOE-B curve proposes that the principal stresses should be used for fatigue calculation. Particular care is also taken in chosen the pressure ranges. Work conducted by API 1156 [17] concluded that pressure cycling can be categorised into three pressure regimes; low range pressure cycle (0-50% MOP), High range pressure cycle (50-100% MOP) and full range pressure cycle (0-100% MOP). The full pressure range is used to calculate the SCF. Once the SCF are calculated using finite element method, the calculated SCFs are used with equation (4-1) to determine the fatigue life of the dent.

4.3 Proposed fatigue analysis procedure

The core of this study is to be able to develop an algorithm for calculating fatigue life of pipeline with dents. The following outlines the steps to be followed to evaluate the fatigue live using the DOE B curve

1. Determine the dent size, pipe diameter and thickness, dent length and pipe grade
2. Determine the mean pressure
3. Determine the stress concentration factor from the Artificial neural network equation (to be discussed in chapter 6)
4. Substitute the calculated SCF into equation 4-1 which is the mathematical representation of the DOE-B curve to calculate the fatigue life

The purpose of this proposed procedure is to present an alternative to the current method for calculating SCF. This method provides an easier way to calculate the SCF without having to run an expensive experimental program and extensive finite element analysis.

4.4 Validation with experimental data

Many researchers have developed empirical and numerical models to estimate the fatigue life of pipeline with dents, some of which are developed for plain dents and some for dents associated with mechanical damages. The methodology involves using published fatigue S-N curves from an appropriate design code and accounting for stress concentration in the dents by the use of stress concentration factors (SCF). Some of these researchers include PRCI [25, 32], EPRG [27], API [17] and ASME [3]. PRCI used the API RP2A curve X', EPRG used the DIN 2413 curve, and API used the ASME BPVC Div. 2 curve. For most experimental data, the cycles to failure are recorded and the stress concentration factor is determined by numerical analysis. The stresses in the pipe cannot be directly measured from the experimental data and as such cannot be directly compared with the FE results. Different researchers use different SN curves and the fatigue lives measured with each curve are different. Some SN Curves are very conservative in predicting the fatigue life while some are less conservative in predicting the fatigue life. BMT fleet [5] in a report compared the various curves used in dent assessment. The demonstration was done using the experimental

data from the joint PRCI/DOT full scale experimental project along with a selected sample of experimental results from two of the other experimental programs for which data was available [17,36]. Table 4-1 below summarises the difference between the experimental data from reference [17, 36] and two of the SN curves as illustrated by BMT fleet [5]. Figure 4-1 also shows the plot comparing the experimental data and the curves

Ref	**Specimen**	**Exp'mtl (cycles)**	**ASME BPVC Div2 (cycles)**	**DOE-B curve (cycles)**
17	3D	89684	82889	87514
	3E	80880	75623	63402
	3F	100943	145906	9887
	5D	62970	89060	195857
	5E	73977	109641	269756
36	UD12A-	31045	78228	393711
	CD24A'-	4687	61801	35506
	UL12A-	15213	171935	644451

Table 4-1 comparison of experimental and estimated fatigue lives for specimens [17,36]

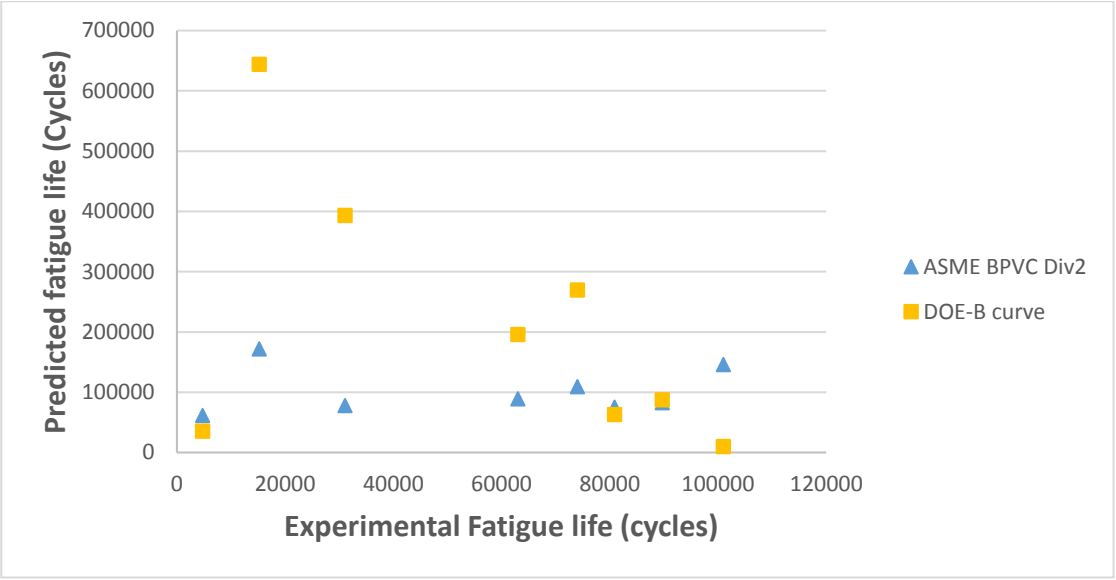

Figure 4-1 comparison of predicted and experimental fatigue lives[17,36]

From figure 4-1, it can be seen that there is a lot of scatter in the results. Some SN curves overestimated the fatigue life while some underestimated it. To validate the FEA results in this study, the strain in the dent was directly compared as it was not possible to directly compare the stresses from the available test data. The test data by Lancaster and Palmer [12] was used for this comparison. In this study, a 100mm diameter pipe with thickness of 1.848mm was dented to a depth of 13% d/D. The strain concentration factor was measured at different levels of pressure at a distance 0.4D along the line of axial symmetry of the dent. The strain concentration factor were computed by dividing the measured strain in the dent by the calculated value of the hoop strain remote from the dent given by the equation below

$$\boldsymbol{\varepsilon_h} = \frac{pD}{2Et} \qquad \textbf{(4-2)}$$

Where ε_h is the hoop strain remote from the dent, p is the pressure, D is the external diameter of the pipe, E is the young's modulus and t is the pipe thickness. A finite element study was done to simulate the experimental procedure and the results were compared with that of experimental data. Table 4-2 shows the comparison between the experimental data and the FE results.

D/t	d/D (%)	σ_y (Mpa)	Pressure(Mpa)	SCF* (exp'mtl)	SCF* (FEA)	% error
54.1	13	163	0.1	10	8.5	15
			2.1	22	19.6	10.9
			6.6	16	15	6.25

SCF*: Strain concentration factor

Table 4-2 comparison of strain concentration factor

The table above shows a good correlation between the experimental data and the FEA results with a maximum percentage error of 15%

4.5 Validation with analytical solution

Rosenfeld [11] in a bid to develop guidelines that enables pipeline operators to assess the severity of dents on the basis of their fatigue life developed an analytical model for calculating the stress range and the fatigue life of plain dents. This project was primarily designed to investigate the re-rounding behaviour of an unconstrained dent in the pipeline. In the course of the project, an equation was developed to estimate the stress range at the peak of the dent. This mathematical model is comprehensive and takes into account the effect of the initial spring back of the dent after formation and the subsequent rerounding effect on the dent depth to estimate the stress range for any pressure cycle operating on the dent. The equation for calculating the stress range is:

$$\Delta\boldsymbol{\sigma} = \left(\frac{\Delta \boldsymbol{p_a D}}{\boldsymbol{2t}}\right)\left(\mathbf{2} + \frac{\mathbf{6}\left(\Delta \boldsymbol{d}^{+} + \Delta \boldsymbol{d}^{-}\right)}{\boldsymbol{t}}\right) \qquad \textbf{(4-3)}$$

where Δp_a = applied cyclic pressure range

D = outer diameter

t = wall thickness

Δd^{+} = outward dent displacement

Δd^{-} = inward dent displacement

The above equation was used to validate the finite element models. Table 4-3 compares the results obtained from the FE models and the analytical equation. It shows some selected models with varying diameter to thickness ratio (D/t), SMYS and dent depth (H_o). All results were recorded at a pressure range of 0-72%SMYS

D/t	σ_y(Mpa)	H_o	Element size(mm)	Δσ(FE) (Mpa)	Δσ(Analytical) (Mpa)[11]	% error
18.6	692	5.8	3	1004	1051.8	4.5
18.6	448	1.6	3	616	648.5	5
18.5	552	5	3	914	820.2	11.4
25	552	7.5	2.5	801	897.3	10.7
40	317	6.7	2.5	520	587.2	11.5
62	317	1.8	2.5	454	497.0	8.7
96	692	3.9	2	791	850	6.9

Table 4-3 comparison of FE and Analytical[11] results

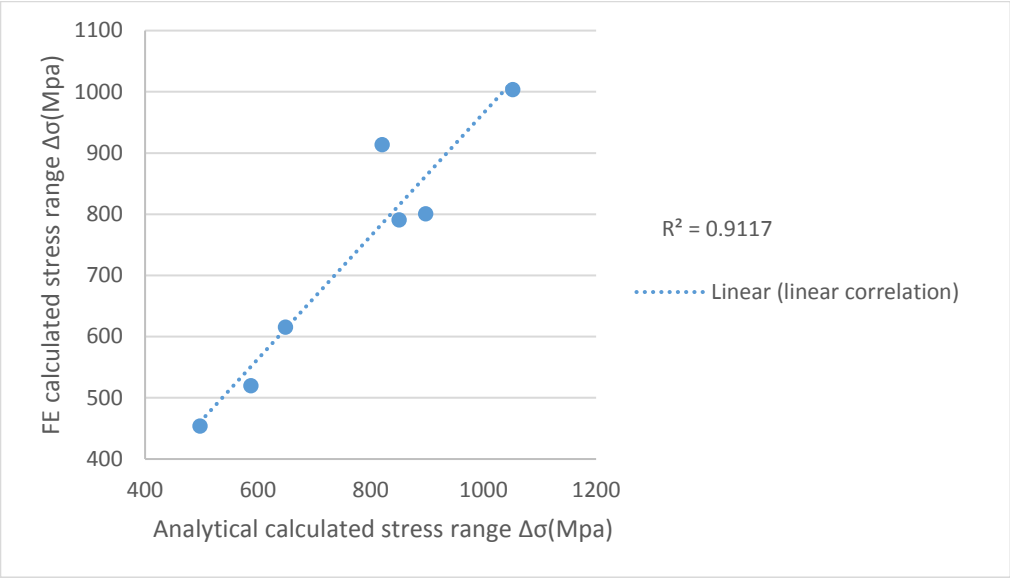

Figure 4-2 linear correlation between FE predicted results and analytical predicted results

From table 4-3, it can be seen that FE results show good correlation with the analytical results with the with the highest percentage error being 11.5%. This shows that the FE models are quite accurate. The element size applied at the dent region to achieve the notch stress is also seen in the table 4-3. Details of the element size and mesh description for all models is seen in section 3.3.4 in chapter 3. Figure 4-2 shows the linear correlation between the FE predicted results and the analytical results, it shows a good correlation with an R-square value of 0.91. This value is an indication of a very good correlation

4.6 Finite element model

The set-up of this analysis is the same as described in chapter 3. A quarter pipe and indenter are modelled taking advantage of the shape of the pipes and indenter. Pipes of different grades and varying D/t ratios are modelled. The pipe grades used are similar to the API 5L seamless line pipe. A sufficient length of the pipe is used to avoid interaction with the boundaries. A 219.07mm diameter dome shaped and a 609.6mm x 304.5mm x 50.8mm bar-shaped indenter is equally used to simulate a circumferential and longitudinal dent. Four different dent depth ranging from 2%d/D to 10%d/D are simulated to investigate the effect of dent geometry. Four different pipe grades(X46, X65, X80 and X100) are analysed to investigate the effect of pipe materials on dent

fatigue. Similarly, eight pipes with a different diameter to thickness ratio D/t ranging from 18-96 are analysed to investigate the effect of pipe geometry as seen in table 3-1. Finally, two ranges of pressure (50% and 72%SMYS) are applied to the pipe to see the effect of pressure range. The material modelling is the same as described in section 3.2.2 in chapter 3. Similarly the elements used is the same as described in section 3.2.3. The meshing procedure and the boundary conditions are the same as described in section 3.2.4 and 3.2.5 respectively.

4.6.1 Loading

In a typical offshore and onshore environment, pipelines may be subjected to other loads such as high temperature and external pressure. To simplify the model, such loads are not accounted for and as such are not included in the loading procedure

The loading took the following sequence;

1. Displacement is applied on the indenter to create a dent with the depth higher than the required dent depth
2. The indenter is removed to allow spring back with the spring back depth being the measured dent depth.
3. Internal pressure is applied to the internal surface of the pipe. An initial pressure of 80% MOP is applied, afterwards, a pressure range of between 0 to 50%SMYS and 72%SMYS is applied
4. The internal pressure is removed to determine reround depth.

It is assumed that dents are introduced at zero pressure. The required dent depths are the ones measured after spring back. It is difficult to get the exact dent depth after spring back; however, the values measured are as close to the required depth. A pressure range of 0 to 50%SMYS and 0 to 72%SMYS is applied on the internal pipe walls and the SCF is computed at 50% and 72%SMYS pressure ranges. The pressure is then removed to see the residual depth.

It is important to know the type of stress to be recorded as different SN curves use a different type of stresses. The notch stresses recorded in this study are the maximum

principal stresses as used in the DOE B-curve [106] and these stresses can be gotten by following the modelling procedure as described in section 3.3 in chapter 3 and by using the correct element size as shown in table 3-3 and 3-4.

4.6.2 Variables considered

As discussed in the literature review, factors that affect the accurate prediction of stress include pipe geometry, which is presented by the diameter to thickness ratio (D/t), the dent length to external diameter ratio (L/D), and dent depth to pipe diameter ratio (d/D), pipe material and pressure range. These variables are used as input data for an artificial neural network which is discussed later in chapter 6. Table 4-3 shows these variables.

D/t	18.6, 25, 32, 40, 50, 62, 80, 90
Pipe grades	X46, X65, X80, X100
H_0(%)	2, 5, 7, 10
Indenter type	Dome and Bar
Pressure(% SMYS)	50, 72

Table 4-4 variables considered

4.6.3 Parametric study

In order to adequately predict the SCF with an artificial neural network, a parametric data sets of the inputs and output variables are needed. This has led to a parametric study which is conducted on a variety of pipe with different pipe materials, dent shape and dent depths to extract the SCF associated with each dent scenario. The SCFs are extracted by dividing the stress range over the pressure range. The SCF can then be used with DOE-B curve to calculate the fatigue life with equation (4-1).

4.7 Results

4.7.1 Stress locations

The results from this study shows that stress concentration factor is influenced by the pipe geometry, dent geometry, pipe material and pressure range. When the pipes are dented, there is an increase in the stress concentration in the dented areas. The location of the maximum stress is found around the dented region and can either be at rim or root of the dent. The location of the maximum stress is dependent on the length to width ratio of the dent. Figures 4-3 and 4-4 represent a typical dent profile of a Dome and bar indenter model for an X46 pipe grade. This profile was measured at the end of the second load step during the loading sequence. The profile for a 2%, 5%, 7% and 10% dent depth are included in the figures. Figures 4-5 and 4-6 show the location of maximum stress for a dome and bar model respectively. The location of the maximum stress is the likely region of the formation of crack, which can propagate and eventually lead to failure. As cyclic pressure is applied on the pipe, the location of the maximum 1st principal stress is dependent on the pipe geometry, dent geometry and pipe material. However, they are all found at the dent region.

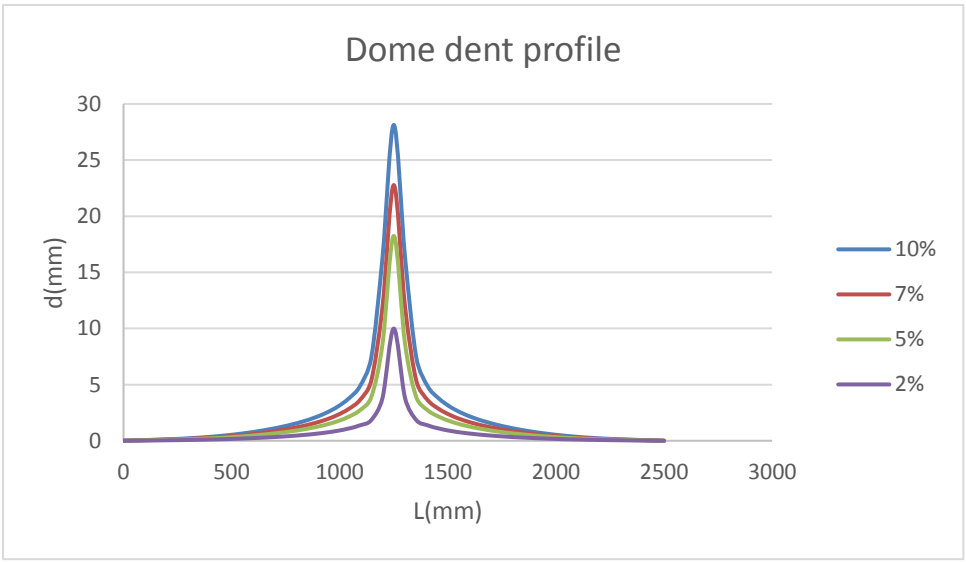

Figure 4-3 Dome dent profile for an X46 pipe grade

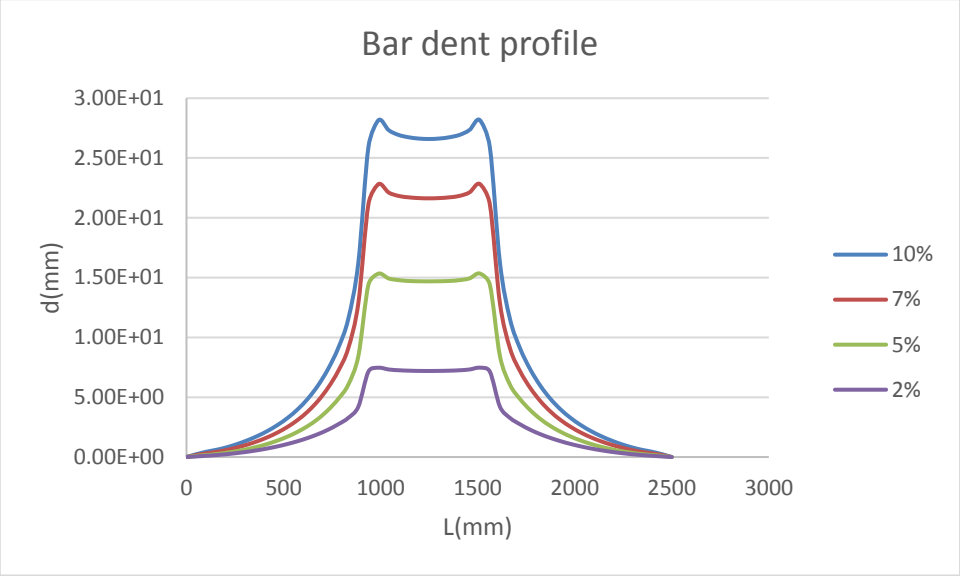

Figure 4-4 Bar dent profile for an X46 pipe grade

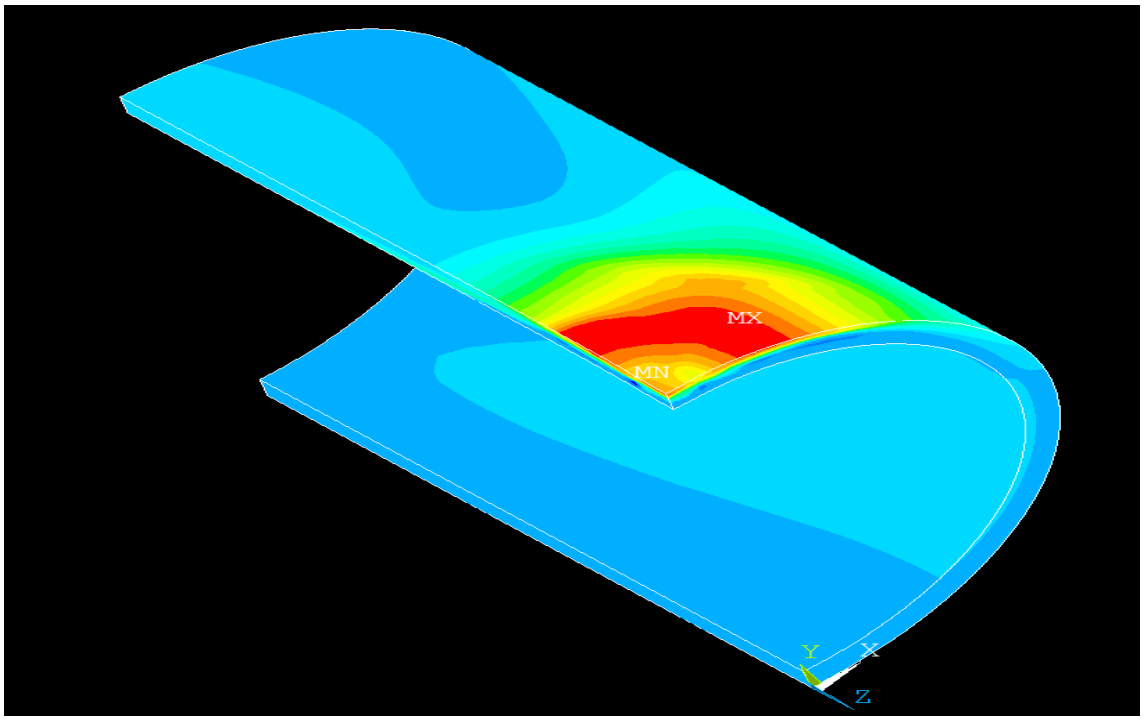

Figure 4-5 maximum stress location for a dome dent

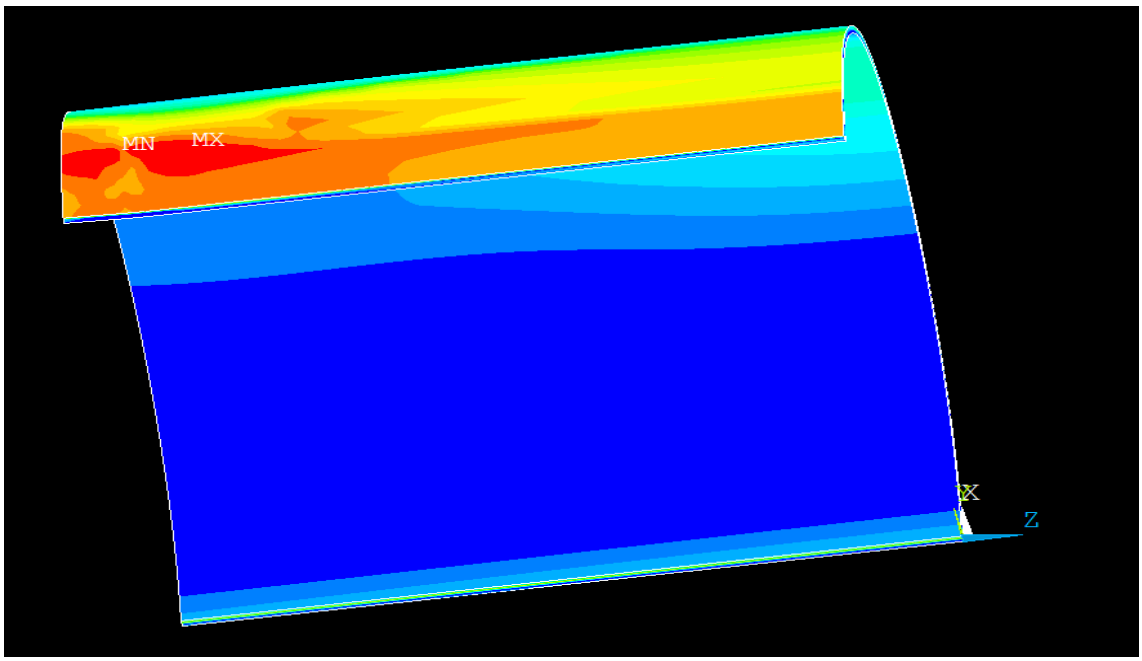

Figure 4-6 Maximum stress location for a bar dent

4.7.2 Effect of pipe geometry on SCF

From past literature, the pipe geometry has been seen to influence the stress concentration factor. Results from this study indicate that stress concentration factor increases with increasing diameter to thickness ratio D/t. This, in turn, will give a corresponding decrease in the fatigue life. Both the dome and bar dent show that Stress concentration factor increased as D/t increased. Figure 4-6 below shows the effect of pipe geometry for a 2% dome and bar indenter models for all pipe grades. It can be seen that the SCF appears to increase in a linear manner for both the bar and dome models for all pipe grades. The SCFs are plotted for both the 50% and 72%SMYS pressure range. Appendix C.1.1 and C.1.2 also shows the effect of pipe geometry on SCF on the other dent depths and they all show similar pattern.

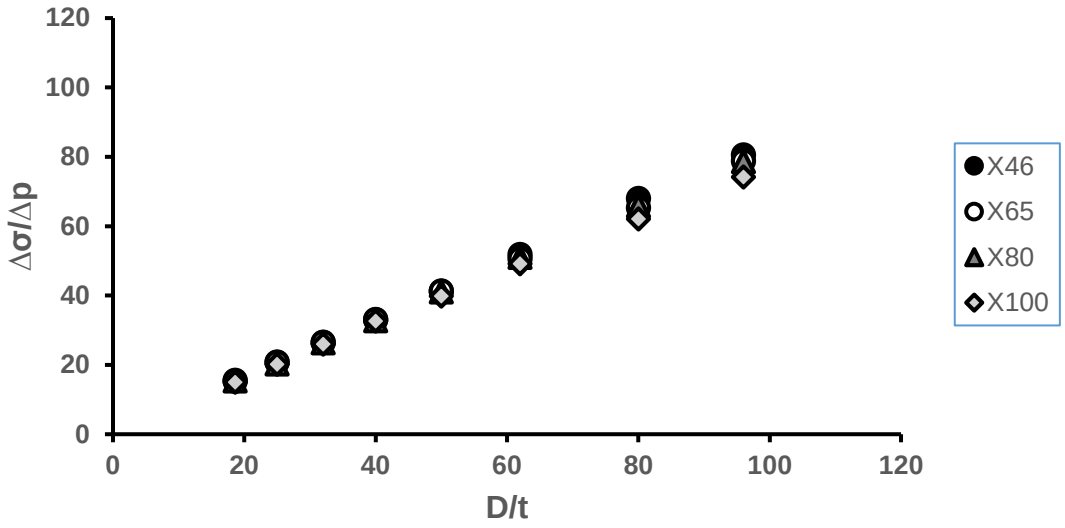

(a) 2% d/D at 72SMYS for dome dent

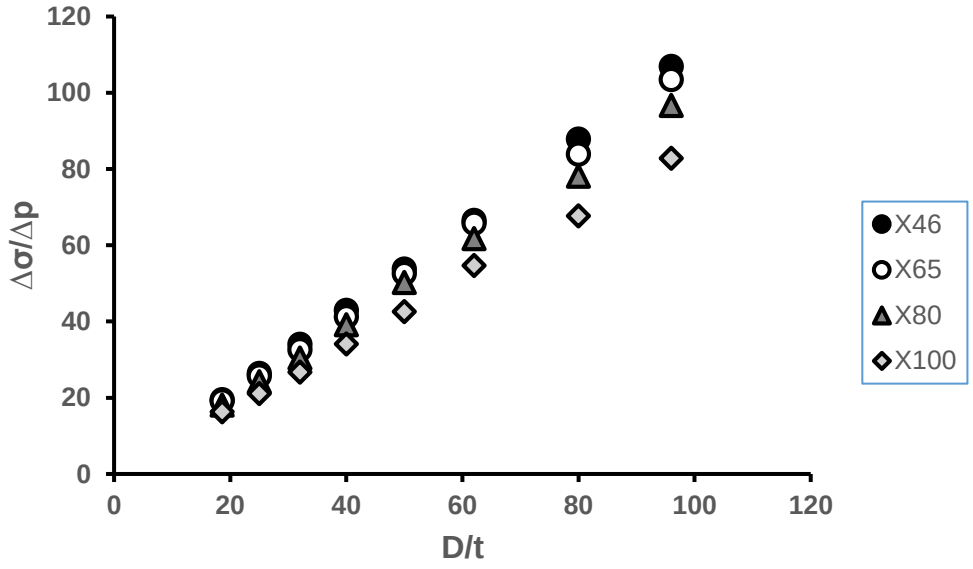

(b) 2%d/D at 50% SMYS for dome dent

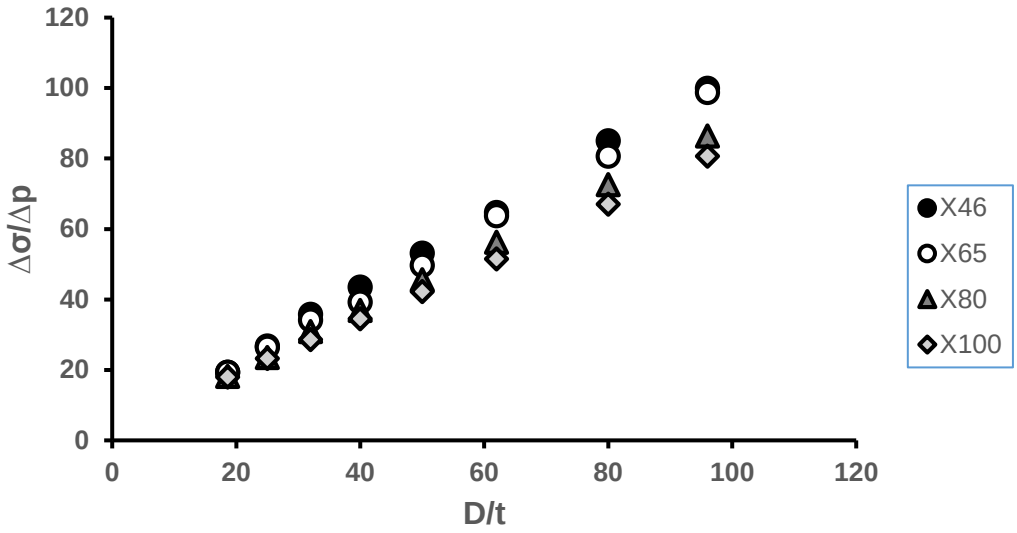

(c) 2% d/D at 50% SMYS for bar dent

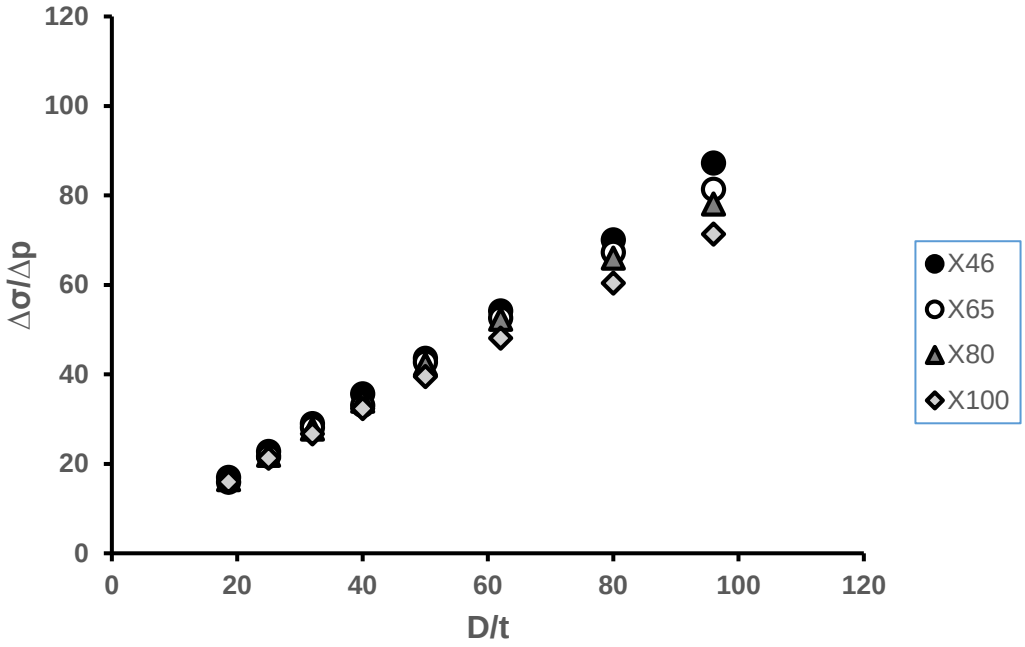

(d) 2% d/D at 72%SMYS for bar dent

Figure 4-7 Effect of pipe geometry and pipe grade on SCF for a 2% dome (a,b) and bar (c,d) indenter models

4.7.3 Effect of pipe grade on SCF

Results from this study show that the material grade in terms of the specified minimum yield stress 'SMYS' can influence the fatigue life of a pipe with dents. Results show that pipes with higher material strengths have higher notch stresses compared to the lower pipe grades. This can be seen in table 4-3 in section 4.5. However, the ratio of the stress range over the pressure range $\Delta\sigma/\Delta p$ appears higher in the lower pipe grades compared to the higher pipe grades as shown figure 4-7. This appears to be true for other dent depth as seen in appendix C.1.1 and C.1.2. This effect could be attributed to the fact that the operating pressure is a function of the pipe's yield strength, diameter and thickness. Pipes with higher strength have higher operating pressure magnitude. When pipes with higher material strengths are pressurised, there is increased rerounding due to the increased pressure magnitude. As a consequence, the dent depth is reduced thereby reducing its susceptibility to higher stress concentration. Observations from the results show that the difference in ratio($\Delta\sigma/\Delta p$) between pipe grades are smaller for pipes with smaller D/t. However, the difference in ratio between pipes grades increases as D/t increases further. It can also be seen from figure 4-7 that the difference is more for 50%SMYS pressure range compared to the 72% SMYS range.

4.7.4 Effect of dent geometry on SCF

The results from this study also show that longitudinal dents exhibit higher SCF compared to a circumferential dent. Figure 4-8 shows plots for both longitudinal and circumferential dents for an 18.6 D/t ratio and X46 pipe grade. The SCFs are plotted against the dent depth. These plots show that SCF is higher in the longitudinal dent of same dent depth. From the result, it is also clear that dent with higher dent depth exhibits higher stress concentration factor. Other pipe grades and D/t show similar pattern.

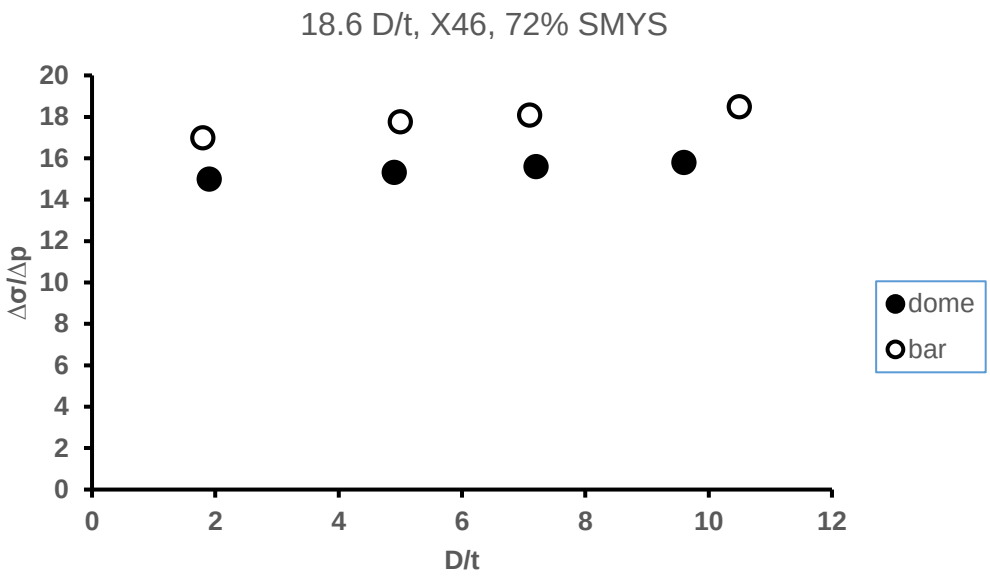

Figure 4-8 Effect of dent geometry

4.7.5 Effect of mean internal pressure

The result shows that internal pressure range can affect stress concentration. An internal pressure range of up to 50% and 72% SMYS is applied to the pipe. Results from this study indicate that SCF is higher in the 50% SMYS pressure range compared to the 72% SMYS pressure range. This is so because, as internal pressure is applied to the pipe wall, the dent begins to reround. As internal pressure is applied further, the dent depth is reduced accordingly, which leads to less stress concentration around the dent region. Figures 4-9 and 4-10 show the effects of pressure range for a 2% dent depth with X46 material for dome and bar dent.

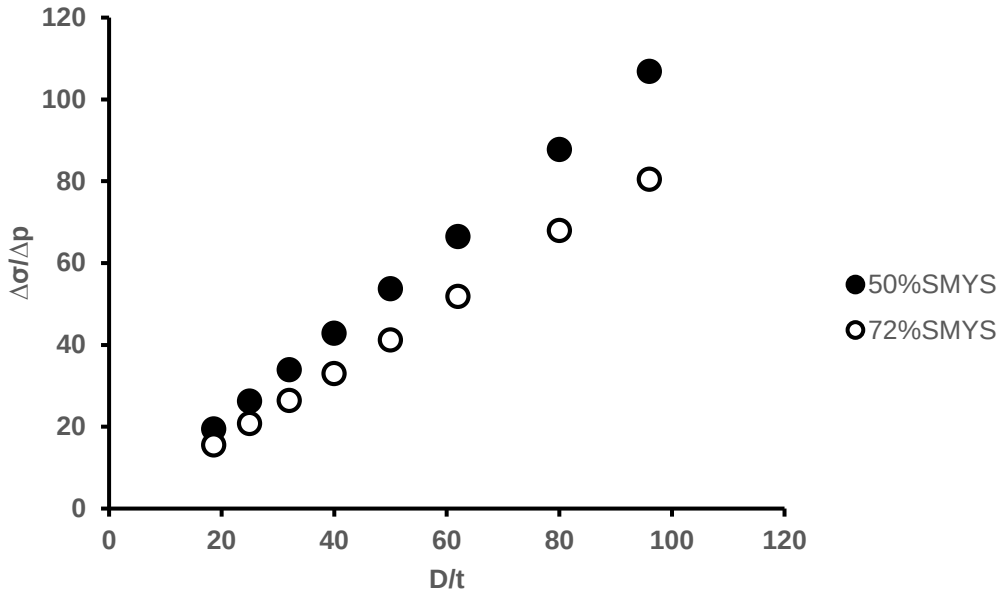

Figure 4-9 Effect of pressure range for a 2% d/D, X46 dome dent

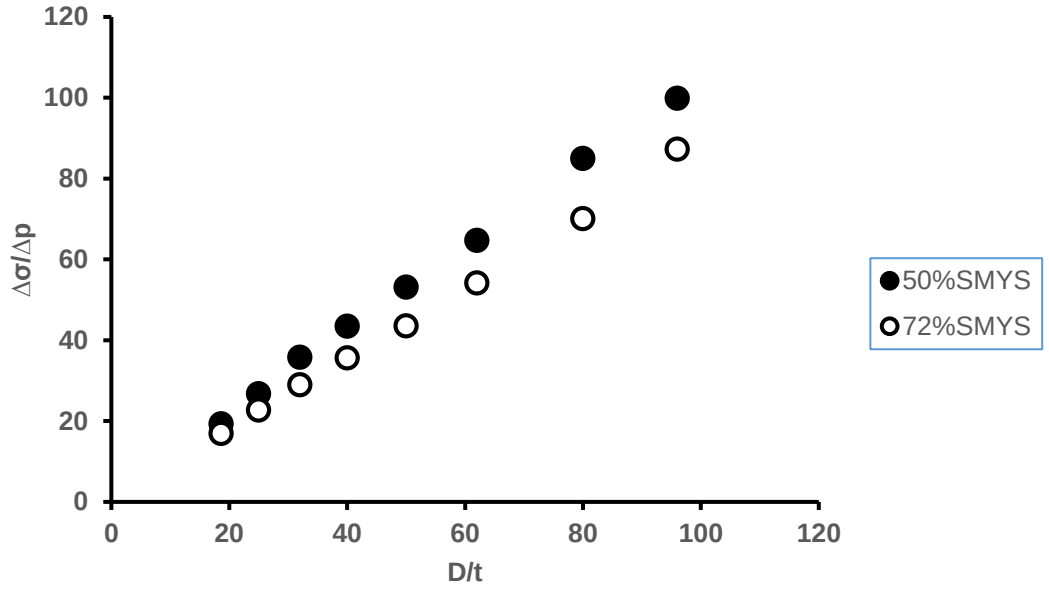

(b)

Figure 4-10 Effect of pressure range for a 2% d/D, X46 bar dent

4.8 Summary of results and conclusions

As part of a study to develop an algorithm for the evaluation of dent severity and fatigue, this study extracts stress concentration factor (SCF) from dome and bar dents under cyclic loading. A parametric range of industry pipes is analysed under various conditions to see its effect on dent severity. Result from this study has shown that

- Pipes with higher material strength exhibit higher notch stresses compared to pipes with lower material strength . However, due to the effect of the operating pressure, the ratio of the stress range to the pressure range($\Delta\sigma/\Delta p$) appears lower for pipes with higher material strength. The results also show that the difference in SCF between pipe grades are smaller for pipes with smaller D/t. However, the difference in SCF between pipes grades increases as D/t increases further. It can also be seen from the result that the difference is more for 50%SMYS pressure range compared to the 72% SMYS range.
- Stress concentration increases with increasing pipe D/t ratio
- Bar dents show higher stress concentration compared to dome dents. It is also clear from the result that dent with higher dent depth exhibit higher stress concentration factor.
- SCF is higher in the 50% SMYS pressure range compared to the 72% SMYS pressure range. This is so because, as internal pressure is applied to the pipe wall, the dent begins to reround. As internal pressure is applied further, the dent depth reduces thereby reducing the stress concentration around the dent region

The results were validated with experimental and analytical solutions and they both show good correlation. This shows that the FE models are quite accurate and can be confidently used to develop the ANN models. The parametric dataset from the FEA study is used to train an artificial neural network using the parameters as input data to predict the SCF.

CHAPTER 5

STRAIN-BASED ASSESSMENT OF PLAIN DENTS

5.1 Introduction

Over the years, dent depth was used by various codes to determine dent severity. These codes include ASME 2006, DNV 2007, EPRG. Recent studies have however shown that dent depth alone is not sufficient enough to determine the severity of dents. The local strain concentration in the pipe has been found to be a better predictor of dent severity. As a result, ASME introduced a strain based assessment in its 2004 version of the ASME B31.8 code. This code also provides a formula for calculating the total strain. This code accepts dent of any depth as long as the associated strain level does not exceed 6%. The ASME code only considers the dent geometric properties. However, just like the stress approach, there is another parameter that may influence the strain in the pipeline. This parameter is the pipe grade . This study will investigate these parameters and how they influence the prediction of strain in the pipeline. The objectives of this chapter include

- Improving the understanding of strain distribution in pipeline with dents
- Identifying the most important parameters which influence the strain in dents
- Creating database for development of an ANN-based formula in chapter 6 using the above parameters

The purpose of this chapter is to create an alternative method to the ASME B31.8 formula for the strain-based assessment. The ANN-formula include the effect of pipe grades as opposed to the ASME formula that only considers the geometric properties of the pipe and dent. The ANN-based formula provides a more comprehensive method for calculating the maximum strain as it looks into all the parameters considered by ASME and also looking at an additional parameter not considered by ASME. The proposed procedure for calculating strain in dent is discussed in chapter 7.

5.2 Current method for estimating strain in pipeline

Strain act on both the longitudinal and circumferential axis of a pipe and each axis have two types of strain acting on them. They include the bending and membrane strain.

According to the ASME B31.8 document [19], the maximum strain in dent is estimated by first evaluating each strain component separately then assuming each component occur coincidentally at the dent apex, the components are combined to give the total strain. The membrane strain is constant throughout the pipe wall but the circumferential strain varies through the pipe wall about the neutral axis. The bending strain in the circumferential direction (ε_1) and the bending and membrane strains in the longitudinal direction (ε_2 and ε_3) are shown in the equations 5-1, 5-2 and 5-3

$$\varepsilon_1 = \left(\frac{t}{2}\right)\left(\frac{1}{R_0} - \frac{1}{R_1}\right) \quad \textbf{(5-1)}$$

$$\varepsilon_2 = -\left(\frac{t}{2}\right)\left(\frac{1}{R_2}\right) \quad \textbf{(5-2)}$$

$$\varepsilon_3 = \left(\frac{1}{2}\right)\left(\frac{d}{L}\right)^2 \quad \textbf{(5-3)}$$

Where t, d and L are the wall thickness, dent depth and dent length in the longitudinal direction respectively; R_o is the radius of curvature of the undeformed pipe surface (equal to half of the nominal pipe outside diameter): R_1 and R_2 are radii of curvature measured in the transverse and longitudinal planes through the dent. This is depicted in figure 5-1.

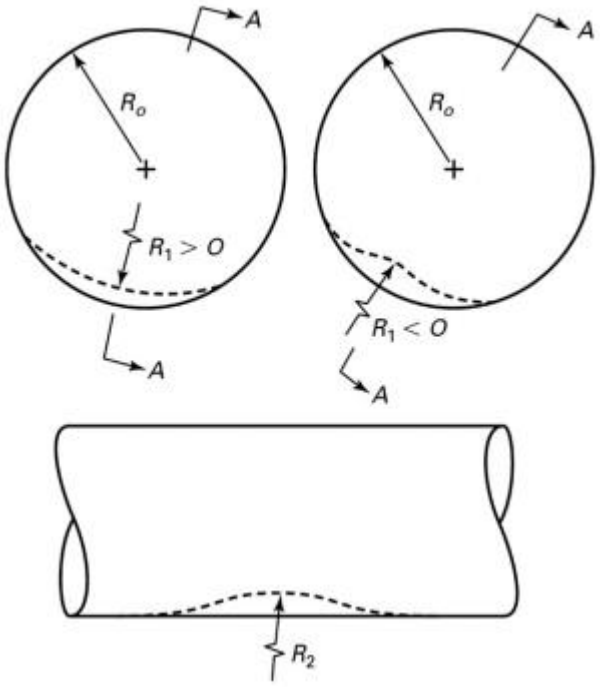

Figure 5-1 Dent geometry [21]

The total combined strain at the inside and outside pipe surface according to ASME B31.8 respectively is given by equation 5-4 and 5-5 respectively

$$\varepsilon_i = [\varepsilon_1^2 - \varepsilon_1(\varepsilon_2 + \varepsilon_3) + (\varepsilon_2 + \varepsilon_3)^2]^{\frac{1}{2}} \quad \textbf{(5-4)}$$

$$\varepsilon_o = [\varepsilon_1^2 - \varepsilon_1(-\varepsilon_2 + \varepsilon_3) + (-\varepsilon_2 + \varepsilon_3)^2]^{\frac{1}{2}} \quad \textbf{(5-5)}$$

In the equation above, it is assumed that the strain combines at the dent apex and therefore is the location for the maximum strain. The overall strain is given by

$$\varepsilon_{max} = Max\{\varepsilon_i, \varepsilon_o\} \quad \textbf{(5-6)}$$

The ASME B31.8 document provides a method for calculating the membrane strain in the longitudinal direction and assumes that the membrane strain in the circumferential direction is negligible.

Noronha Jr et al [21], however, demonstrated that the ASME B31.8 [19] equations were derived considering incorrect plane strain assumptions and therefore their use can lead to inaccurate results. They came up with new equations to calculate the combined strain considering the plain strain state which are :

$$\varepsilon_i = \frac{2}{3}[\varepsilon_1^2 - \varepsilon_1(\varepsilon_2 + \varepsilon_3) + (\varepsilon_2 + \varepsilon_3)^2]^{\frac{1}{2}} \quad \textbf{(5-7)}$$

$$\varepsilon_o = \frac{2}{3}[\varepsilon_1^2 - \varepsilon_1(-\varepsilon_2 + \varepsilon_3) + (-\varepsilon_2 + \varepsilon_3)^2]^{\frac{1}{2}} \quad \textbf{(5-8)}$$

It can be observed that the equations are similar to that of the ASME equations except for the fact that they are preceded by the constant (2/3). They argued that in the derivation of the equations, the assumption that the radial strains are negligible is questionable since it means that at the dent region, the pipe wall is subjected to plane strain state, which is not true. They further went ahead to develop equations for the combined strain considering the radial components with the remit that strains in this region are mainly in the plastic range where the incompressibility condition may be applied. The modified equations considering the radial components are as follows

$$\varepsilon_i = \frac{2}{\sqrt{3}}\sqrt{\varepsilon_1^2 + \varepsilon_1(\varepsilon_2 + \varepsilon_3) + (\varepsilon_2 + \varepsilon_3)^2} \quad \textbf{(5-9)}$$

$$\varepsilon_o = \frac{2}{\sqrt{3}}\sqrt{\varepsilon_1^2 - \varepsilon_1(-\varepsilon_2 + \varepsilon_3) + (-\varepsilon_2 + \varepsilon_3)^2} \quad \textbf{(5-10)}$$

They compared the results from these equations to that of a finite element study and the results were in close agreement as opposed to the ASME equation which under predicted the strain

5.3 Finite Element Model

Similar to the SN approach, a finite element model is used to investigate the effect of parameters like dent geometry, pipe geometry and pipe grade on the strain distribution in dented pipeline.

The model used is similar to the one used for the SN approach. It uses a non-linear elastic-plastic finite element analysis for the study. The geometry creation is the same as described in section 3.2.1 in chapter 3. A quarter model of both the pipe and indenter are modelled taking advantage of the symmetry of the pipe and indenter. The material modelling is also the same as described in section 3.2.2. Four different pipe grades are used to determine the effect of pipe material on the strain distribution in the pipeline. 8 different pipes with varying diameter to thickness ratio D/t as seen in table 3-1 in chapter 3. Two types of indenter (Dome and bar) are used to simulate circumferential and longitudinal dents respectively. The element used and the meshing procedure are the same as described in section 3.2.3 and 3.2.4 respectively. The same element size as described in table 3-3 and 3-3 is used to achieve the notch strain. Similarly, the boundary conditions are the same as described in section 3.2.5.

5.3.1 Loading

The loading took the following sequence

1. The pipe is indented at zero pressure to a depth higher than the expected dent depth. This is done because the pipe is expected to experience some spring back and the spring back depth is the measured dent depth
2. The indenter is then removed to allow spring back in the pipe

It is important to note that the dent depth considered for this assessment is the dent depth after spring back and can be viewed as a construction dent. However an ANN-based formula is given in chapter 6 that gives the relationship between spring back depth and reround depth considering various parameters.

5.3.2 Parametric study

A parametric study is conducted to evaluate the effect of the various parameters including, dent geometry, pipe geometry and pipe grade that might affect the strain prediction in the pipe. As discussed earlier, the current method for assessing strain as

proposed by ASME only considers the geometric properties of the pipe. This study aims to consider the other parameters that might influence the strain in the pipeline. In order to this, 8 different pipes with D/t ranging between 18.5 to 96 are modelled to study the effect of pipe geometry, 4 different dent depths are considered to study the effect of dent geometry on the strains. Similarly, 4 different pipe grades are used to study the effect of pipe material. The table showing these variables is seen in table 4-1 in chapter 4. The parametric data set obtained from this study is eventually used to train an artificial neural network ANN to predict the strain in the pipeline.

5.4 Effect of important variables on strain

As discussed earlier, two components of strain act in a pipeline; the circumferential and longitudinal strain. The total strain in the pipeline is a combination of the two strains. Circumferential, longitudinal. The location of the maximum strain is found at the dent apex for both the dome and bar indenter model as seen in figure 5-2 and 5-3 respectively. The maximum strains recorded are obtained during spring back at zero pressure The strain values extracted from the FEA study are the equivalent Von Mises strain. Table 5-1 and 5-2 shows the total strain recorded at spring back for the dome and bar indenter models respectively. From the results, it is seen that the various parameters affect the strain as is discussed below

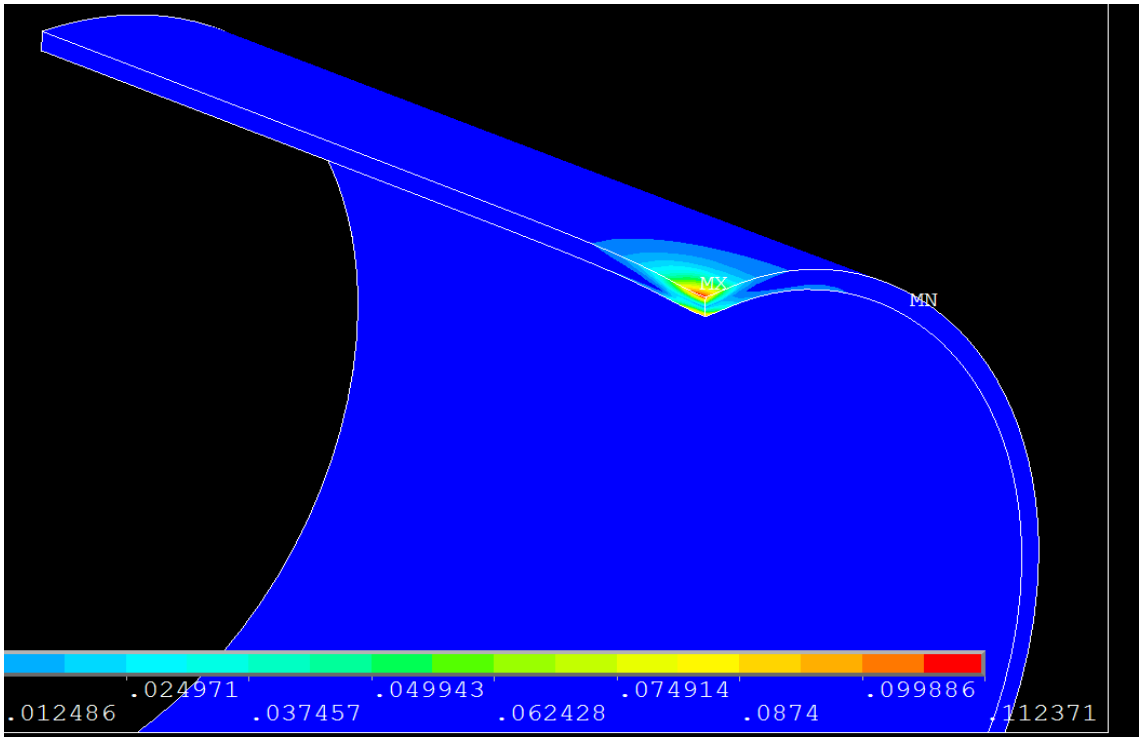

Figure 5-2 Location of maximum strain after spring back for dome indenter

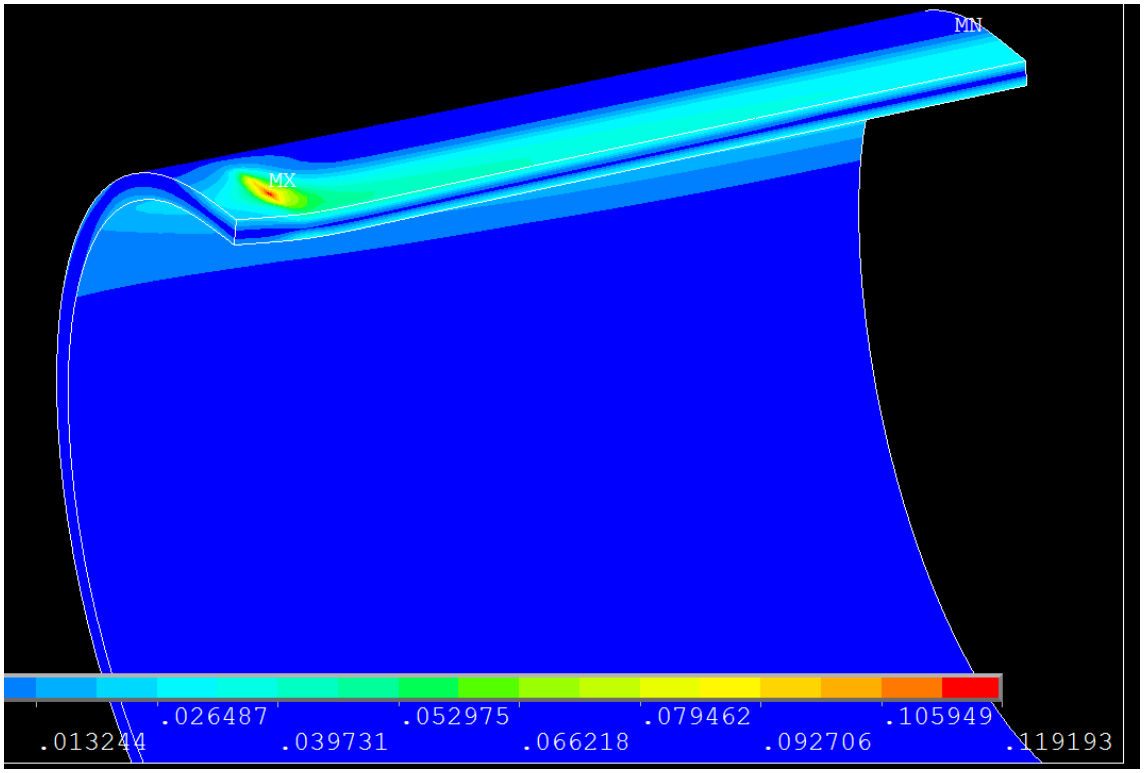

Figure 5-3 Location of maximum strain after spring back for a bar indenter

D/t	X46		X65		X80		X100	
	d/D (%)[1]	Dome	d/D(%)[1]	Dome	d/D(%)[1]	Dome	d/D(%)[1]	Dome
		ε_t		ε_t		ε_t		ε_t
18.6	1.9	0.099	1.6	0.087	2.3	0.118	1.9	0.099
25	1.8	0.1	2	0.11	1.6	0.098	1.8	0.1
32	2.2	0.123	1.8	0.11	2.2	0.13	2.2	0.123
40	1.7	0.11	1.6	0.1	2.2	0.13	1.7	0.11
50	1.8	0.104	1.6	0.098	2.3	0.115	1.8	0.104

62	1.8	0.091	2.5	0.086	2.2	0.092	1.8	0.091
80	2.2	0.069	2.3	0.067	2.6	0.067	2.2	0.069
96	1.9	0.05	2.1	0.049	2.6	0.051	1.9	0.05
18.6	4.9	0.15	4.5	0.15	5	0.16	4.9	0.15
25	5.7	0.186	4.6	0.16	5.4	0.2	5.7	0.186
32	4.3	0.158	4.6	0.147	5	0.18	4.3	0.158
40	5.3	0.14	4.6	0.13	5.1	0.156	5.3	0.14
50	4.4	0.112	4.7	0.104	5.5	0.118	4.4	0.112
62	5	0.091	4.8	0.087	5.8	0.092	5	0.091
80	4.6	0.069	5.5	0.065	5.5	0.066	4.6	0.069
96	4.9	0.049	5.6	0.048	5.6	0.05	4.9	0.049
18.6	7.2	0.185	7	0.18	7.8	0.198	7.2	0.185
25	6.9	0.19	7.3	0.17	7.5	0.21	6.9	0.19
32	6	0.165	6.6	0.15	7.2	0.18	6	0.165
40	6.7	0.14	6.9	0.129	7.4	0.155	6.7	0.14
50	7	0.109	6.6	0.103	7.7	0.117	7	0.109
62	6.9	0.086	6.9	0.083	7.7	0.091	6.9	0.086
80	7	0.064	7	0.063	7.5	0.066	7	0.064
96	7	0.049	7.6	0.049	7.7	0.05	7	0.049
18.6	9.6	0.196	9.1	0.19	10.2	0.21	9.6	0.196
25	9.5	0.19	10.1	0.17	10.8	0.21	9.5	0.19
32	9.1	0.165	9.9	0.15	10.5	0.18	9.1	0.165
40	10.3	0.14	9.6	0.13	10.5	0.157	10.3	0.14
50	9.4	0.109	9.9	0.1	10.8	0.118	9.4	0.109
62	9.7	0.085	10.5	0.082	10.6	0.091	9.7	0.085

80	9.8	0.065	10	0.06	10.6	0.066	9.8	0.065
96	9.9	0.049	10.8	0.049	11.3	0.057	9.9	0.049

[1] Measured dent depth after spring back

Table 5-1 Total strain measured at spring back for dome indenter models

D/t	**X46**		**X65**		**X80**		**X100**	
	d/D (%)[1]	**Bar**	**d/D(%)[1]**	**Bar**	**d/D(%)[1]**	**Bar**	**d/D(%)[1]**	**Bar**
		ε_t		**ε_t**		**ε_t**		**ε_t**
18.6	1.8	0.13	1.9	0.13	1.9	0.15	1.5	0.13
25	1.9	0.095	1.9	0.094	1.8	0.1	1.7	0.095
32	2.1	0.069	1.9	0.069	2	0.077	1.8	0.069
40	2.1	0.049	1.9	0.051	1.9	0.054	2	0.052
50	1.9	0.037	1.8	0.04	1.9	0.04	1.9	0.04
62	2.2	0.034	1.9	0.036	2.1	0.03	1.8	0.032
80	1.6	0.025	2.1	0.029	2.1	0.028	1.6	0.024
96	1.8	0.024	2.4	0.024	1.9	0.023	1.5	0.019
18.6	5	0.245	4.7	0.208	5.3	0.27	4.6	0.024
25	4.8	0.157	4.7	0.145	5	0.175	5	0.16
32	5.1	0.11	4.8	0.104	5	0.117	5.3	0.109
40	5.3	0.077	4.8	0.072	4.9	0.075	5.3	0.068
50	4.8	0.054	4.7	0.05	5.4	0.054	5.1	0.05
62	5.1	0.041	5.3	0.047	6	0.062	4.5	0.045
80	4.6	0.031	5.3	0.05	5.6	0.067	4.6	0.05
96	5.1	0.036	5.2	0.047	5.9	0.062	4.4	0.046
18.6	7.1	0.27	6.5	0.22	7.3	0.029	7.1	0.0275

25	7.4	0.178	6.7	0.159	7	0.188	7.2	0.175
32	7.4	0.12	6.2	0.11	6.9	0.123	7.1	0.11
40	7.3	0.081	7	0.076	7.5	0.08	7	0.072
50	6.3	0.057	7.2	0.072	7.8	0.094	7	0.084
62	7.3	0.056	6.8	0.061	7.3	0.07	6.3	0.064
80	6.3	0.049	7.7	0.084	6.7	0.085	6.3	0.082
96	6.8	0.05	7.5	0.067	7.6	0.076	7.3	0.068
18.6	10.5	0.029	9.8	0.24	9.5	0.31	10	0.29
25	9.6	0.18	10.2	0.167	9.7	0.19	10.2	0.19
32	10.1	0.13	10.6	0.14	9.9	0.16	10.4	0.167
40	10.6	0.103	8.7	0.086	10.6	0.13	10.2	0.129
50	11.4	0.11	9.1	0.097	11	0.136	9.7	0.118
62	9.6	0.076	9.8	0.09	11.2	0.122	10.3	0.11
80	10.5	0.106	10	0.11	10.6	0.13	9	0.114
96	11	0.076	11	0.08	11.4	0.09	10.5	0.084

[1] Measured dent depth after spring back

Table 5-2 Total strain measured at spring back for bar indenter models

5.4.1 Effect of pipe geometry on strain

Pipe geometry is one of the parameters that influence the strain concentration in the pipeline. From the result, it is seen that the circumferential, longitudinal and total strain reduces as the diameter to thickness ratio (D/t) of the pipe increases. Figure 5-4 and 5-5 below represents a graph showing the effect of the diameter to thickness ratio (D/t) of the pipe on strain for a dome and bar indenter model respectively. It shows the result of a 5% dent depth for an equivalent pipe grade. From Figure 5-4, it is seen that the circumferential strain is higher than the longitudinal strain and decreases as the D/t increases. However, figure 5-5 shows the opposite with the longitudinal strain higher than the circumferential strain. A plot of other dent depths can be seen in appendix D

and they all show similar trend. From this results, one can conclude that circumferential dents have a higher strain in the circumferential direction and the longitudinal dents have a higher strain in the longitudinal direction compared to the circumferential direction. A particular observation from the results shows that the difference between the circumferential and longitudinal strain is higher in circumferential dent compared to that of the longitudinal dent.

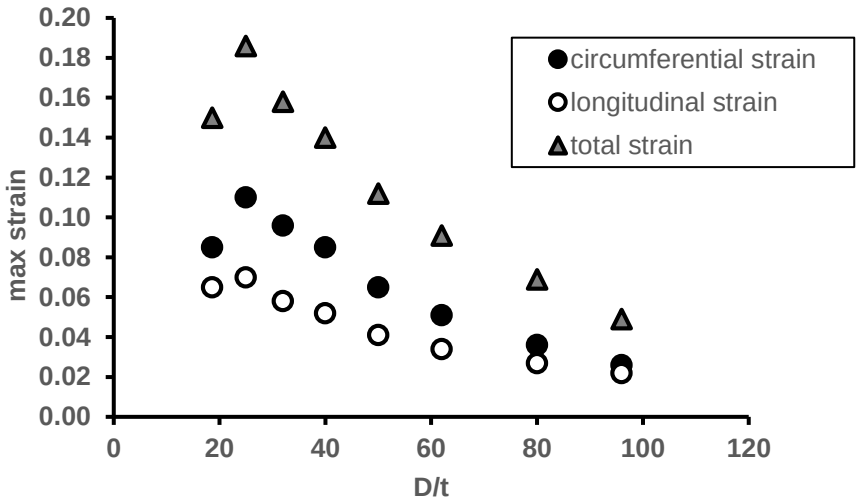

Figure 5-4 Effect of pipe geometry on strain for a 5% dome dent for X46 pipe grade

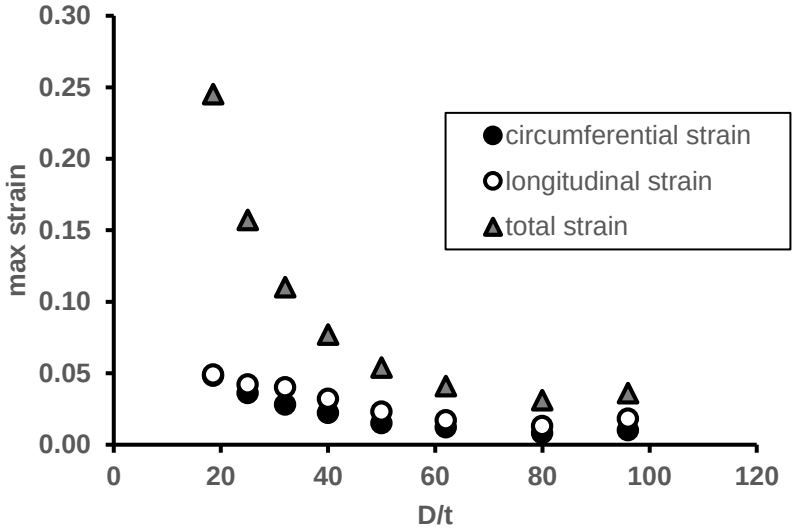

Figure 5-5 Effect of pipe geometry on strain for a 5% bar dent for X46 pipe grade

5.4.2 Effect of dent geometry on strain

The dent orientation and dent depths are some of the parameters that affect the strains in the pipeline. This section investigates how these parameters influence the strain distribution. The result from the study has shown that the total strain in a dent is higher in a longitudinal dent compared to a circumferential dent. Figure 5-6 shows a graph of strain versus the dent depth for both the longitudinal and circumferential dent for an 18.5 D/t. It clearly shows the longitudinal dent at the top of the graph indicating higher strain. Similarly, an increase in dent depth gives a corresponding increase in the strain for both dent models. The dent geometry also determines the location of the maximum strain. Though the maximum strain is situated at the apex of the dent depth as seen in figure 5-2 and 5-3, the location of the strains are different for each dent type. The maximum strain is located at the bottom of the dent and is centralised for a dome dent, however, the bar dent has the maximum strain located at the far end of the dent.

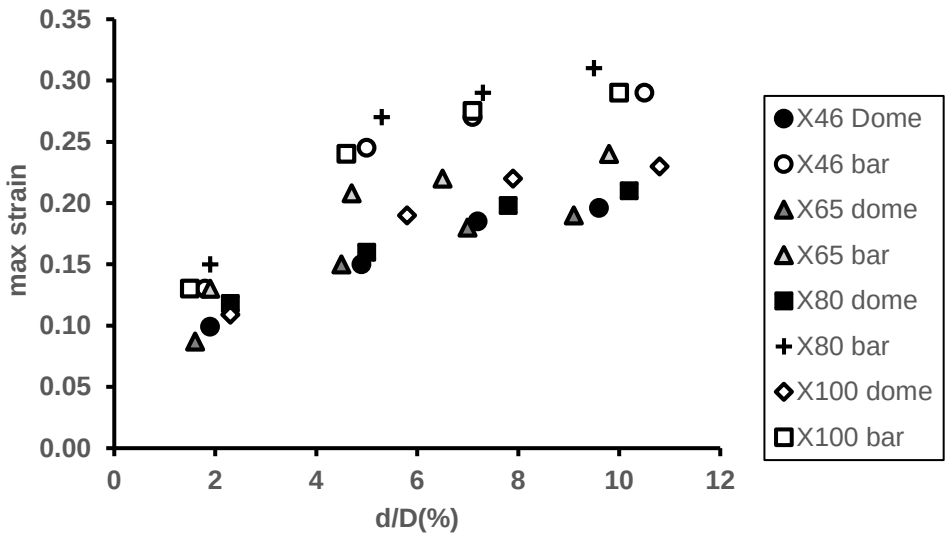

Figure 5-6 Effect of dent geometry on strain for an 18.6 D/t for all dent depths and pipe grades

5.4.3 Effect of pipe grades on strains

As discussed earlier in the chapter, the ASME method for evaluating strains in dent only considers the geometric properties of the pipe dent. Studies have shown that other parameters like pipe grades can influence the strain prediction in the pipe. This study investigates the effect of the pipe grades on the magnitude and distribution of the strains in the pipeline. Figure 5-7 and 5-8 below shows a plot of the strain versus the D/t for a 10% dent depth for the four different pipe grades. Figure 5-7 represents plots for the dome indenter and figure 5-8 represents plots for the bar indenter. From figure 5-7, a noticeable difference is seen in the strain magnitude up until a D/t of 50. Though it does not follow a definite pattern, the higher pipe grades appear to have higher strain. As the D/t increases further, the difference in the strain are quite small. Other dent depth appears to follow the same pattern for the dome dent as seen in appendix D.2. Figure 5-8, however, doesn't follow a particular pattern. Some of the dent depths as shown in appendix D.2 shows a minimal difference in the strain for all pipe grades. One of the parameters that might cause the irregular pattern observed here is the dent depth, the measured dent for each pipe grades are different, and the dent depth has been observed to be a critical factor in influencing the strain.

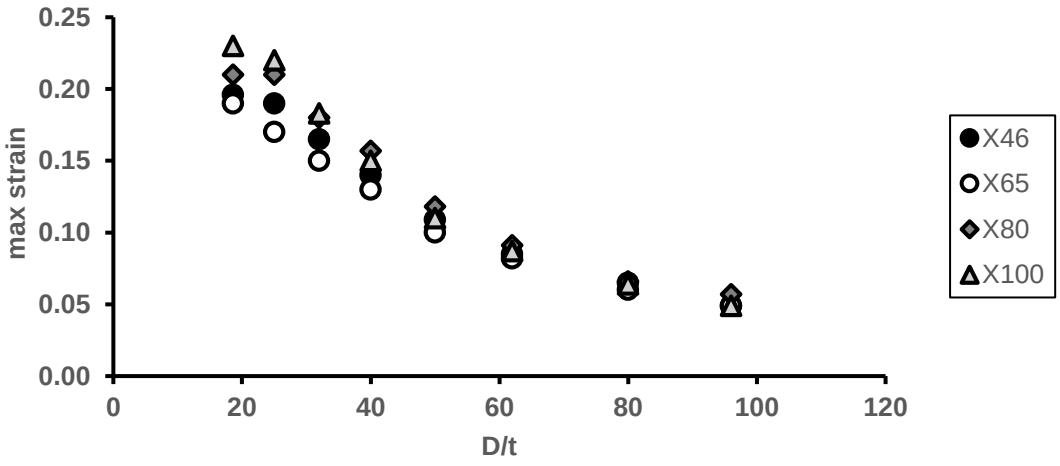

Figure 5-7 Effect of pipe grade on strain for a 10% dome dent

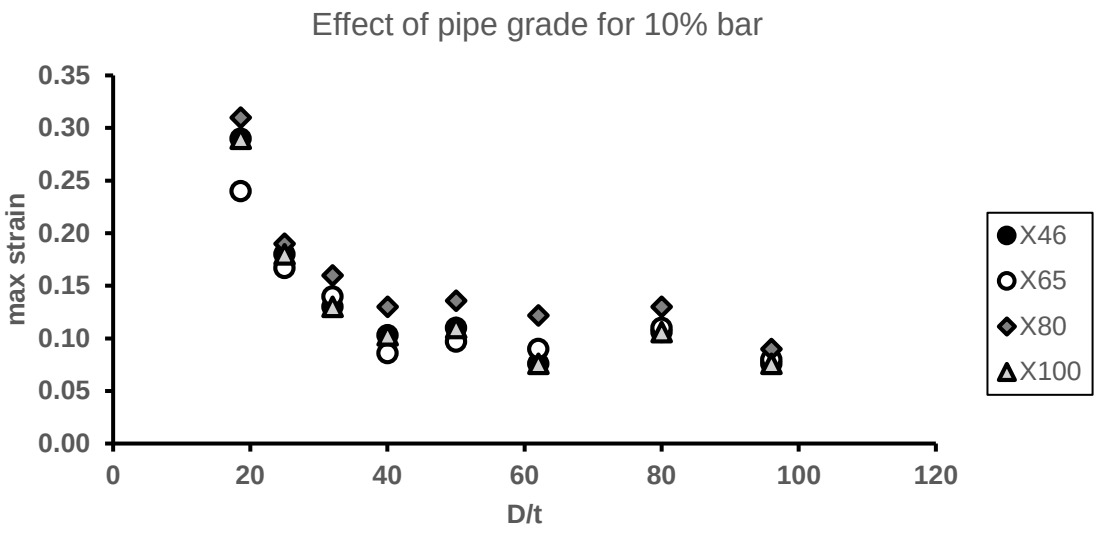

Figure 5-8 Effect of pipe grade on strain for a 10% bar dent

5.4.4 Comparison between ASME B31.8 , Modified ASME [21] and FEA predicted strain

This section compares the total strain predicted using the ASME equation, Noronha et al [21] and the predicted FEA strain. To do the comparison, the strain data extracted from the X65 grade models are used, the dent depth of 2%, 5%, 7% and 10% for all diameter to thickness ratios (D/t) are compared. Table 5-3 below compares the total strain at the outer surface of the pipe between the FEA predicted strain, the ASME predicted strain and Noronha et al[21] using the equations as described in equations 5-5 and 5-10 respectively. The dome indenter model is used to do the comparison. Figure 5-9 also shows the graph of FEA predicted strain versus ASME predicted strain and Noronha et al predicted strain.

D/t	Diameter (mm)	Thickness (mm)	Measured dent depth (%)	FEA predicted strain	ASME predicted strain[19]		Noronha et al [21]	
					Strain value	% error	Strain value	% error
18.6	323.62	17.399	1.6	0.087	0.12	33.58	0.10	16.82

25	323.62	12.944	2	0.11	0.09	21.35	0.11	2.20
32	323.62	10.1131	1.8	0.11	0.07	38.62	0.12	9.49
40	323.62	8.0905	1.6	0.1	0.05	46.01	0.10	2.90
50	323.62	6.4724	1.6	0.098	0.04	55.93	0.09	13.46
62	323.62	5.2196	2.5	0.086	0.03	59.48	0.08	7.31
80	323.62	4.04525	2.3	0.067	0.03	59.70	0.06	12.79
96	323.62	3.371	2.1	0.049	0.02	54.09	0.05	5.29
18.6	323.62	17.399	4.5	0.15	0.12	22.22	0.14	7.15
25	323.62	12.944	4.6	0.16	0.09	45.79	0.16	2.48
32	323.62	10.1131	4.6	0.147	0.07	53.97	0.14	8.63
40	323.62	8.0905	4.6	0.13	0.05	58.41	0.11	14.51
50	323.62	6.4724	4.7	0.104	0.04	58.43	0.10	9.35
62	323.62	5.2196	4.8	0.087	0.03	59.93	0.08	13.44
80	323.62	4.04525	5.5	0.065	0.03	58.42	0.06	4.57
96	323.62	3.371	5.6	0.048	0.02	53.09	0.05	1.51
18.6	323.62	17.399	7	0.18	0.12	35.41	0.21	13.98
25	323.62	12.944	7.3	0.17	0.09	49.12	0.16	9.18
32	323.62	10.1131	6.6	0.15	0.07	54.96	0.14	11.00
40	323.62	8.0905	6.9	0.129	0.05	58.09	0.12	8.46
50	323.62	6.4724	6.6	0.103	0.04	58.03	0.10	8.29
62	323.62	5.2196	6.9	0.083	0.03	57.98	0.08	3.48
80	323.62	4.04525	7	0.063	0.03	57.10	0.06	5.94
96	323.62	3.371	7.6	0.049	0.02	54.01	0.05	8.72
18.6	323.62	17.399	9.1	0.19	0.12	38.86	0.21	9.14
25	323.62	12.944	10.1	0.17	0.09	49.14	0.16	9.22

32	323.62	10.1131	9.9	0.15	0.07	54.96	0.13	16.87
40	323.62	8.0905	9.6	0.13	0.05	58.43	0.11	14.54
50	323.62	6.4724	9.9	0.1	0.04	56.75	0.10	5.10
62	323.62	5.2196	10.5	0.082	0.03	57.45	0.08	2.18
80	323.62	4.04525	10	0.06	0.03	54.93	0.06	5.65
96	323.62	3.371	10.8	0.049	0.02	33.58	0.05	8.66

Table 5-3 Comparison of FEA predicted strain, ASME predicted strain[19] and Noronha et al strain[21] for a dome model X65 pipe grade

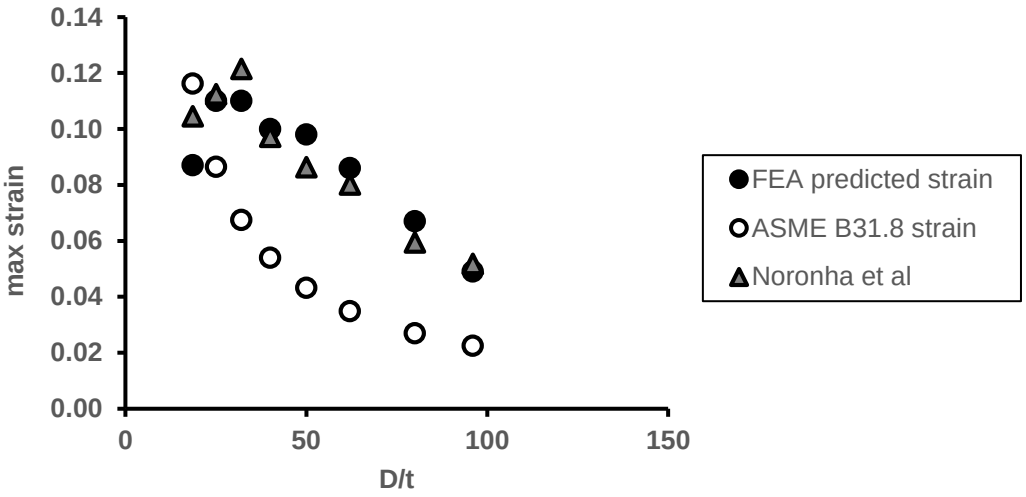

(a)

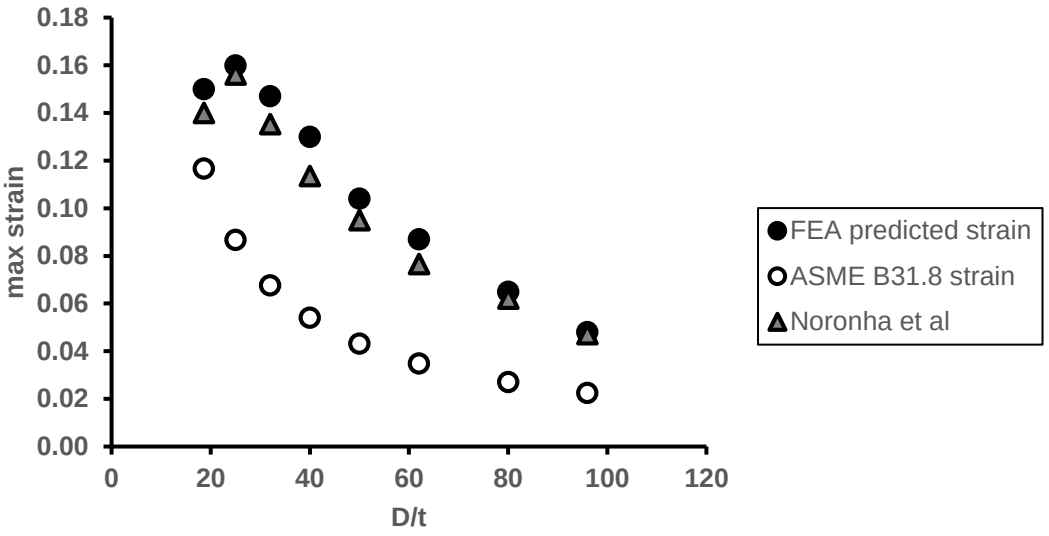
0.18
0.16
0.14
0.12
0.10
0.08
0.06
0.04
0.02
0.00
max strain
0
20
40
60
80
100
120
D/t
FEA predicted strain
ASME B31.8 strain
Noronha et al

(b)

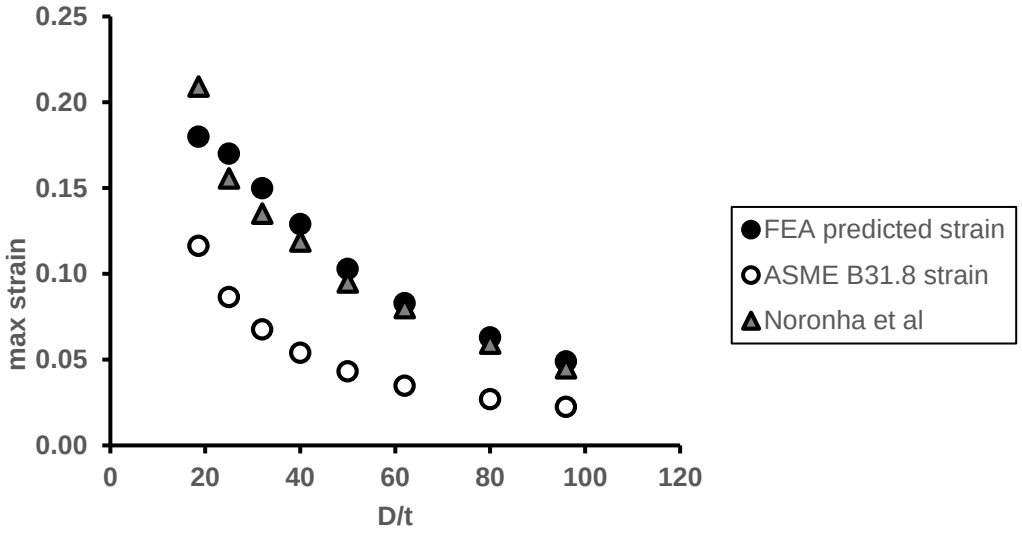
0.25
0.20
0.15
0.10
0.05
0.00
max strain
0
20
40
60
80
100
120
D/t
FEA predicted strain
ASME B31.8 strain
Noronha et al

(c)

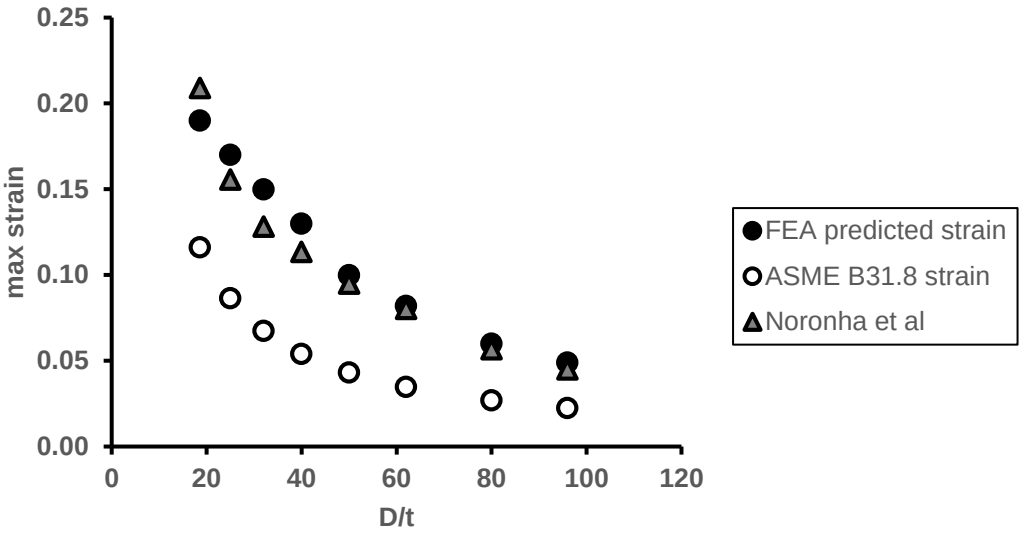

(d)

Figure 5-9 Comparison of FEA predicted strain, ASME predicted strain[19] and Noronha et al strain[21] for a 2%(a), 5%(b), 7%(c) and 10%(d) dent depth

From the results, it can be observed that all methods follow a similar pattern, however, the ASME formula under-predicted the strain. The conservation in the ASME result could be due to the fact that the ASME formula only considers the geometric properties of the pipe and also does not consider the radial components of the strain. The formula proposed by Noronha et al [21] however shows a very good correlation with the FE results. This calls for a revision of the ASME B31.8 document. The notch strain is achieved by following the modelling procedure as described in chapter 3. The element size that was used to achieve the notch strain is seen in table 3-3 and 3-4

5.5 Summary of results and conclusion

The results above have shown how various parameters like pipe geometry, dent geometry and pipe material can affect the total strain in the dent. These parameters are very important in predicting the total strain. From the discussions presented above, the below conclusions can be drawn

1. Circumferential strains are higher in circumferential dents compared to longitudinal strains and reduce as the diameter to thickness ratio increases

2. Longitudinal strains are higher in longitudinal dent compared to circumferential strains and reduce as D/t increases
3. The difference between the circumferential and longitudinal strain is higher in circumferential dent compared to that of the longitudinal dent.
4. The total strain in a dent is higher in a longitudinal dent compared to a circumferential dent
5. As the dent depth increases, there is a corresponding increase in the strain for both dent models
6. Pipes with higher material grades exhibits higher strain and the difference in strain level gets smaller as the Diameter to thickness (D/t) increases
7. The ASME and the FEA predicted strain shows similarity in patterns in regards to how the parameters affect the strain, however, the ASME equation under-predicted the strain
8. The proposed formula by Noronha el al[21] gave a good correlation to the FEA results
9. ASME needs to revise equation to consider the radial components of the strain and also consider plane strain state

The objective of this chapter is to study the effect of these parameters on the strain prediction. The data extracted from the FEA study is eventually used to train an artificial neural network (ANN) in chapter 6 to be able to predict the maximum strain level in the pipeline. The ANN-based formula will present a more comprehensive method for evaluating the total strain in the dent as it includes the effect of pipe grade which was not considered in the ASME equation.

CHAPTER 6

ARTIFICIAL NEURAL NETWORK APPLICATION FOR PREDICTING REROUNDING, SCF AND STRAIN IN DENTED PIPELINE

6.1 Introduction

Artificial neural network is a method than can be used to predict data through learning. It derives its origin from the human nervous system which consist of a large parallel interconnection of a large number of neuron. These neurons are interconnected in a very complex way between each other to create a network. The artificial neural network mimics a small part of the human brain to perform some specific task such as data classification or pattern recognition through a learning process.

An artificial neural network consists of a set of neurons or processing element (PE) that are connected by links of certain numeric weights. Each neuron has

- a set of input links from other neurons
- a set of output links from other neurons
- a current activation function
- an activation function to compute the activation level in the next time step

A typical neuron is seen in figure 2-7 in the literature review. From the figure x_1, x_2…x_n are the inputs, w1j, w2j….wnj are the weights. The total weighted input is the sum of the input activation multiplied by their respective weights as shown by equation 6-1

$$G = \sum_{i=0} W_{ij} x_i \qquad \textbf{(6-1)}$$

A typical neural network architecture will consist of an input layer, one or more hidden layer, and an output layer. The input layer represents the information that is being fed into the system. The hidden layer is dictated by the activities of the input units and the

weights between the input and hidden layer. The output layer relies on the action of the hidden layer and weights between the input and output layer.

For this study, only one hidden layer is used because its efficiency is enough for this application.

The number of neurons in the input layer is equal to the number of input variables, similarly, the number of output layer is equal to the number of output variables. The accuracy of the model is determined by the number of neurons in the hidden layer. The relationship between the input x_j and output y_p of a single perceptron is given by the expression below

$$y_p = f\left(\sum_{j=1}^{N} w_p^j x_j + b_p\right) \qquad \textbf{(6-2)}$$

Where w_p^j are the weights, b_p is a constant usually referred to as bias and $f(\,)$ is the activation function [6]. The number of weights and biases to be determined depends on the network architecture itself. It can be determined by the equation (6-3).

$$(n_i \times n_h) + (n_h \times n_o) + (n_h + n_o) \qquad \textbf{(6-3)}$$

Where n_i is the number of inputs, n_h is the number of processing elements in the hidden layer and n_o is the number of output.

There are several algorithms that can be used to train a neural network. Some of them include back-propagation, genetic algorithm, and particle swam optimisation. For this study, the back propagation algorithm is used as it is the fastest and the most common technique. It also gives insight on how the weights and biases can affect the behaviour of the network.

Suppose we have an input layer X and an output layer Y with the transpose of the vector of the input variables is $\mathbf{X}^T = (x_1, x_2, x_3, \ldots x_n)$ and the transpose of the output variable as $\mathbf{Y}^T = (y_1, y_2, y_3, \ldots y_l)$. The mathematical expression between the input and output is given by equation (6-4).

$$\mathrm{Y} = f\left\{W_2^T \mathrm{x}\left[f\left(W_1 \mathrm{x} \left\langle \begin{matrix} I \\ X \end{matrix} \right\rangle\right)\right]\right\} \qquad \textbf{(6-4)}$$

Where I is a unit one by one unit matrix and the expressions of matrices W_1 and W_2^T are

$$\mathrm{W1} = \begin{bmatrix} b_1 & wih_1^1 & wih_1^2 & \cdots & wih_1^n \\ . & . & . & . & . \\ b_m & wih_m^1 & wih_m^2 & \ldots & wih_m^n \end{bmatrix} \qquad \textbf{(6-5)}$$

$$W_2^T = \begin{bmatrix} c_1 & who_1^1 & who_1^2 & \cdots & who_1^m \\ . & . & . & . & . \\ c_L & who_L^1 & who_L^2 & \ldots & who_L^m \end{bmatrix} \qquad \textbf{(6-6)}$$

The behaviour of an ANN greatly depends on the activation function, weights, and biases. There are different types of activation functions. The most common ones are the logistic sigmoid and the hyperbolic tangent transfer functions. Both functions are compared to determine the one that best predicts the SCF. The expressions for both the logsig and hyperbolic tangent functions are given below

$$Logsig = Y = \frac{1}{1 + e^{-x}} \qquad \textbf{(6-7)}$$

$$\text{Hyperbolic tangent} = Y = \frac{e^{x} - e^{-x}}{e^{x} + e^{-x}} \qquad \textbf{(6-8)}$$

In this Study, ANN is used to predict the total rerounding, stress concentration factor and the maximum strain in the dent. A commercial software MATLAB by MATHWORKS is used to develop the model. The ANN architecture constitute of an input layer with 4 input variable for the strain and rerounding model and 5 input variables for the SCF models. It consist of one hidden layer and one output layer with one output variable. The performance of the network is measured by alternating the number of neurons in the hidden layer, the transfer functions, and the weights. The ranges of the input variables are seen in table 6-1.

	D/t		**d/D**		**L/D**		**σy**		**P_{mean}**	
	Dome	Bar	Dome	Bar	Dome	Bar	Dome	Bar	Dome	Bar
Minimum	18.6	18.6	1.3	1.5	0.2163	2.9046	317	317	3.55	3.55
Maximum	96	96	11.3	11.4	3.6154	6.1183	690	690	48.07	48.07

Table 6-1 input variable ranges for ANN models

6.2 Constitutive ANN model for rerounding prediction

In this study, artificial neural network is used is to predict the reround depth of a dent in a pipeline. Two separate models are developed to predict the dome dents and bar dents. There are several training algorithms that can be used to train the data. It is difficult to determine the training algorithm that will be fastest for a given problem. The speed is dependent on many factors such as the number of data points in the training set, the complexity of the problem, the number of weights and biases, error goals and whether or not the network is being used for pattern recognition or regression. For this study, the Levenberg-Marquardt function is used as it the most common training function and has been proven to give good fits. The network will have one hidden layer as this is sufficient enough to perform the analysis. However, different number of processing elements are varied to determine the one that gives the best performance with minimal errors. The two transfer functions (logarithmic sigmoid and hyperbolic tangent) is also varied to determine the one that gives the best performance. The input and the output variables vary within a wide range and it is common practice to

normalise the data to linearly transform these sets into a similar range of variability. For this study a non-linear nominalisation of both the input and output data is done and this has been shown to improve the ANN training stability and consequently a higher degree of accuracy. Higher and lower bounds of normalisations are dictated by saturation limits of the activation functions: [0, 1] for sigmoidal and [−1, 1] for tangential hyperbolic functions. For some applications where extrapolation outside the boundaries of the input data could be a requirement, input/output data normalisation within a closer range of [0.2, 0.8] or [0.3, 0.7] is recommended [48]. The formula used to normalise the data to a range of [D,R] is given below

$$X_{normalised} = ax + b \quad \textbf{(6-9)}$$

$$a = \frac{D-R}{x_{max}-x_{min}} \quad \textbf{(6-10)}$$

$$b = D - ax_{max} \quad \textbf{(6-11)}$$

Where x_{max} and x_{min} are the maximum and minimum values of the variable. In this study, D = 0.95 and R= 0.05.

6.2.1 ANN Architecture for dome model

The model architecture consist of three (3) layers; the input, hidden and output layers as seen in figure 6-1 below. The input layer consist of four variables which include the diameter to thickness ratio of the pipe (D/t) representing the pipe geometric property, dent depth after spring back (%d/D) and Length to diameter ratio (L/D) representing the dent geometric properties. The 4th input variable the yield strength of the pipe representing the pipe material property. It is assumed that the pipe is pressurised up to the maximum allowable operating pressure(MAOP). The hidden layer consist of 10 processing elements and the output represents the predicted reround depth. This model also makes use of the tansig activation function. This model is chosen because

it gave the best overall performance with minimal errors. Before this model was chosen several analysis was done by varying the number of processing elements in the hidden layer and also varying the activation functions. The data used for the analysis are the normalised data generated from the parametric study done using FEA. The generated dataset are fed into the network to train it. The table below shows the comparison in performance between the different number of processing elements and the activation functions. It shows the mean squared error, Root mean square error, Coefficient of variation and the R-squared value.

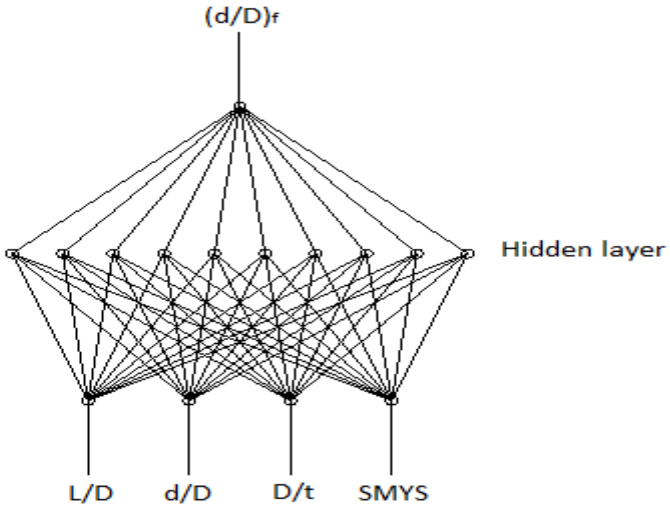

Figure 6-1 Network architecture for a dome rerounding

No of PEs	Logsig				Tansig			
	MSE	RMSE	COV (%)	R square	MSE	RMSE	COV	R square
5	0.000227	0.0181	5.2	0.99	0.000237	0.0178	5	0.9710
10	0.0000888	0.0164	4.6	0.99	0.0000972	0.0146	4.1	0.99
15	0.0000187	0..0203	9.5	0.97	0.0000374	0.215	6.0	0.98

Table 6-2 Comparison of the performances for varying processing elements and activation functions for a dome reround depth

The performances of each network is shown in table 6-2. From the table, it can be seen that the network architecture that gave the best performance is the network with 10 processing elements and a tansig activation function. This network gave the minimal error with a coefficient of variation 4.1 %. The linear correlation between ANN predicted reround depth and the FEA reround depth is seen in figure 6-2 below with an R-square value of 0.99. A good correlation is seen in the graph with a sum of square error of 0.0270.

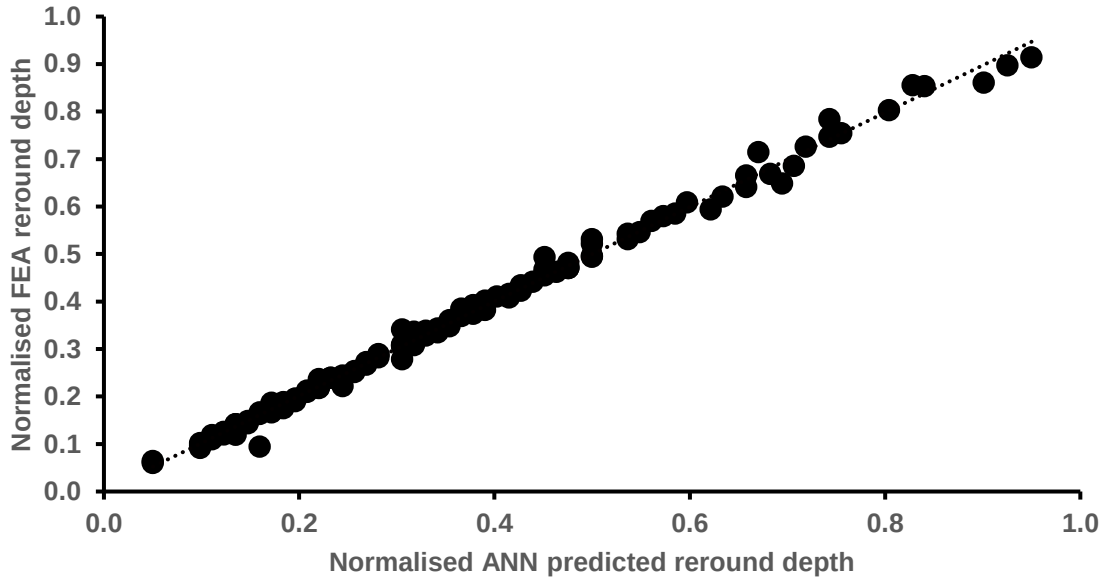

Figure 6-2 Graph of ANN predicted dome reround depth versus FEA predicted depth

As discussed earlier, the performance of the network is dependent on weights and bias values, the number of processing element, the activation function and the training algorithm, the weight and bias matrices of the network that gave the best performance are seen in the set of equations below

$$W_1 = \begin{bmatrix} -0.51279 & 1.514 & 1.2128 & -1.4739 \\ -0.95193 & 1.6421 & -0.60832 & -1.4918 \\ 1.5826 & 0.078602 & 0.18563 & 1.9112 \\ 1.5492 & 1.325 & -1.4138 & 0.20881 \\ -0.70308 & 0.35891 & -1.5832 & 1.7517 \\ 0.75434 & -1.5207 & -1.602 & 0.86623 \\ -0.41945 & -2.0519 & 1.2213 & 0.56599 \\ 1.7727 & -0.49457 & -0.025636 & 1.6764 \\ 1.0944 & 1.0124 & -1.263 & 1.5428 \\ -1.227 & 1.2006 & -0.018417 & 1.8029 \end{bmatrix} \quad \textbf{(6-12)}$$

$$W_2^T = \begin{bmatrix} -0.71276 \\ 0.52149 \\ 0.16063 \\ 0.69917 \\ 0.0395 \\ -0.02922 \\ 0.43003 \\ -0.38837 \\ -0.0027195 \\ 0.57202 \end{bmatrix} \quad \textbf{(6-13)}$$

$$B_1 = \begin{bmatrix} 2.4896 \\ 1.9363 \\ -1.3831 \\ -0.82986 \\ 0.27662 \\ 0.27662 \\ -0.82986 \\ 1.3831 \\ 1.9363 \\ -2.4896 \end{bmatrix} \quad \textbf{(6-14)}$$

$$B_2 = [0] \quad \textbf{(6-15)}$$

Where W_1 is is the weight matrix from the input to the hidden layer, W_2^T is the transposed weight matrix from hidden layer to output, B1 is the bias matrix from the input to hidden layer and B2 is the bias value from hidden layer to output. The mathematical relationship between the inputs and the output is seen in equation 6-4

6.2.2 ANN Architecture for bar model

Similar to the dome model, the network consist of 3 layers, the input, hidden and the output layer. The input layer consist of the four input variables, which include the diameter to thickness ratio (D/t), the length to diameter ratio (L/D), the dent depth %d/D and the yield stress (σy). The input value ranges are seen in table 6-1 above .The output layer is the final dent depth after pressure. The network is equally trained by varying the number of processing elements (PE) and the transfer function. The Lavenberg-Marquardt training algorithm is also used for this analysis. After running the analysis, the model that gives the best performance is the model with 15 hidden processing elements and the tansig activation function. A table showing the performance of each analysis is shown below. Figure 6-3 below represent the network architecture for the bar model which shows the 4 input variable, 15 hidden processing element and the output

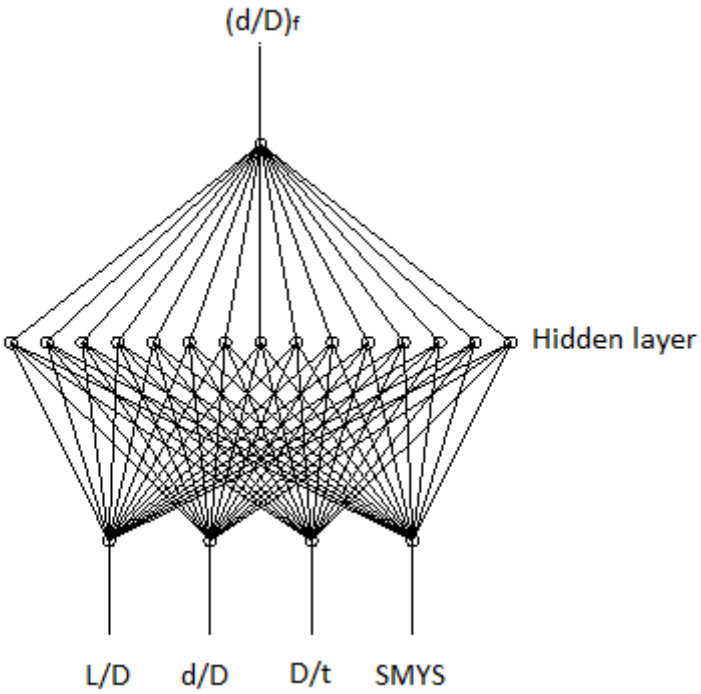

Figure 6-3 Network architecture for a bar rerounding

No of PEs	Logsig				Tansig			
	MSE	RMSE	COV (%)	R square	MSE	RMSE	COV	R square
5	0.0000943	0.0144	3.7	0.99	0.000107	0.0159	4.1	0.99
10	0.0000409	0.0253	6.5	0.98	0.0000217	0.0146	3.7	0.99
15	0.0000237	0.0157	4.0	0.99	0.00000501	0.0124	3.2	0.99

Table 6-3 Comparison of the performances for varying processing elements and activation functions for a bar reround depth

From table 6-3, it can be seen that the network that gives the best performance is the network with 15 hidden processing elements with Tansig activation function. The network has a mean square error value of 5.01E-06 and a coefficient of variation of 3.2. The linear regression between the predicted values and actual gives a good fit as shown below with R-square value of 0.99.

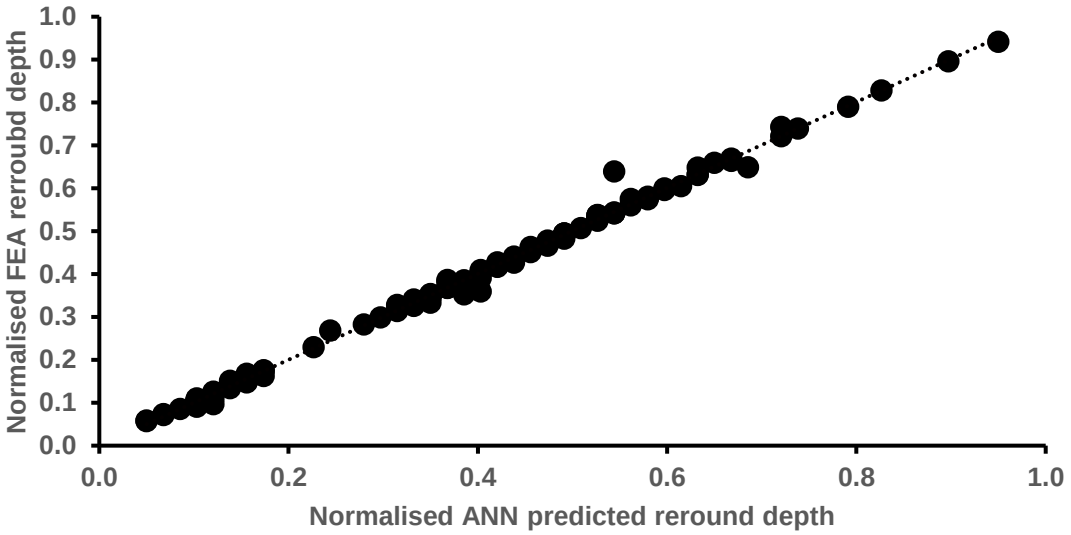

Figure 6-4 Graph of ANN predicted bar reround depth versus FEA predicted depth

From Table 6-3, it can be seen that the logsig transfer function equally gives a very good performance with low coefficient of variation. However, the aim is to select the network with the best performance, hence, the reason why the logsig function is

chosen. The matrix equation of the weights and bias values that gave the best person is seen below. The equation governing the inputs and the output is seen in equation 6-4.

$$W_1 = \begin{bmatrix} 1.7477 & -1.51 & 0.45195 & -1.4326 \\ -0.49476 & -1.9224 & 1.4499 & -1.2445 \\ -2.131 & 1.6495 & -0.57256 & -0.031926 \\ -1.0876 & -2.1164 & -0.59595 & 1.2545 \\ -0.36429 & 1.7115 & 1.9475 & 0.85818 \\ 0.39473 & 0.95808 & -1.9228 & 1.6793 \\ -1.0952 & -0.052464 & 1.774 & 1.8005 \\ 0.61102 & 0.46654 & 2.4555 & -0.98528 \\ 1.1858 & -1.4749 & 1.6628 & 1.1158 \\ -1.3316 & -0.19693 & -1.9204 & -1.4461 \\ -1.3198 & 1.5975 & -0.82145 & -1.6194 \\ -1.5524 & 0.35738 & -1.2571 & 1.8636 \\ -1.9496 & 0.22738 & 1.9335 & 0.00024136 \\ -0.45562 & -1.6126 & -2.1837 & -0.12063 \\ 0.046921 & -0.06629 & 1.3209 & 2.4165 \end{bmatrix} \quad \textbf{(6-16)}$$

$$W_2^T = \begin{bmatrix} 0.14162 \\ 0.15167 \\ 0.46332 \\ 0.39378 \\ 0.098895 \\ -0.40872 \\ -0.33523 \\ 0.49822 \\ -0.60754 \\ -0.013017 \\ -0.42805 \\ 0.61702 \\ 0.27417 \\ 0.00060793 \\ -0.037 \end{bmatrix} \quad \textbf{(6-17)}$$

$$B1 = \begin{bmatrix} -2.7552 \\ 2.3616 \\ 1.968 \\ 1.5744 \\ 1.1808 \\ -0.7872 \\ 0.3936 \\ 0 \\ 0..3936 \\ -0.7872 \\ -1.1808 \\ -1.5744 \\ -1.968 \\ -2.3616 \\ 2.7552 \end{bmatrix} \quad \textbf{(6-18)}$$

$$B_2 = [0] \quad \textbf{(6-19)}$$

6.3 Comparison between Experimental, FEA and ANN result

Figure 6-5 show a comparison between experimental result [17], FEA results and ANN predicted results. Selected input variables of a dome model from the experimental data are simulated in the ANN network to predict the rerounding depth. The predicted values shows a good correlation with the experimental results. This shows the level of accuracy of the ANN-based method and can be confidently applied to predict the rerounding depth

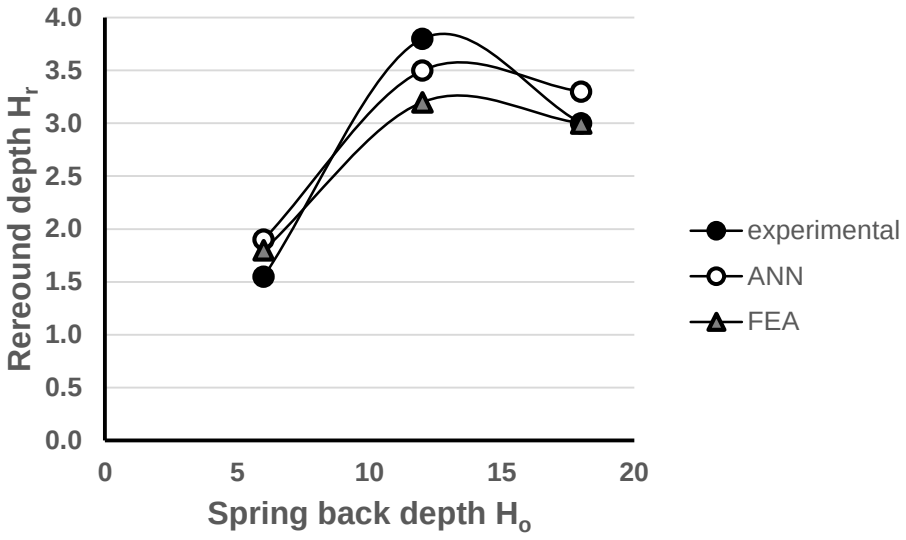

Figure 6-5 Graph of ANN predicted bar reround depth versus FEA predicted de

6.4 Constitutive ANN model for SCF prediction

In this study, ANN is used to predict the SCF associated with each dent scenario. Two separate ANN models are created to predict the SCF associated with longitudinal and circumferential dents respectively. Similar to the reround models, this study will make use of a single hidden layer with varying processing elements as this is sufficient enough to give the required performance. The Lavenberg-Marquardt training algorithm is also used in this study to train the network. The two common activation functions are investigated to see which one gives the best performance. As discussed earlier, the effect of parameters such as dent geometry, pipe geometry, pipe material and pressure range are studied. These parameters represent the input parameters in the network and the SCF represents the output. The individual parameters include D/t and L/D ratio for the dent geometry, D/t ratio for the pipe geometry, σy for pipe specified minimum yield stress (SMYS) and P_{mean} representing the effect of mean pressure. The data for these parameters are extracted from FE results from the parametric study.

These data are divided into 3 subsets, one for training the network, the second for testing and the last set of data are used for validation. For this study, 70% of the data are used for training, 15% for testing and 15% for validation.

6.4.1 ANN Architecture for dome model

The ANN architecture constitute of an input layer with 5 input variable, one hidden layer and one output layer with one output variable. The input variables include the diameter to thickness ratio (D/t), length to diameter ratio (L/D), dent depth after spring back (%d/D), the yield stress (σy) and the mean pressure (P_{mean}). The output represents the predicted SCF. The performance of the network is measured by alternating the number of neurons in the hidden layer, the transfer functions, and the weights. The number of neurons in the hidden layer varies between 5 and 15. Both the logsig and tansig functions are also compared to see the one that gives the best performance. The performance of the network is measured by the mean squared error (MSE) and the coefficient of variation between the predicted and actual output. The input ranges used are seen in table 6-1. Figure 6-6 shows the network architecture dome model. Both the input and output variables are normalised as seen in equation 6.9. The network that gives the best performance is the network with 5 processing elements in the hidden layer and a logsig activation function. Table 6-4 shows the performance of each network.

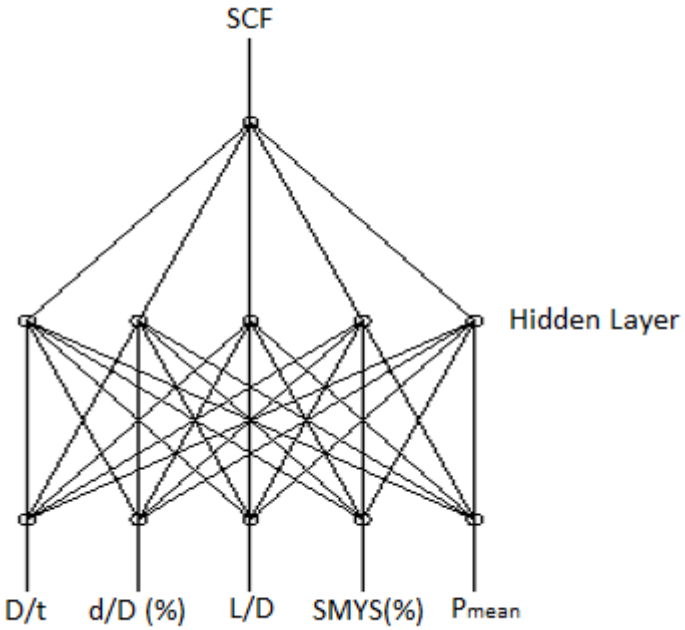

Figure 6-6 Network architecture for predicting SCF in a dome dent

No of PEs	Logsig			Tansig		
	MSE	COV (%)	R square	MSE	COV (%)	R square
5	0.0000985	4.7	0.99	0.000128	6.8	0.96
10	0.0000687	4.9	0.99	0.0000786	5.4	0.98
15	0.0000574	5.7	0.98	0.0000552	5.3	0.98

Table 6-4 Comparison of the performances for varying processing elements and activation functions for a dome SCF

The table above shows the performance of each network. The logsig activation function gave better performance with the best network having 5 hidden processing elements with the lowest coefficient of variation of 4.7. Figure 6-7 shows the linear regression graph of the ANN predicted SCF and the FEA predicted SCF

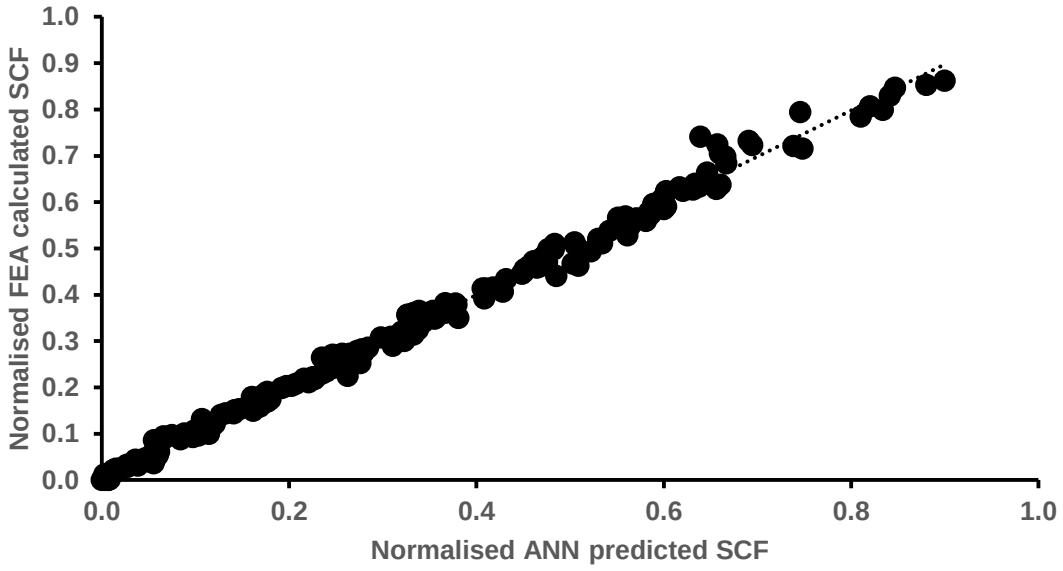

Figure 6-7 Graph of ANN predicted SCF versus FEA predicted SCF for dome dent

The linear regression gives a good fit with an R-square value of 0.99 . The weights and bias matrix equations for this network is given below and the mathematical expression

between the input and output is given in equation 6-4 where W_1 is is the weight matrix from the input to the hidden layer, W_2^T is the transposed weight matrix from hidden layer to output, B_1 is the bias matrix from the input to hidden layer and B_2 is the bias value from hidden layer to output.

$$W_1 = \begin{bmatrix} 1.6689 & -2.1342 & -1.8156 & -1.899 & 0.82586 \\ 1.9343 & -1.0558 & 2.2431 & -0.37294 & -2.2131 \\ -1.7942 & 0.2255 & 2.199 & 1.9997 & 1.6793 \\ 1.9745 & 2.1853 & -0.069854 & 1.3957 & 2.073 \\ 0.67914 & 2.3854 & 1.5407 & 2.3577 & 0.91709 \end{bmatrix} \quad \textbf{(6-20)}$$

$$\boldsymbol{w_2^T} = [1.3903\ 1.3115\ -0.58134\ 0.83866\ -1.7737] \quad \textbf{(6-21)}$$

$$B1 = \begin{bmatrix} 3.8632 \\ -1.9316 \\ 0 \\ 1.9316 \\ -3.8632 \end{bmatrix} \quad \textbf{(6-22)}$$

$$B_2 = [-0.59271] \quad \textbf{(6-23)}$$

6.4.2 ANN Architecture for bar model

The network for the bar model share similar architecture and settings as the dome model. After training the networks, the network that gives the best performance is the network with 5 processing elements and a logsig transfer function. The network architecture is the same as the dome model as seen in figure 6-6. Table 6-5 below also show the performance of each network.

No of PEs	Logsig			Tansig		
	MSE	COV (%)	R square	MSE	COV (%)	R square
5	0.0000886	3.5	0.99	0.000985	12.4	0.94
10	0.0000925	5.3	0.98	0.000745	9.85	0.96
15	0.0000798	5.6	0.98	0.000521	7.7	0.97

Table 6-5 Comparison of the performances for varying processing elements and activation functions for a bar SCF

From the table above the logsig function gave better performance compared to the tansig function. This network has a mean squared error value of 8.86E-05. The linear regression is also plotted below and it gives a good fit with an R-square value of 0.99 and a coefficient of variation of 3.5%

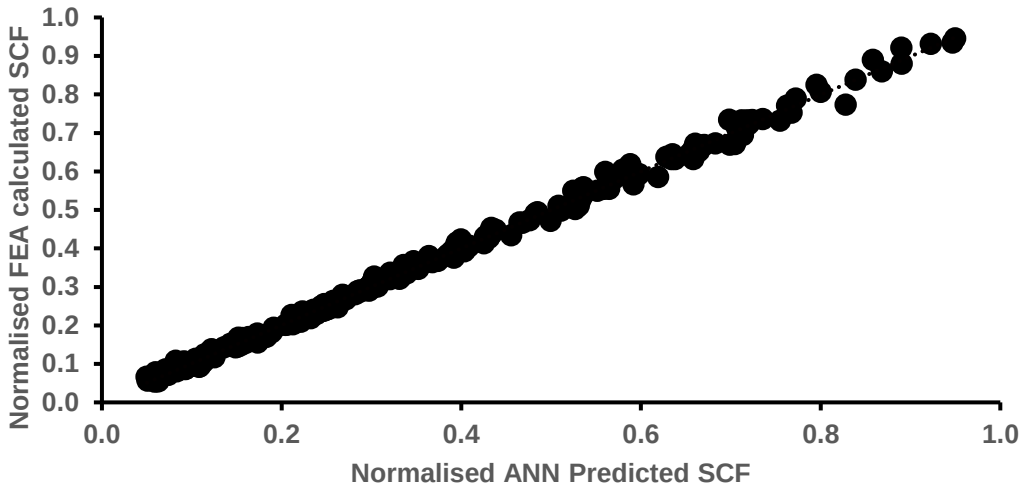

Figure 6-8 linear regression graph for ANN predicted SCF versus FEA predicted SCF for bar dent

The values of the weight and biases of the network are seen in the equations below where equation 6-24 is the weight matrix from the input to the hidden layer, equation 6-25 is the transposed weight matrix from hidden layer to output, equation 6-26 is the

bias matrix from the input to hidden layer and equation 6-27 is the bias value from hidden layer to output. The mathematical expression between the input and output is given in equation 6-4.

$$W_1 = \begin{bmatrix} 0.94276 & 0.49931 & -0.33592 & 1.6789 & 3.2947 \\ -2.2601 & 2.552 & 0.31962 & -1.0121 & 1.4756 \\ 2.4692 & 1.2598 & -1.3487 & -2.1102 & 0.98426 \\ 1.8301 & 2.0653 & 1.5172 & -0.14883 & -2.233 \\ -1.5154 & -0.47222 & 0.027508 & -0.97318 & -3.3853 \end{bmatrix} \quad \textbf{(6-24)}$$

$$\boldsymbol{w_2^T} = [0.2339\ -0.77856\ 1.7176\ 1.8798\ -0.83406] \quad \textbf{(6-25)}$$

$$B1 = \begin{bmatrix} -3.8632 \\ 1.9316 \\ 0 \\ 1.9316 \\ -3.8632 \end{bmatrix} \quad \textbf{(6-26)}$$

$$B_2 = [-1.1093] \quad \textbf{(6-27)}$$

6.5 Constitutive ANN model for Strain prediction

One of the objectives of this study is to review the existing method for calculating strains in the pipe. Previous chapter has shown how the ASME B31.8 code under-predicts the total strain in the pipe. This study uses artificial neural network to predict the total strain in the pipe. Data from finite element study is used to train the network. The network has 3 layers (input, hidden and output layer). The input layer consist of the 4 input variable (D/t, L/D,d/D and σy), the hidden layer varies different number of processing elements and the output predicts the maximum strain after spring back. The network share similar attributes as mentioned in previous models.

6.5.1 ANN Architecture for dome model

The network consist of 3 layers with the input layer consisting of the four input variable. 6 networks are trained with varying processing elements and transfer functions. The network that gives best performance is the network with 10 processing elements in the hidden layer and uses the logsig activation function. The table showing the performance of each network is seen below. The network architecture for the chosen model is seen below. The figure shows the four input variables D/t, L/D, d/D and SMYS. The dent depth used is the dent depth after spring back. The middle layer which is the hidden layer shows the 10 processing elements and the output layer shows the predicted maximum strain.

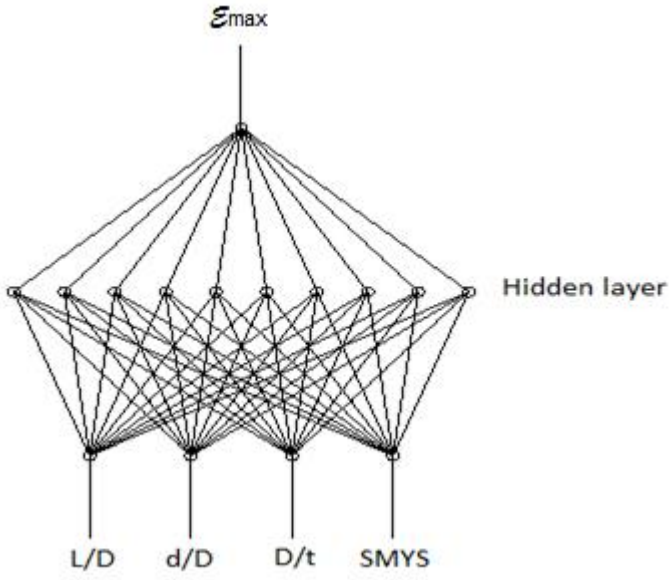

Figure 6-9 Network architecture for predicting strain in dome dent

No of PEs	Logsig				Tansig			
	MSE	RMSE	COV (%)	R square	MSE	RMSE	COV (%)	R square
5	2.19E-5	0.0167	14.3	0.9	1.33E-4	0.0157	13.5	0.9

10	7.44E-6	0.0057	4.9	0.99	1.0E-4	0.0213	18	0.8
15	1.76E-5	0.0132	11.3	0.93	1.1E-5	0.0131	11	0.93

Table 6-6 Comparison of the performances for varying processing elements and activation functions for a dome dent

From the table 6-6 , it is seen that the tansig function gave better performance for 5 processing elements in the hidden layer. For 10 processing elements, the logsig gave the best performance which is the overall best performance of all the network. As the processing elements increased to 15, the tansig function gave a slightly better performance. This network chosen has a mean squared error value of 7.44 E-6. The linear regression is also plotted below. The regression is shown to give a good fit with an R-square value of 0.99 and a coefficient of variation of 4.9%.

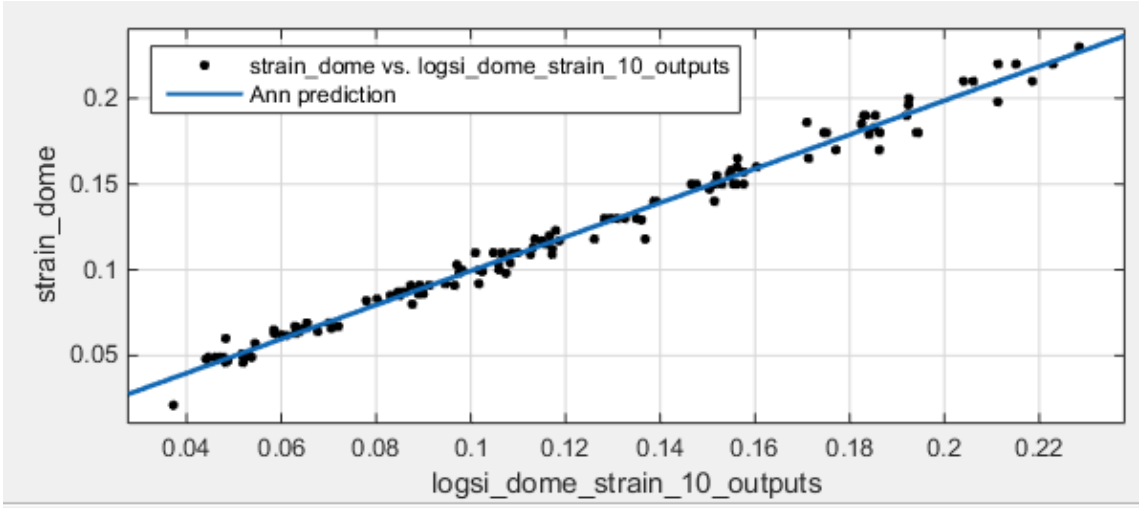

Figure 6-10 linear regression graph for ANN predicted Strain versus FEA predicted Strain for dome dent

The values of the weight and biases of the network are seen in the equations below. The mathematical expression between the input and output is given in equation 6-4. From the equations below, W_1 is is the weight matrix from the input to the hidden layer, W_2^T is the transposed weight matrix from hidden layer to output, B_1 is the bias matrix from the input to hidden layer and B_2 is the bias value from hidden layer to output.

$$W_1 = \begin{bmatrix} -1.2742 & 4.1782 & 4.9577 & 0.83736 \\ 1.2959 & -1.815 & -1.5486 & -4.8245 \\ 0.32557 & 4.0402 & -5.9636 & -0.14593 \\ 2.0322 & -1.1188 & -3.3968 & -5.0411 \\ 0.35635 & 0.38461 & 0.89538 & 0.39628 \\ 1.5228 & -0.2715 & -4.1469 & -1.1585 \\ -4.1396 & 10.5104 & -6.4896 & -1.3508 \\ 4.0038 & -6.55377 & 9.6739 & -2.0073 \\ 4.1277 & -4.1606 & 7.054 & -1.0131 \\ -12.0869 & 4.8778 & -6.8317 & 1.4395 \end{bmatrix} \quad \textbf{(6-28)}$$

$$W_2^T = \begin{bmatrix} 1.625 \\ -3.5264 \\ 3.63 \\ 3.3811 \\ -4.2908 \\ -1.5609 \\ 0.46118 \\ -3.1732 \\ 10.163 \\ 10.3806 \end{bmatrix} \quad \textbf{(6-29)}$$

$$B1 = \begin{bmatrix} 7.7983 \\ 0.17913 \\ -10.6615 \\ 0.11379 \\ 0.2713 \\ 0.14576 \\ -5.1871 \\ 9.9569 \\ 9.8298 \\ -19.4016 \end{bmatrix} \quad \textbf{(6-30)}$$

$$B_2 = [-5.5664] \quad \textbf{(6-31)}$$

6.5.2 ANN Architecture for bar model

The network shares similar characteristic and settings as described in section 6.4.1. Table 6-6 below shows the performance of each network. The network with the best performance is the network with 15 processing elements in the hidden layer and a logsig activation function. The network architecture of the chosen model is given below

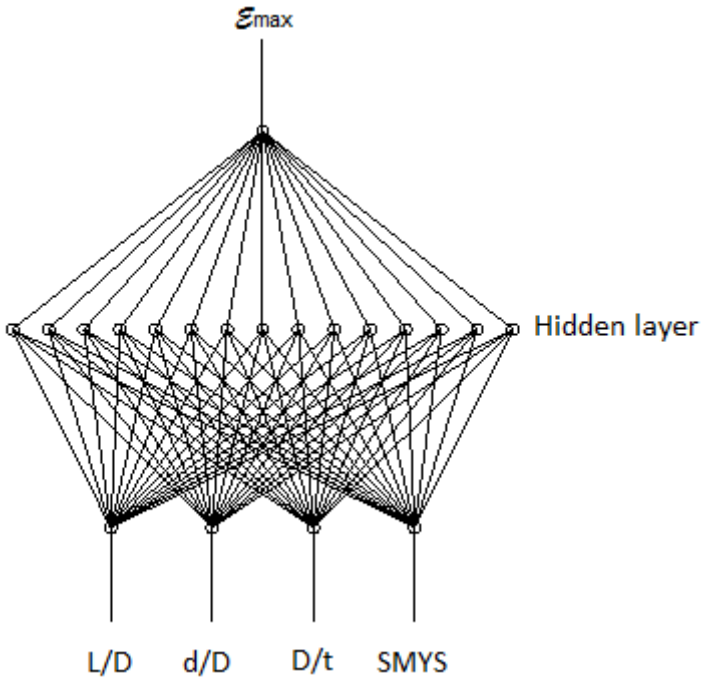

Figure 6-11 Network architecture for predicting strain in bar dent

No of PEs	Logsig				Tansig			
	MSE	RMSE	COV (%)	R square	MSE	RMSE	COV (%)	R square
5	5.82E-5	0.0116	11.2	0.97	1.05E-5	0.0104	10	0.97
10	2.56E-5	0.0101	9.7	0.97	1.03E-5	0.0104	10	0.97
15	5.64E-6	0.0091	8.8	0.98	1.41E-5	0.0121	11.7	0.97

Table 6-7 Comparison of the performances for varying processing elements and activation functions for a bar dent

From table 6-7, it is seen that the tansig function gave a better performance for 5 and 10 processing elements. However, as the processing elements increased further, the logsig function gave better performance. The network with the overall best performance has 15 processing element and logsig activation function. The means squared error of this network is 5.64 x 10^{-6} .The linear regression of the ANN predicted strain and the FE predicted strain is seen in figure 6-12.

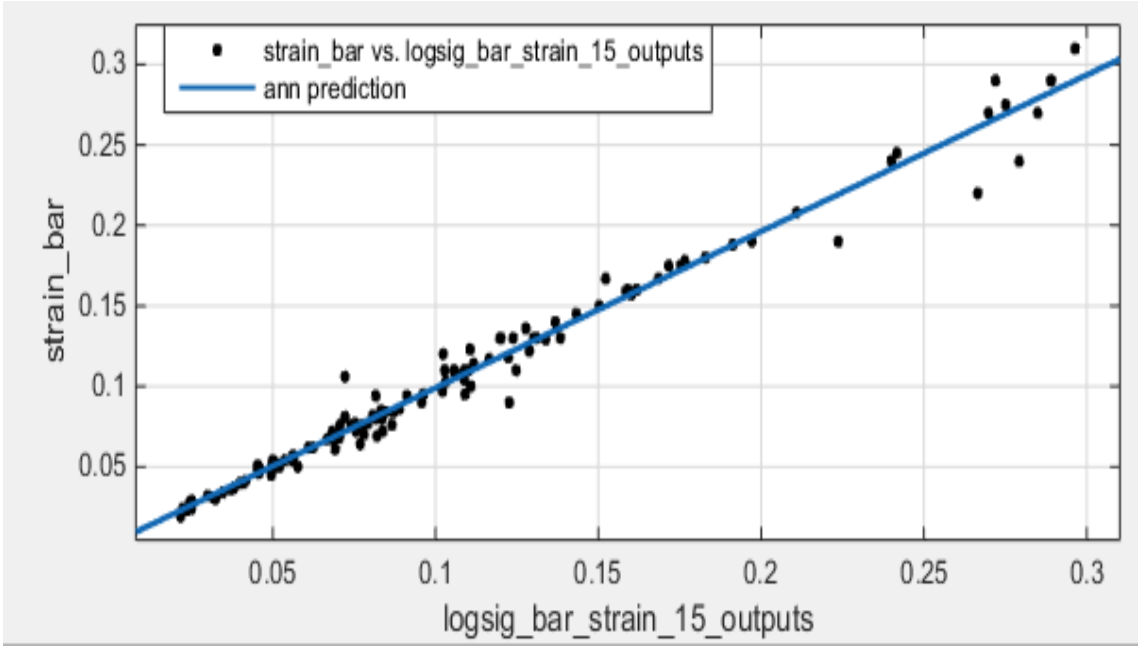

Figure 6-12 linear regression graph for ANN predicted Strain versus FEA predicted Strain for bar dent

The regression above shows a good with an R-square value of 0.98 and coefficient of variation of 8.8%. The values of the weight and biases of the network are seen in the equations below. The mathematical expression between the inputs and output is given in equation 6-4.

$$W_1 = \begin{bmatrix} 4.2981 & -1.9781 & -0.76656 & -2.8241 \\ -2.0227 & -1.9545 & -3.8026 & 4.166 \\ 2.5933 & 3.4971 & -5.2272 & 0.65328 \\ -6.3702 & -0.11286 & 3.9084 & 0.24412 \\ 3.1061 & -1.3944 & 3.2589 & -2.6161 \\ 4.0088 & 2.6785 & 1.2342 & -0.67948 \\ 0.1094 & 1.9516 & 0.97041 & 5.7258 \\ 1.8014 & 3.7107 & 3.6772 & 1.0424 \\ 2.0231 & -1.6587 & -8.8934 & 1.8008 \\ 5.11 & 3.7729 & 0.71017 & 2.1614 \\ 1.2648 & 2.8214 & 0.26868 & 4.3462 \\ -7.2374 & -0.90969 & -0.68872 & -4.1578 \\ 3.8764 & 1.6143 & 3.335 & 1.4222 \\ 1.015 & 0.9976 & -4.6561 & -1.96 \\ 6.0544 & -0.49504 & 0.16135 & -0.98605 \end{bmatrix} \quad \textbf{(6-32)}$$

$$W_2^T = \begin{bmatrix} 0.33821 \\ 1.7417 \\ 0.19724 \\ 0.54557 \\ -0.098531 \\ 0.012167 \\ 1.0903 \\ 0.26616 \\ -1.0953 \\ -1.2505 \\ 0.81836 \\ 0.92209 \\ 0.35059 \\ 2.7291 \\ -5.793 \end{bmatrix} \quad \textbf{(6-33)}$$

$$B1 = \begin{bmatrix} -6.7108 \\ -1.2191 \\ 1.9344 \\ 2.1239 \\ 4.9549 \\ -0.53593 \\ 1.2506 \\ -0.91194 \\ 0.64421 \\ 0.643 \\ -5.0216 \\ -8.1726 \\ -2.1728 \\ -5.4958 \\ 4.4971 \end{bmatrix} \quad \textbf{(6-34)}$$

$$B_2 = [-1.4414] \quad \textbf{(6-35)}$$

6.6 Summary and conclusion

This chapter uses artificial neural network to predict the final dent depth (reround depth) after pressurisation and the stress concentration factor in the dent. It is also used predict the maximum strain in pipeline dents. The rationale behind this is to develop a means of predicting the reround depth, SCF and strain without having to run expensive experimental program and extensive finite element analysis. The parameters that affect the rerounding, SCF and maximum strain as discussed in chapter 3, 4 and 5 respectively are used to train the ANN to be able to predict the reround depth, SCF and strain. Two separate models are trained to predict dome and bar dents respectively for each result. The networks have one hidden layer as this is sufficient enough to perform the analysis. Different number of processing elements are used for each result to determine the network that best give a good fit with minimal errors. The Levenberg-Marquardt function is used as it is the most common training function and has be proven to give good fits. The two transfer functions (logarithmic sigmoid and hyperbolic tangent) is also investigated to determine the one that gives the best fit. Each network has a model architecture consisting of three (3) layers; the input, hidden and output layers. The input layer consist of four variables which include the diameter to thickness ratio of the pipe (D/t) representing the pipe geometric

property, dent depth (%d/D) and Length to diameter ratio (L/D) representing the dent geometric properties. The 4th input variable is the yield strength of the pipe representing the pipe material property. The hidden layer has a variable number of processing elements ranging between 5 and 15. The numbers are alternated with the two different transfer functions to see the model that gives the best performance. The output predicts the reround dent depth, SCF and strain after spring back. From the results the following can be concluded:

1. For the dome model rerounding result, the network architecture that gave the best performance is the network with 10 processing elements and a tansig activation function. The network gave the minimal error with a coefficient of variation(COV) 4.1 %. The ANN predicted reround depth showed a good correlation with the FEA reround depth with an R-square value of 0.99.
2. For the bar model rerounding result, the network that gives the best performance is the network with 15 hidden processing elements with tansig activation function. The network has a mean square error value of 5.01E-06 and a COV of 3.2%.
3. For the dome model SCF result, the logsig activation function gave better performance with the best network having 5 hidden processing elements and coefficient of variation (COV) of 4.7
4. For the Bar model SCF result, the network that has the best performance is the network with 5 processing elements and a logsig transfer function. This network has a mean squared error value of 8.86E-05. The linear regression gives good fit with an R-square value of 0.99 and a coefficient of variation of 3.5%
5. For the dome model strain result, the logsig function gave the best performance with 10 processing elements and a COV of 4.9%
6. For the bar model strain result, the network with the overall best performance has 15 processing element and logsig activation function. and a COV of 8.8%.

Altogether, the ANN-based method have shown a good degree of reliability with low coefficient of variation for all models. These low coefficient of variation increases the confidence in the use of the ANN-based formula

CHAPTER 7

PROPOSED PROCEDURE FOR DENT ASSESSMENT

Previous chapters have the described past and current methods for evaluating dent severity. It described the strain-based assessment and the fatigue assessment. The strain-based assessment was proposed by ASME B31.8 and equations 5-4 and 5-5 was given in order to find the total strain in the dent. Fatigue assessment, however, has been done by various researchers to calculate the fatigue life of pipelines with dent. This is done by extracting SCF from experimental data or finite element analysis and using it with an SN curve in order to determine the fatigue life. Experiments are expensive and finite element analysis are time consuming. This chapter proposes the use of the artificial neural network for both strain based assessment and fatigue assessment. This method eliminates the process of having to run an expensive experimental program or running an extensive finite element study in order to calculate the SCF used in fatigue assessment and strain used in strain based assessment.

The application of ANN is new and unique in dent assessment. Apart from the fact that it will save time and money, it has a very good accuracy in predicting the SCF and maximum strain. What makes the ANN application unique is its ability to learn. Unlike other methods such as curve fitting, ANN studies patterns and trends through the data provided. The accuracy of the ANN depends on the number of training data. A wider range of data is recommended when using ANN. The more the training data, the more the accuracy of the predicted results. The ANN application in dent assessment is easy and straightforward. All that is required is the need to know the values of the input parameters. Once the input parameters are known and inputted into the ANN model, it predicts the results with good accuracy

A large data base of SCFs was generated from a prior finite element study which analysed the effect of various parameters on the fatigue life of pipeline with dents. A wider range of pipe grades, pipe geometry, dent geometry and pressure range was analysed in order to give the large database of SCFs. This was then used to train the

ANN in order to predict the SCF. Similarly, ANN is used to predict the maximum strain in the pipe. It also considers the effective various parameters on the prediction of strain. The ANN is also used to predict the rerounding depth after pressurisation. The strain assessment includes the effect of pipe grade which was not included in the ASME B31.8 code. A flow chart showing this procedure is seen in figure 7-1 and each component of the flow chart is further explained below

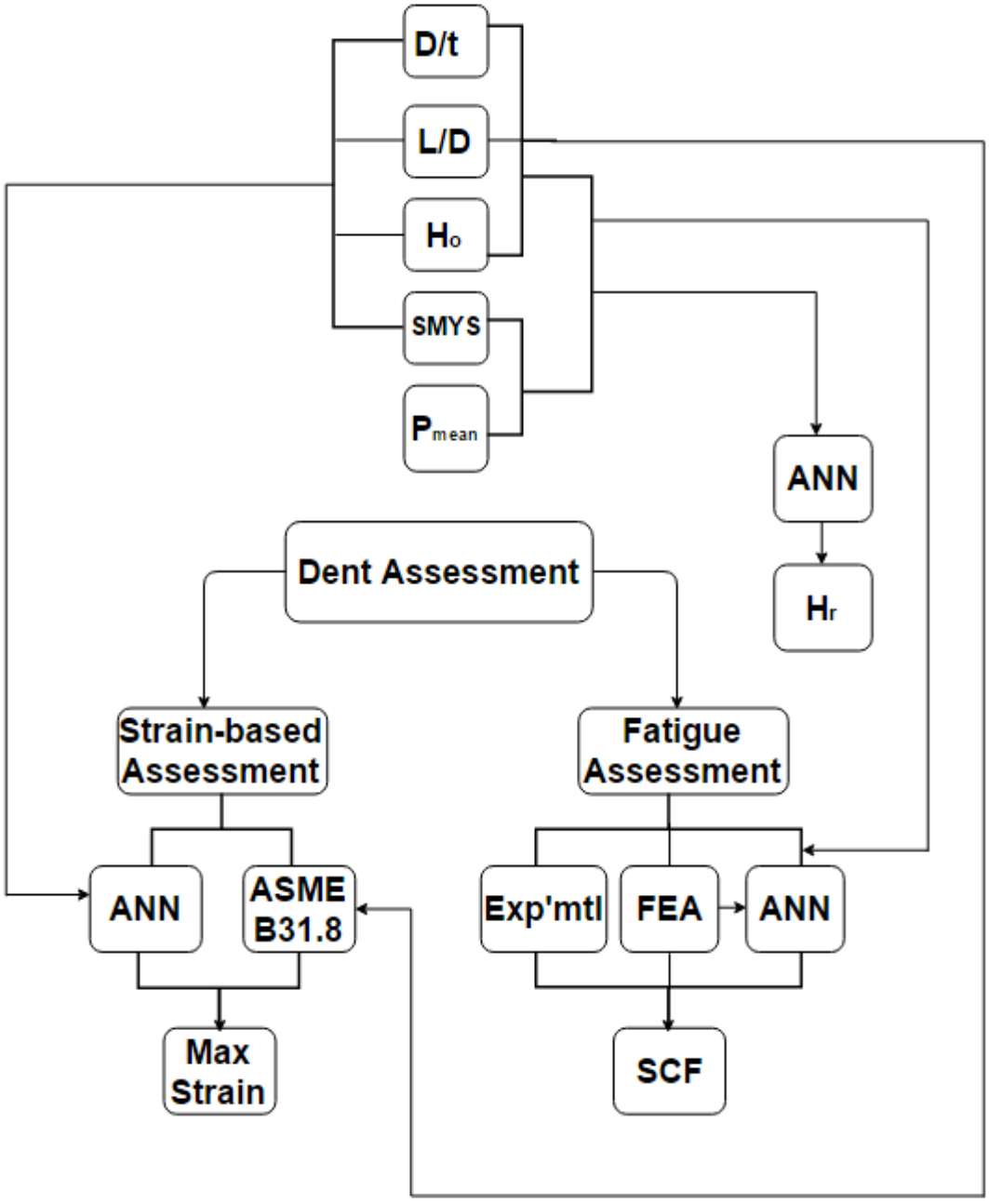

Figure 7-1 Flow chart for Dent assessment

In previous chapters, the various parameters that influence the fatigue and maximum strain was discussed , the parameters include, dent geometry, pipe geometry, pipe grade and mean pressure. The dent geometry factor is represented as the dent depth (H_o) and the ratio of the dent length to the diameter of the pipe (L/D). The pipe geometry is represented as a ratio of the pipe diameter to the thickness of the pipe (D/t). Similarly, the pipe grade is represented by the specified minimum yield stress(SMYS). Finally the pressure range is represented by the mean pressure in the pipe.

In order to carry out a dent assessment using the proposed methods, these parameters needs to be known. It is important to note that the dent depth considered in the proposed methods is the dent depth after spring back (H_o). However, an ANN-based formula in chapter 6 show the relationship between the spring back dent depth and the reround dent depth (H_r).

7.1 Proposed fatigue assessment procedure

The stress concentration factor (SCF) used in fatigue assessment have over the years been derived empirically or using finite element analysis. These methods can be very expensive and time consuming. This section proposes an alternative method for calculating the SCF using the ANN-based formula. The ANN application eliminates the need to run extensive FE study and expensive experimental program, thereby saving time and money. The ANN-based formula also considers the various parameters that affect the SCF in pipe which were not systematically considered by previous researchers. It gets its training data from a prior FE study done in chapter 4. In order to improve the accuracy the ANN formula, a wider range of dataset is needed. As a result, a parametric range of industry standard pipes was analysed with different dent orientation and depths. A total of 256 analyses was done to generate the data needed to train the network. The 256 analyses was achieved by creating an Ansys parametric design language (APDL). With the APDL, parameters can be changed to create new models. Details of how the models were created and analysed can be seen in chapter 3. The parameters considered in the FE study includes the pipe diameter to thickness

ratio (D/t), dent depth after spring back(H_o),the length of dent to diameter ratio (L/D), pipe grade(σ_y) and the mean pressure (%SMYS). The accuracy of the ANN-based formula depends on the accuracy of the FE result. The accuracy of FE result was tested by validating it with experimental data and analytical models. The validation shows that the FE results were quite accurate with a maximum percentage error of 15%. With the FE results being accurate, the data generated can be confidently used to train the network. The data was normalised and divided into 3 sets. 70% of the datasets was used for training, 15% was used for testing and the remaining 15% was used for validation. Two ANN models are created for dome models and longitudinally aligned bar models. The architecture consist of 3 layers(input, hidden and output). Each models have 5 processing elements in the hidden layer and use the sigmoid activation function.

In order to use the ANN-based formula, the 5 input parameters needs to be determined. It assumed in this procedure that the dent has already been introduced before the pipe is pressurised. Hence, the dent depth required is the depth after spring back. An ANN-based formula was created in chapter 6 to give the relationship between the spring-back dent depth and reround dent depth.

In order to use the ANN-based formula, the following steps should be followed :

1. Determine the spring back dent depth(H_o), the length of dent to diameter ratio (L/D), the diameter to thickness ratio (D/t) of the pipe, the yield strength of the pipe and the mean operating pressure
2. Normalise the data using equation 6-9
3. If it is a dome model, apply the weights ,biases and sigmoid transfer function as seen in equation 6-2. The values of the weights and biases are seen in equations 6-20, 6-21, 6-22 and 6-23
4. If it is a bar model, apply the weights, biases and sigmoid transfer function as seen in equation 6-2. The values of the weights and biases are seen in equations 6-24, 6-25, 6-26 and 6-27
5. Insert the above parameters into the governing equation relating the output(SCF) to the inputs(H_o,L/D, D/t, σy and P_{mean}) as shown in equation 6-4 to predict the normalised SCF.
6. De-normalise the value of SCF to get the actual SCF using equation 6-9.

7. Apply SCF with DOE-B curve to calculate the fatigue life

7.2 Proposed strain-based assessment procedure

Dent depth alone was used to measure dent severity in the past. ASME B31.8 code gave a recommendation that the total strain in the pipe could be a better measure of the dent severity. It proposed an equation as seen in equation 5-4 and 5-5 to calculate the maximum strain in the inner and outer walls of the pipe respectively. However, the proposed ASME equation only considers the geometric property of the pipe and dent. FEA studies in chapter 4 indicated that other parameter like pipe grade could influence the maximum strain in the pipe. The proposed method incorporates the influence of the pipe grade and is proposed to replace the ASME B31.8 equation. An ANN-based formula is used to predict the maximum strain in the pipe. The parameters used to train the network include D/t, H_o, L/D and σ_y. The pressure range was not included as part of the parameters. The strain data used in training the network was extracted from a prior finite element analysis done on a parametric range of industry pipe with different sizes and shapes of dents. The proposed ANN has 3 layers(input, hidden and output layer). The dome and the bar model has 10 and 15 processing elements respectively in the hidden layer. The sigmoid transfer function is used for both models. The following steps should be followed in order to use the ANN-based formula for strain-based assessment:

1. Determine the spring back dent depth H_o, the length of dent to diameter ratio (L/D), the diameter to thickness ratio (D/t) and the yield strength of the pipe.
2. Normalise the data using equation 6-9
3. If it is a dome model, apply the weights ,biases and sigmoid transfer function as seen in equation 6-2. The values of the weights and biases are seen in equations 6-28, 6-29, 6-30 and 6-31
4. If it is a bar model, apply the weights, biases and sigmoid transfer function as seen in equation 6-2. The values of the weights and biases are seen in equations 6-32, 6-33, 6-34 and 6-35
5. Insert the above parameters into the governing equation relating the output(maximum strain) to the inputs(H_o,L/D, D/t and σy) as shown in equation 6-4 to predict the normalised maximum strain.

6. De-normalise the value of strain to get the actual maximum strain using equation 6-9.

7.3 Summary and conclusion

The aim of this research is to provide an alternative and easier method for assessing dent severity in pipeline. Both the strain based and fatigue assessment was considered in this research. The SCF used in fatigue assessment was previously determined empirically or using finite element analysis which are expensive and time consuming. This research presents the ANN-based formula which eliminates the need for an expensive experimental program or extensive finite element analysis to calculate the SCF. The data used for training was gotten from an extensive finite element analysis that investigated the various parameters that affects the SCF in the pipe in a parametric study. The accuracy of the FEA model was determined by validating it with experimental data. The FE results were accurate with a maximum percentage error of 15%. The accuracy of the FE results raised confidence in the data used for training the ANN. ANN models were created for both dome and bar model. Both models showed good accuracy with the coefficient of variation (COV) of 4.7% for dome model and 3.5% for bar model. They both have a linear correlation of 0.99 which indicates that the models are quite accurate.

ANN-based formula was also used in strain-based assessment. It was used to predict the maximum strain in the dent. The training data was also gotten from a FE parametric study that included the study of the effect of pipe grades which was not considered by the ASME B31.8 formula. ANN Models were created for both the dome and the bar indenter. Both models showed good accuracy with a COV of 4.9% for dome model and 8.8% for bar. The linear correlation is 0.99 and 0.98 respectively which indicates they are quite accurate.

In conclusion, both the strain-based and fatigue ANN models have shown good accuracy and can be used to replace the current assessment methods. This will help save time and money in assessing dent in pipelines.

CHAPTER 8

CONCLUSION AND RECOMMENDATION FOR FURTHER STUDIES

8.1 Conclusion

Results have shown that some basic parameters influence the rerounding depth, stress concentration and strain in the dent. These parameters include dent geometry, pipe geometry, pipe material and pressure range.

Study of the pipe response to denting have shown that the pipe geometry influences both the spring back and rerounding of the dent. The ratio of the initial dent depth to the elastic spring back increases with increasing D/t. Similarly, the ratio of the measured dent depth to final dent depth (after pressurisation) increases with a corresponding increase in the D/t. The dent geometry also influenced the spring back and rerounding. The ratio of the initial dent to the measured dent is higher for longer dents compared to shorter dents. This is an indication that elastic recovery is higher in longer dents compared to shorter dents. However, the ratio of the measured depth to the final depth reduces as the dent depth increases. This clearly shows that deeper dents have less elastic recovery than shallow dents. From the study, it is seen that the ratio of the measured depth to the final depth is higher for longer dents compared to shorter dents. On the contrary to spring back, the ratio of the measured to final depths increases as the dent depth increases.

The study also indicated that both the ratio of the initial to the measured depth and the ratio of the measured depth to the final depth increases with increasing pipe grades. This confirms that pipes with lesser strength exhibit less elastic spring back and rerounding compared to pipes with higher material strength. These results were validated with experimental data and a good agreement was observed between them.

Results from the study of the effect of aforementioned parameters show that pipes with higher material strengths have higher notch stresses compared to the lower pipe grades. However, the ratio of the stress range over the pressure range $\Delta\sigma/\Delta p$ appears higher in the lower pipe grades compared to the higher pipe grades. The result also

show that the difference in SCF between pipe grades are smaller for pipes with smaller D/t. However, the difference in SCF between pipes grades increases as D/t increases further. It can also be seen from the result that the difference is more for 50%SMYS pressure range compared to the 72% SMYS range. It has also shown that Stress concentration increases with increasing pipe D/t ratio of equal dent depth and material grade. From the result, bar dents show higher stress concentration compared to dome dents of similar dent depth. It is also clear from the result that dent with higher dent depth exhibit higher stress concentration factor. Furthermore, it can be seen from the result that SCF is higher in the 50% SMYS pressure range compared to the 72% SMYS pressure range. The results were validated with both experimental data and analytical solutions. A good correlation was seen in both when compared to the FE results. This is an indication that the FE models were accurate and the data generated can be confidently used for the ANN application

Results from the strain study has shown that circumferential strains are higher in circumferential dents compared to longitudinal strains and reduce as the diameter to thickness ratio increases. As such, longitudinal strains are higher in longitudinal dent compared to circumferential strains and reduce as D/t increases. Results have also showed that the difference between the circumferential and longitudinal strain is higher in circumferential dent compared to that of the longitudinal dent. It has also shown that the total strain in a dent is higher in a longitudinal dent compared to a circumferential dent. As the dent depth increases, there is a corresponding increase in the strain for both dent models. Pipes with higher material grades exhibits higher strain and the difference in strain level gets smaller as the Diameter to thickness (D/t) increases. The results when compared to the ASME B31.8 equation shows similarity in patterns in regards to how the parameters affect the strain, however, the ASME equation under-predicted the strain. This could be attributed to that fact that the ASME equation does not consider plane strain state and also not considering radial components as pointed out by Noronha et al[21]. The FE results were further validated with the equation proposed by Noronha et al and a good correlation was seen between them

The data generated from the above studies were fed into an artificial neural network ANN. The network was used to predict the rerounding depth, SCF and the maximum strain in the dent. Two models each are created to predict for longitudinal and

circumferential dents. Each networks have one hidden layer. Different number of processing elements are varied for each result to determine the one that gives the best performance. The Levenberg-Marquardt function is used as it the most common training function and has be proven to give good fits. Two transfer functions (logarithmic sigmoid and hyperbolic tangent) is also varied to determine the one that gives the best fit. Each network has a model architecture consisting of three (3) layers; the input, hidden and output layers. The input layer consist of four variable parameters which include D/t, L/D, d/D% and SMYS.

For the rerounding prediction ANN analysis, the network architecture that gave the best performance for the dome model is the network with 10 processing elements and a tansig activation function. The network gave the minimal error with a coefficient of variation (COV) of 4.1 %. The linear correlation between ANN predicted reround depth and the FEA reround depth showed a good correlation with an R-square value of 0.99. Similarly for the bar model, the network with the best performance is the network with 15 hidden processing elements and a tansig activation function. The network has a mean square error value of 5.01E-06 and a coefficient of variation of 3.2. The linear regression between the predicted values and actual gives a good fit with R-square value of 0.99.

The same analysis was run to predict the SCF. For the dome model, the logsig activation function gave better performance with the best network having 5 hidden processing elements. The linear regression gives a good fit with an R-square value of 0.99 and a coefficient of variation of 4.7. The Bar model has a network with 5 processing elements and a logsig transfer function. This network has a mean squared error value of 8.86E-5. The linear regression gives good fit with an R-square value of 0.99 and a coefficient of variation of 3.5 %.

From the strain prediction study, the best network for the dome model is network with 10 processing elements and a logsig activation function. The network has a mean squared error value of 7.44 E-6. The regression is shown to give a good fit with an R-square value of 0.99 and a coefficient of variation of 4.9%. Similarly for the bar model, the network with the overall best performance has 15 processing element and logsig activation function. The means squared error of this network is 5.64 x 10-6 .The linear

correlation shows a good fit with an R-square value of 0.98 and coefficient of variation of 8.8%.

In general, all the ANN models have shown very good performance as they all show a COV of less than 10% and good R-squared value. These models will eliminate the need for running an extensive finite element study or setting up expensive experimental program to get the stress and strain data for a given dent. Once the variable parameters are known, these models are able to predict the result with minimal errors. By reason of its efficiency and possibly potential for further expansion, the technique will be attractive to pipeline operators to effectively determine the severity of dents in pipeline.

8.2 Limitations and recommendation for further studies

Because of the time constraint and availability of research, the accomplishment of set objectives is normally constrained. As such, it has not been possible to extensively investigate all areas of interest

The efficiency of the artificial neural network is determined by the amount of training data it has. In theory, the more the data, the better the prediction. One of the main objectives of this is to study how various parameters would affect the SCF, strain and rerounding. These parameters include: dent geometry, pipe geometry, pipe material and pressure cycling. The dent depth and the dent length have been used to characterise the dent geometry. However the dent width and acute angle of the dent could also influence the stress and the strain. The dent was measured up to 10% d/D because 10% is the maximum acceptable dent by industry standard. From this study, it is seen that a dent of 10% d/D might not potentially pose any danger to the pipeline. It recommended that the dent with an acute angle is studied to see its influence on the stresses and strain. Furthermore, it is recommended that dent depths greater than 10%d/D be studied to see its effect on the strain and stress. This will create a wider range of training data for the artificial neural network

This study has only considered four material grades for its analysis. It is recommended that more pipe grades are analysed to increase the data range required for training

Furthermore, pressure was applied up to 50% and 72%SMYS. A wider range of pressure cycles would increase the SCF data available for training. It is therefore recommended that a wider range of pressure cycles be considered for future research.

By including the above suggested parameters, a larger database of training, testing and validation data will be available and this well help improve the efficiencies of the models.

Furthermore, the Levenberg-Marquardt training algorithm was the only algorithm used in this study. There are several other training algorithms available in matlab that could be used to train the network. It recommended that some this training algorithms are considered for future studies

REFERENCES

1. Cosham, A. and P. Hopkins, *The effect of dents in pipelines—guidance in the pipeline defect assessment manual.* International Journal of Pressure Vessels and Piping, 2004. **81**(2): p. 127-139.

2. Race, J.M., *REPORT PREPARED FOR UKOPA.* 2008.

3. Rosenfeld, M.J., *Proposed new guidelines for ASME B31. 8 on assessment of dents and mechanical damage.* Gas Research Institute, 2001.

4. Belanos, S.P. and R.S. Ryan, *Dents in pipe.* Oil and Gas Journal, 1958. 56: p. 155-161.

5. Technology, B.F., *Dent Fatigue Life Assessment, DOT# 432 Closeout Report.* 2012.

6. Wang, K.C. and E.D. Smith, *The Effect of Mechanical Damage on Fracture Initiation in Line Pipe, Part I: Dents*1982: Energy, Mines and Resources Canada, Canada Centre for Mineral and Energy Technology.

7. Tyson, W.R. and K.C. Wang, *Effects of External Damage (Gouges and Dents) on Performance of Linepipe. A Review of Work at MTL, CANMET.* Canadian Centre for Mineral and Energy Technology (CANMET), Canada, Report MTL, 1988: p. 88-34.

8. Ong, L.S., A.K. Soh, and J.H. Ong, *Experimental and finite element investigation of a local dent on a pressurized pipe.* The Journal of Strain Analysis for Engineering Design, 1992. **27**(3): p. 177-185.

9. Bjørnøy, O.H., et al. *Residual Strength of Dented Pipelines DNV Test Results*. in *The Tenth International Offshore and Polar Engineering Conference*. 2000. International Society of Offshore and Polar Engineers.

10. Maxey, W.A., *Analysis made of outside-force damage to pipelines.* Oil Gas J.;(United States), 1987. **85**(20).

11. Rosenfeld, M.J. *Investigations of dent rerounding behavior*. in *The 1998 International Pipeline Conference, IPC. Part 1(of 2)*. 1998.

12. Lancaster, E.R. and S.C. Palmer. *Experimental study of strains caused by pressurisation of pipes with dents*. in *The Fourth International Offshore and Polar Engineering Conference*. 1994. International Society of Offshore and Polar Engineers.

13. Macdonald, K.A. and A. Cosham, *Best practice for the assessment of defects in pipelines–gouges and dents.* Engineering Failure Analysis, 2005. **12**(5): p. 720-745.

14. Kiefner, J.F. *Fracture initiation*. in *Paper G, Proceedings of the 4th Symposium on Line Pipe Research, Pipeline Research Committee of the American Gas Association, Dallas, Texas, USA, AGA Catalogue*. 1969.

15. Zarea, M., et al. *Numerical models for static denting and dynamic puncture of gas transmission linepipe and their validation*. in *International Pipeline Conference*. 1996.

16. Brooker, D.C., *Denting of pressurised pipelines under localised radial loading.* International journal of mechanical sciences, 2004. **46**(12): p. 1783-1805.

17. Alexander, C.R. and J.F. Kiefner. *Effects of smooth and rock dents on liquid petroleum pipelines*. in *1999 API Pipeline Conference, Dallas, Texas*. 1997.

18. Kiefner, J.F. and C.R. Alexander, *Repair of Pipeline Dents Containing Minor Scratches.* PRCI Report on Contract No. PR, 1999: p. 218-9508.

19. American Society of Mechanical Engineers, *Gas Transmission and Distribution Piping systems.* ASME B31.8, 2007.

20. Le Bastard, A.l. *Influence of internal pressure for depth measurement on a dent*. in *2006 International Pipeline Conference*. 2006. American Society of Mechanical Engineers.

21. Noronha Jr, D.B., et al., *Procedures for the strain based assessment of pipeline dents.* International Journal of Pressure Vessels and Piping, 2010. **87**(5): p. 254-265.

22. Noronha, D.B., et al. *The use of B-splines in the Assessment of strain levels associated with plain dents*. in *Proceedings of RPC2005, Rio pipeline conference and exposition, Rio de Janeiro, Brazil*. 2005.

23. Dawson, S.J., A. Russell, and A. Patterson. *Emerging techniques for enhanced assessment and analysis of dents*. in *2006 International Pipeline Conference*. 2006. American Society of Mechanical Engineers.

24. Alexander, C.R. *Analysis of dented pipeline considering constrained and unconstrained dent configurations*. in *1999 Energy Sources Technology Conference & Exhibition, Sheraton Astrodome Hotel, Houston, Texas*. 1999.

25. Fowler, J.R., et al., *Fatigue life of pipelines with dents and gouges subjected to cyclic internal pressure.* Petroleum Division (Publication) PD69, ASME, 1995: p. 17-35.

26. DIN2413, *Design of Steel pressure Pipe.* Deutshe Norm, 1993.

27. R.J.Bood, M.R.G., U. Marewski, P.Roovers, M. Steiner, M.Zaream, *EPRG Methods for Assessing the Tolerance and Resistance of Pipelines to External Damage Part 1 and 2.* R International, 1999.

28. DoE, O.I., *Guidance on Design and Construction.* London, April, 1984.

29. American Petroleum, I., *Recommended practice 2A: planning, designing, and constructing fixed offshore platforms*2003: American Petroleum Institute.

30. Rosenfeld, M.J., *Development of a Model for Fatigue Rating Shallow Unrestrained Dents.* PRCI/AGA Catalog, 1997(L51741).

31. Fowler, J.R., Katsounas A.T,Boubendier R.,, *Criteria for Dent Acceptabilily of Offshore Pipelines.* Pipeline research council international, PRCI Report PR-201-927, 1992.

32. Rosenfeld, M.J., *Guidelines for the Assessment of Dents on Welds.* PRCI Report on Contract No. PR, 1999: p. 218-9822.

33. Engineering ToolBox, E. *Strain life Fatigue Analysis*. 2008 [cited 2014 6th February]; Available from: http://www.fea-optimization.com/ETBX/strainlife_help.html.

34. Beller, M., C. Mattheck, and J. Zimmermann. *Stress concentrations in pipelines due to the presence of dents*. in *The First International Offshore and Polar Engineering Conference*. 1991. International Society of Offshore and Polar Engineers.

35. Rinehart, A.J. and P.B. Keating. *Predicting the fatigue life of long dents in petroleum pipelines*. in *ASME 2002 21st International Conference on Offshore Mechanics and Arctic Engineering*. 2002. American Society of Mechanical Engineers.

36. Keating, P.B. and R. Hoffmann, *Fatigue behavior of dented petroleum pipelines.* Texas A&M University Final Report to US Department of Transportation, 1997.

37. de Carvalho Pinheiro, B., I.P. Pasqualino, and S.r.B. da Cunha. *Stress concentration factors of dented pipelines*. in *2006 International Pipeline Conference*. 2006. American Society of Mechanical Engineers.

38. Dinovitzer, A., et al. *Geometric dent characterization*. in *2002 4th International Pipeline Conference*. 2002. American Society of Mechanical Engineers.

39. Kiefner, J.F. *Dealing with Low-Frequency-Welded ERW Pipe and Flash-Welded Pipe with Respect to HCA-Related Integrity Assessments*. in *ASME 2002 Engineering Technology Conference on Energy*. 2002. American Society of Mechanical Engineers.

40. Warman, D.J., et al. *Management of pipeline dents and mechanical damage in gas pipelines*. in *2006 International Pipeline Conference*. 2006. American Society of Mechanical Engineers.

41. Baker, M., *Dent Study-Final Report.* TTO Number 10, Integrity Management Program, Delivery Order DTRS56-02-D-70036, DOT Research and Special Programs Administration, Office of Pipeline Safety. 2004.

42. International, P. *TDW Unveills New Leakage Inspection Tools*. 2010 [cited 2014 26th January]; Available from: http://pipelinesinternational.com/news/tdw_unveils_new_leakage_inspection_tool/043974/.

43. Electric, G. *Geometry Assessment solutions*. 2014 [cited 2014 March 16th]; Available from: http://www.geenergy.com/products_and_services/services/pipeline_integrity_services/geometry_assessment_solutions.jsp.

44. International, P. *Design Improvement On a new Generation UT in-Line Inspection crack tool: A Case Study*. 2012 [cited 2014 12th March]; Available from: http://pipelinesinternational.com/news/design_improvements_on_a_new_generation_ut_in-line_inspection_crack_tool_a_/078989/.

45. Race, J.M., et al. *UKOPA dent assessment algorithms: a strategy for prioritising pipeline dents*. in *2010 8th International Pipeline Conference*. 2010. American Society of Mechanical Engineers.

46. Dinovitzer, A. *Dent Integrity Assessment*. in *API 54th Annual Pipeline Conference*. 2003.

47. Rosenfeld, M.J., et al. *Deterministic Assessment of Minor Mechanical Damage on Pipelines*. in *2006 International Pipeline Conference*. 2006. American Society of Mechanical Engineers.

48. Pu, Yongchang, and Ehsan Mesbahi. "Application of artificial neural networks to evaluation of the ultimate strength of steel panels." *Engineering Structures* 28.8 (2006): 1190-1196.

49. Stergiou, C.and Siganos D. 1996. *Introduction to neural networks* [Online]. Availableat :https://www.doc.ic.ac.uk/~nd/surprise_96/journal/vol4/cs11/report.html#Introduction to neural networks [Accessed: 25 July 2016].

50. Strandberg P.2014. Neural networks used for climate change calculations [Online]. Available at http://www.global-warming-and-the-climate.com/climate-forcing.htm [Accessed; 25 July 2016]

51. Technobium. 2016 .Stock market prediction using neuroph neural networks [Online]. Available at http://technobium.com/stock-market-prediction-using-neuroph-neural-networks/ [Accessed 25 July 2016]

52. Ansys Mechanical APDL [computer program].Ver 16, United states of America: sharcnet;2016

53. Specification, A.P.I., 2004. 5L, Specification for Line Pipe. *Edition March*.

54. Wang, R.Y., Kania, R., Arumugam, U. and Gao, M., 2012, September. A Combined Approach to Characterization of Dent with Metal Loss. In *2012 9th International Pipeline Conference* (pp. 209-216). American Society of Mechanical Engineers.

55. Rafi, A.N.M., Das, S., Ghaednia, H., Silva, J., Kania, R. and Wang, R., 2012. Revisiting ASME strain-based dent evaluation criterion. *Journal of Pressure Vessel Technology*, *134*(4), p.041101.

56. Tinacos, K., Cazenave, P., Gao, M., Krishnamurthy, R., Seman, D. and Jones, C., 2012, September. ILI Based Dent Screening and Strain Based Analysis. In *2012 9th International Pipeline Conference* (pp. 727-734). American Society of Mechanical Engineers.

57. Arumugam, U., Gao, M., Krishnamurthy, R., Wang, R. and Kania, R., 2012, September. Root Cause Analysis of Dent with Crack: A Case Study. In *2012 9th International Pipeline Conference* (pp. 735-746). American Society of Mechanical Engineers.

58. Kiefner, J.F., Kolovich, C., Kolovich, k., 2006, “Pipeline Incidents Caused by Mechanical Damage,” Presentation at the Mechanical Damage Technical Workshop,Houston, USA

59. Lukasiewicz, S.A., Czyz, J. A., Sun, C., Adeeb, S., 2006, “Calculation of Strains in dents based in High Resolution In-Line Caliper Survey,” ASME 6th International Pipeline Conference, Calgary, Alberta, Canada

60. Leis, B.N., Forte, T.P. and Zhu, X., 2004, January. Integrity analysis for dents in pipelines. In *2004 International Pipeline Conference* (pp. 1247-1258). American Society of Mechanical Engineers.

61. Leis, B.N., Bubenik, T.A., Francini, R.B., Nestleroth, J.B. and Davis, R.J., 2000. Recent Developments in Avoiding, Detecting, and Assessing Severity of Mechanical Damage. In *Pipeline Technology: Proceedings of the 3rd International Pipeline Technology Conference, Brugge, Belgium, May 21-24, 2000* (Vol. 1, p. 389). Gulf Professional Publishing.

62. Lukasiewicz, S.A., Czyz, J.A., Sun, C. and Adeeb, S., 2006, January. Calculation of strains in dents based on high resolution in-line caliper survey. In *2006 International Pipeline Conference* (pp. 129-134). American Society of Mechanical Engineers.

63. McCoy, J. and Ironside, S., 2004, January. Dent management program. In *2004 International Pipeline Conference* (pp. 1211-1217). American Society of Mechanical Engineers.

64. Ironside, S.D. and Carroll, L.B., 2002, January. Pipeline dent management program. In *2002 4th International Pipeline Conference* (pp. 1859-1864). American Society of Mechanical Engineers.

65. Hart, J.D., Powell, G.H., Maple, J.A., Stevick, G.R. and Norton, J.D., 1998, June. Fatigue damage calculations for a dented and ovalled section of the TransAlaska Pipeline System at Thompson Pass. In *1998 2nd International Pipeline Conference* (pp. 263-272). American Society of Mechanical Engineers.

66. Dinovitzer, A.S., Lazor, R.B., Walker, R. and Bayley, C., 1999, June. A pipeline dent assessment model. In *Proceedings of the 18th International Conference on OMAE* (pp. 11-16).

67. Dieter, G.E. and Bacon, D.J., 1986. *Mechanical metallurgy* (Vol. 3). New York: McGraw-Hill.

68. Dinovitzer, A., Bhatia, A., Walker, R. and Lazor, R., 2000, October. A Pipeline Dent Assessment Model Considering Localised Effects. In *2000 3rd International Pipeline Conference* (pp. V002T06A008-V002T06A008). American Society of Mechanical Engineers.

69. Davis, P.M., Dubois, J., Olcese, A., Uhlig, F., Larivé, J.F. and Martin, D.E., 2006. Performance of European cross-country oil pipelines. *Statistical summary of reported spillages*, *54*.

70. Czyz, J.A., Lukasiewicz, S.A., Sun, C. and Adeeb, S., 2008. Calculating dent strain. *Pipeline and Gas Technology*, *2*, pp.38-45.

71. Browne, D. and Hicks, R., 2005. UKOPA Pipeline Fault Database, Pipeline Product Loss Incidents (1962-2004). *Fourth Report of the UKOPA Fault Database Management Group prepared by Advantica for FDMG, UKOPA, UK*.

72. ASTM, A.E., 2003. 1049–Standard practices for cycle counting in fatigue analysis. *West Conshohocken (PA)*.

73. Boiler, A.S.M.E. and Code, P.V., 2010. Section VIII Division 1. *UG-126 Pressure Relief Valves to UG-129 Marking, ASME International, New York, NY*.

74. American Society of Mechanical Engineers, 1992. *Liquid Transportation Systems for Hydrocarbons, Liquid Petroleum Gas, Anhydrous Ammonia, and Alcohols: ASME B31. 4*. American Society of Mechanical Engineers.

75. Beuker, T. and Rahe, F., 2005. High-quality, smart pig dent inspection complies with rules for gas, liquid lines. *Pipeline & gas journal*, *232*(3), pp.40-44.

76. Clapham, L., Babbar, V. and Rubinshteyn, A., 2006, January. Understanding Magnetic Flux Leakage Signals from Dents. In *2006 International Pipeline Conference* (pp. 27-34). American Society of Mechanical Engineers.

77. EGIG *Gas pipeline incidents: 6th Report of the European Gas Incident Data Group, 2005*

78. Fowler, J. R. "Criteria for dent acceptability in offshore pipeline." In *Offshore Technology Conference*. Offshore Technology Conference, 1993.

79. Johnston, D.C. and Hrncir, T.G., Using In-line Inspection to Address Deformations Containing Near-neutral pH Stress Corrosion Cracking. 2002. *Calgary, Alta., Canada: American Society of Mechanical Engineers*.

80. Lyons, D., 2002. *Western European cross-country oil pipelines 30-year performance statistics*. CONCAWE.

81. Roovers, P., Bood, R., Galli, M., Marewski, U., Steiner, M. and Zaréa, M., 2000. EPRG methods for assessing the tolerance and resistance of pipelines to external damage. *Pipeline technology*, *2*, pp.405-425.

82. Rosenfeld, M.J., Porter, P.C. and Cox, J.A., 1998, June. Strain estimation using Vetco deformation tool data. In *1998 2nd International Pipeline Conference* (pp. 389-397). American Society of Mechanical Engineers

83. Rosenfeld, M.J., 2001. *Proposed New Guidelines for ASME B31. 8 on Assessment of Dents and Mechanical Damage: Topical Report*. Gas Research Institute.

84. Rosenfeld, M.J., Pepper, J.W. and Leewis, K., 2002, January. Basis of the new criteria in ASME B31. 8 for prioritization and repair of mechanical damage. In *2002 4th International Pipeline Conference* (pp. 647-658). American Society of Mechanical Engineers.

85. Stevick, G.R., Hart, J.D. and Flanders, B., 1998, June. Fatigue curves for damage calculations for a dented and ovalled section of the TransAlaska Pipeline System. In *1998 2nd International Pipeline Conference* (pp. 273-278). American Society of Mechanical Engineers.

86. Standard, A.P.I., 2001. 1160 Managing System Integrity for Hazardous Liquid Pipelines. *Firs Edition, November*.

87. Hopkins, P., Jones, D.G. and Clyne, A., 1989, February. The significance of dents and defects in transmission pipelines. In *International Conference on Pipework Engineering and Operations, London* (pp. 137-145).

88. Eiber, R.J., 1981. *The Effects of Dents on Failure Characteristics of Line Pipe*. American Gas Assn.

89. Eiber, R.J., 1979. Causes of pipeline failures probed. *Oil and Gas J.*, *77*(52), pp.80-88.

90. Edward, D.C., 1988. A theoretical analysis of the formation of dents in pipeline under station condition. *British Gas. Engineering Research Station, Report*, *4080*.

91. Hopkins, P. and Corbin, P., 1988, September. A study of external damage of pipelines. In *Seventh american gas association symposium, Calgary, Alberta, Canada*.

92. Hopkins, P., JONES, D. and Clyne, A., 1983. Recent studies of the significance of mechanical damage in pipelines.

93. Wang, S.C., 2003. Artificial neural network. In *Interdisciplinary computing in java programming* (pp. 81-100). Springer US.

94. Hepner, G. F. (1990). Artificial neural network classification using a minimal training set. Comparison to conventional supervised classification. *Photogrammetric Engineering and Remote Sensing*, *56*(4), 469-473.

95. Hill, T., Marquez, L., O'Connor, M. and Remus, W., 1994. Artificial neural network models for forecasting and decision making. *International journal of forecasting*, *10*(1), pp.5-15.

96. Dreiseitl, S. and Ohno-Machado, L., 2002. Logistic regression and artificial neural network classification models: a methodology review. *Journal of biomedical informatics*, *35*(5), pp.352-359.

97. Elhewy, A.H., Mesbahi, E. and Pu, Y., 2006. Reliability analysis of structures using neural network method. *Probabilistic Engineering Mechanics*, *21*(1), pp.44-53.

98. Hopkins, P., Corder, I. and Corbin, P., 1992, June. The resistance of gas transmission pipelines to mechanical damage. In *International Conference on Pipeline Reliability.* (Vol. 2, p. 1992).

99. Hertz-Clémens, S., 2006, January. Experimental and Numerical Modelling of Pipeline Denting. In *2006 International Pipeline Conference* (pp. 171-179). American Society of Mechanical Engineers.

100. Karamanos, S.A. and Andreadakis, K.P., 2006. Denting of internally pressurized tubes under lateral loads. *International Journal of Mechanical Sciences*, *48*(10), pp.1080-1094.

101. Gresnigt, A.M., Karamanos, S.A. and Andreadakis, K.P., 2007. Lateral loading of internally pressurized steel pipes. *Journal of Pressure Vessel Technology*, *129*(4), pp.630-638.

102. Hopkins, P., 1992, April. The application of fitness for purpose methods to defects detected in offshore transmission pipelines. In *Conference on welding and weld performance in the process industry, London* (pp. 27-28).

103. Gao, M., McNealy, R., Krishnamurthy, R. and Colquhoun, I., 2008, January. Strain-based models for dent assessment: a review. In *2008 7th International Pipeline Conference* (pp. 823-830). American Society of Mechanical Engineers.

104. FEA for all. 2013. What is an FEA solver? [Online]. Available at http://feaforall.com/what-is-an-fea-solver/# [accessed 27 February 2017]

105. Fowler, J.R., Alexander, C.R., Kovach, P.J. and Connelly, L.M., 1994. *Cyclic Pressure Fatigue Life of Pipelines With Plain Dents, Dents With Gouges, and Dents With Welds* (No. AGA--94015627). American Gas Association, Inc., Arlington, VA (United States); Stress Engineering Services, Inc., Houston, TX (United States).

106.] Durowoju, M, Pu, Y, Benson, S & Race, J 2016, 'Fatigue assessment of pipeline with plain dents under cyclic pressure loading using finite element method' pp. 1-10.

APPENDICES

Appendix A Spring Back Result

This section shows the table comparing the ratio of the initial dent depth (H_i) to the spring back depth (H_o)for all pipe grades and diameter to thickness ratio (D/t). It shows the comparison for both the dome and bar models. It also shows the other graphs showing the effect of dent geometry, pipe geometry and pipe grade on the spring back depth of dents as discussed in chapter 3.

DOME

d/D (%)	D/t	X46			X65			X80			X100		
		H_i (%)	H_o (%)	H_i/H_o	H_i (%)	H_o (%)	H_i/H_o	H_i (%)	H_o (%)	H_i/H_o	H_i (%)	H_o (%)	H_i/H_o
2	18.6	2.78	1.90	1.46	2.78	1.60	1.74	3.71	2.30	1.61	4.02	2.30	1.75
	25	2.78	1.80	1.55	3.40	2.00	1.70	4.64	1.60	2.90	4.33	2.30	1.88
	32	3.40	2.20	1.55	3.40	1.80	1.89	4.02	2.20	1.83	4.02	1.80	2.23
	40	3.09	1.70	1.82	3.40	1.60	2.12	4.33	2.20	1.97	4.64	2.00	2.32
	50	3.09	1.80	1.72	3.71	1.60	2.32	4.94	2.30	2.15	4.94	1.90	2.60
	62	3.09	1.80	1.72	5.25	2.50	2.10	5.25	2.20	2.39	5.87	2.10	2.80
	80	3.09	2.20	1.40	5.56	2.30	2.42	6.80	2.60	2.61	5.25	1.30	4.04
	96	2.78	1.90	1.46	5.87	2.10	2.80	6.80	2.60	2.61	6.49	1.60	4.06
5	18.6	5.87	4.90	1.20	6.18	4.50	1.37	6.49	5.00	1.30	8.03	5.80	1.39
	25	7.11	5.70	1.25	6.49	4.60	1.41	7.11	5.40	1.32	8.34	5.70	1.46
	32	5.56	4.30	1.29	6.80	4.60	1.48	7.11	5.00	1.42	8.03	5.00	1.61
	40	7.11	5.30	1.34	7.11	4.60	1.55	8.03	5.10	1.58	8.96	5.30	1.69
	50	6.49	4.40	1.47	7.42	4.70	1.58	8.96	5.50	1.63	8.96	4.90	1.83
	62	7.11	5.00	1.42	8.34	4.80	1.74	10.20	5.80	1.76	10.20	5.00	2.04
	80	7.73	4.60	1.68	10.51	5.50	1.91	11.43	5.50	2.08	11.43	4.70	2.43
	96	9.27	4.90	1.89	11.74	5.60	2.10	12.98	5.60	2.32	11.43	3.90	2.93
7	18.6	8.03	7.20	1.12	8.65	7.00	1.24	9.89	7.80	1.27	10.51	7.90	1.33
	25	8.03	6.90	1.16	8.96	7.30	1.23	9.89	7.50	1.32	10.51	7.50	1.40
	32	7.42	6.00	1.24	8.96	6.60	1.36	9.58	7.20	1.33	10.51	7.10	1.48

	40	8.65	6.70	1.29	9.58	6.90	1.39	10.82	7.40	1.46	11.43	7.30	1.57
	50	9.58	7.00	1.37	9.89	6.60	1.50	11.74	7.70	1.52	11.74	6.90	1.70
	62	10.20	6.90	1.48	11.12	6.90	1.61	12.98	7.70	1.69	13.29	7.10	1.87
	80	11.43	7.00	1.63	12.67	7.00	1.81	14.21	7.50	1.90	14.52	6.50	2.23
	96	12.36	7.00	1.77	15.14	7.60	1.99	16.69	7.70	2.17	16.07	6.20	2.59
10	18.6	10.51	9.60	1.09	10.82	9.10	1.19	11.74	10.20	1.15	13.60	10.80	1.26
	25	10.82	9.50	1.14	12.36	10.10	1.22	13.29	10.80	1.23	14.52	11.00	1.32
	32	10.82	9.10	1.19	12.67	9.90	1.28	13.60	10.50	1.29	14.21	10.20	1.39
	40	12.67	10.30	1.23	12.67	9.60	1.32	14.52	10.50	1.38	14.21	9.60	1.48
	50	12.36	9.40	1.31	13.91	9.90	1.40	15.76	10.80	1.46	15.14	9.50	1.59
	62	13.60	9.70	1.40	15.76	10.50	1.50	17.30	10.60	1.63	16.69	9.40	1.78
	80	15.14	9.80	1.55	17.00	10.00	1.70	18.85	10.60	1.78	18.85	9.10	2.07
	96	16.38	9.90	1.65	19.78	10.80	1.83	21.94	11.30	1.94	23.18	10.10	2.29

BAR

d/D (%)	D/t	X46			X65			X80			X100		
		H_i (%)	H_o (%)	H_i/H_o	H_i (%)	H_o (%)	H_i/H_o	H_i (%)	H_o (%)	H_i/H_o	H_i (%)	H_o (%)	H_i/H_o
2	18.6	3.40	1.80	1.89	4.02	1.90	2.11	4.33	1.90	2.28	4.33	1.50	2.88
	25	4.02	1.90	2.11	4.64	1.90	2.44	4.94	1.80	2.75	5.25	1.70	3.09
	32	4.64	2.10	2.21	5.25	1.90	2.76	5.87	2.00	2.94	6.18	1.80	3.43
	40	5.25	2.10	2.50	5.87	1.90	3.09	6.49	1.90	3.42	7.42	2.00	3.71
	50	5.56	1.90	2.93	6.49	1.80	3.61	7.42	1.90	3.90	8.34	1.90	4.39
	62	6.80	2.20	3.09	7.73	1.90	4.07	8.96	2.10	4.27	9.27	1.80	5.15
	80	7.11	1.60	4.44	9.58	2.10	4.56	10.82	2.10	5.15	10.82	1.60	6.76
	96	8.34	1.80	4.64	11.74	2.40	4.89	12.36	1.90	6.51	12.05	1.50	8.03
5	18.6	6.80	5.00	1.36	7.11	4.70	1.51	8.03	5.30	1.52	8.03	4.60	1.75
	25	7.11	4.80	1.48	7.73	4.70	1.64	8.65	5.00	1.73	9.58	5.00	1.92
	32	8.03	5.10	1.58	8.65	4.80	1.80	9.58	5.00	1.92	11.12	5.30	2.10
	40	8.96	5.30	1.69	9.58	4.80	2.00	10.51	4.90	2.14	12.36	5.30	2.33
	50	9.27	4.80	1.93	10.82	4.70	2.30	12.67	5.40	2.35	14.21	5.10	2.79

	62	10.82	5.10	2.12	12.98	5.30	2.45	15.14	6.00	2.52	14.83	4.50	3.30
	80	11.74	4.60	2.55	14.83	5.30	2.80	17.30	5.60	3.09	17.30	4.60	3.76
	96	13.60	5.10	2.67	16.07	5.20	3.09	18.85	5.90	3.19	18.85	4.40	4.28
7	18.6	8.96	7.10	1.26	8.96	6.50	1.38	10.20	7.30	1.40	10.82	7.10	1.52
	25	9.89	7.40	1.34	9.89	6.70	1.48	10.82	7.00	1.55	12.05	7.20	1.67
	32	10.51	7.40	1.42	10.20	6.20	1.64	11.74	6.90	1.70	13.29	7.10	1.87
	40	11.12	7.30	1.52	12.05	7.00	1.72	13.60	7.50	1.81	14.52	7.00	2.07
	50	11.12	6.30	1.77	13.60	7.20	1.89	15.45	7.80	1.98	17.00	7.00	2.43
	62	13.29	7.30	1.82	14.52	6.80	2.14	16.38	7.30	2.24	17.30	6.30	2.75
	80	13.91	6.30	2.21	17.30	7.70	2.25	17.92	6.70	2.67	19.78	6.30	3.14
	96	15.45	6.80	2.27	18.85	7.50	2.51	21.01	7.60	2.76	23.48	7.30	3.22
10	18.6	12.36	10.50	1.18	12.36	9.80	1.26	12.36	9.50	1.30	13.91	10.00	1.39
	25	12.05	9.60	1.26	13.60	10.20	1.33	13.60	9.70	1.40	15.45	10.20	1.51
	32	13.29	10.10	1.32	14.83	10.60	1.40	14.83	9.90	1.50	17.00	10.40	1.63
	40	14.52	10.60	1.37	13.91	8.70	1.60	16.69	10.60	1.57	18.23	10.20	1.79
	50	16.07	11.40	1.41	15.45	9.10	1.70	18.23	11.00	1.66	20.39	9.70	2.10
	62	15.45	9.60	1.61	17.30	9.80	1.77	20.09	11.20	1.79	21.63	10.30	2.10
	80	17.92	10.50	1.71	19.78	10.00	1.98	22.25	10.60	2.10	23.18	9.00	2.58
	96	19.78	11.00	1.80	22.87	11.00	2.08	25.96	11.40	2.28	27.81	10.50	2.65

A.1 Effect of pipe goemtery on spring back

A.1.1 Effect on circumferential dents

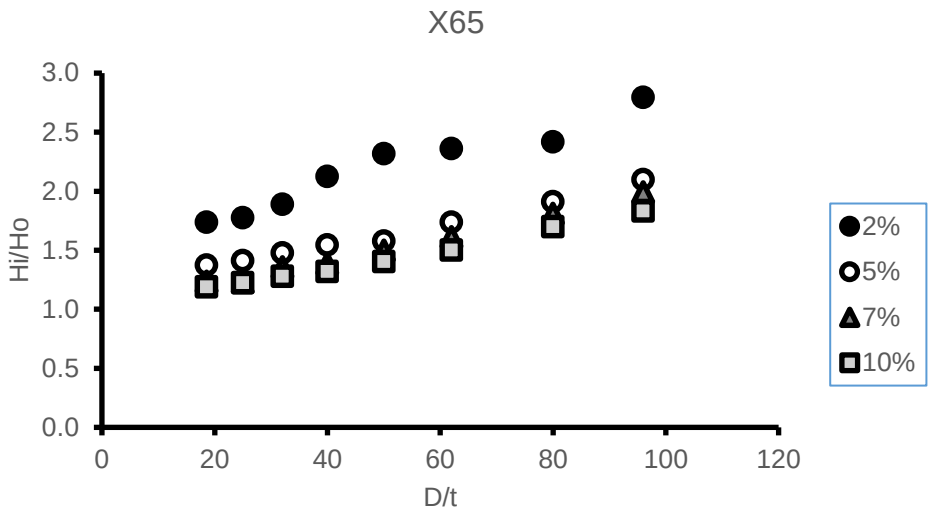

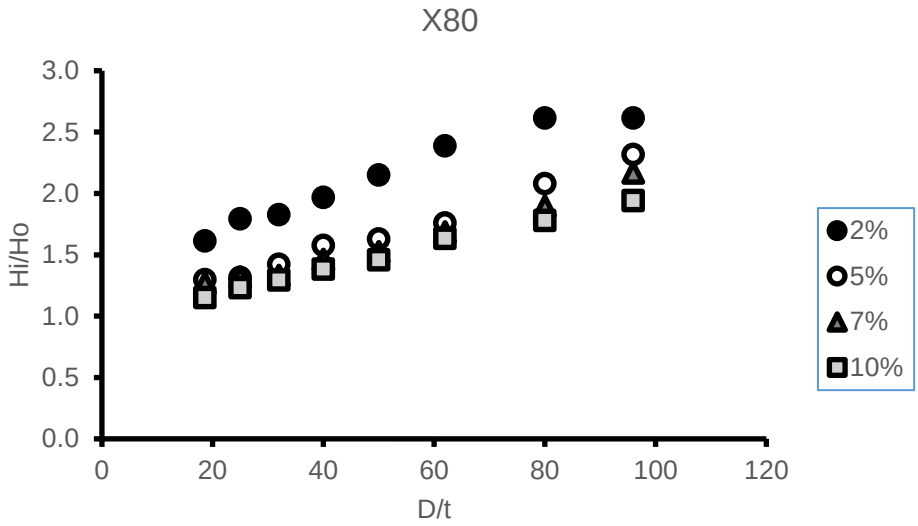

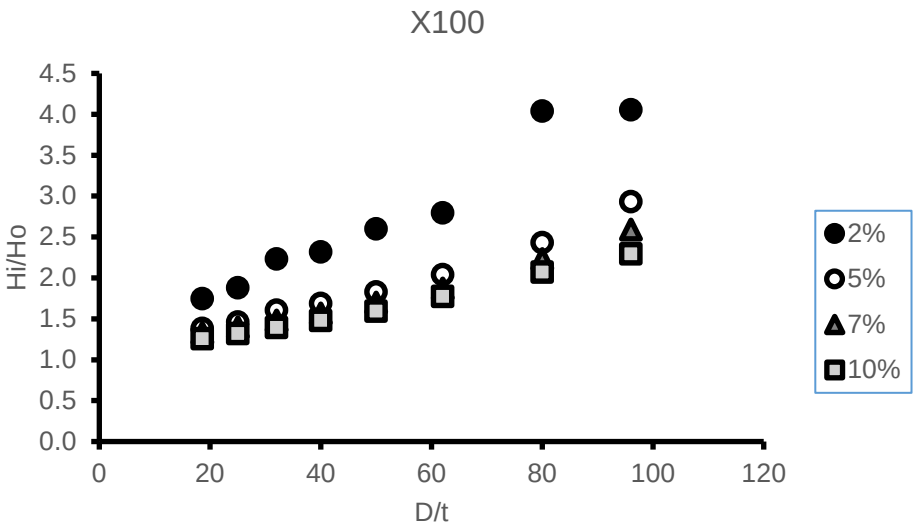

A.1.2 Effect on longitudinal dents

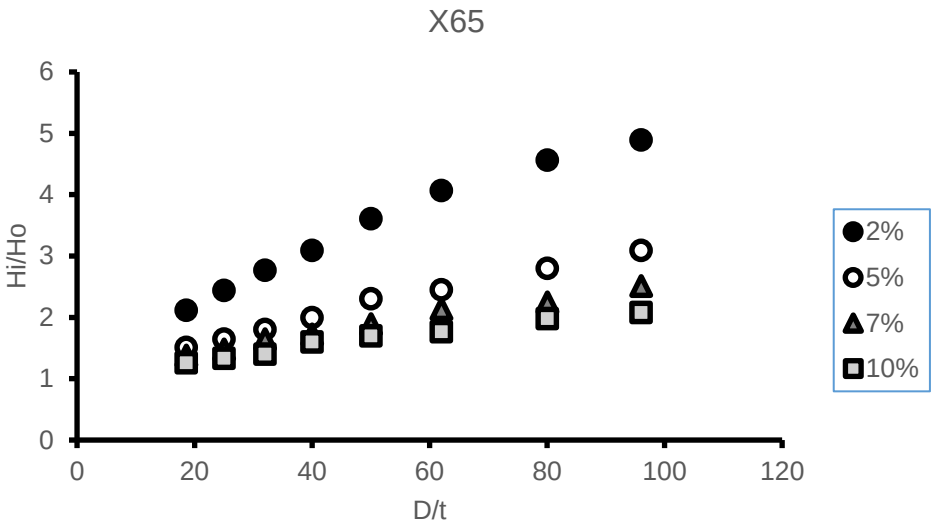

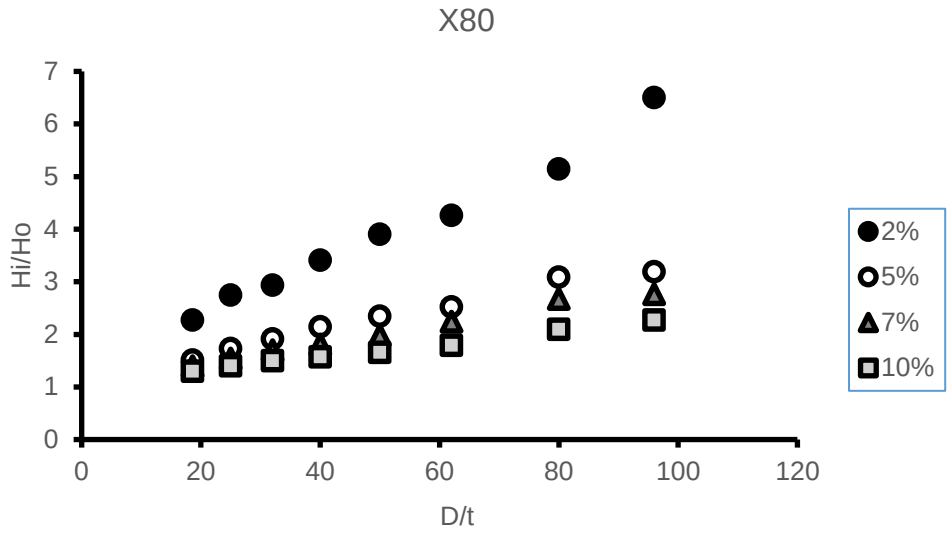
X80
Hi/Ho
D/t
0
1
2
3
4
5
6
7
0
20
40
60
80
100
120
2%
5%
7%
10%

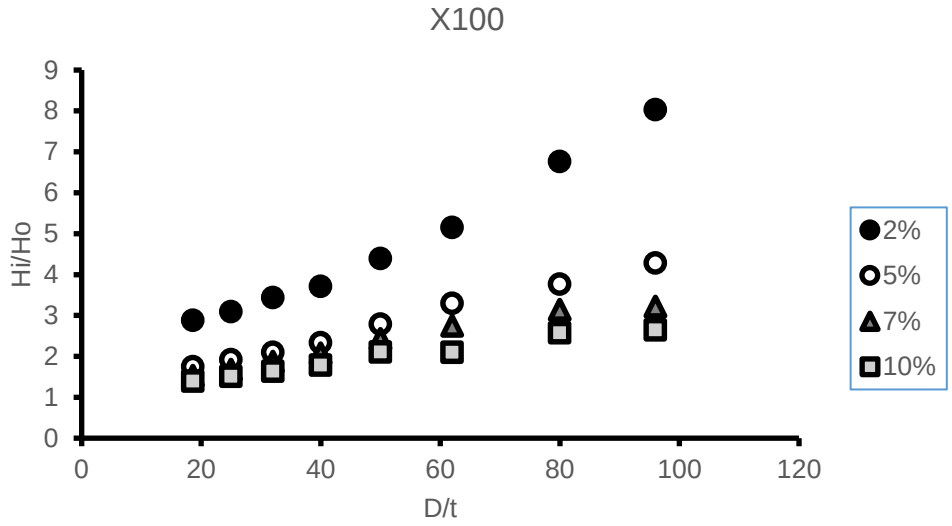
X100
Hi/Ho
D/t
0
1
2
3
4
5
6
7
8
9
0
20
40
60
80
100
120
2%
5%
7%
10%

A.2 Effect of dent goemtery on spring back

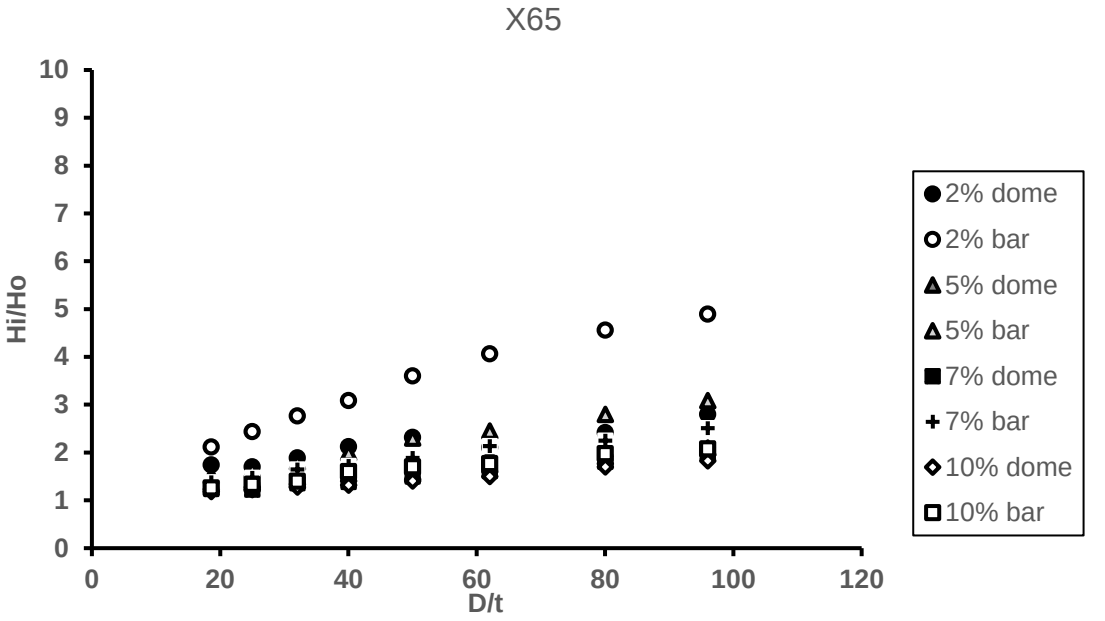

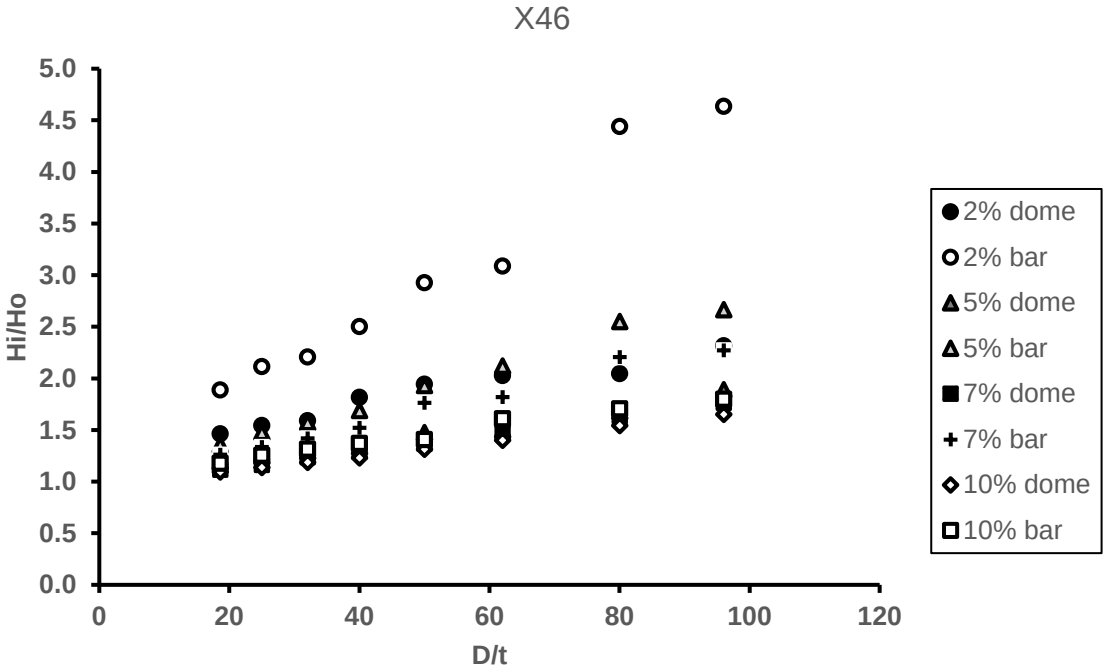

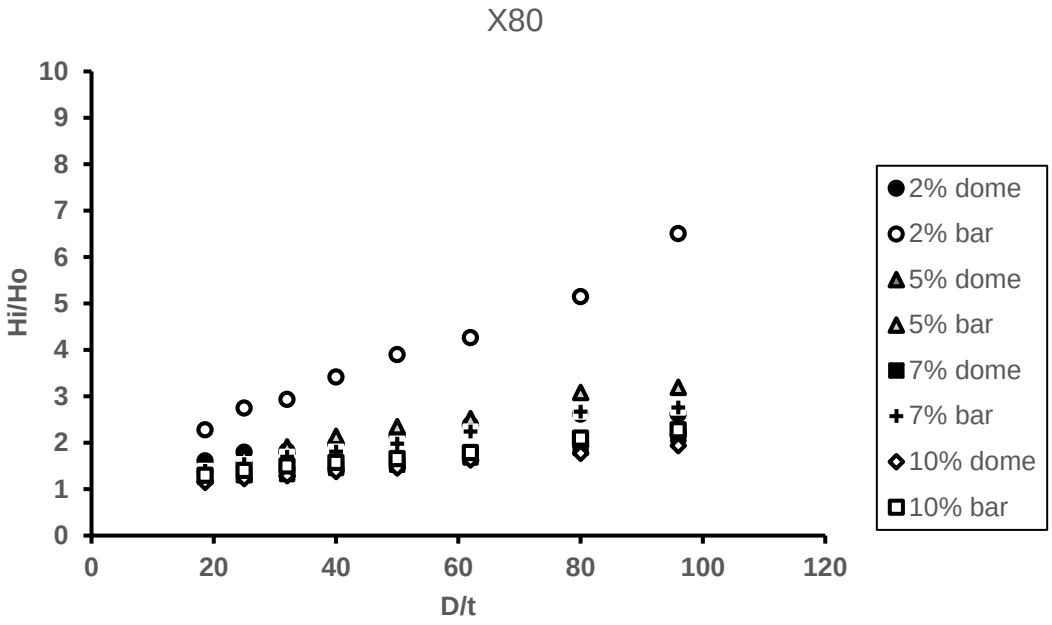

A.3 Effect of pipe grades on spring back

A.3.1 Effect on circumferential dents

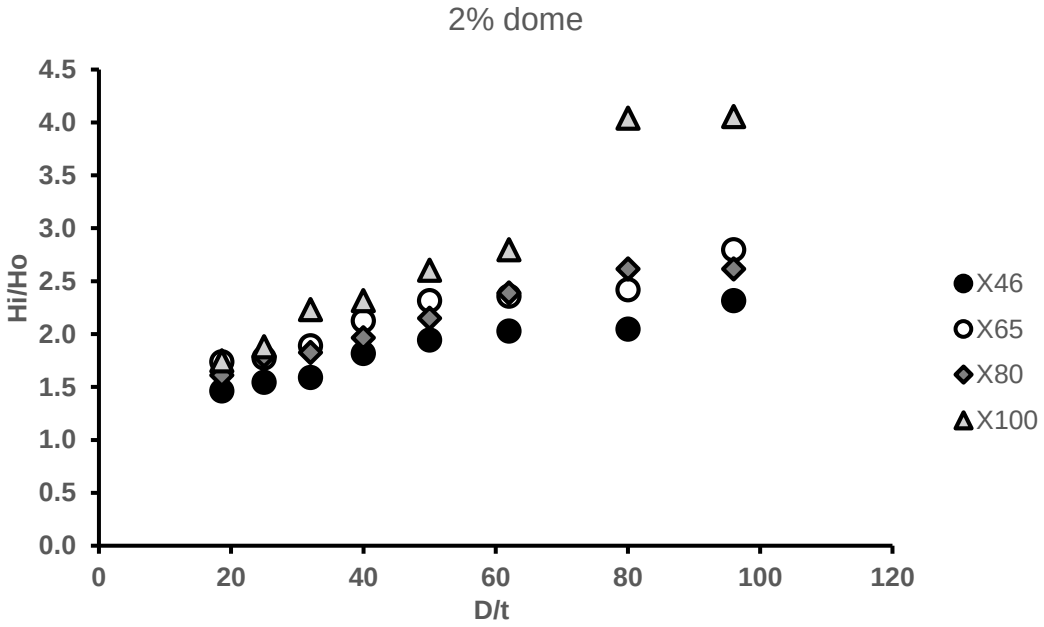

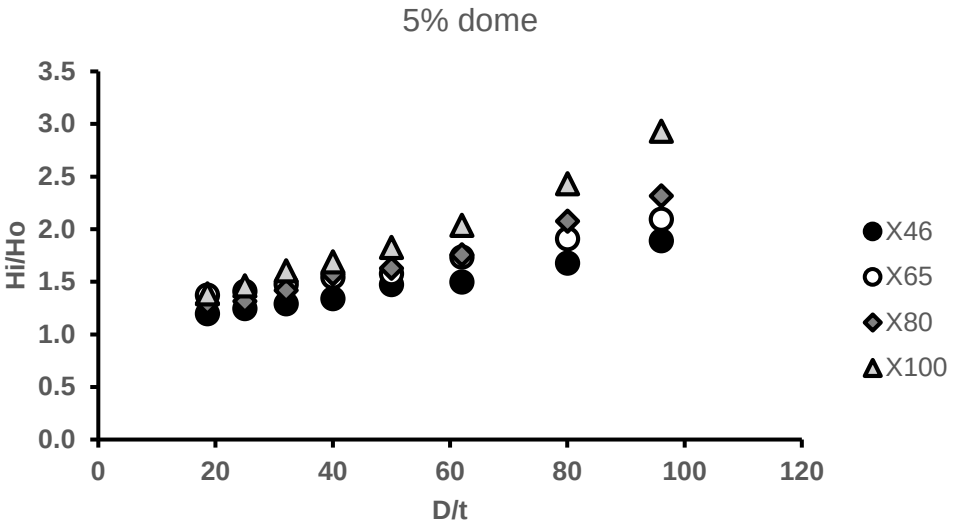
5% dome
Hi/Ho
3.5
3.0
2.5
2.0
1.5
1.0
0.5
0.0
0
20
40
60
80
100
120
D/t
X46
X65
X80
X100

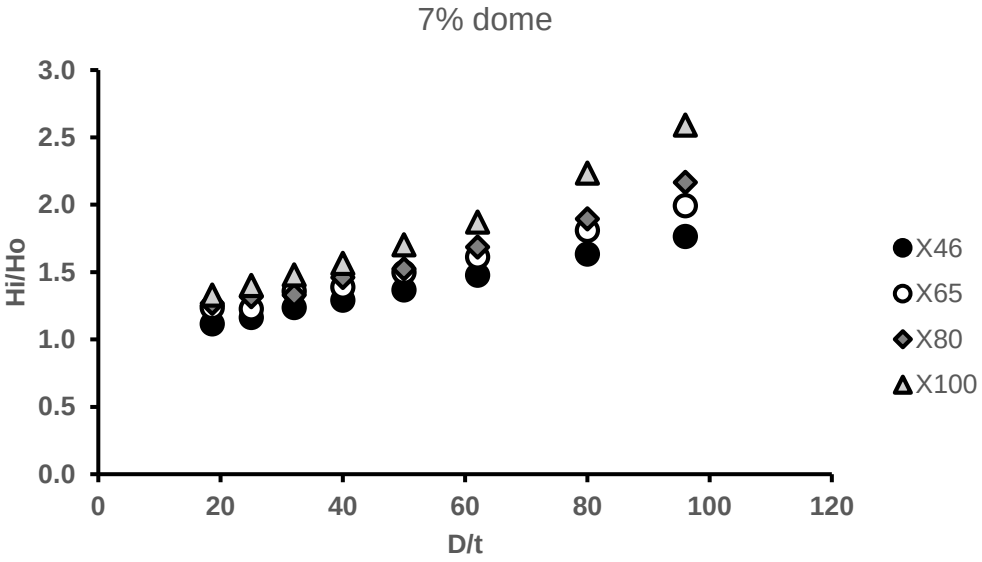
7% dome
Hi/Ho
3.0
2.5
2.0
1.5
1.0
0.5
0.0
0
20
40
60
80
100
120
D/t
X46
X65
X80
X100

A.3.2 Effect on longitudinal dents

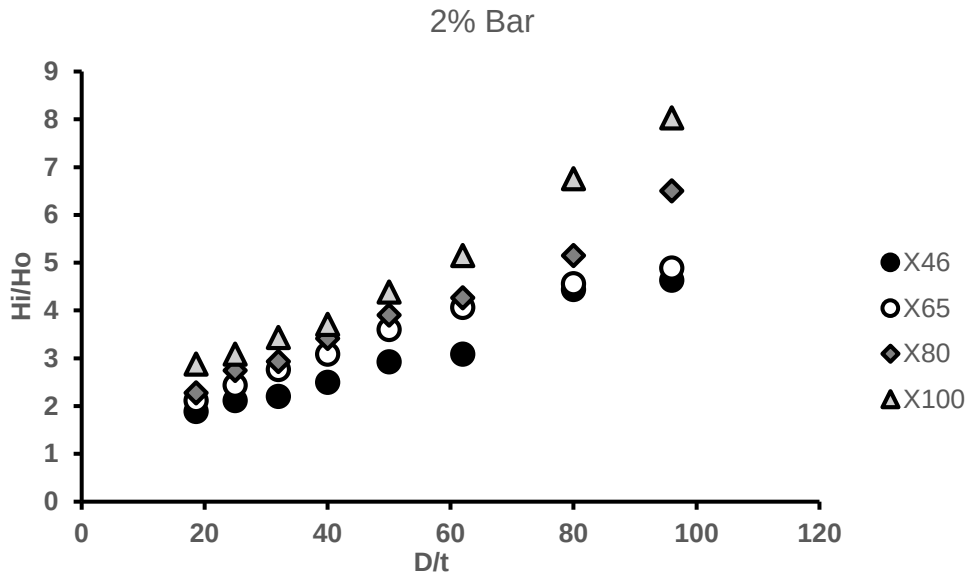

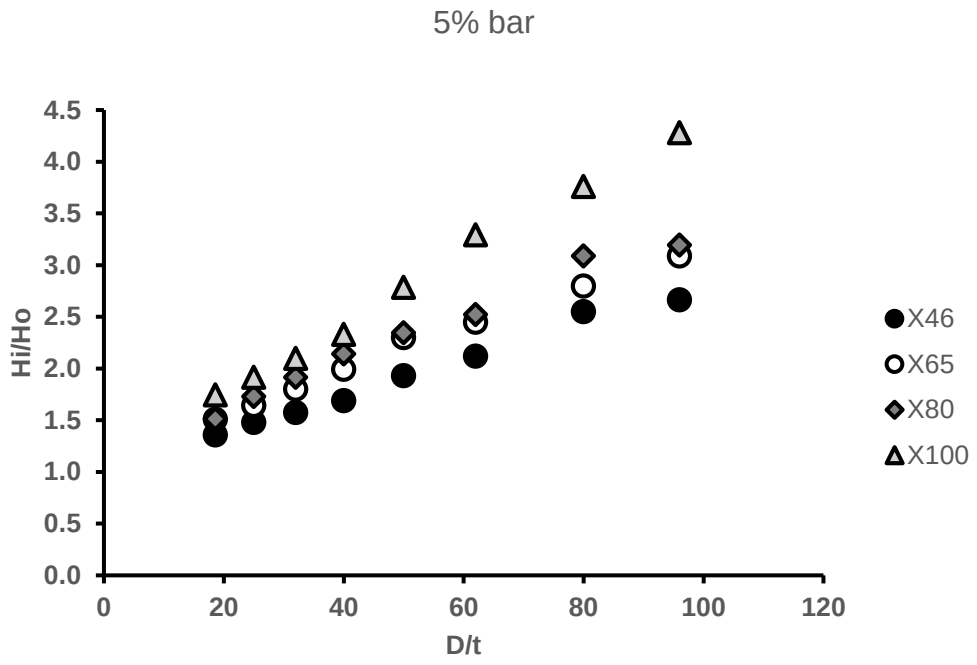

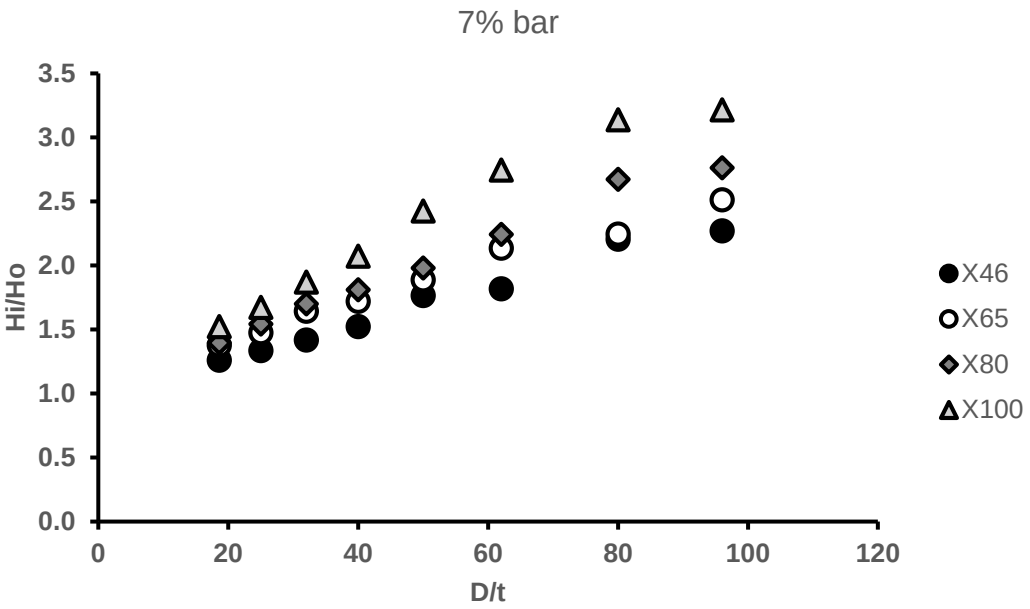
7% bar
3.5
3.0
2.5
2.0
1.5
1.0
0.5
0.0
Hi/Ho
0
20
40
60
80
100
120
D/t
X46
X65
X80
X100

Appendix B Rerounding Result

This section shows the table comparing the ratio of the measured(spring back) dent depth (H_o) to the reround depth (H_r)for all pipe grades and diameter to thickness ratio (D/t). it shows the comparison for both the dome and bar models. It also shows the other graphs showing the effect of dent geometry, pipe geometry and pipe grade on the reround depth of dents as discussed in chapter 3.

Dome models

d/D (%)	D/t	X46			X65			X80			X100		
		H_o	H_f	H_o/H_f	H_o	H_f	H_o/H_f	H_o	H_f	H_o/H_f	H_o	H_f	H_o/H_f
2	18.6	1.90	1.70	1.12	1.60	1.50	1.07	2.30	2.10	1.10	2.30	2.00	1.15
	25	1.80	1.60	1.13	2.00	1.80	1.11	1.60	1.40	1.14	2.30	1.90	1.21
	32	2.20	1.90	1.16	1.80	1.40	1.29	2.20	1.80	1.22	1.80	1.40	1.29
	40	1.70	1.40	1.21	1.60	1.30	1.23	2.20	1.70	1.29	2.00	1.40	1.43
	50	1.80	1.40	1.29	1.60	1.20	1.33	2.30	1.70	1.35	1.90	1.30	1.46
	62	1.80	1.30	1.38	2.50	1.60	1.56	2.20	1.40	1.57	2.10	1.20	1.75
	80	2.20	1.40	1.57	2.30	1.80	1.28	2.60	1.40	1.86	1.30	0.70	1.86
	96	1.90	1.10	1.73	2.10	1.10	1.91	2.60	1.10	2.36	1.60	0.70	2.29
5	18.6	4.90	4.40	1.11	4.50	4.00	1.13	5.00	4.40	1.14	5.80	4.70	1.23
	25	5.70	4.70	1.21	4.60	3.80	1.21	5.40	4.00	1.35	5.70	4.20	1.36
	32	4.30	3.40	1.26	4.60	2.70	1.70	5.00	3.70	1.35	5.00	3.30	1.52
	40	5.30	3.70	1.43	4.60	3.20	1.44	5.10	3.40	1.50	5.30	2.90	1.83
	50	4.40	2.90	1.52	4.70	2.80	1.68	5.50	3.10	1.77	4.90	2.30	2.13
	62	5.00	2.60	1.92	4.80	2.50	1.92	5.80	2.60	2.23	5.00	1.90	2.63
	80	4.60	2.10	2.19	5.50	2.10	2.62	5.50	2.00	2.75	4.70	1.40	3.36
	96	4.90	1.80	2.72	5.60	1.90	2.95	5.60	1.70	3.29	3.90	1.60	2.44
7	18.6	7.20	6.20	1.16	7.00	5.90	1.19	7.80	6.50	1.20	7.90	6.10	1.30
	25	6.90	5.50	1.25	7.30	5.40	1.35	7.50	5.70	1.32	7.50	5.10	1.47
	32	6.00	4.40	1.36	6.60	3.00	2.20	7.20	4.80	1.50	7.10	4.20	1.69
	40	6.70	4.20	1.60	6.90	3.90	1.77	7.40	4.20	1.76	7.30	3.50	2.09
	50	7.00	3.70	1.89	6.60	3.30	2.00	7.70	3.50	2.20	6.90	2.80	2.46
	62	6.90	3.10	2.23	6.90	2.90	2.38	7.70	3.00	2.57	7.10	2.30	3.09

	80	7.00	2.50	2.80	7.00	2.40	2.92	7.50	2.40	3.13	6.50	1.70	3.82
	96	7.00	2.10	3.33	7.60	2.20	3.45	7.70	2.10	3.67	6.20	1.40	4.43
10	18.6	9.60	7.90	1.22	9.10	7.10	1.28	10.20	8.10	1.26	10.80	7.70	1.40
	25	9.50	6.90	1.38	10.10	6.40	1.58	10.80	7.20	1.50	11.00	6.40	1.72
	32	9.10	5.70	1.60	9.90	3.00	3.30	10.50	5.80	1.81	10.20	5.00	2.04
	40	10.30	5.20	1.98	9.60	4.40	2.18	10.50	4.90	2.14	9.60	4.00	2.40
	50	9.40	4.20	2.24	9.90	3.80	2.61	10.80	4.10	2.63	9.50	3.20	2.97
	62	9.70	3.60	2.69	10.50	3.40	3.09	10.60	3.50	3.03	9.40	2.60	3.62
	80	9.80	3.00	3.27	10.00	2.80	3.57	10.60	2.90	3.66	9.10	2.10	4.33
	96	9.90	2.80	3.54	10.80	2.90	3.72	11.30	2.80	4.04	10.10	2.20	4.59

Bar models

d/D (%)	D/t	X46			X65			X80			X100		
		H_o	H_f	H_o/H_f	H_o	H_f	H_o/H_f	H_o	H_f	H_o/H_f	H_o	H_f	H_o/H_f
2	18.6	1.80	1.40	1.29	1.90	1.50	1.27	1.90	1.50	1.27	1.50	1.10	1.36
	25	1.90	1.50	1.27	1.90	1.40	1.36	1.80	1.30	1.38	1.70	1.10	1.55
	32	2.10	1.40	1.50	1.90	1.30	1.46	2.00	1.40	1.43	1.80	1.10	1.64
	40	2.10	1.40	1.50	1.90	1.20	1.58	1.90	1.20	1.58	2.00	1.10	1.82
	50	1.90	1.20	1.58	1.80	1.10	1.64	1.90	1.10	1.73	1.90	1.10	1.73
	62	2.20	1.30	1.69	1.90	1.10	1.73	2.10	1.20	1.75	1.80	0.90	2.00
	80	1.60	0.90	1.78	2.10	1.10	1.91	2.10	1.20	1.75	1.60	0.80	2.00
	96	1.80	1.00	1.80	2.40	1.40	1.71	1.90	1.10	1.73	1.50	0.80	1.88
5	18.6	5.00	3.60	1.39	4.70	3.30	1.42	5.30	3.50	1.51	4.60	2.90	1.59
	25	4.80	3.10	1.55	4.70	2.90	1.62	5.00	2.90	1.72	5.00	2.70	1.85
	32	5.10	2.80	1.82	4.80	2.70	1.78	5.00	2.70	1.85	5.30	2.60	2.04
	40	5.30	2.80	1.89	4.80	2.50	1.92	4.90	2.50	1.96	5.30	2.50	2.12
	50	4.80	2.50	1.92	4.70	2.50	1.88	5.40	2.60	2.08	5.10	2.30	2.22
	62	5.10	2.50	2.04	5.30	2.60	2.04	6.00	2.60	2.31	4.50	2.10	2.14
	80	4.60	2.30	2.00	5.30	2.40	2.21	5.60	2.40	2.33	4.60	1.90	2.42
	96	5.10	2.40	2.13	5.20	2.20	2.36	5.90	2.30	2.57	4.40	1.80	2.44

7	18.6	7.10	4.60	1.54	6.50	4.10	1.59	7.30	4.30	1.70	7.10	4.00	1.78
	25	7.40	4.10	1.80	6.70	3.60	1.86	7.00	3.70	1.89	7.20	3.50	2.06
	32	7.40	3.60	2.06	6.20	3.20	1.94	6.90	3.30	2.09	7.10	3.20	2.22
	40	7.30	3.30	2.21	7.00	3.20	2.19	7.50	3.30	2.27	7.00	2.90	2.41
	50	6.30	3.00	2.10	7.20	3.10	2.32	7.80	3.10	2.52	7.00	2.80	2.50
	62	7.30	3.00	2.43	6.80	2.90	2.34	7.30	2.90	2.52	6.30	2.50	2.52
	80	6.30	2.80	2.25	7.70	2.90	2.66	6.70	2.60	2.58	6.30	2.40	2.63
	96	6.80	2.80	2.43	7.50	2.90	2.59	7.60	2.80	2.71	7.30	2.50	2.92
10	18.6	10.50	5.90	1.78	9.80	5.20	1.88	9.50	5.00	1.90	10.00	5.60	1.79
	25	9.60	4.70	2.04	10.20	4.60	2.22	9.70	4.40	2.20	10.20	4.30	2.37
	32	10.10	4.20	2.40	10.60	4.10	2.59	9.90	3.90	2.54	10.40	3.80	2.74
	40	10.60	3.90	2.72	8.70	3.50	2.49	10.60	3.70	2.86	10.20	3.40	3.00
	50	11.40	3.70	3.08	9.10	3.30	2.76	11.00	3.50	3.14	9.70	3.10	3.13
	62	9.60	3.30	2.91	9.80	3.30	2.97	11.20	3.50	3.20	10.30	3.20	3.22
	80	10.50	3.50	3.00	10.00	3.50	2.86	10.60	3.60	2.94	9.00	2.90	3.10
	96	11.00	3.60	3.06	11.00	3.80	2.89	11.40	3.80	3.00	10.50	3.30	3.18

B.1 Effect of pipe goemtery on rerounding

B.1.1 Effect on circumferential dents

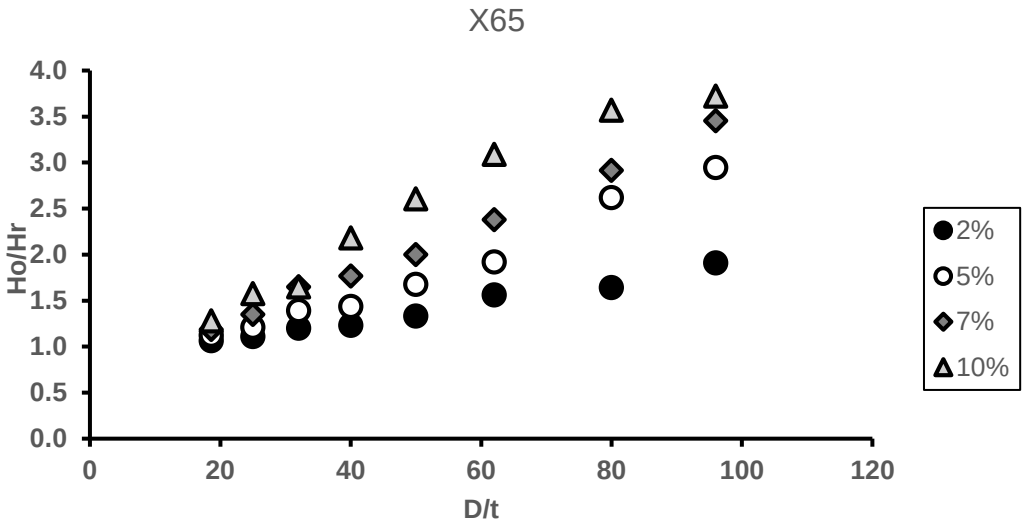

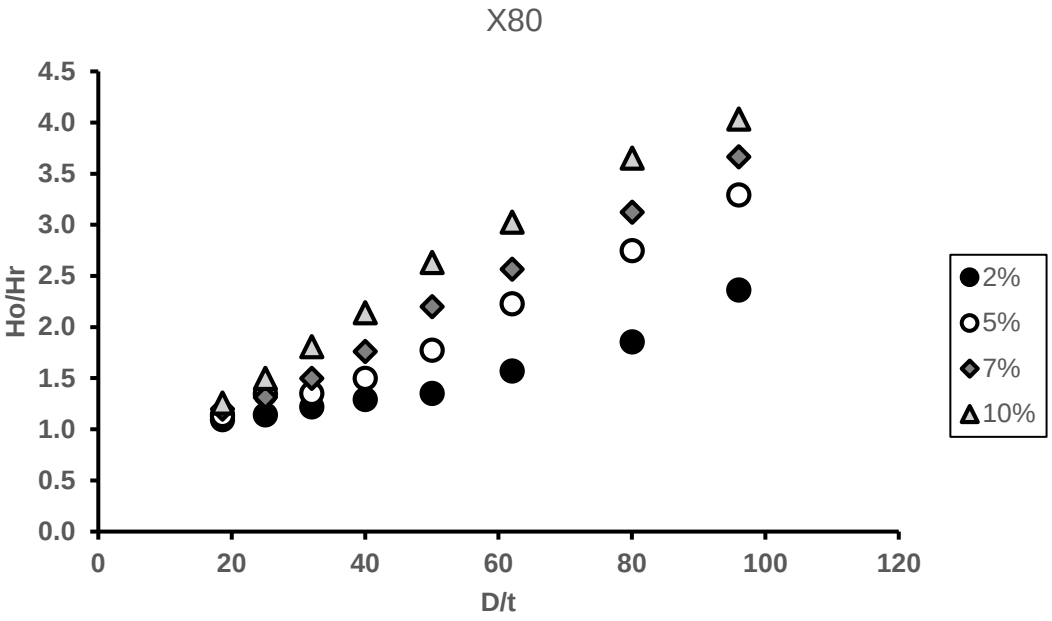
X80
Ho/Hr
D/t
0.0
0.5
1.0
1.5
2.0
2.5
3.0
3.5
4.0
4.5
0
20
40
60
80
100
120
2%
5%
7%
10%

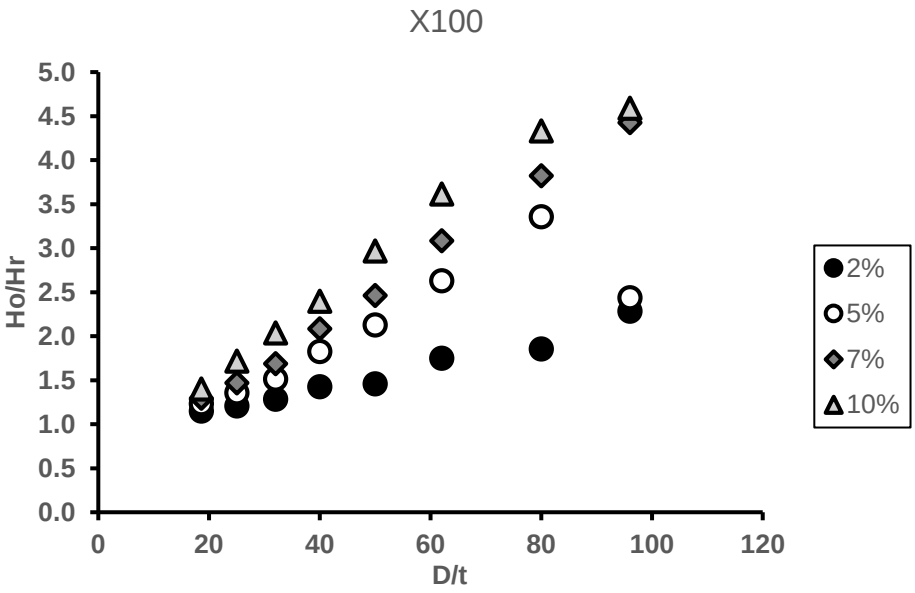
X100
Ho/Hr
D/t
0.0
0.5
1.0
1.5
2.0
2.5
3.0
3.5
4.0
4.5
5.0
0
20
40
60
80
100
120
2%
5%
7%
10%

B.1.2 Effect on longitudinal dents

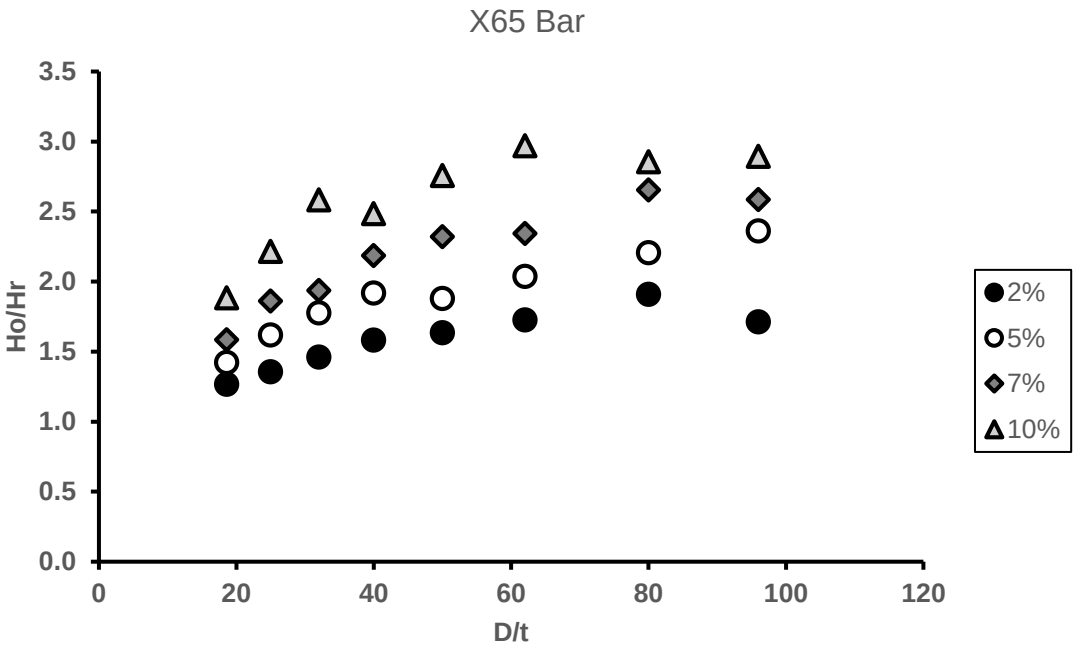

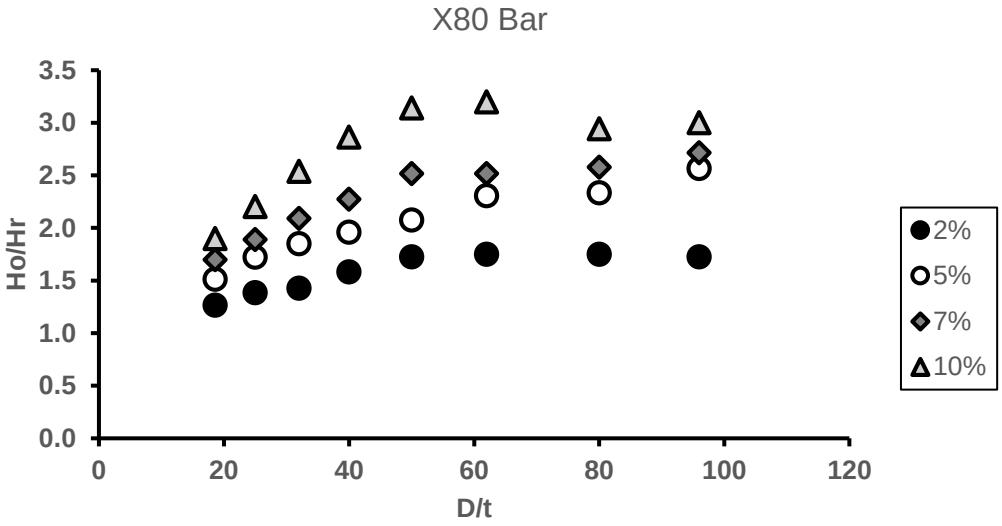

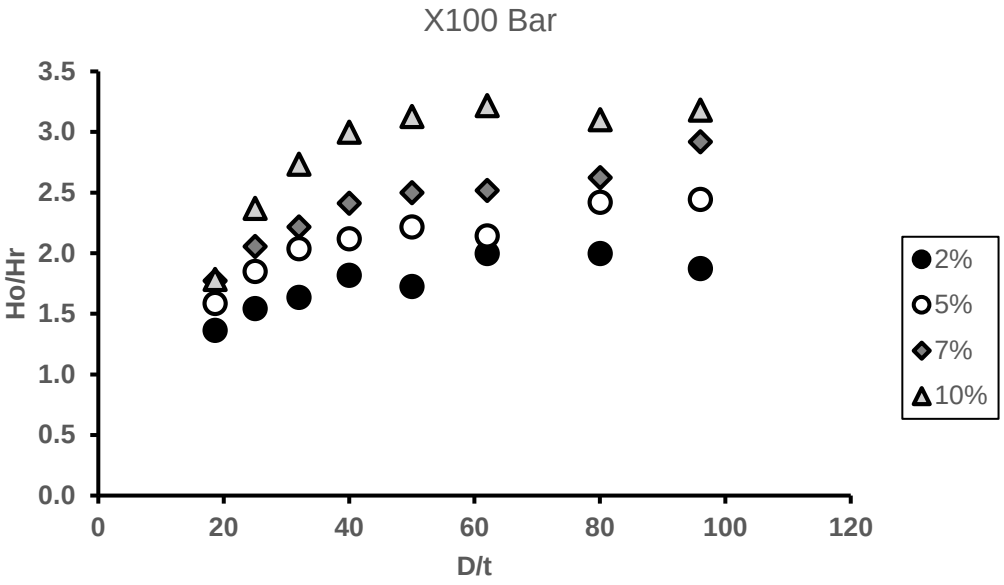

B.2 Effect of dent goemtery on rerounding

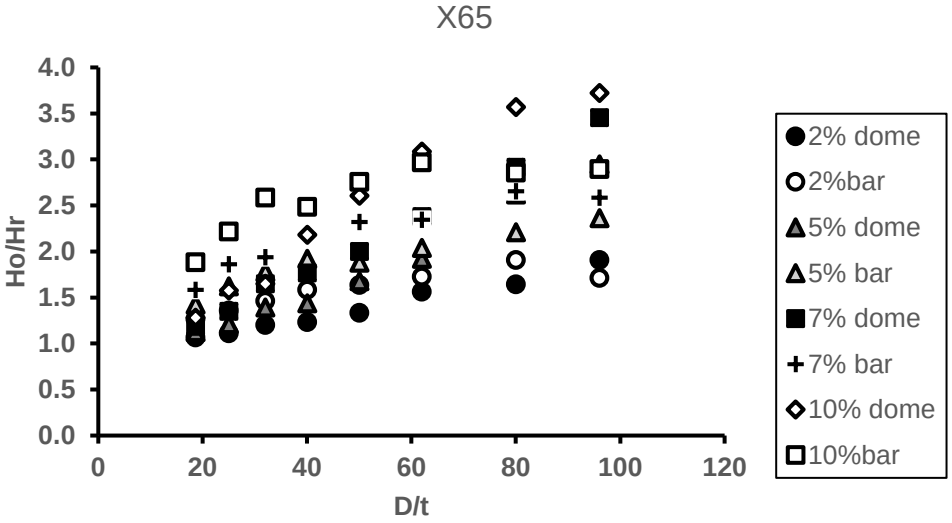

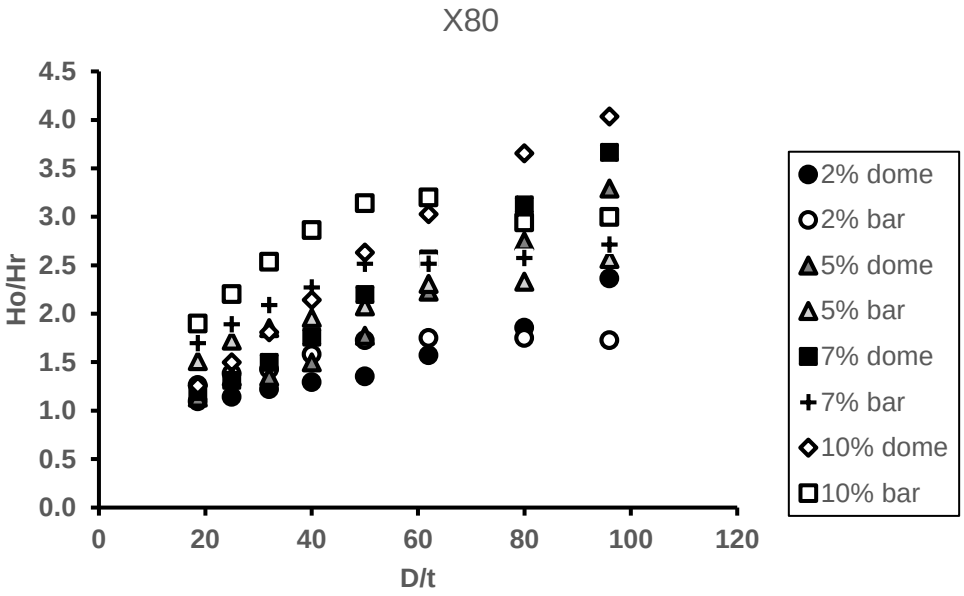
X80
Ho/Hr
D/t
0.0
0.5
1.0
1.5
2.0
2.5
3.0
3.5
4.0
4.5
0
20
40
60
80
100
120
2% dome
2% bar
5% dome
5% bar
7% dome
7% bar
10% dome
10% bar

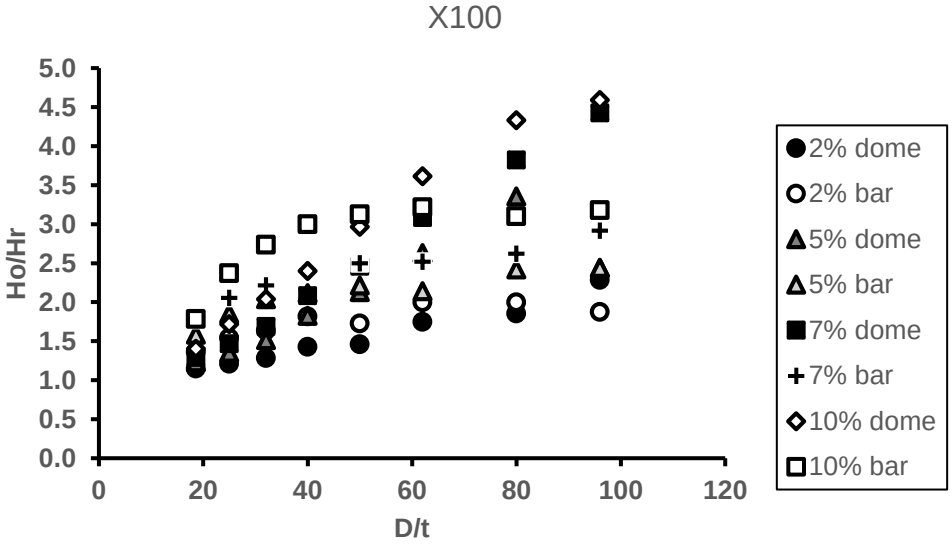
X100
Ho/Hr
D/t
0.0
0.5
1.0
1.5
2.0
2.5
3.0
3.5
4.0
4.5
5.0
0
20
40
60
80
100
120
2% dome
2% bar
5% dome
5% bar
7% dome
7% bar
10% dome
10% bar

B.3 Effect of pipe grade on rerounding

B.3.1 Effect on circumferential dents

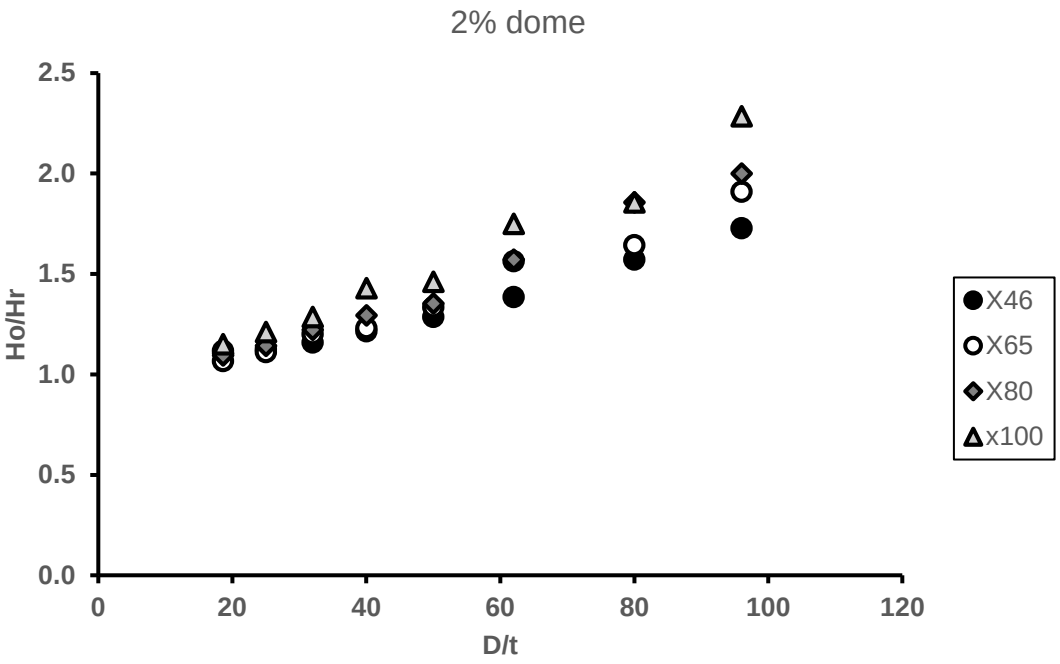

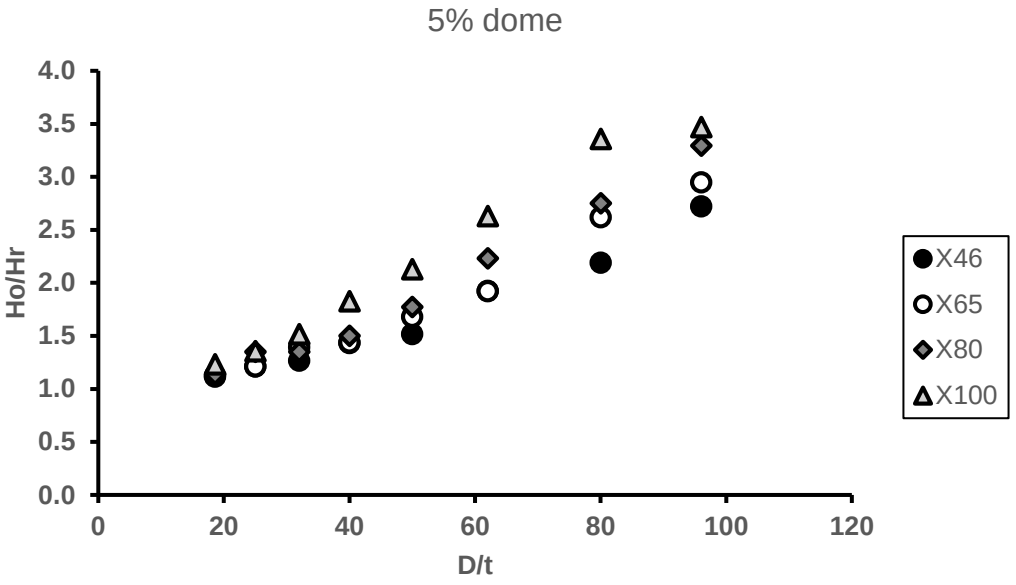

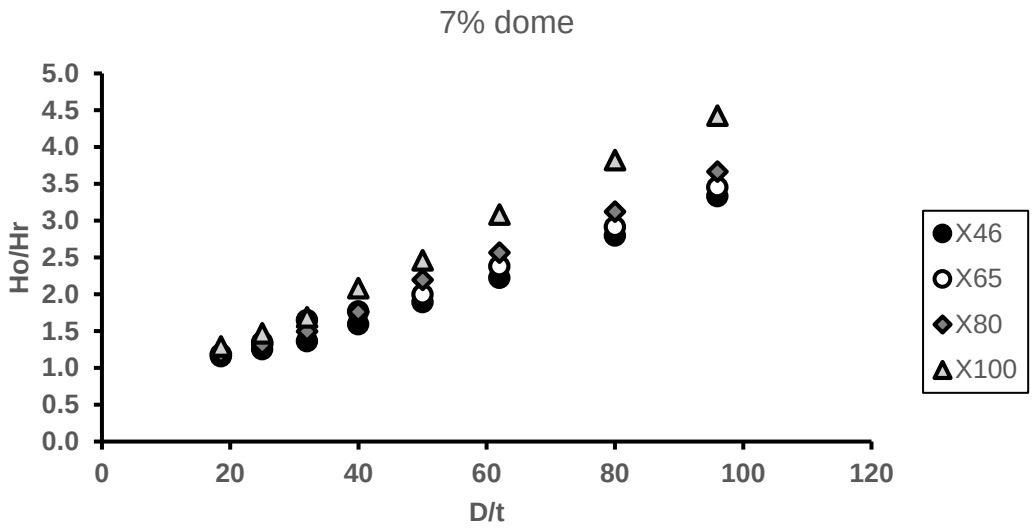

B.3.2 Effect on longitudinal dents

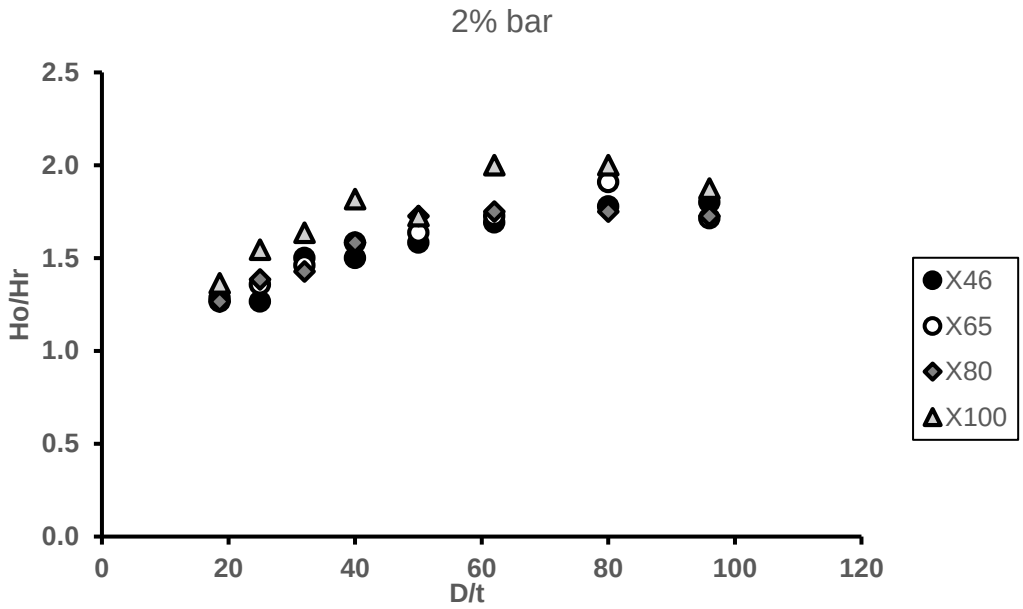

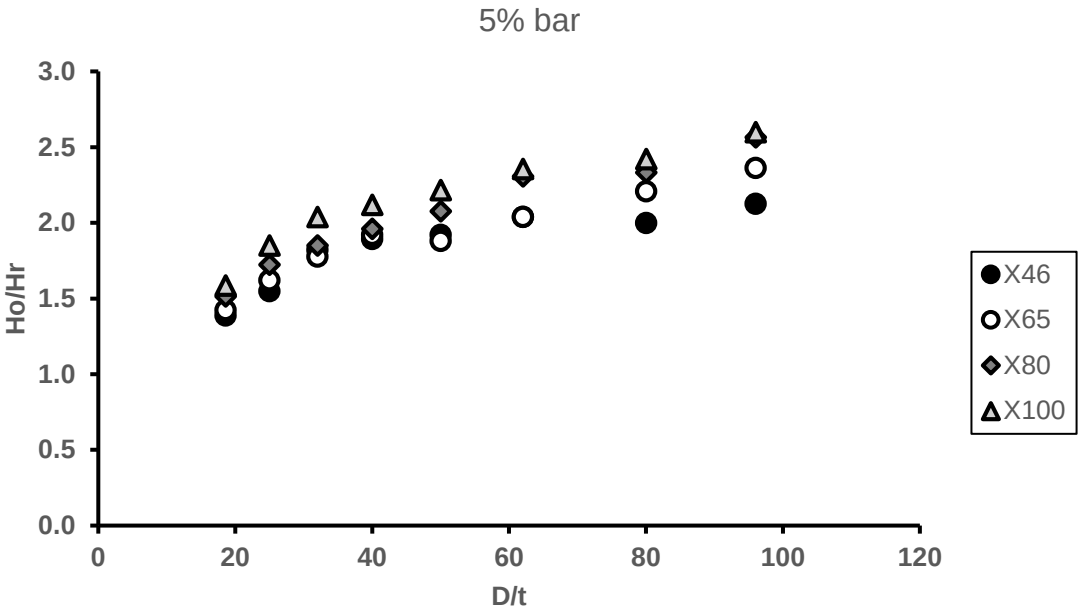
5% bar
3.0
2.5
2.0
1.5
1.0
0.5
0.0
Ho/Hr
0
20
40
60
80
100
120
D/t
X46
X65
X80
X100

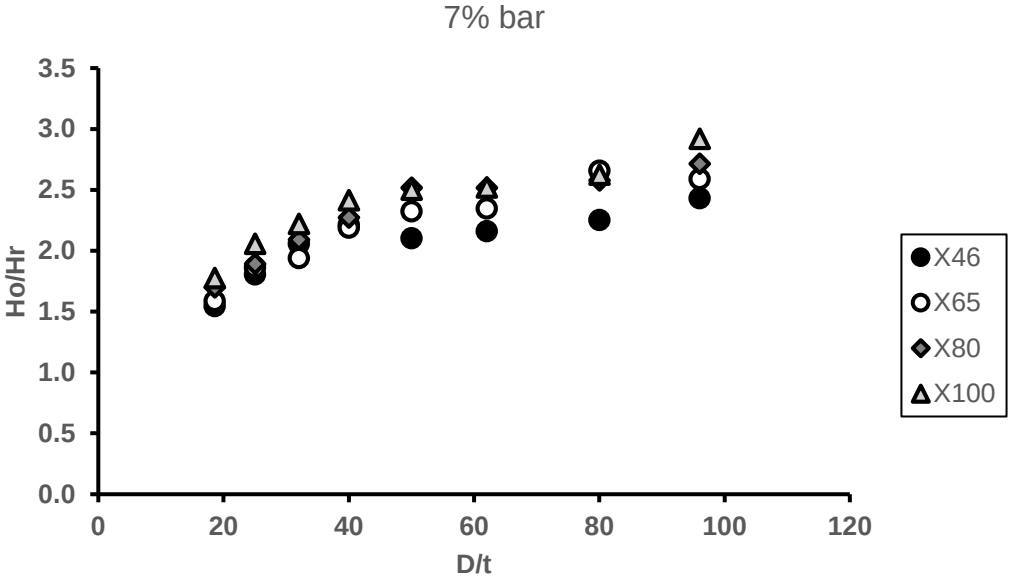
7% bar
3.5
3.0
2.5
2.0
1.5
1.0
0.5
0.0
Ho/Hr
0
20
40
60
80
100
120
D/t
X46
X65
X80
X100

Appendix C SCF Results

This section shows other graphs illustrating the effects of pipe geometry and pipe grades on the SCF in dented pipelines as discussed in chapter 4.it shows the results for different dent depths at different pressure ranges for both the dome and bar dent.

C.1 Effect of pipe goemtery and pipe grade on SCF

C.1.1 Effect on dome dents

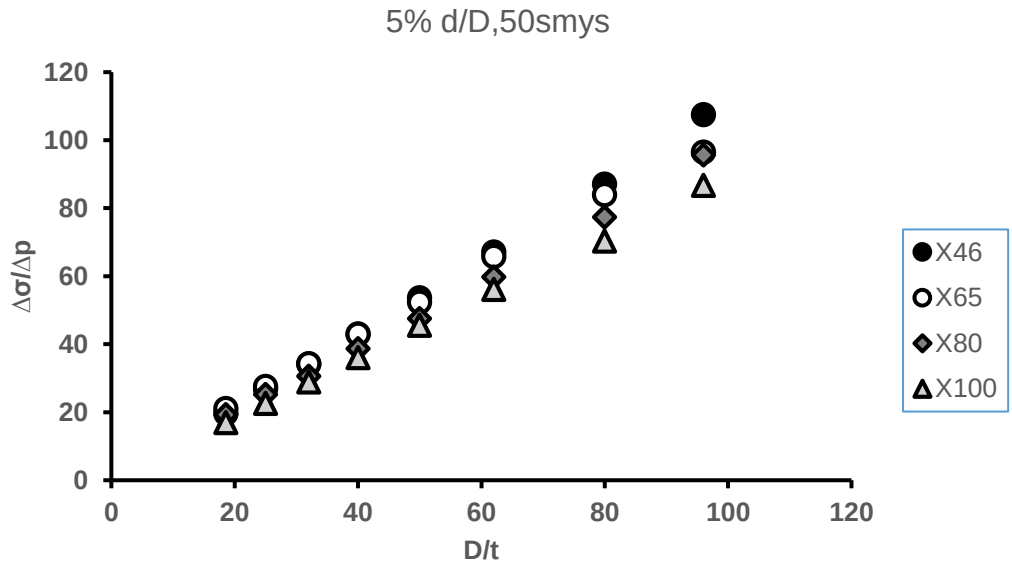

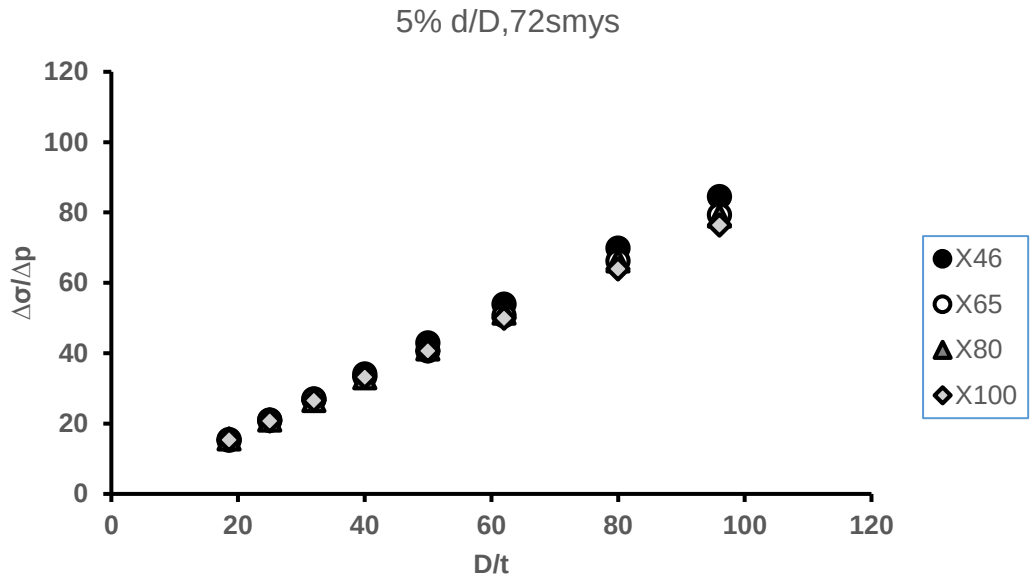

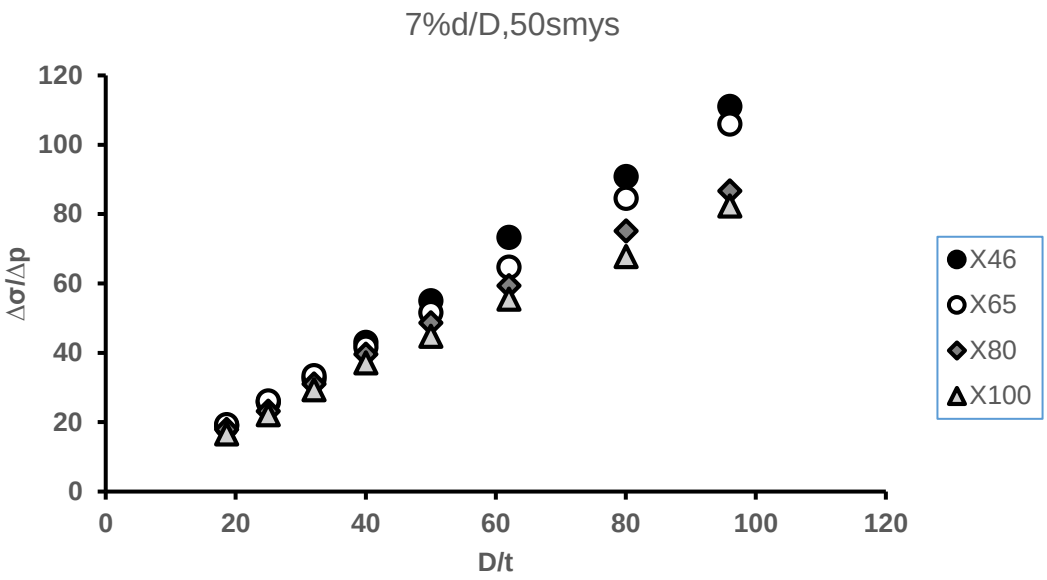
7%d/D,50smys
120
100
80
60
40
20
0
Δσ/Δp
0
20
40
60
80
100
120
D/t
X46
X65
X80
X100

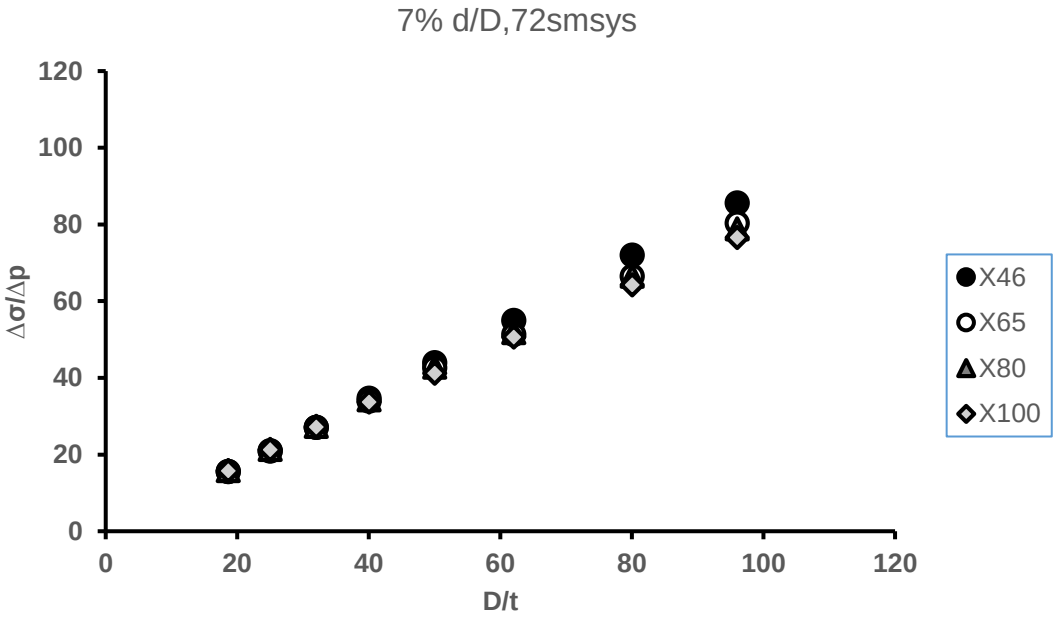
7% d/D,72smsys
120
100
80
60
40
20
0
Δσ/Δp
0
20
40
60
80
100
120
D/t
X46
X65
X80
X100

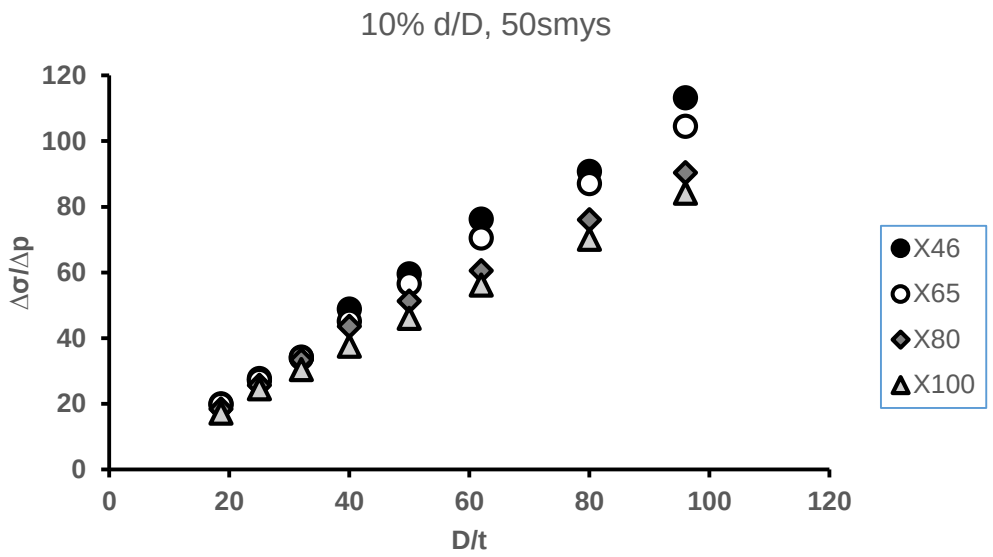
10% d/D, 50smys
Δσ/Δp
D/t
0
20
40
60
80
100
120
X46
X65
X80
X100

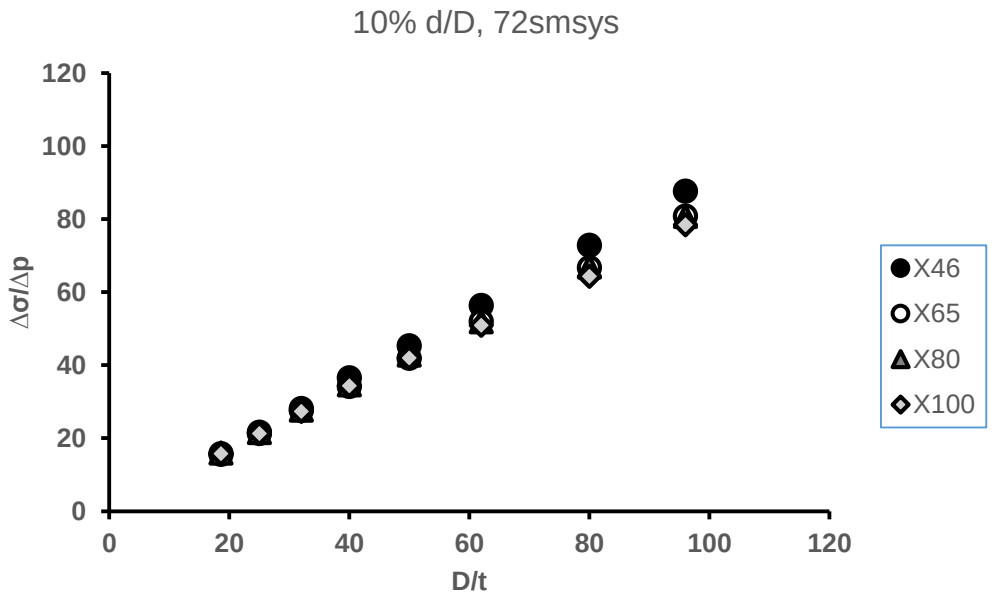
10% d/D, 72smsys
Δσ/Δp
D/t
0
20
40
60
80
100
120
X46
X65
X80
X100

C.1.2 Effect on bar dents

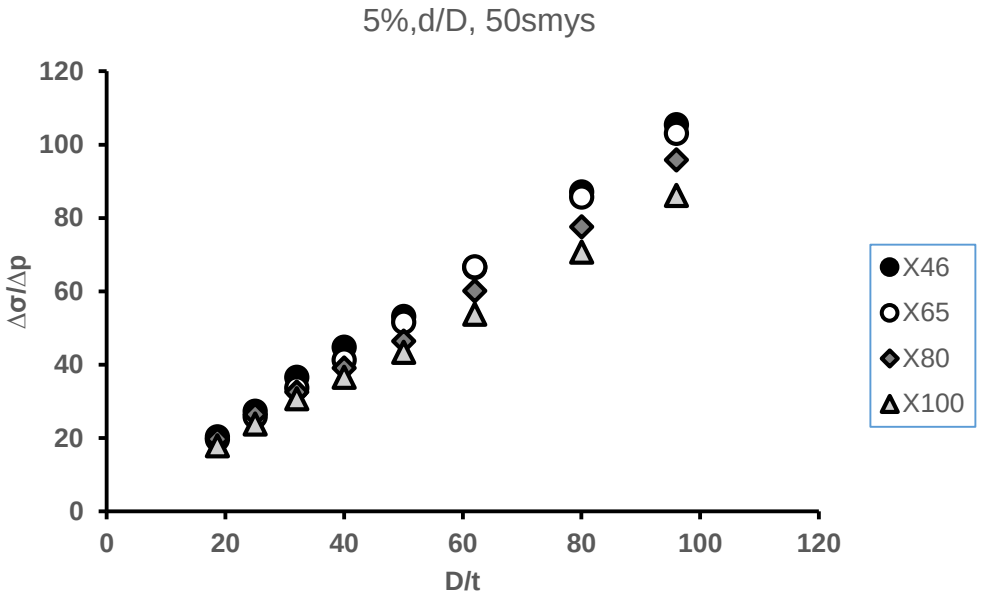

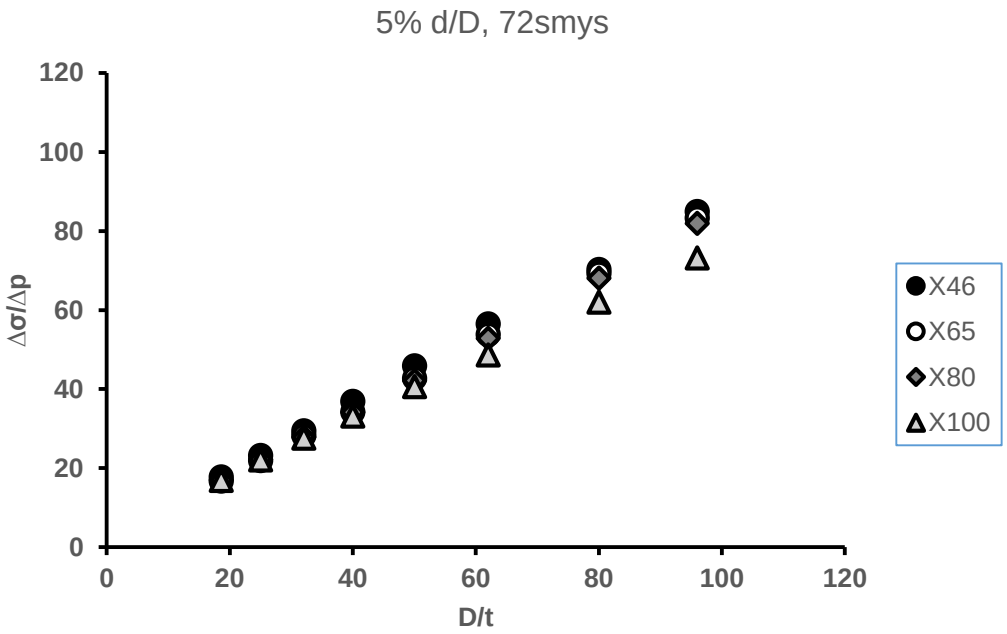

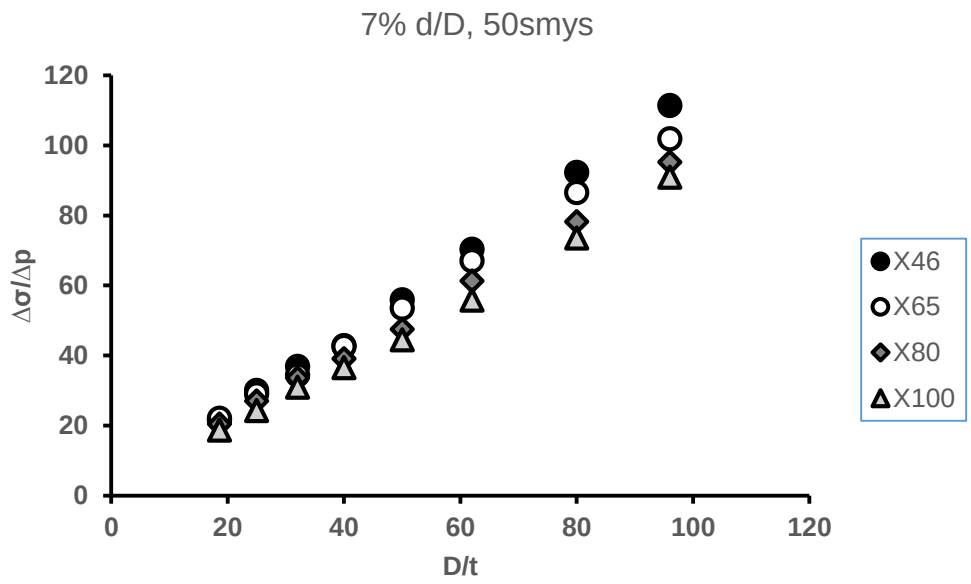
7% d/D, 50smys
Δσl/Δp
D/t
0
20
40
60
80
100
120
X46
X65
X80
X100

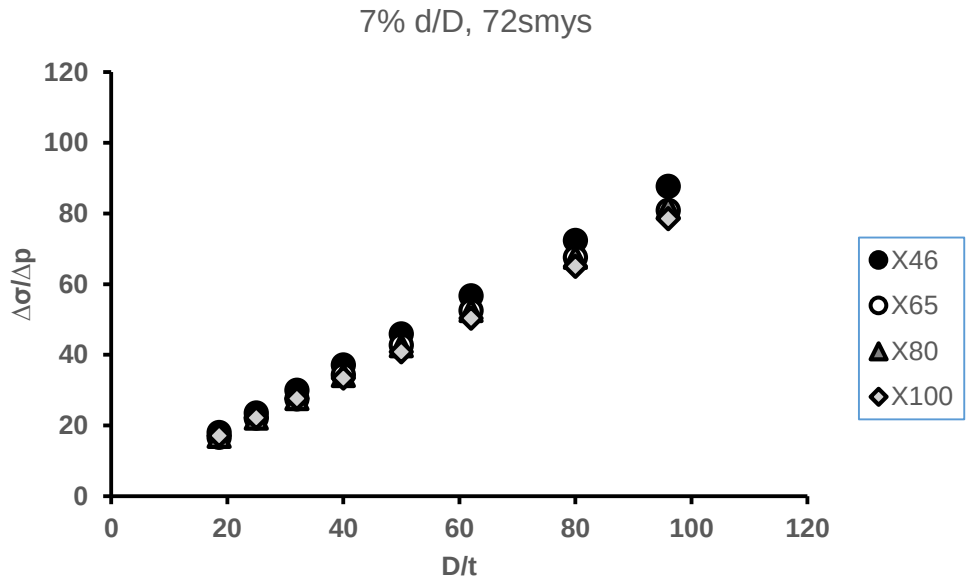
7% d/D, 72smys
Δσl/Δp
D/t
0
20
40
60
80
100
120
X46
X65
X80
X100

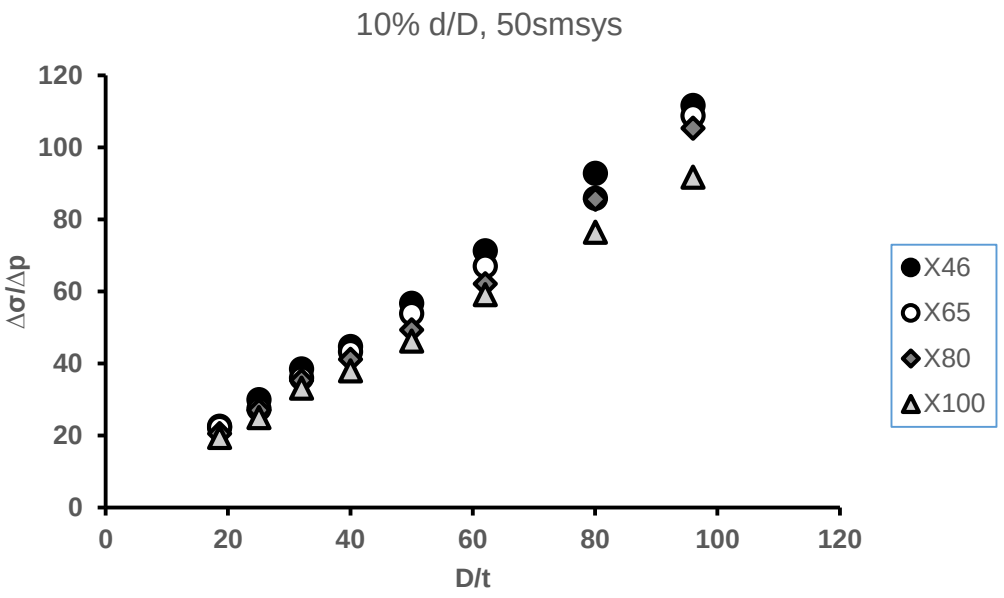
10% d/D, 50smsys
Δσ/Δp
D/t
0
20
40
60
80
100
120
X46
X65
X80
X100

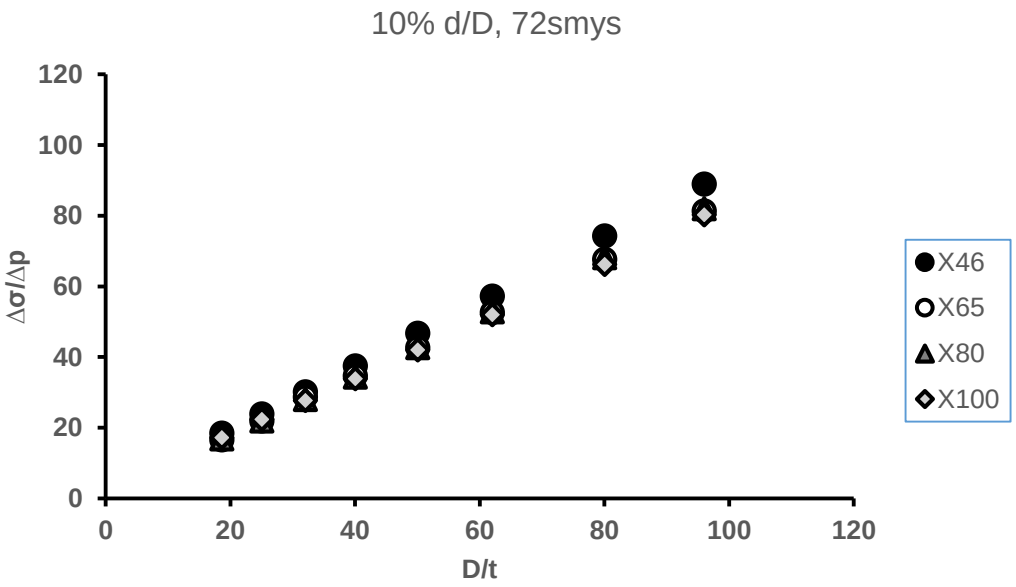
10% d/D, 72smys
Δσ/Δp
D/t
0
20
40
60
80
100
120
X46
X65
X80
X100

Appendix D Strain Results

This section shows the other graphs illustrating the effects of pipe geometry and pipe grades on the maximum strain for both the dome and bar dents as discussed in chapter 5. It compares the effect on different dent depths.

D.1 Effect of pipe goemtery on Strain

D.1.1 Effect on dome dents

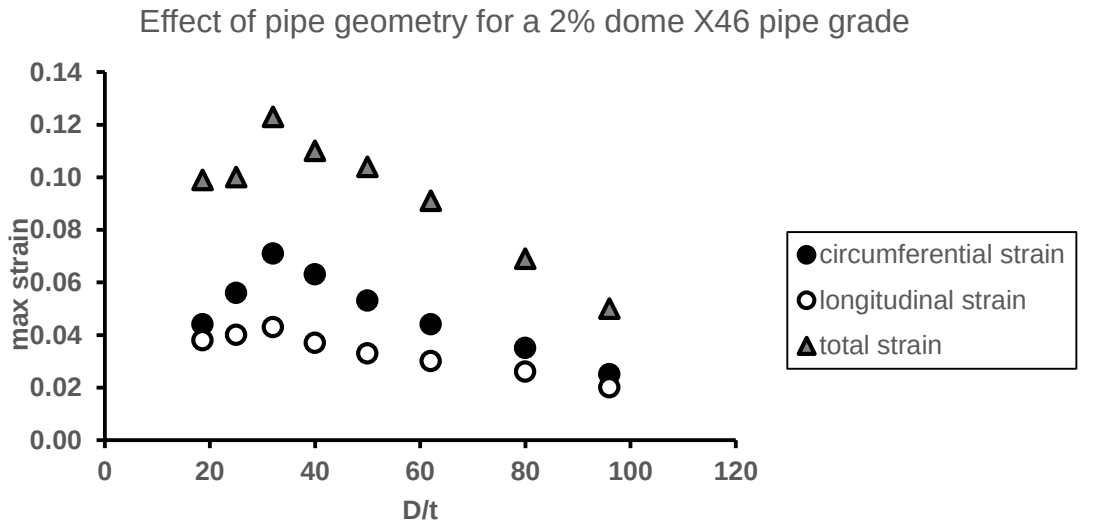

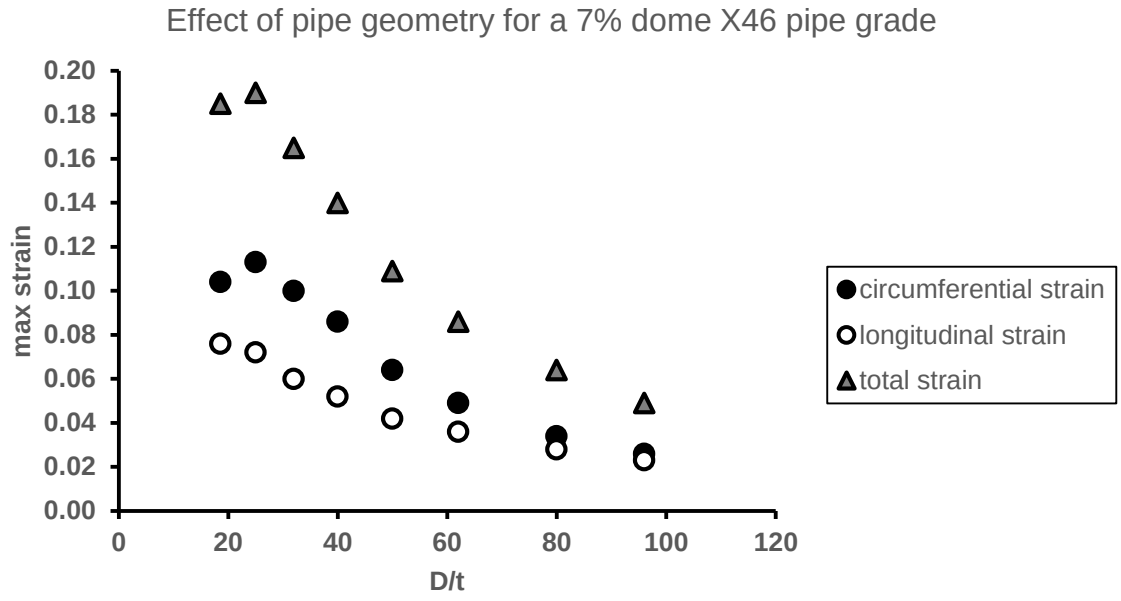

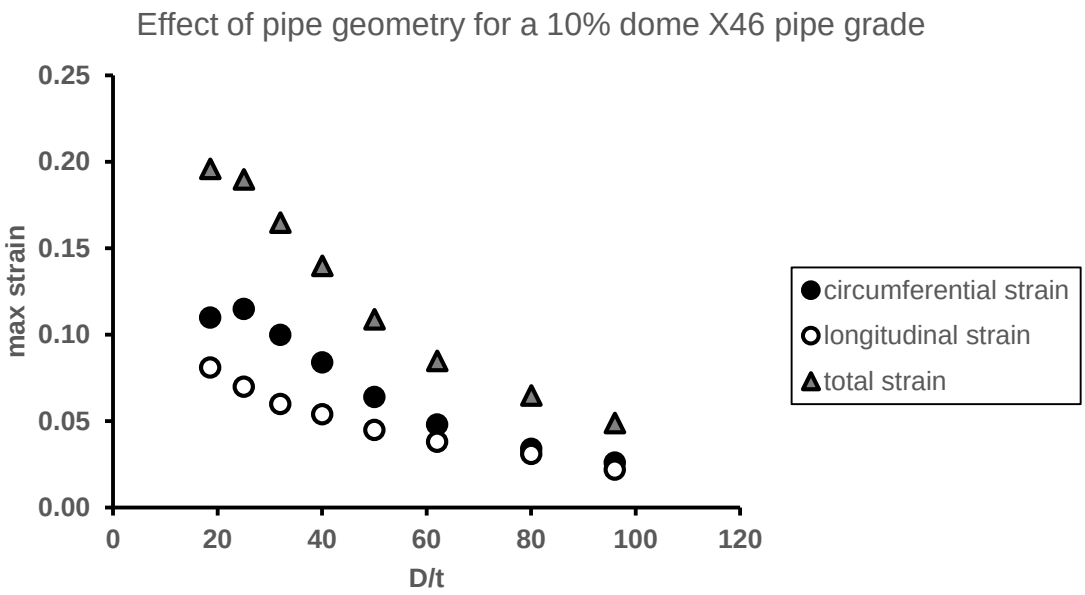

D.1.2 Effect on bar dents

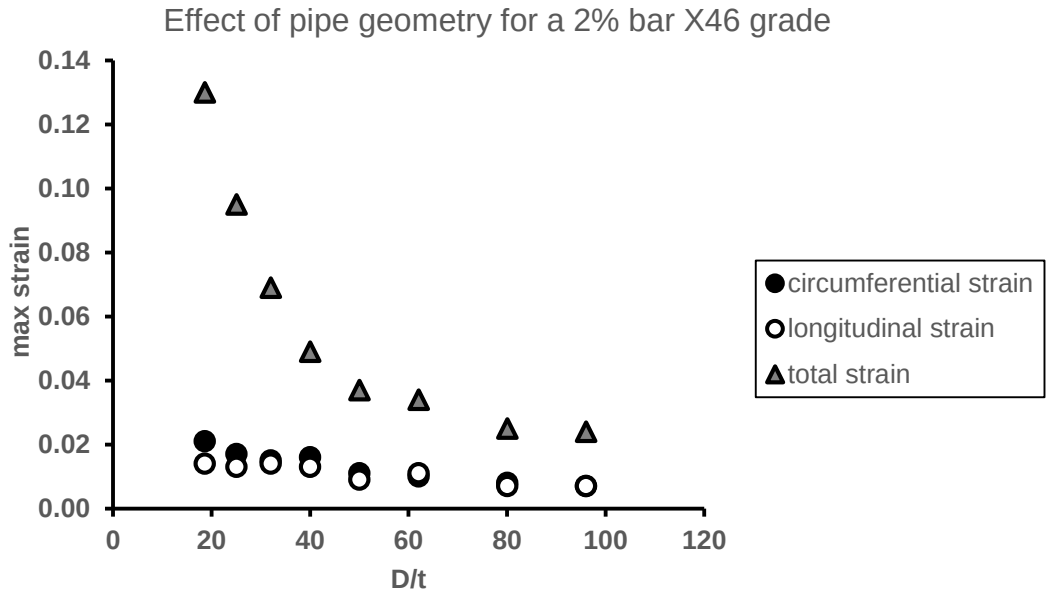

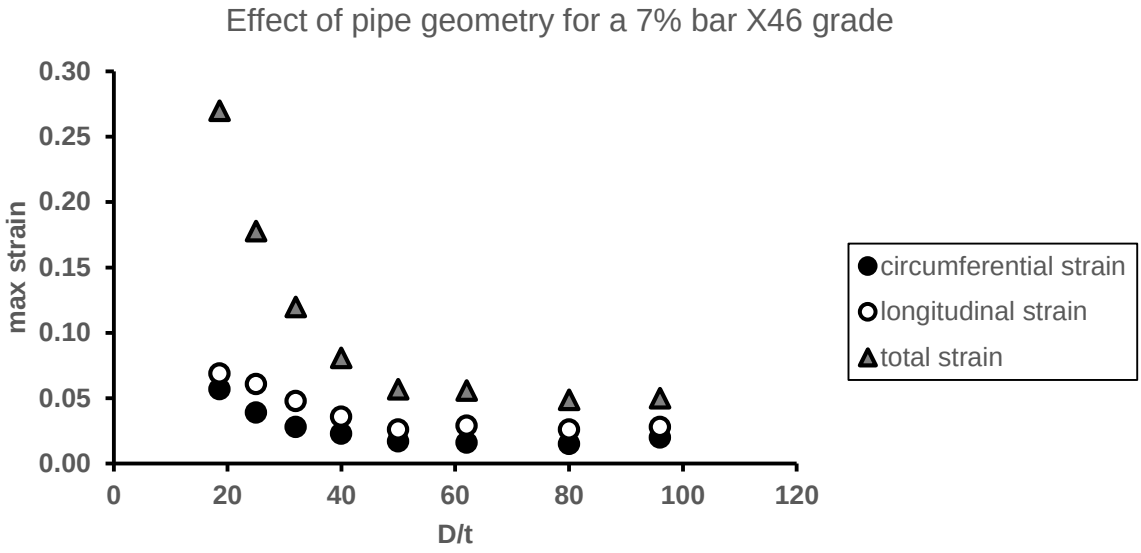
Effect of pipe geometry for a 7% bar X46 grade
max strain
0.30
0.25
0.20
0.15
0.10
0.05
0.00
0
20
40
60
80
100
120
D/t
circumferential strain
longitudinal strain
total strain

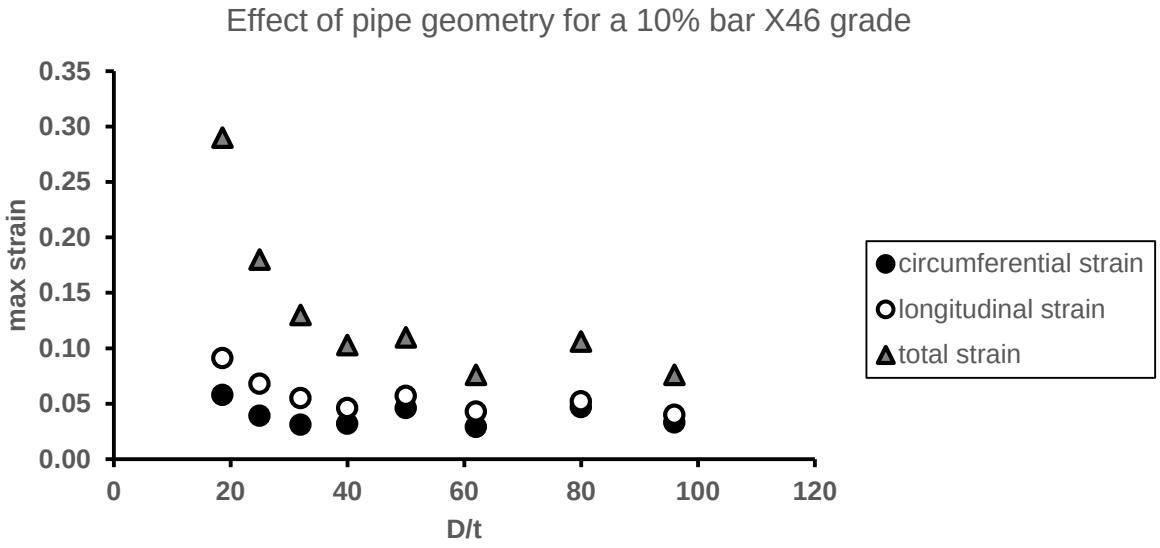
Effect of pipe geometry for a 10% bar X46 grade
max strain
0.35
0.30
0.25
0.20
0.15
0.10
0.05
0.00
0
20
40
60
80
100
120
D/t
circumferential strain
longitudinal strain
total strain

D.2 Effect of pipe grade on Strain

D.2.1 Effect on dome dents

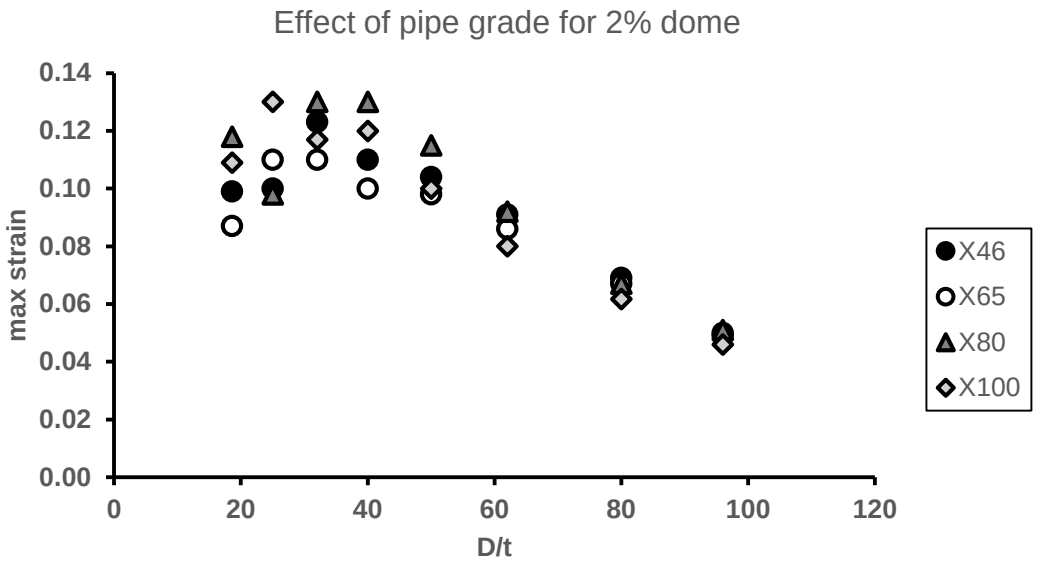

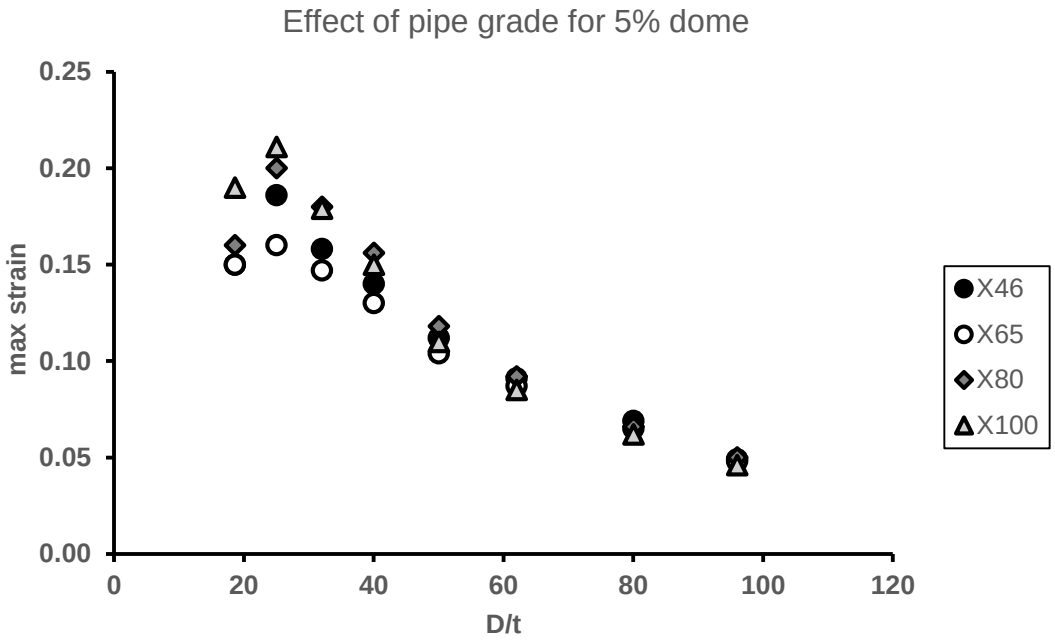

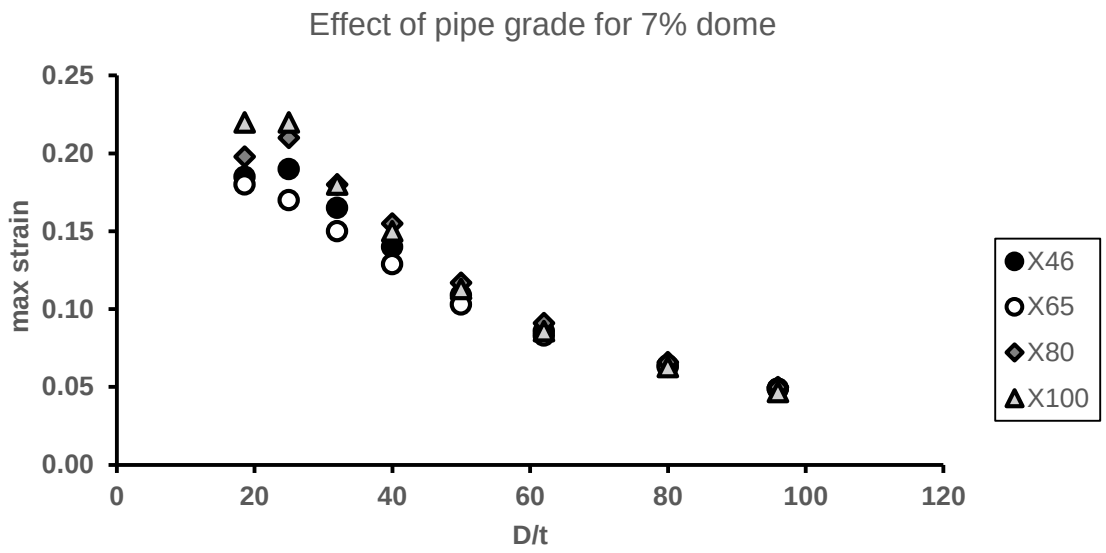

D.2.2 Effect on bar dents

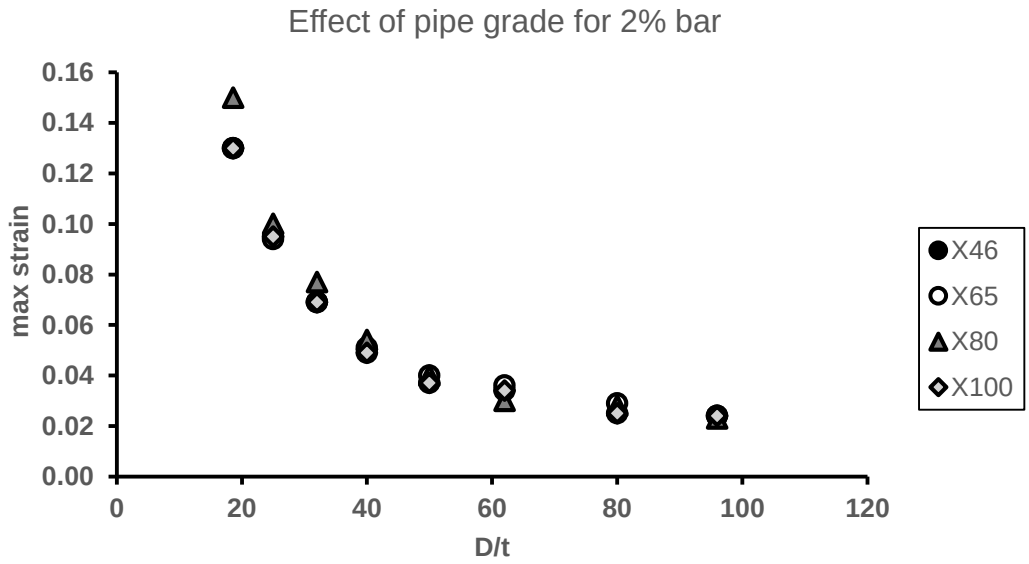

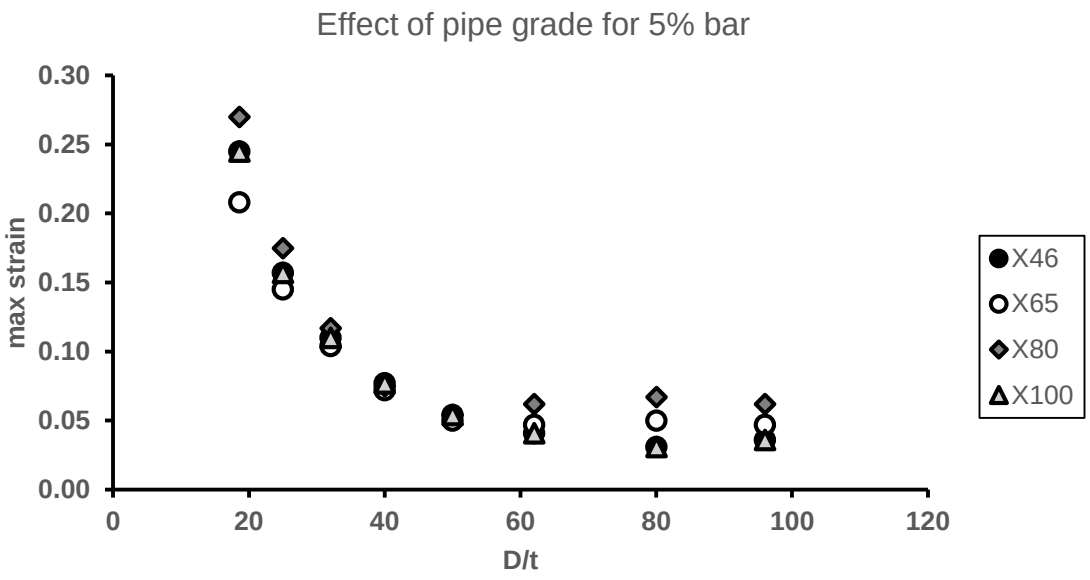
Effect of pipe grade for 5% bar
max strain
0.30
0.25
0.20
0.15
0.10
0.05
0.00
0
20
40
60
80
100
120
D/t
X46
X65
X80
X100

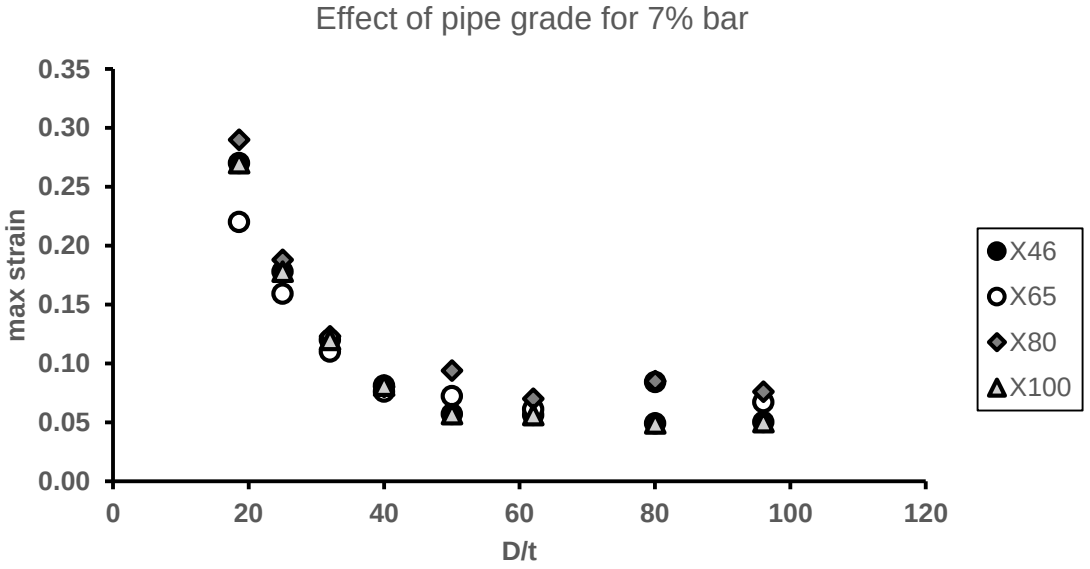
Effect of pipe grade for 7% bar
max strain
0.35
0.30
0.25
0.20
0.15
0.10
0.05
0.00
0
20
40
60
80
100
120
D/t
X46
X65
X80
X100

Appendix E Ansys mechanical APDL log file

This section shows the Ansys parametric design language (APDL) used for modelling both the dome and the bar dents. With APDL, several models can be created by changing the parameters highlighted in red and copying and pasting in the command window. The APDL file also contains comments highlighting the purpose of a particular command in order to help a first time user understand the command. The comments section begins with an exclamation mark(!) followed by the word comment and this is not part of the codes.it should be noted that sentences in italics are not part of the codes and is only used to describe a particular command or variable

E.1 Apdl file for a dome dent

! comments: setting preferences- the below codes helps select static structural analysis by disabling every other analysis settings, static structural is set as 1 and all other analysis set as 0 as shown by the red highlights

```
/NOPR
KEYW,PR_SET,1
KEYW,PR_STRUC,1
KEYW,PR_THERM,0
KEYW,PR_FLUID,0
KEYW,PR_ELMAG,0
KEYW,MAGNOD,0
KEYW,MAGEDG,0
KEYW,MAGHFE,0
KEYW,MAGELC,0
KEYW,PR_MULTI,0
/GO
!*
/COM,
/COM,Preferences for GUI filtering have been set to display:
/COM,  Structural
!*
```

! comments: Selecting elements; This is the section where elements are selected

```
/PREP7
!*
ET,1,SOLID186
!*
ET,2,TARGE170
!*
ET,3,CONTA174
!*
```

! comments: defining real constant; for older version of ansys, the real constants of element needs to be defined, however, some of the new elements do not require real constants

```
R,1, , ,
!*
R,2,,,, ,,
```

```
RMORE,,,, ,,
RMORE,,,, ,,
RMORE,,,, ,,
RMORE,,,,,,
RMORE,,,,,
!*
!*
```

! comments: defining material properties; here the material model and properties are defined

```
MPTEMP,,,,,,,,
MPTEMP,1,0
MPDATA,EX,1,,210000                    ! Young's modulus
MPDATA,PRXY,1,,0.3                     ! Poisson ratio
TB,KINH,1,1,11,0
TBTEMP,0
TBPT,,0.002211904762,464.5             ! stress-strain data
TBPT,,0.05,560
TBPT,,0.1,625
TBPT,,0.2,690
TBPT,,0.3,750
TBPT,,0.4,775
TBPT,,0.5,800
TBPT,,0.6,825
TBPT,,0.8,860
TBPT,,0.9,880
TBPT,,1,900
```

! comments: defining key points; this is the point where the geometry creation starts, four key points are created with the first key point starting from the origin as indicated as 0,0,0. The second key point shows the thickness of the pipe. The 3rd and 4th key point completes the quarter symmetry of the pipe

```
K,1,0,0,0,
K,2,0,17.399,0,
K,3,0,306.221,0,
K,4,0,323.62,0,
KPLOT
```

! comments: key points 5,6 and 7 defines the radius of the outer and inner wall of the pipe. These points are created in order to be able to create arcs joining the points

```
K,5,161.81,161.81,0,
K,6,144.411,161.81,0,
K,7,0,161.81,0,
```

! comments: Creating lines between key points

```
LSTR,      1,      2
LSTR,      3,      4
!*
```

! comments: creating arcs between key points

```
LARC,4,5,7,161.81,                     ! radius of outer wall
!*
LARC,1,5,7,161.81,
!*
LARC,3,6,7,144.411,                    ! radius of inner wall
!*
LARC,6,2,7,144.411,
LSTR,      6,      5
LPLOT
/PNUM,KP,0
/PNUM,LINE,1
/PNUM,AREA,0
/PNUM,VOLU,0
```

```
/PNUM,NODE,0
/PNUM,TABN,0
/PNUM,SVAL,0
/NUMBER,0
!*
/PNUM,ELEM,0
/REPLOT
!*

! comments :creating areas between lines

al,2,3,5,7
al,1,4,6,7

! comments: Extruding areas; the areas are extruded 3 times to create the 3 different volumes. Both the upper and
lower half needs to be extruded

VOFFST,1,328.605, ,

VOFFST,3,200, ,

VOFFST,8,721.395, ,

VOFFST,2,328.605, ,

VOFFST,18,200, ,

VOFFST,23,721.395, ,

! comments: Creating key point to draw dome indenter

K,100,0,323.62,,                    ! start of the key point which is at the top of the pipe in order to simulate contact
K,101,0,433.355,,
K,102,109.535,433.355,

! comments: creating lines between key points

LSTR,    100,    101
LSTR,    101,    102
!*

! comments: creating arc between key points

LARC,102,100,101,109.535,                ! radius of the dome

LPLOT
al,56,57,58

FLST,2,1,5,ORDE,1
FITEM,2,33
FLST,8,2,3
FITEM,8,101
FITEM,8,100
VROTAT,P51X, , , , , ,P51X, ,360,4,

FLST,2,3,6,ORDE,2
FITEM,2,7
FITEM,2,-9

! comments: deleting unwanted volume

VDELE,P51X, , ,1
APLOT
LPLOT
VPLOT
```

```
! comments: defining element size for indenter

ESIZE,10,0,                              ! element size
MSHAPE,0,3D
MSHKEY,1
!*
CM,_Y,VOLU
VSEL, , , ,      10
CM,_Y1,VOLU
CHKMSH,'VOLU'
CMSEL,S,_Y
!*

! comments:  meshing the  indenter

VMESH,_Y1
!*
CMDELE,_Y
CMDELE,_Y1
CMDELE,_Y2
!*
VPLOT

! comments: adding the three volumes in the pipe

vadd,3,6
vadd,2,5
vadd,1,4
VPLOT

LPLOT

FLST,5,4,4,ORDE,4
FITEM,5,12
FITEM,5,-13
FITEM,5,36
FITEM,5,-37
CM,_Y,LINE
LSEL, , , ,P51X
CM,_Y1,LINE
CMSEL,,_Y
!*
FLST,5,4,4,ORDE,4
FITEM,5,12
FITEM,5,-13
FITEM,5,36
FITEM,5,-37
CM,_Y,LINE
LSEL, , , ,P51X
CM,_Y1,LINE
CMSEL,,_Y
!*

! comments: line sizing; this is the point where the lines are divided to create the number of elements and bias

LESIZE,_Y1, , ,80,3, , , ,1                    ! 80 is the number of division and 3 is the bias factor
!*
FLST,5,4,4,ORDE,4
FITEM,5,3
FITEM,5,5
FITEM,5,9
FITEM,5,11
CM,_Y,LINE
LSEL, , , ,P51X
CM,_Y1,LINE
CMSEL,,_Y
```

```
!*
LESIZE,_Y1, , ,30, , , , ,1
!*
FLST,5,4,4,ORDE,4
FITEM,5,4
FITEM,5,6
FITEM,5,49
FITEM,5,-50
CM,_Y,LINE
LSEL, , , ,P51X
CM,_Y1,LINE
CMSEL,,_Y
!*
LESIZE,_Y1, , ,20, , , , ,1
!*
FLST,5,4,4,ORDE,4
FITEM,5,1
FITEM,5,-2
FITEM,5,8
FITEM,5,32
CM,_Y,LINE
LSEL, , , ,P51X
CM,_Y1,LINE
CMSEL,,_Y
!*
LESIZE,_Y1, , ,6, , , , ,1
!*
CM,_Y,VOLU
VSEL, , , ,      2
CM,_Y1,VOLU
CHKMSH,'VOLU'
CMSEL,S,_Y
!*
```

! comments: meshing the main volume of the pipe

```
VSWEEP,_Y1
!*
CMDELE,_Y
CMDELE,_Y1
CMDELE,_Y2
!*
VPLOT
```

! comment: defining element size for the other volumes

```
ESIZE,60,0,                          ! element size
VPLOT
FLST,5,2,6,ORDE,2
FITEM,5,3
FITEM,5,7
CM,_Y,VOLU
VSEL, , , ,P51X
CM,_Y1,VOLU
CHKMSH,'VOLU'
CMSEL,S,_Y
!*
```

! comments: meshing other volumes

```
VSWEEP,_Y1
!*
CMDELE,_Y
CMDELE,_Y1
CMDELE,_Y2
!*
```

! comments: selecting the target area

```
ASEL,S, , ,      44
APLOT

/REPLO  NSLA,S,1
NPLOT
```

! comments: selecting target nodes from the area

```
FLST,5,784,1,ORDE,5
FITEM,5,2
FITEM,5,38
FITEM,5,-73
FITEM,5,785
FITEM,5,-1531
NSEL,R, , ,P51X
CM,target,NODE
CMSEL,A,target
/MREP,EPLOT
ALLSEL,ALL
VPLOT
```

! comments: selecting contact nodes

```
NSEL,S,LOC,X,0,161.81                    ! location on the x axis
NPLOT
NSEL,R,LOC,Y,306.221,323.62              ! location on the y axis
NPLOT
NSEL,R,LOC,Z,0,-140                      ! location on the Z axis
NPLOT
```

! comments: automatically selected nodes based on the location selected(no need to copy and paste as it automatically generated using the above commands)

```
FLST,5,7547,1,ORDE,897
FITEM,5,785
FITEM,5,14499
FITEM,5,-14543
FITEM,5,14613
FITEM,5,-14702
FITEM,5,14737
FITEM,5,-14781
FITEM,5,14851
FITEM,5,-14940
FITEM,5,14975
FITEM,5,-15019
FITEM,5,15089
FITEM,5,-15178
FITEM,5,15213
FITEM,5,-15257
FITEM,5,15327
FITEM,5,-15416
FITEM,5,15451
FITEM,5,-15495
FITEM,5,15565
FITEM,5,-15654
FITEM,5,15689
FITEM,5,-15891
FITEM,5,15899
FITEM,5,-15905
FITEM,5,16288
FITEM,5,-16295
FITEM,5,16339
FITEM,5,-16354
```

FITEM,5,16377
FITEM,5,-16383
FITEM,5,16429
FITEM,5,-16442
FITEM,5,16466
FITEM,5,-16471
FITEM,5,16519
FITEM,5,-16530
FITEM,5,16555
FITEM,5,-16559
FITEM,5,16609
FITEM,5,-16618
FITEM,5,16644
FITEM,5,-16647
FITEM,5,16700
FITEM,5,-16706
FITEM,5,16734
FITEM,5,-16735
FITEM,5,16765
FITEM,5,-16781
FITEM,5,17349
FITEM,5,-17356
FITEM,5,17399
FITEM,5,-17415
FITEM,5,17437
FITEM,5,-17444
FITEM,5,17487
FITEM,5,-17503
FITEM,5,17525
FITEM,5,-17532
FITEM,5,17575
FITEM,5,-17591
FITEM,5,17613
FITEM,5,-17620
FITEM,5,17663
FITEM,5,-17679
FITEM,5,17701
FITEM,5,-17708
FITEM,5,17751
FITEM,5,-17767
FITEM,5,17789
FITEM,5,-17796
FITEM,5,17839
FITEM,5,-17855
FITEM,5,17877
FITEM,5,-17884
FITEM,5,17927
FITEM,5,-17943
FITEM,5,17965
FITEM,5,-17972
FITEM,5,18015
FITEM,5,-18031
FITEM,5,18053
FITEM,5,-18060
FITEM,5,18103
FITEM,5,-18119
FITEM,5,18141
FITEM,5,-18148
FITEM,5,18191
FITEM,5,-18207
FITEM,5,18229
FITEM,5,-18236
FITEM,5,18279
FITEM,5,-18295
FITEM,5,18317
FITEM,5,-18324

FITEM,5,18367
FITEM,5,-18383
FITEM,5,18405
FITEM,5,-18412
FITEM,5,18455
FITEM,5,-18471
FITEM,5,18493
FITEM,5,-18500
FITEM,5,18543
FITEM,5,-18559
FITEM,5,18581
FITEM,5,-18588
FITEM,5,18631
FITEM,5,-18647
FITEM,5,18669
FITEM,5,-18676
FITEM,5,18719
FITEM,5,-18735
FITEM,5,18757
FITEM,5,-18764
FITEM,5,18807
FITEM,5,-18823
FITEM,5,18845
FITEM,5,-18852
FITEM,5,18895
FITEM,5,-18911
FITEM,5,18933
FITEM,5,-18940
FITEM,5,18983
FITEM,5,-18999
FITEM,5,19021
FITEM,5,-19028
FITEM,5,19071
FITEM,5,-19087
FITEM,5,19109
FITEM,5,-19116
FITEM,5,19159
FITEM,5,-19175
FITEM,5,19197
FITEM,5,-19204
FITEM,5,19247
FITEM,5,-19263
FITEM,5,19285
FITEM,5,-19292
FITEM,5,19335
FITEM,5,-19351
FITEM,5,19373
FITEM,5,-19380
FITEM,5,19423
FITEM,5,-19439
FITEM,5,19461
FITEM,5,-19468
FITEM,5,19511
FITEM,5,-19527
FITEM,5,19549
FITEM,5,-19556
FITEM,5,19599
FITEM,5,-19615
FITEM,5,19637
FITEM,5,-19644
FITEM,5,19687
FITEM,5,-19703
FITEM,5,19725
FITEM,5,-19732
FITEM,5,19775
FITEM,5,-19791

FITEM,5,19813
FITEM,5,-19820
FITEM,5,19863
FITEM,5,-19879
FITEM,5,19901
FITEM,5,-19908
FITEM,5,19951
FITEM,5,-19967
FITEM,5,19989
FITEM,5,-19996
FITEM,5,20039
FITEM,5,-20055
FITEM,5,20077
FITEM,5,-20084
FITEM,5,20127
FITEM,5,-20143
FITEM,5,20165
FITEM,5,-20172
FITEM,5,20215
FITEM,5,-20231
FITEM,5,20253
FITEM,5,-20260
FITEM,5,20303
FITEM,5,-20319
FITEM,5,20341
FITEM,5,-20348
FITEM,5,20391
FITEM,5,-20407
FITEM,5,20429
FITEM,5,-20436
FITEM,5,20479
FITEM,5,-20495
FITEM,5,20517
FITEM,5,-20524
FITEM,5,20567
FITEM,5,-20583
FITEM,5,20605
FITEM,5,-20612
FITEM,5,20655
FITEM,5,-20671
FITEM,5,20693
FITEM,5,-20700
FITEM,5,20743
FITEM,5,-20759
FITEM,5,20781
FITEM,5,-20788
FITEM,5,20831
FITEM,5,-20847
FITEM,5,20869
FITEM,5,-20876
FITEM,5,20919
FITEM,5,-20935
FITEM,5,20957
FITEM,5,-20964
FITEM,5,21007
FITEM,5,-21023
FITEM,5,21045
FITEM,5,-21052
FITEM,5,21095
FITEM,5,-21111
FITEM,5,21133
FITEM,5,-21140
FITEM,5,21183
FITEM,5,-21199
FITEM,5,21221
FITEM,5,-21228

FITEM,5,21271
FITEM,5,-21287
FITEM,5,41214
FITEM,5,-41219
FITEM,5,41352
FITEM,5,-41362
FITEM,5,41432
FITEM,5,-41442
FITEM,5,41878
FITEM,5,-41922
FITEM,5,41957
FITEM,5,-42001
FITEM,5,42036
FITEM,5,-42080
FITEM,5,42115
FITEM,5,-42159
FITEM,5,42194
FITEM,5,-42238
FITEM,5,42273
FITEM,5,-42317
FITEM,5,42352
FITEM,5,-42396
FITEM,5,42431
FITEM,5,-42475
FITEM,5,42510
FITEM,5,-42554
FITEM,5,42589
FITEM,5,-42633
FITEM,5,42668
FITEM,5,-43162
FITEM,5,43542
FITEM,5,-43586
FITEM,5,43621
FITEM,5,-43665
FITEM,5,43700
FITEM,5,-43744
FITEM,5,43779
FITEM,5,-43823
FITEM,5,43858
FITEM,5,-43902
FITEM,5,43937
FITEM,5,-43981
FITEM,5,44016
FITEM,5,-44060
FITEM,5,44095
FITEM,5,-44139
FITEM,5,44174
FITEM,5,-44218
FITEM,5,44253
FITEM,5,-44297
FITEM,5,44332
FITEM,5,-44826
FITEM,5,45206
FITEM,5,-45250
FITEM,5,45285
FITEM,5,-45329
FITEM,5,45364
FITEM,5,-45408
FITEM,5,45443
FITEM,5,-45487
FITEM,5,45522
FITEM,5,-45566
FITEM,5,45601
FITEM,5,-45645
FITEM,5,45680
FITEM,5,-45724

FITEM,5,45759
FITEM,5,-45803
FITEM,5,45838
FITEM,5,-45882
FITEM,5,45917
FITEM,5,-45961
FITEM,5,45997
FITEM,5,-46006
FITEM,5,46008
FITEM,5,-46017
FITEM,5,46019
FITEM,5,-46028
FITEM,5,46030
FITEM,5,-46039
FITEM,5,46041
FITEM,5,-46050
FITEM,5,46052
FITEM,5,-46061
FITEM,5,46063
FITEM,5,-46072
FITEM,5,46074
FITEM,5,-46083
FITEM,5,46085
FITEM,5,-46094
FITEM,5,46096
FITEM,5,-46105
FITEM,5,46107
FITEM,5,-46116
FITEM,5,46118
FITEM,5,-46127
FITEM,5,46129
FITEM,5,-46138
FITEM,5,46140
FITEM,5,-46149
FITEM,5,46151
FITEM,5,-46160
FITEM,5,46162
FITEM,5,-46171
FITEM,5,46173
FITEM,5,-46182
FITEM,5,46184
FITEM,5,-46193
FITEM,5,46195
FITEM,5,-46204
FITEM,5,46206
FITEM,5,-46215
FITEM,5,46217
FITEM,5,-46226
FITEM,5,46228
FITEM,5,-46237
FITEM,5,46239
FITEM,5,-46248
FITEM,5,46250
FITEM,5,-46259
FITEM,5,46261
FITEM,5,-46270
FITEM,5,46272
FITEM,5,-46281
FITEM,5,46283
FITEM,5,-46292
FITEM,5,46294
FITEM,5,-46303
FITEM,5,46305
FITEM,5,-46314
FITEM,5,46316
FITEM,5,-46325

FITEM,5,46327
FITEM,5,-46336
FITEM,5,46338
FITEM,5,-46347
FITEM,5,46349
FITEM,5,-46358
FITEM,5,46360
FITEM,5,-46369
FITEM,5,46371
FITEM,5,-46380
FITEM,5,46382
FITEM,5,-46391
FITEM,5,46393
FITEM,5,-46402
FITEM,5,46404
FITEM,5,-46413
FITEM,5,46415
FITEM,5,-46424
FITEM,5,46426
FITEM,5,-46435
FITEM,5,46437
FITEM,5,-46446
FITEM,5,46448
FITEM,5,-46457
FITEM,5,46459
FITEM,5,-46468
FITEM,5,46470
FITEM,5,-46479
FITEM,5,46481
FITEM,5,-46490
FITEM,5,46870
FITEM,5,-46914
FITEM,5,46949
FITEM,5,-46993
FITEM,5,47028
FITEM,5,-47072
FITEM,5,47107
FITEM,5,-47151
FITEM,5,47186
FITEM,5,-47230
FITEM,5,47344
FITEM,5,-47388
FITEM,5,47423
FITEM,5,-47467
FITEM,5,47502
FITEM,5,-47546
FITEM,5,47581
FITEM,5,-47625
FITEM,5,47662
FITEM,5,-47670
FITEM,5,47673
FITEM,5,-47681
FITEM,5,47684
FITEM,5,-47692
FITEM,5,47695
FITEM,5,-47703
FITEM,5,47706
FITEM,5,-47714
FITEM,5,47717
FITEM,5,-47725
FITEM,5,47728
FITEM,5,-47736
FITEM,5,47739
FITEM,5,-47747
FITEM,5,47750
FITEM,5,-47758

FITEM,5,47761
FITEM,5,-47769
FITEM,5,47772
FITEM,5,-47780
FITEM,5,47783
FITEM,5,-47791
FITEM,5,47794
FITEM,5,-47802
FITEM,5,47805
FITEM,5,-47813
FITEM,5,47816
FITEM,5,-47824
FITEM,5,47827
FITEM,5,-47835
FITEM,5,47838
FITEM,5,-47846
FITEM,5,47849
FITEM,5,-47857
FITEM,5,47860
FITEM,5,-47868
FITEM,5,47871
FITEM,5,-47879
FITEM,5,47882
FITEM,5,-47890
FITEM,5,47893
FITEM,5,-47901
FITEM,5,47904
FITEM,5,-47912
FITEM,5,47915
FITEM,5,-47923
FITEM,5,47926
FITEM,5,-47934
FITEM,5,47937
FITEM,5,-47945
FITEM,5,47948
FITEM,5,-47956
FITEM,5,47959
FITEM,5,-47967
FITEM,5,47970
FITEM,5,-47978
FITEM,5,47981
FITEM,5,-47989
FITEM,5,47992
FITEM,5,-48000
FITEM,5,48003
FITEM,5,-48011
FITEM,5,48014
FITEM,5,-48022
FITEM,5,48025
FITEM,5,-48033
FITEM,5,48036
FITEM,5,-48044
FITEM,5,48047
FITEM,5,-48055
FITEM,5,48058
FITEM,5,-48066
FITEM,5,48069
FITEM,5,-48077
FITEM,5,48080
FITEM,5,-48088
FITEM,5,48091
FITEM,5,-48099
FITEM,5,48102
FITEM,5,-48110
FITEM,5,48113
FITEM,5,-48121

FITEM,5,48124
FITEM,5,-48132
FITEM,5,48135
FITEM,5,-48143
FITEM,5,48146
FITEM,5,-48154
FITEM,5,48613
FITEM,5,-48657
FITEM,5,48692
FITEM,5,-48736
FITEM,5,48771
FITEM,5,-48815
FITEM,5,48850
FITEM,5,-48894
FITEM,5,49008
FITEM,5,-49052
FITEM,5,49087
FITEM,5,-49131
FITEM,5,49166
FITEM,5,-49210
FITEM,5,49245
FITEM,5,-49289
FITEM,5,49327
FITEM,5,-49334
FITEM,5,49338
FITEM,5,-49345
FITEM,5,49349
FITEM,5,-49356
FITEM,5,49360
FITEM,5,-49367
FITEM,5,49371
FITEM,5,-49378
FITEM,5,49382
FITEM,5,-49389
FITEM,5,49393
FITEM,5,-49400
FITEM,5,49404
FITEM,5,-49411
FITEM,5,49415
FITEM,5,-49422
FITEM,5,49426
FITEM,5,-49433
FITEM,5,49437
FITEM,5,-49444
FITEM,5,49448
FITEM,5,-49455
FITEM,5,49459
FITEM,5,-49466
FITEM,5,49470
FITEM,5,-49477
FITEM,5,49481
FITEM,5,-49488
FITEM,5,49492
FITEM,5,-49499
FITEM,5,49503
FITEM,5,-49510
FITEM,5,49514
FITEM,5,-49521
FITEM,5,49525
FITEM,5,-49532
FITEM,5,49536
FITEM,5,-49543
FITEM,5,49547
FITEM,5,-49554
FITEM,5,49558
FITEM,5,-49565

FITEM,5,49569
FITEM,5,-49576
FITEM,5,49580
FITEM,5,-49587
FITEM,5,49591
FITEM,5,-49598
FITEM,5,49602
FITEM,5,-49609
FITEM,5,49613
FITEM,5,-49620
FITEM,5,49624
FITEM,5,-49631
FITEM,5,49635
FITEM,5,-49642
FITEM,5,49646
FITEM,5,-49653
FITEM,5,49657
FITEM,5,-49664
FITEM,5,49668
FITEM,5,-49675
FITEM,5,49679
FITEM,5,-49686
FITEM,5,49690
FITEM,5,-49697
FITEM,5,49701
FITEM,5,-49708
FITEM,5,49712
FITEM,5,-49719
FITEM,5,49723
FITEM,5,-49730
FITEM,5,49734
FITEM,5,-49741
FITEM,5,49745
FITEM,5,-49752
FITEM,5,49756
FITEM,5,-49763
FITEM,5,49767
FITEM,5,-49774
FITEM,5,49778
FITEM,5,-49785
FITEM,5,49789
FITEM,5,-49796
FITEM,5,49800
FITEM,5,-49807
FITEM,5,49811
FITEM,5,-49818
FITEM,5,50356
FITEM,5,-50400
FITEM,5,50435
FITEM,5,-50479
FITEM,5,50514
FITEM,5,-50558
FITEM,5,50751
FITEM,5,-50795
FITEM,5,50830
FITEM,5,-50874
FITEM,5,50909
FITEM,5,-50953
FITEM,5,50993
FITEM,5,-50998
FITEM,5,51004
FITEM,5,-51009
FITEM,5,51015
FITEM,5,-51020
FITEM,5,51026
FITEM,5,-51031

FITEM,5,51037
FITEM,5,-51042
FITEM,5,51048
FITEM,5,-51053
FITEM,5,51059
FITEM,5,-51064
FITEM,5,51070
FITEM,5,-51075
FITEM,5,51081
FITEM,5,-51086
FITEM,5,51092
FITEM,5,-51097
FITEM,5,51103
FITEM,5,-51108
FITEM,5,51114
FITEM,5,-51119
FITEM,5,51125
FITEM,5,-51130
FITEM,5,51136
FITEM,5,-51141
FITEM,5,51147
FITEM,5,-51152
FITEM,5,51158
FITEM,5,-51163
FITEM,5,51169
FITEM,5,-51174
FITEM,5,51180
FITEM,5,-51185
FITEM,5,51191
FITEM,5,-51196
FITEM,5,51202
FITEM,5,-51207
FITEM,5,51213
FITEM,5,-51218
FITEM,5,51224
FITEM,5,-51229
FITEM,5,51235
FITEM,5,-51240
FITEM,5,51246
FITEM,5,-51251
FITEM,5,51257
FITEM,5,-51262
FITEM,5,51268
FITEM,5,-51273
FITEM,5,51279
FITEM,5,-51284
FITEM,5,51290
FITEM,5,-51295
FITEM,5,51301
FITEM,5,-51306
FITEM,5,51312
FITEM,5,-51317
FITEM,5,51323
FITEM,5,-51328
FITEM,5,51334
FITEM,5,-51339
FITEM,5,51345
FITEM,5,-51350
FITEM,5,51356
FITEM,5,-51361
FITEM,5,51367
FITEM,5,-51372
FITEM,5,51378
FITEM,5,-51383
FITEM,5,51389
FITEM,5,-51394

FITEM,5,51400
FITEM,5,-51405
FITEM,5,51411
FITEM,5,-51416
FITEM,5,51422
FITEM,5,-51427
FITEM,5,51433
FITEM,5,-51438
FITEM,5,51444
FITEM,5,-51449
FITEM,5,51455
FITEM,5,-51460
FITEM,5,51466
FITEM,5,-51471
FITEM,5,51477
FITEM,5,-51482
FITEM,5,52099
FITEM,5,-52143
FITEM,5,52178
FITEM,5,-52222
FITEM,5,52494
FITEM,5,-52538
FITEM,5,52573
FITEM,5,-52617
FITEM,5,52659
FITEM,5,-52662
FITEM,5,52670
FITEM,5,-52673
FITEM,5,52681
FITEM,5,-52684
FITEM,5,52692
FITEM,5,-52695
FITEM,5,52703
FITEM,5,-52706
FITEM,5,52714
FITEM,5,-52717
FITEM,5,52725
FITEM,5,-52728
FITEM,5,52736
FITEM,5,-52739
FITEM,5,52747
FITEM,5,-52750
FITEM,5,52758
FITEM,5,-52761
FITEM,5,52769
FITEM,5,-52772
FITEM,5,52780
FITEM,5,-52783
FITEM,5,52791
FITEM,5,-52794
FITEM,5,52802
FITEM,5,-52805
FITEM,5,52813
FITEM,5,-52816
FITEM,5,52824
FITEM,5,-52827
FITEM,5,52835
FITEM,5,-52838
FITEM,5,52846
FITEM,5,-52849
FITEM,5,52857
FITEM,5,-52860
FITEM,5,52868
FITEM,5,-52871
FITEM,5,52879
FITEM,5,-52882

FITEM,5,52890
FITEM,5,-52893
FITEM,5,52901
FITEM,5,-52904
FITEM,5,52912
FITEM,5,-52915
FITEM,5,52923
FITEM,5,-52926
FITEM,5,52934
FITEM,5,-52937
FITEM,5,52945
FITEM,5,-52948
FITEM,5,52956
FITEM,5,-52959
FITEM,5,52967
FITEM,5,-52970
FITEM,5,52978
FITEM,5,-52981
FITEM,5,52989
FITEM,5,-52992
FITEM,5,53000
FITEM,5,-53003
FITEM,5,53011
FITEM,5,-53014
FITEM,5,53022
FITEM,5,-53025
FITEM,5,53033
FITEM,5,-53036
FITEM,5,53044
FITEM,5,-53047
FITEM,5,53055
FITEM,5,-53058
FITEM,5,53066
FITEM,5,-53069
FITEM,5,53077
FITEM,5,-53080
FITEM,5,53088
FITEM,5,-53091
FITEM,5,53099
FITEM,5,-53102
FITEM,5,53110
FITEM,5,-53113
FITEM,5,53121
FITEM,5,-53124
FITEM,5,53132
FITEM,5,-53135
FITEM,5,53143
FITEM,5,-53146
FITEM,5,53842
FITEM,5,-53886
FITEM,5,54237
FITEM,5,-54281
FITEM,5,54325
FITEM,5,-54326
FITEM,5,54336
FITEM,5,-54337
FITEM,5,54347
FITEM,5,-54348
FITEM,5,54358
FITEM,5,-54359
FITEM,5,54369
FITEM,5,-54370
FITEM,5,54380
FITEM,5,-54381
FITEM,5,54391
FITEM,5,-54392

FITEM,5,54402
FITEM,5,-54403
FITEM,5,54413
FITEM,5,-54414
FITEM,5,54424
FITEM,5,-54425
FITEM,5,54435
FITEM,5,-54436
FITEM,5,54446
FITEM,5,-54447
FITEM,5,54457
FITEM,5,-54458
FITEM,5,54468
FITEM,5,-54469
FITEM,5,54479
FITEM,5,-54480
FITEM,5,54490
FITEM,5,-54491
FITEM,5,54501
FITEM,5,-54502
FITEM,5,54512
FITEM,5,-54513
FITEM,5,54523
FITEM,5,-54524
FITEM,5,54534
FITEM,5,-54535
FITEM,5,54545
FITEM,5,-54546
FITEM,5,54556
FITEM,5,-54557
FITEM,5,54567
FITEM,5,-54568
FITEM,5,54578
FITEM,5,-54579
FITEM,5,54589
FITEM,5,-54590
FITEM,5,54600
FITEM,5,-54601
FITEM,5,54611
FITEM,5,-54612
FITEM,5,54622
FITEM,5,-54623
FITEM,5,54633
FITEM,5,-54634
FITEM,5,54644
FITEM,5,-54645
FITEM,5,54655
FITEM,5,-54656
FITEM,5,54666
FITEM,5,-54667
FITEM,5,54677
FITEM,5,-54678
FITEM,5,54688
FITEM,5,-54689
FITEM,5,54699
FITEM,5,-54700
FITEM,5,54710
FITEM,5,-54711
FITEM,5,54721
FITEM,5,-54722
FITEM,5,54732
FITEM,5,-54733
FITEM,5,54743
FITEM,5,-54744
FITEM,5,54754
FITEM,5,-54755

```
FITEM,5,54765
FITEM,5,-54766
FITEM,5,54776
FITEM,5,-54777
FITEM,5,54787
FITEM,5,-54788
FITEM,5,54798
FITEM,5,-54799
FITEM,5,54809
FITEM,5,-54810
NSEL,R, , ,P51X
CM,contact,NODE
CMSEL,A,contact
/MREP,EPLOT
ALLSEL,ALL
VPLOT

! comments: creating contact pair

/COM, CONTACT PAIR CREATION - START
CM,_NODECM,NODE
CM,_ELEMCM,ELEM
CM,_KPCM,KP
CM,_LINECM,LINE
CM,_AREACM,AREA
CM,_VOLUCM,VOLU
/GSAV,cwz,gsav,,temp
MP,MU,1,0.2                    ! coefficient of friction
MAT,1
MP,EMIS,1,7.88860905221e-031
R,3
REAL,3
ET,4,170
ET,5,175
R,3,,,1.0,0.1,0,
RMORE,,,1.0E20,0.0,1.0,
RMORE,0.0,0,1.0,,1.0,0.5
RMORE,0,1.0,1.0,0.0,,1.0
RMORE,10.0
KEYOPT,5,4,0
KEYOPT,5,5,3
KEYOPT,5,7,0
KEYOPT,5,8,0
KEYOPT,5,9,1
KEYOPT,5,10,2
KEYOPT,5,11,0
KEYOPT,5,12,0
KEYOPT,5,2,0
KEYOPT,4,5,0
! Generate the target surface
NSEL,S,,,TARGET
CM,_TARGET,NODE
TYPE,4
ESLN,S,0
ESURF
CMSEL,S,_ELEMCM
! Generate the contact surface
NSEL,S,,,CONTACT
CM,_CONTACT,NODE
TYPE,5
ESLN,S,0
ESURF
ALLSEL
ESEL,ALL
ESEL,S,TYPE,,4
ESEL,A,TYPE,,5
```

```
ESEL,R,REAL,,3
/PSYMB,ESYS,1
/PNUM,TYPE,1
/NUM,1
EPLOT
ESEL,ALL
ESEL,S,TYPE,,4
ESEL,A,TYPE,,5
ESEL,R,REAL,,3
CMSEL,A,_NODECM
CMDEL,_NODECM
CMSEL,A,_ELEMCM
CMDEL,_ELEMCM
CMSEL,S,_KPCM
CMDEL,_KPCM
CMSEL,S,_LINECM
CMDEL,_LINECM
CMSEL,S,_AREACM
CMDEL,_AREACM
CMSEL,S,_VOLUCM
CMDEL,_VOLUCM
/GRES,cwz,gsav
CMDEL,_TARGET
CMDEL,_CONTACT
/COM, CONTACT PAIR CREATION - END
/MREP,EPLOT
ALLSEL,ALL
/REPLOT
VPLOT
```

! comments: defining major volumes and area for viewing results

```
CM,indenter,VOLU
CMSEL,A,indenter
CMDELE,indenter
VSEL,R, , ,      10
CM,indenter,VOLU
CMSEL,A,indenter
VSEL,R, , ,      2
CM,keyvolume,VOLU
CMSEL,A,keyvolume
ASEL,R, , ,      5
CM,extarea,AREA
CMSEL,A,extarea
ASEL,R, , ,      7
CM,intarea,AREA
CMSEL,A,intarea
/MREP,EPLOT
ALLSEL,ALL
VPLOT
FINISH
CMDELE,INTAREA
CMDELE,KEYVOLUME
VSEL,R, , ,      2
CM,keyvolume,VOLU
CMSEL,A,keyvolume
ASEL,R, , ,      7
CM,intarea,AREA
CMSEL,A,intarea
/MREP,EPLOT
ALLSEL,ALL
VPLOT
/MREP,EPLOT
ALLSEL,ALL
VPLOT
```

```
! comments: Applying boundary conditions and loading

/SOLU
FLST,2,10,5,ORDE,10
FITEM,2,1
FITEM,2,-2
FITEM,2,4
FITEM,2,9
FITEM,2,14
FITEM,2,19
FITEM,2,24
FITEM,2,29
FITEM,2,33
FITEM,2,42
DA,P51X,SYMM
FLST,2,3,4,ORDE,3
FITEM,2,36
FITEM,2,44
FITEM,2,52
!*
/GO
DL,P51X, ,UY,0
/VIEW,  1, -0.413493917123    ,  0.194139313190E-01, -0.910299884529
/ANG,   1,  -4.24338859683
/REPLO
FLST,2,2,5,ORDE,2
FITEM,2,13
FITEM,2,35
!*
/GO
DA,P51X,UZ,0
FLST,2,1,5,ORDE,1
FITEM,2,44
!*
/GO
DA,P51X,UX,0
FLST,2,1,5,ORDE,1
FITEM,2,44
!*
/GO
DA,P51X,UZ,0
FLST,2,1,5,ORDE,1
FITEM,2,44
!*
/GO
DA,P51X,UY,-9                          ! initial dent depth before removal of indenter
LSWRITE,1,                             ! Defining load steps
FLST,2,1,5,ORDE,1
FITEM,2,44
!*
/GO
DA,P51X,ALL,0                          ! removing indenter
LSWRITE,2,
FLST,2,6,5,ORDE,6
FITEM,2,7
FITEM,2,12
FITEM,2,17
FITEM,2,23
FITEM,2,30
FITEM,2,37
/GO
!*
SFA,P51X,1,PRES,27.6                   ! applying pressure
LSWRITE,3,
FLST,2,6,5,ORDE,6
FITEM,2,7
```

```
FITEM,2,12
FITEM,2,17
FITEM,2,23
FITEM,2,30
FITEM,2,37
/GO
!*
SFA,P51X,1,PRES,34.6
LSWRITE,4,
FLST,2,6,5,ORDE,6
FITEM,2,7
FITEM,2,12
FITEM,2,17
FITEM,2,23
FITEM,2,30
FITEM,2,37
/GO
!*
SFA,P51X,1,PRES,24.1
LSWRITE,5,
FLST,2,6,5,ORDE,6
FITEM,2,7
FITEM,2,12
FITEM,2,17
FITEM,2,23
FITEM,2,30
FITEM,2,37
/GO
!*
SFA,P51X,1,PRES,0
LSWRITE,6,
FLST,2,6,5,ORDE,6
FITEM,2,7
FITEM,2,12
FITEM,2,17
FITEM,2,23
FITEM,2,30
FITEM,2,37
/GO
!*
SFA,P51X,1,PRES,24.1
LSWRITE,7,
FLST,2,6,5,ORDE,6
FITEM,2,7
FITEM,2,12
FITEM,2,17
FITEM,2,23
FITEM,2,30
FITEM,2,37
/GO
!*
SFA,P51X,1,PRES,34.6
LSWRITE,8,
FLST,2,6,5,ORDE,6
FITEM,2,7
FITEM,2,12
FITEM,2,17
FITEM,2,23
FITEM,2,30
FITEM,2,37
/GO
!*
SFA,P51X,1,PRES,0
LSWRITE,9,
FLST,2,6,5,ORDE,6
FITEM,2,7
```

```
FITEM,2,12
FITEM,2,17
FITEM,2,23
FITEM,2,30
FITEM,2,37
/GO
!*
SFA,P51X,1,PRES,24.1
LSWRITE,10,
FLST,2,6,5,ORDE,6
FITEM,2,7
FITEM,2,12
FITEM,2,17
FITEM,2,23
FITEM,2,30
FITEM,2,37
/GO
!*
SFA,P51X,1,PRES,34.6
LSWRITE,11,
FLST,2,6,5,ORDE,6
FITEM,2,7
FITEM,2,12
FITEM,2,17
FITEM,2,23
FITEM,2,30
FITEM,2,37
/GO
!*
SFA,P51X,1,PRES,0                    ! removing pressure
LSWRITE,12,
!*

! comments: defining non-linear settings

ANTYPE,0
NLGEOM,1
NSUBST,100,1000,10                   ! defining sub-steps
OUTRES,ERASE
OUTRES,ALL,1
AUTOTS,1
LNSRCH,1
TIME,1
/nerr,10000,10000,off

! comments: Solving by load steps
LSSOLVE,1,12,1,
FINISH

! comments: post processing phase

/POST1
/SHOW,WIN32C
SET,FIRST
/PLOPTS,INFO,3
/CONTOUR,ALL,18
/PNUM,MAT,1
/NUMBER,1
/REPLOT,RESIZE
SET,,,,,,,15
PLESOL,S,1

SET,,,,,,,30
PLESOL,S,1
SET,,,,,,,180
PLESOL,S,1
```

```
SET,,,,,,,165
PLESOL,S,1

SET,,,,,,,150
PLESOL,S,1
PLNSOL,S,1
SET,,,,,,,165
PLNSOL,S,1
! /UIS,ABORT,1
/SHOW,WIN32
/REPLOT,RESIZE
FINISH
! /EXIT,ALL
```

E.2 Apdl file for a bar dent

! comments: setting preferences- the below codes helps select static structural analysis by disabling every other analysis settings, static structural is set as 1 and all other analysis set as 0 as shown by the red highlights

```
/NOPR
KEYW,PR_SET,1
KEYW,PR_STRUC,1
KEYW,PR_THERM,0
KEYW,PR_FLUID,0
KEYW,PR_ELMAG,0
KEYW,MAGNOD,0
KEYW,MAGEDG,0
KEYW,MAGHFE,0
KEYW,MAGELC,0
KEYW,PR_MULTI,0
/GO
!*
/COM,
/COM,Preferences for GUI filtering have been set to display:
/COM,  Structural
!*
```

! comments: Selecting elements; This is the section where elements are selected

```
/PREP7
!*
ET,1,SOLID186
!*
ET,2,TARGE170
!*
ET,3,CONTA174
!*
```

! comments: defining real constant; for older version of ansys, the real constants of element needs to be defined, however, some of the new elements do not require real constants

```
R,1, , ,
!*
R,2,,,, ,,
RMORE,,,, ,,
RMORE,,,, ,,
RMORE,,,, ,,
RMORE,,,,,,
RMORE,,,,,
!*
```

! comments: defining material properties; here the material model and properties are defined

```
MPTEMP,,,,,,,,
MPTEMP,1,0
MPDATA,EX,1,,210000                    ! Young's modulus
MPDATA,PRXY,1,,0.3                     ! Poisson ratio
/CWD,'D:\ansys'
!*
TB,KINH,1,1,8,0
TBTEMP,0
TBPT,,0.0015,315                       ! stress-strain data
TBPT,,0.003,337
TBPT,,0.012,374
TBPT,,0.02,386
TBPT,,0.05,418
TBPT,,0.07,430
TBPT,,0.09,437
TBPT,,0.135,443
```

! comments: defining key points; this is the point where the geometry creation starts, four key points are created with the first key point starting from the origin as indicated as 0,0,0. The second key point shows the thickness of the pipe. The 3rd and 4th key point completes the quarter symmetry of the pipe

```
K,1,0,0,0,
K,2,0,17.399,0,
K,3,0,306.221,0,
K,4,0,323.62,0,
KPLOT
```

! comments: key points 5,6 and 7 defines the radius of the outer and inner wall of the pipe. These points are created in order to be able to create arcs joining the points

```
K,5,161.81,161.81,0,
K,6,144.411,161.81,0,
K,7,0,161.81,0,
```

! comments: Creating lines between key points

```
LSTR,      1,      2
LSTR,      3,      4
!*
```

! comments: creating arcs between key points

```
LARC,4,5,7,161.81,                     ! radius of outer wall
!*
LARC,1,5,7,161.81,
!*
LARC,3,6,7,144.411,                    ! radius of inner wall
!*
LARC,6,2,7,144.411,
LSTR,      6,      5
LPLOT
/PNUM,KP,0
/PNUM,LINE,1
/PNUM,AREA,0
/PNUM,VOLU,0
/PNUM,NODE,0
/PNUM,TABN,0
/PNUM,SVAL,0
/NUMBER,0
!*
/PNUM,ELEM,0
/REPLOT
!*
```

! comments :creating areas between lines

```
al,2,3,5,7
al,1,4,6,7

! comments: Extruding areas; the areas are extruded 3 times to create the 3 different volumes. Both the upper and
lower half needs to be extruded

VOFFST,1,328.605, ,

VOFFST,3,200, ,

VOFFST,8,721.395, ,
/
VOFFST,2,328.605, ,

VOFFST,18,200, ,

VOFFST,23,721.395, ,

! comments: Creating key point to draw bar indenter

K,100,0,323.62,,                    ! start of the key point which is at the top of the pipe in order to simulate contact
K,101,0,374.42,,
K,102,90,374.42,,
K,103,90,323.62,,

! comments: creating lines between key points

LSTR,     100,     101
LSTR,     101,     102
LSTR,     102,     103

LPLOT
LSTR,     100,     103
LFILLT,57,58,15, ,
!*
LFILLT,59,58,15, ,

! comments: creating area between lines

al,56,57,60,58,61,59
!*

! comments: extruding area to give length of indenter

VOFFST,33,304.8, ,          ! length of indenter
VPLOT
VPLOT
vadd,3,6
vadd,2,5
vadd,1,4
LPLOT

! comments: defining element size for indenter

ESIZE,10,0,                 ! element size
CM,_Y,VOLU
VSEL, , , ,      7
CM,_Y1,VOLU
CHKMSH,'VOLU'
CMSEL,S,_Y
!*

! comments:  meshing the  indenter

VSWEEP,_Y1
```

```
!*
CMDELE,_Y
CMDELE,_Y1
CMDELE,_Y2
!*
VPLOT
LPLOT

FLST,5,4,4,ORDE,4
FITEM,5,12
FITEM,5,-13
FITEM,5,36
FITEM,5,-37
CM,_Y,LINE
LSEL, , , ,P51X
CM,_Y1,LINE
CMSEL,,_Y
!*

! comments: line sizing; this is the point where the lines are divided to create the number of elements

LESIZE,_Y1, , ,90, , , , ,1          ! 90 is the number of division
!*
FLST,5,4,4,ORDE,4
FITEM,5,3
FITEM,5,5
FITEM,5,9
FITEM,5,11
CM,_Y,LINE
LSEL, , , ,P51X
CM,_Y1,LINE
CMSEL,,_Y
!*
LESIZE,_Y1, , ,30, , , , ,1
!*
FLST,5,4,4,ORDE,4
FITEM,5,4
FITEM,5,6
FITEM,5,49
FITEM,5,-50
CM,_Y,LINE
LSEL, , , ,P51X
CM,_Y1,LINE
CMSEL,,_Y
!*
LESIZE,_Y1, , ,20, , , , ,1
!*
FLST,5,4,4,ORDE,4
FITEM,5,1
FITEM,5,-2
FITEM,5,8
FITEM,5,32
CM,_Y,LINE
LSEL, , , ,P51X
CM,_Y1,LINE
CMSEL,,_Y
!*
LESIZE,_Y1, , ,6, , , , ,1
!*
CM,_Y,VOLU
VSEL, , , ,      2
CM,_Y1,VOLU
CHKMSH,'VOLU'
CMSEL,S,_Y
!*
```

```
! comments: meshing the main volume of the pipe

VSWEEP,_Y1
!*
CMDELE,_Y
CMDELE,_Y1
CMDELE,_Y2
!*
VPLOT

! comment: defining element size for the other volumes

ESIZE,45,0,                    ! element size
FLST,5,2,6,ORDE,2
FITEM,5,3
FITEM,5,8
CM,_Y,VOLU
VSEL, , , ,P51X
CM,_Y1,VOLU
CHKMSH,'VOLU'
CMSEL,S,_Y
!*

! comments: meshing other volumes

VSWEEP,_Y1
!*
CMDELE,_Y
CMDELE,_Y1
CMDELE,_Y2
!*
FLST,5,2,5,ORDE,2
FITEM,5,39
FITEM,5,-40

! comments: selecting the target area

ASEL,S, , ,P51X
APLOT
NSLA,S,1
NPLOT

! comments: selecting target nodes from the area

FLST,5,1203,1,ORDE,15
FITEM,5,335
FITEM,5,-346
FITEM,5,366
FITEM,5,857
FITEM,5,-887
FITEM,5,2083
FITEM,5,-3124
FITEM,5,3142
FITEM,5,-3150
FITEM,5,3154
FITEM,5,-3156
FITEM,5,3177
FITEM,5,-3219
FITEM,5,3313
FITEM,5,-3374
NSEL,R, , ,P51X
CM,target,NODE
CMSEL,A,target
/MREP,EPLOT
ALLSEL,ALL
VPLOT
```

! comments: selecting contact nodes

```
NSEL,S,LOC,X,0,161.81                    ! location on the x axis
NPLOT
NSEL,R,LOC,Y,306.221,323                 ! location on the y axis
NPLOT
NSEL,R,LOC,Z,0,-304                      ! location on the Z axis
NPLOT
```

! comments: automatically selected nodes based on the location selected(no need to copy and paste as it automatically generated using the above commands)

```
FLST,5,13155,1,ORDE,1486
FITEM,5,11385
FITEM,5,-11466
FITEM,5,11480
FITEM,5,-11643
FITEM,5,11650
FITEM,5,-11731
FITEM,5,11745
FITEM,5,-11908
FITEM,5,11915
FITEM,5,-11996
FITEM,5,12010
FITEM,5,-12173
FITEM,5,12180
FITEM,5,-12261
FITEM,5,12275
FITEM,5,-12438
FITEM,5,12445
FITEM,5,-12526
FITEM,5,12540
FITEM,5,-12703
FITEM,5,12710
FITEM,5,-12879
FITEM,5,12976
FITEM,5,-12981
FITEM,5,13364
FITEM,5,-13371
FITEM,5,13415
FITEM,5,-13430
FITEM,5,13453
FITEM,5,-13459
FITEM,5,13505
FITEM,5,-13518
FITEM,5,13542
FITEM,5,-13547
FITEM,5,13595
FITEM,5,-13606
FITEM,5,13631
FITEM,5,-13635
FITEM,5,13685
FITEM,5,-13694
FITEM,5,13720
FITEM,5,-13723
FITEM,5,13776
FITEM,5,-13782
FITEM,5,13810
FITEM,5,-13811
FITEM,5,13844
FITEM,5,-13857
FITEM,5,14425
FITEM,5,-14431
FITEM,5,14475
FITEM,5,-14488
```

FITEM,5,14513
FITEM,5,-14519
FITEM,5,14563
FITEM,5,-14576
FITEM,5,14601
FITEM,5,-14607
FITEM,5,14651
FITEM,5,-14664
FITEM,5,14689
FITEM,5,-14695
FITEM,5,14739
FITEM,5,-14752
FITEM,5,14777
FITEM,5,-14783
FITEM,5,14827
FITEM,5,-14840
FITEM,5,14865
FITEM,5,-14871
FITEM,5,14915
FITEM,5,-14928
FITEM,5,14953
FITEM,5,-14959
FITEM,5,15003
FITEM,5,-15016
FITEM,5,15041
FITEM,5,-15047
FITEM,5,15091
FITEM,5,-15104
FITEM,5,15129
FITEM,5,-15135
FITEM,5,15179
FITEM,5,-15192
FITEM,5,15217
FITEM,5,-15223
FITEM,5,15267
FITEM,5,-15280
FITEM,5,15305
FITEM,5,-15311
FITEM,5,15355
FITEM,5,-15368
FITEM,5,15393
FITEM,5,-15399
FITEM,5,15443
FITEM,5,-15456
FITEM,5,15481
FITEM,5,-15487
FITEM,5,15531
FITEM,5,-15544
FITEM,5,15569
FITEM,5,-15575
FITEM,5,15619
FITEM,5,-15632
FITEM,5,15657
FITEM,5,-15663
FITEM,5,15707
FITEM,5,-15720
FITEM,5,15745
FITEM,5,-15751
FITEM,5,15795
FITEM,5,-15808
FITEM,5,15833
FITEM,5,-15839
FITEM,5,15883
FITEM,5,-15896
FITEM,5,15921
FITEM,5,-15927

FITEM,5,15971
FITEM,5,-15984
FITEM,5,16009
FITEM,5,-16015
FITEM,5,16059
FITEM,5,-16072
FITEM,5,16097
FITEM,5,-16103
FITEM,5,16147
FITEM,5,-16160
FITEM,5,16185
FITEM,5,-16191
FITEM,5,16235
FITEM,5,-16248
FITEM,5,16273
FITEM,5,-16279
FITEM,5,16323
FITEM,5,-16336
FITEM,5,16361
FITEM,5,-16367
FITEM,5,16411
FITEM,5,-16424
FITEM,5,16449
FITEM,5,-16455
FITEM,5,16499
FITEM,5,-16512
FITEM,5,16537
FITEM,5,-16543
FITEM,5,16587
FITEM,5,-16600
FITEM,5,16625
FITEM,5,-16631
FITEM,5,16675
FITEM,5,-16688
FITEM,5,16713
FITEM,5,-16719
FITEM,5,16763
FITEM,5,-16776
FITEM,5,16801
FITEM,5,-16807
FITEM,5,16851
FITEM,5,-16864
FITEM,5,16889
FITEM,5,-16895
FITEM,5,16939
FITEM,5,-16952
FITEM,5,16977
FITEM,5,-16983
FITEM,5,17027
FITEM,5,-17040
FITEM,5,17065
FITEM,5,-17071
FITEM,5,17115
FITEM,5,-17128
FITEM,5,17153
FITEM,5,-17159
FITEM,5,17203
FITEM,5,-17216
FITEM,5,17241
FITEM,5,-17247
FITEM,5,17291
FITEM,5,-17304
FITEM,5,17329
FITEM,5,-17335
FITEM,5,17379
FITEM,5,-17392

FITEM,5,17417
FITEM,5,-17423
FITEM,5,17467
FITEM,5,-17480
FITEM,5,17505
FITEM,5,-17511
FITEM,5,17555
FITEM,5,-17568
FITEM,5,17593
FITEM,5,-17599
FITEM,5,17643
FITEM,5,-17656
FITEM,5,17681
FITEM,5,-17687
FITEM,5,17731
FITEM,5,-17744
FITEM,5,17769
FITEM,5,-17775
FITEM,5,17819
FITEM,5,-17832
FITEM,5,17857
FITEM,5,-17863
FITEM,5,17907
FITEM,5,-17920
FITEM,5,17945
FITEM,5,-17951
FITEM,5,17995
FITEM,5,-18008
FITEM,5,18033
FITEM,5,-18039
FITEM,5,18083
FITEM,5,-18096
FITEM,5,18121
FITEM,5,-18127
FITEM,5,18171
FITEM,5,-18184
FITEM,5,18209
FITEM,5,-18215
FITEM,5,18259
FITEM,5,-18272
FITEM,5,18297
FITEM,5,-18303
FITEM,5,18347
FITEM,5,-18360
FITEM,5,18385
FITEM,5,-18391
FITEM,5,18435
FITEM,5,-18448
FITEM,5,18473
FITEM,5,-18479
FITEM,5,18523
FITEM,5,-18536
FITEM,5,18561
FITEM,5,-18567
FITEM,5,18611
FITEM,5,-18624
FITEM,5,18649
FITEM,5,-18655
FITEM,5,18699
FITEM,5,-18712
FITEM,5,18737
FITEM,5,-18743
FITEM,5,18787
FITEM,5,-18800
FITEM,5,18825
FITEM,5,-18831

FITEM,5,18875
FITEM,5,-18888
FITEM,5,18913
FITEM,5,-18919
FITEM,5,18963
FITEM,5,-18976
FITEM,5,19001
FITEM,5,-19007
FITEM,5,19051
FITEM,5,-19064
FITEM,5,19089
FITEM,5,-19095
FITEM,5,19139
FITEM,5,-19152
FITEM,5,19177
FITEM,5,-19183
FITEM,5,19227
FITEM,5,-19240
FITEM,5,19265
FITEM,5,-19271
FITEM,5,19315
FITEM,5,-19328
FITEM,5,19353
FITEM,5,-19359
FITEM,5,19403
FITEM,5,-19416
FITEM,5,19441
FITEM,5,-19447
FITEM,5,19491
FITEM,5,-19504
FITEM,5,19529
FITEM,5,-19535
FITEM,5,19579
FITEM,5,-19592
FITEM,5,19617
FITEM,5,-19623
FITEM,5,19667
FITEM,5,-19680
FITEM,5,19705
FITEM,5,-19711
FITEM,5,19755
FITEM,5,-19768
FITEM,5,19793
FITEM,5,-19799
FITEM,5,19843
FITEM,5,-19856
FITEM,5,19881
FITEM,5,-19887
FITEM,5,19931
FITEM,5,-19944
FITEM,5,19969
FITEM,5,-19975
FITEM,5,20019
FITEM,5,-20032
FITEM,5,20057
FITEM,5,-20063
FITEM,5,20107
FITEM,5,-20120
FITEM,5,20145
FITEM,5,-20151
FITEM,5,20195
FITEM,5,-20208
FITEM,5,20233
FITEM,5,-20239
FITEM,5,20283
FITEM,5,-20296

FITEM,5,20321
FITEM,5,-20327
FITEM,5,20371
FITEM,5,-20384
FITEM,5,20409
FITEM,5,-20415
FITEM,5,20459
FITEM,5,-20472
FITEM,5,20497
FITEM,5,-20503
FITEM,5,20547
FITEM,5,-20560
FITEM,5,20585
FITEM,5,-20591
FITEM,5,20635
FITEM,5,-20648
FITEM,5,20673
FITEM,5,-20679
FITEM,5,20723
FITEM,5,-20736
FITEM,5,20761
FITEM,5,-20767
FITEM,5,20811
FITEM,5,-20824
FITEM,5,20849
FITEM,5,-20855
FITEM,5,20899
FITEM,5,-20912
FITEM,5,20937
FITEM,5,-20943
FITEM,5,20987
FITEM,5,-21000
FITEM,5,21025
FITEM,5,-21031
FITEM,5,21075
FITEM,5,-21088
FITEM,5,21113
FITEM,5,-21119
FITEM,5,21163
FITEM,5,-21176
FITEM,5,21201
FITEM,5,-21207
FITEM,5,21251
FITEM,5,-21264
FITEM,5,21289
FITEM,5,-21295
FITEM,5,21339
FITEM,5,-21352
FITEM,5,21377
FITEM,5,-21383
FITEM,5,21427
FITEM,5,-21440
FITEM,5,21465
FITEM,5,-21471
FITEM,5,21515
FITEM,5,-21528
FITEM,5,21553
FITEM,5,-21559
FITEM,5,21603
FITEM,5,-21616
FITEM,5,40954
FITEM,5,-40959
FITEM,5,41092
FITEM,5,-41167
FITEM,5,41672
FITEM,5,-41753

FITEM,5,41760
FITEM,5,-41841
FITEM,5,41848
FITEM,5,-41929
FITEM,5,41936
FITEM,5,-42017
FITEM,5,42024
FITEM,5,-42105
FITEM,5,42112
FITEM,5,-42193
FITEM,5,42200
FITEM,5,-42281
FITEM,5,42288
FITEM,5,-42369
FITEM,5,42376
FITEM,5,-42457
FITEM,5,42464
FITEM,5,-42545
FITEM,5,42552
FITEM,5,-43453
FITEM,5,43525
FITEM,5,-43606
FITEM,5,43613
FITEM,5,-43694
FITEM,5,43701
FITEM,5,-43782
FITEM,5,43789
FITEM,5,-43870
FITEM,5,43877
FITEM,5,-43958
FITEM,5,43965
FITEM,5,-44046
FITEM,5,44053
FITEM,5,-44134
FITEM,5,44141
FITEM,5,-44222
FITEM,5,44229
FITEM,5,-44310
FITEM,5,44317
FITEM,5,-44398
FITEM,5,44405
FITEM,5,-45306
FITEM,5,45378
FITEM,5,-45459
FITEM,5,45466
FITEM,5,-45547
FITEM,5,45554
FITEM,5,-45635
FITEM,5,45642
FITEM,5,-45723
FITEM,5,45730
FITEM,5,-45811
FITEM,5,45818
FITEM,5,-45899
FITEM,5,45906
FITEM,5,-45987
FITEM,5,45994
FITEM,5,-46075
FITEM,5,46082
FITEM,5,-46163
FITEM,5,46170
FITEM,5,-46251
FITEM,5,46259
FITEM,5,-46268
FITEM,5,46270
FITEM,5,-46279

FITEM,5,46281
FITEM,5,-46290
FITEM,5,46292
FITEM,5,-46301
FITEM,5,46303
FITEM,5,-46312
FITEM,5,46314
FITEM,5,-46323
FITEM,5,46325
FITEM,5,-46334
FITEM,5,46336
FITEM,5,-46345
FITEM,5,46347
FITEM,5,-46356
FITEM,5,46358
FITEM,5,-46367
FITEM,5,46369
FITEM,5,-46378
FITEM,5,46380
FITEM,5,-46389
FITEM,5,46391
FITEM,5,-46400
FITEM,5,46402
FITEM,5,-46411
FITEM,5,46413
FITEM,5,-46422
FITEM,5,46424
FITEM,5,-46433
FITEM,5,46435
FITEM,5,-46444
FITEM,5,46446
FITEM,5,-46455
FITEM,5,46457
FITEM,5,-46466
FITEM,5,46468
FITEM,5,-46477
FITEM,5,46479
FITEM,5,-46488
FITEM,5,46490
FITEM,5,-46499
FITEM,5,46501
FITEM,5,-46510
FITEM,5,46512
FITEM,5,-46521
FITEM,5,46523
FITEM,5,-46532
FITEM,5,46534
FITEM,5,-46543
FITEM,5,46545
FITEM,5,-46554
FITEM,5,46556
FITEM,5,-46565
FITEM,5,46567
FITEM,5,-46576
FITEM,5,46578
FITEM,5,-46587
FITEM,5,46589
FITEM,5,-46598
FITEM,5,46600
FITEM,5,-46609
FITEM,5,46611
FITEM,5,-46620
FITEM,5,46622
FITEM,5,-46631
FITEM,5,46633
FITEM,5,-46642

FITEM,5,46644
FITEM,5,-46653
FITEM,5,46655
FITEM,5,-46664
FITEM,5,46666
FITEM,5,-46675
FITEM,5,46677
FITEM,5,-46686
FITEM,5,46688
FITEM,5,-46697
FITEM,5,46699
FITEM,5,-46708
FITEM,5,46710
FITEM,5,-46719
FITEM,5,46721
FITEM,5,-46730
FITEM,5,46732
FITEM,5,-46741
FITEM,5,46743
FITEM,5,-46752
FITEM,5,46754
FITEM,5,-46763
FITEM,5,46765
FITEM,5,-46774
FITEM,5,46776
FITEM,5,-46785
FITEM,5,46787
FITEM,5,-46796
FITEM,5,46798
FITEM,5,-46807
FITEM,5,46809
FITEM,5,-46818
FITEM,5,46820
FITEM,5,-46829
FITEM,5,46831
FITEM,5,-46840
FITEM,5,46842
FITEM,5,-46851
FITEM,5,46853
FITEM,5,-46862
FITEM,5,46864
FITEM,5,-46873
FITEM,5,46875
FITEM,5,-46884
FITEM,5,46886
FITEM,5,-46895
FITEM,5,46897
FITEM,5,-46906
FITEM,5,46908
FITEM,5,-46917
FITEM,5,46919
FITEM,5,-46928
FITEM,5,46930
FITEM,5,-46939
FITEM,5,46941
FITEM,5,-46950
FITEM,5,46952
FITEM,5,-46961
FITEM,5,46963
FITEM,5,-46972
FITEM,5,46974
FITEM,5,-46983
FITEM,5,46985
FITEM,5,-46994
FITEM,5,46996
FITEM,5,-47005

FITEM,5,47007
FITEM,5,-47016
FITEM,5,47018
FITEM,5,-47027
FITEM,5,47029
FITEM,5,-47038
FITEM,5,47040
FITEM,5,-47049
FITEM,5,47051
FITEM,5,-47060
FITEM,5,47062
FITEM,5,-47071
FITEM,5,47073
FITEM,5,-47082
FITEM,5,47084
FITEM,5,-47093
FITEM,5,47095
FITEM,5,-47104
FITEM,5,47106
FITEM,5,-47115
FITEM,5,47117
FITEM,5,-47126
FITEM,5,47128
FITEM,5,-47137
FITEM,5,47139
FITEM,5,-47148
FITEM,5,47150
FITEM,5,-47159
FITEM,5,47231
FITEM,5,-47312
FITEM,5,47319
FITEM,5,-47400
FITEM,5,47407
FITEM,5,-47488
FITEM,5,47495
FITEM,5,-47576
FITEM,5,47583
FITEM,5,-47664
FITEM,5,47759
FITEM,5,-47840
FITEM,5,47847
FITEM,5,-47928
FITEM,5,47935
FITEM,5,-48016
FITEM,5,48023
FITEM,5,-48104
FITEM,5,48113
FITEM,5,-48121
FITEM,5,48124
FITEM,5,-48132
FITEM,5,48135
FITEM,5,-48143
FITEM,5,48146
FITEM,5,-48154
FITEM,5,48157
FITEM,5,-48165
FITEM,5,48168
FITEM,5,-48176
FITEM,5,48179
FITEM,5,-48187
FITEM,5,48190
FITEM,5,-48198
FITEM,5,48201
FITEM,5,-48209
FITEM,5,48212
FITEM,5,-48220

FITEM,5,48223
FITEM,5,-48231
FITEM,5,48234
FITEM,5,-48242
FITEM,5,48245
FITEM,5,-48253
FITEM,5,48256
FITEM,5,-48264
FITEM,5,48267
FITEM,5,-48275
FITEM,5,48278
FITEM,5,-48286
FITEM,5,48289
FITEM,5,-48297
FITEM,5,48300
FITEM,5,-48308
FITEM,5,48311
FITEM,5,-48319
FITEM,5,48322
FITEM,5,-48330
FITEM,5,48333
FITEM,5,-48341
FITEM,5,48344
FITEM,5,-48352
FITEM,5,48355
FITEM,5,-48363
FITEM,5,48366
FITEM,5,-48374
FITEM,5,48377
FITEM,5,-48385
FITEM,5,48388
FITEM,5,-48396
FITEM,5,48399
FITEM,5,-48407
FITEM,5,48410
FITEM,5,-48418
FITEM,5,48421
FITEM,5,-48429
FITEM,5,48432
FITEM,5,-48440
FITEM,5,48443
FITEM,5,-48451
FITEM,5,48454
FITEM,5,-48462
FITEM,5,48465
FITEM,5,-48473
FITEM,5,48476
FITEM,5,-48484
FITEM,5,48487
FITEM,5,-48495
FITEM,5,48498
FITEM,5,-48506
FITEM,5,48509
FITEM,5,-48517
FITEM,5,48520
FITEM,5,-48528
FITEM,5,48531
FITEM,5,-48539
FITEM,5,48542
FITEM,5,-48550
FITEM,5,48553
FITEM,5,-48561
FITEM,5,48564
FITEM,5,-48572
FITEM,5,48575
FITEM,5,-48583

FITEM,5,48586
FITEM,5,-48594
FITEM,5,48597
FITEM,5,-48605
FITEM,5,48608
FITEM,5,-48616
FITEM,5,48619
FITEM,5,-48627
FITEM,5,48630
FITEM,5,-48638
FITEM,5,48641
FITEM,5,-48649
FITEM,5,48652
FITEM,5,-48660
FITEM,5,48663
FITEM,5,-48671
FITEM,5,48674
FITEM,5,-48682
FITEM,5,48685
FITEM,5,-48693
FITEM,5,48696
FITEM,5,-48704
FITEM,5,48707
FITEM,5,-48715
FITEM,5,48718
FITEM,5,-48726
FITEM,5,48729
FITEM,5,-48737
FITEM,5,48740
FITEM,5,-48748
FITEM,5,48751
FITEM,5,-48759
FITEM,5,48762
FITEM,5,-48770
FITEM,5,48773
FITEM,5,-48781
FITEM,5,48784
FITEM,5,-48792
FITEM,5,48795
FITEM,5,-48803
FITEM,5,48806
FITEM,5,-48814
FITEM,5,48817
FITEM,5,-48825
FITEM,5,48828
FITEM,5,-48836
FITEM,5,48839
FITEM,5,-48847
FITEM,5,48850
FITEM,5,-48858
FITEM,5,48861
FITEM,5,-48869
FITEM,5,48872
FITEM,5,-48880
FITEM,5,48883
FITEM,5,-48891
FITEM,5,48894
FITEM,5,-48902
FITEM,5,48905
FITEM,5,-48913
FITEM,5,48916
FITEM,5,-48924
FITEM,5,48927
FITEM,5,-48935
FITEM,5,48938
FITEM,5,-48946

FITEM,5,48949
FITEM,5,-48957
FITEM,5,48960
FITEM,5,-48968
FITEM,5,48971
FITEM,5,-48979
FITEM,5,48982
FITEM,5,-48990
FITEM,5,48993
FITEM,5,-49001
FITEM,5,49004
FITEM,5,-49012
FITEM,5,49172
FITEM,5,-49253
FITEM,5,49260
FITEM,5,-49341
FITEM,5,49348
FITEM,5,-49429
FITEM,5,49436
FITEM,5,-49517
FITEM,5,49612
FITEM,5,-49693
FITEM,5,49700
FITEM,5,-49781
FITEM,5,49788
FITEM,5,-49869
FITEM,5,49876
FITEM,5,-49957
FITEM,5,49967
FITEM,5,-49974
FITEM,5,49978
FITEM,5,-49985
FITEM,5,49989
FITEM,5,-49996
FITEM,5,50000
FITEM,5,-50007
FITEM,5,50011
FITEM,5,-50018
FITEM,5,50022
FITEM,5,-50029
FITEM,5,50033
FITEM,5,-50040
FITEM,5,50044
FITEM,5,-50051
FITEM,5,50055
FITEM,5,-50062
FITEM,5,50066
FITEM,5,-50073
FITEM,5,50077
FITEM,5,-50084
FITEM,5,50088
FITEM,5,-50095
FITEM,5,50099
FITEM,5,-50106
FITEM,5,50110
FITEM,5,-50117
FITEM,5,50121
FITEM,5,-50128
FITEM,5,50132
FITEM,5,-50139
FITEM,5,50143
FITEM,5,-50150
FITEM,5,50154
FITEM,5,-50161
FITEM,5,50165
FITEM,5,-50172

FITEM,5,50176
FITEM,5,-50183
FITEM,5,50187
FITEM,5,-50194
FITEM,5,50198
FITEM,5,-50205
FITEM,5,50209
FITEM,5,-50216
FITEM,5,50220
FITEM,5,-50227
FITEM,5,50231
FITEM,5,-50238
FITEM,5,50242
FITEM,5,-50249
FITEM,5,50253
FITEM,5,-50260
FITEM,5,50264
FITEM,5,-50271
FITEM,5,50275
FITEM,5,-50282
FITEM,5,50286
FITEM,5,-50293
FITEM,5,50297
FITEM,5,-50304
FITEM,5,50308
FITEM,5,-50315
FITEM,5,50319
FITEM,5,-50326
FITEM,5,50330
FITEM,5,-50337
FITEM,5,50341
FITEM,5,-50348
FITEM,5,50352
FITEM,5,-50359
FITEM,5,50363
FITEM,5,-50370
FITEM,5,50374
FITEM,5,-50381
FITEM,5,50385
FITEM,5,-50392
FITEM,5,50396
FITEM,5,-50403
FITEM,5,50407
FITEM,5,-50414
FITEM,5,50418
FITEM,5,-50425
FITEM,5,50429
FITEM,5,-50436
FITEM,5,50440
FITEM,5,-50447
FITEM,5,50451
FITEM,5,-50458
FITEM,5,50462
FITEM,5,-50469
FITEM,5,50473
FITEM,5,-50480
FITEM,5,50484
FITEM,5,-50491
FITEM,5,50495
FITEM,5,-50502
FITEM,5,50506
FITEM,5,-50513
FITEM,5,50517
FITEM,5,-50524
FITEM,5,50528
FITEM,5,-50535

FITEM,5,50539
FITEM,5,-50546
FITEM,5,50550
FITEM,5,-50557
FITEM,5,50561
FITEM,5,-50568
FITEM,5,50572
FITEM,5,-50579
FITEM,5,50583
FITEM,5,-50590
FITEM,5,50594
FITEM,5,-50601
FITEM,5,50605
FITEM,5,-50612
FITEM,5,50616
FITEM,5,-50623
FITEM,5,50627
FITEM,5,-50634
FITEM,5,50638
FITEM,5,-50645
FITEM,5,50649
FITEM,5,-50656
FITEM,5,50660
FITEM,5,-50667
FITEM,5,50671
FITEM,5,-50678
FITEM,5,50682
FITEM,5,-50689
FITEM,5,50693
FITEM,5,-50700
FITEM,5,50704
FITEM,5,-50711
FITEM,5,50715
FITEM,5,-50722
FITEM,5,50726
FITEM,5,-50733
FITEM,5,50737
FITEM,5,-50744
FITEM,5,50748
FITEM,5,-50755
FITEM,5,50759
FITEM,5,-50766
FITEM,5,50770
FITEM,5,-50777
FITEM,5,50781
FITEM,5,-50788
FITEM,5,50792
FITEM,5,-50799
FITEM,5,50803
FITEM,5,-50810
FITEM,5,50814
FITEM,5,-50821
FITEM,5,50825
FITEM,5,-50832
FITEM,5,50836
FITEM,5,-50843
FITEM,5,50847
FITEM,5,-50854
FITEM,5,50858
FITEM,5,-50865
FITEM,5,51113
FITEM,5,-51194
FITEM,5,51201
FITEM,5,-51282
FITEM,5,51289
FITEM,5,-51370

FITEM,5,51553
FITEM,5,-51634
FITEM,5,51641
FITEM,5,-51722
FITEM,5,51729
FITEM,5,-51810
FITEM,5,51822
FITEM,5,-51827
FITEM,5,51833
FITEM,5,-51838
FITEM,5,51844
FITEM,5,-51849
FITEM,5,51855
FITEM,5,-51860
FITEM,5,51866
FITEM,5,-51871
FITEM,5,51877
FITEM,5,-51882
FITEM,5,51888
FITEM,5,-51893
FITEM,5,51899
FITEM,5,-51904
FITEM,5,51910
FITEM,5,-51915
FITEM,5,51921
FITEM,5,-51926
FITEM,5,51932
FITEM,5,-51937
FITEM,5,51943
FITEM,5,-51948
FITEM,5,51954
FITEM,5,-51959
FITEM,5,51965
FITEM,5,-51970
FITEM,5,51976
FITEM,5,-51981
FITEM,5,51987
FITEM,5,-51992
FITEM,5,51998
FITEM,5,-52003
FITEM,5,52009
FITEM,5,-52014
FITEM,5,52020
FITEM,5,-52025
FITEM,5,52031
FITEM,5,-52036
FITEM,5,52042
FITEM,5,-52047
FITEM,5,52053
FITEM,5,-52058
FITEM,5,52064
FITEM,5,-52069
FITEM,5,52075
FITEM,5,-52080
FITEM,5,52086
FITEM,5,-52091
FITEM,5,52097
FITEM,5,-52102
FITEM,5,52108
FITEM,5,-52113
FITEM,5,52119
FITEM,5,-52124
FITEM,5,52130
FITEM,5,-52135
FITEM,5,52141
FITEM,5,-52146

FITEM,5,52152
FITEM,5,-52157
FITEM,5,52163
FITEM,5,-52168
FITEM,5,52174
FITEM,5,-52179
FITEM,5,52185
FITEM,5,-52190
FITEM,5,52196
FITEM,5,-52201
FITEM,5,52207
FITEM,5,-52212
FITEM,5,52218
FITEM,5,-52223
FITEM,5,52229
FITEM,5,-52234
FITEM,5,52240
FITEM,5,-52245
FITEM,5,52251
FITEM,5,-52256
FITEM,5,52262
FITEM,5,-52267
FITEM,5,52273
FITEM,5,-52278
FITEM,5,52284
FITEM,5,-52289
FITEM,5,52295
FITEM,5,-52300
FITEM,5,52306
FITEM,5,-52311
FITEM,5,52317
FITEM,5,-52322
FITEM,5,52328
FITEM,5,-52333
FITEM,5,52339
FITEM,5,-52344
FITEM,5,52350
FITEM,5,-52355
FITEM,5,52361
FITEM,5,-52366
FITEM,5,52372
FITEM,5,-52377
FITEM,5,52383
FITEM,5,-52388
FITEM,5,52394
FITEM,5,-52399
FITEM,5,52405
FITEM,5,-52410
FITEM,5,52416
FITEM,5,-52421
FITEM,5,52427
FITEM,5,-52432
FITEM,5,52438
FITEM,5,-52443
FITEM,5,52449
FITEM,5,-52454
FITEM,5,52460
FITEM,5,-52465
FITEM,5,52471
FITEM,5,-52476
FITEM,5,52482
FITEM,5,-52487
FITEM,5,52493
FITEM,5,-52498
FITEM,5,52504
FITEM,5,-52509

FITEM,5,52515
FITEM,5,-52520
FITEM,5,52526
FITEM,5,-52531
FITEM,5,52537
FITEM,5,-52542
FITEM,5,52548
FITEM,5,-52553
FITEM,5,52559
FITEM,5,-52564
FITEM,5,52570
FITEM,5,-52575
FITEM,5,52581
FITEM,5,-52586
FITEM,5,52592
FITEM,5,-52597
FITEM,5,52603
FITEM,5,-52608
FITEM,5,52614
FITEM,5,-52619
FITEM,5,52625
FITEM,5,-52630
FITEM,5,52636
FITEM,5,-52641
FITEM,5,52647
FITEM,5,-52652
FITEM,5,52658
FITEM,5,-52663
FITEM,5,52669
FITEM,5,-52674
FITEM,5,52680
FITEM,5,-52685
FITEM,5,52691
FITEM,5,-52696
FITEM,5,52702
FITEM,5,-52707
FITEM,5,52713
FITEM,5,-52718
FITEM,5,53054
FITEM,5,-53135
FITEM,5,53142
FITEM,5,-53223
FITEM,5,53494
FITEM,5,-53575
FITEM,5,53582
FITEM,5,-53663
FITEM,5,53677
FITEM,5,-53680
FITEM,5,53688
FITEM,5,-53691
FITEM,5,53699
FITEM,5,-53702
FITEM,5,53710
FITEM,5,-53713
FITEM,5,53721
FITEM,5,-53724
FITEM,5,53732
FITEM,5,-53735
FITEM,5,53743
FITEM,5,-53746
FITEM,5,53754
FITEM,5,-53757
FITEM,5,53765
FITEM,5,-53768
FITEM,5,53776
FITEM,5,-53779

FITEM,5,53787
FITEM,5,-53790
FITEM,5,53798
FITEM,5,-53801
FITEM,5,53809
FITEM,5,-53812
FITEM,5,53820
FITEM,5,-53823
FITEM,5,53831
FITEM,5,-53834
FITEM,5,53842
FITEM,5,-53845
FITEM,5,53853
FITEM,5,-53856
FITEM,5,53864
FITEM,5,-53867
FITEM,5,53875
FITEM,5,-53878
FITEM,5,53886
FITEM,5,-53889
FITEM,5,53897
FITEM,5,-53900
FITEM,5,53908
FITEM,5,-53911
FITEM,5,53919
FITEM,5,-53922
FITEM,5,53930
FITEM,5,-53933
FITEM,5,53941
FITEM,5,-53944
FITEM,5,53952
FITEM,5,-53955
FITEM,5,53963
FITEM,5,-53966
FITEM,5,53974
FITEM,5,-53977
FITEM,5,53985
FITEM,5,-53988
FITEM,5,53996
FITEM,5,-53999
FITEM,5,54007
FITEM,5,-54010
FITEM,5,54018
FITEM,5,-54021
FITEM,5,54029
FITEM,5,-54032
FITEM,5,54040
FITEM,5,-54043
FITEM,5,54051
FITEM,5,-54054
FITEM,5,54062
FITEM,5,-54065
FITEM,5,54073
FITEM,5,-54076
FITEM,5,54084
FITEM,5,-54087
FITEM,5,54095
FITEM,5,-54098
FITEM,5,54106
FITEM,5,-54109
FITEM,5,54117
FITEM,5,-54120
FITEM,5,54128
FITEM,5,-54131
FITEM,5,54139
FITEM,5,-54142

FITEM,5,54150
FITEM,5,-54153
FITEM,5,54161
FITEM,5,-54164
FITEM,5,54172
FITEM,5,-54175
FITEM,5,54183
FITEM,5,-54186
FITEM,5,54194
FITEM,5,-54197
FITEM,5,54205
FITEM,5,-54208
FITEM,5,54216
FITEM,5,-54219
FITEM,5,54227
FITEM,5,-54230
FITEM,5,54238
FITEM,5,-54241
FITEM,5,54249
FITEM,5,-54252
FITEM,5,54260
FITEM,5,-54263
FITEM,5,54271
FITEM,5,-54274
FITEM,5,54282
FITEM,5,-54285
FITEM,5,54293
FITEM,5,-54296
FITEM,5,54304
FITEM,5,-54307
FITEM,5,54315
FITEM,5,-54318
FITEM,5,54326
FITEM,5,-54329
FITEM,5,54337
FITEM,5,-54340
FITEM,5,54348
FITEM,5,-54351
FITEM,5,54359
FITEM,5,-54362
FITEM,5,54370
FITEM,5,-54373
FITEM,5,54381
FITEM,5,-54384
FITEM,5,54392
FITEM,5,-54395
FITEM,5,54403
FITEM,5,-54406
FITEM,5,54414
FITEM,5,-54417
FITEM,5,54425
FITEM,5,-54428
FITEM,5,54436
FITEM,5,-54439
FITEM,5,54447
FITEM,5,-54450
FITEM,5,54458
FITEM,5,-54461
FITEM,5,54469
FITEM,5,-54472
FITEM,5,54480
FITEM,5,-54483
FITEM,5,54491
FITEM,5,-54494
FITEM,5,54502
FITEM,5,-54505

FITEM,5,54513
FITEM,5,-54516
FITEM,5,54524
FITEM,5,-54527
FITEM,5,54535
FITEM,5,-54538
FITEM,5,54546
FITEM,5,-54549
FITEM,5,54557
FITEM,5,-54560
FITEM,5,54568
FITEM,5,-54571
FITEM,5,54995
FITEM,5,-55076
FITEM,5,55435
FITEM,5,-55516
FITEM,5,55532
FITEM,5,-55533
FITEM,5,55543
FITEM,5,-55544
FITEM,5,55554
FITEM,5,-55555
FITEM,5,55565
FITEM,5,-55566
FITEM,5,55576
FITEM,5,-55577
FITEM,5,55587
FITEM,5,-55588
FITEM,5,55598
FITEM,5,-55599
FITEM,5,55609
FITEM,5,-55610
FITEM,5,55620
FITEM,5,-55621
FITEM,5,55631
FITEM,5,-55632
FITEM,5,55642
FITEM,5,-55643
FITEM,5,55653
FITEM,5,-55654
FITEM,5,55664
FITEM,5,-55665
FITEM,5,55675
FITEM,5,-55676
FITEM,5,55686
FITEM,5,-55687
FITEM,5,55697
FITEM,5,-55698
FITEM,5,55708
FITEM,5,-55709
FITEM,5,55719
FITEM,5,-55720
FITEM,5,55730
FITEM,5,-55731
FITEM,5,55741
FITEM,5,-55742
FITEM,5,55752
FITEM,5,-55753
FITEM,5,55763
FITEM,5,-55764
FITEM,5,55774
FITEM,5,-55775
FITEM,5,55785
FITEM,5,-55786
FITEM,5,55796
FITEM,5,-55797

FITEM,5,55807
FITEM,5,-55808
FITEM,5,55818
FITEM,5,-55819
FITEM,5,55829
FITEM,5,-55830
FITEM,5,55840
FITEM,5,-55841
FITEM,5,55851
FITEM,5,-55852
FITEM,5,55862
FITEM,5,-55863
FITEM,5,55873
FITEM,5,-55874
FITEM,5,55884
FITEM,5,-55885
FITEM,5,55895
FITEM,5,-55896
FITEM,5,55906
FITEM,5,-55907
FITEM,5,55917
FITEM,5,-55918
FITEM,5,55928
FITEM,5,-55929
FITEM,5,55939
FITEM,5,-55940
FITEM,5,55950
FITEM,5,-55951
FITEM,5,55961
FITEM,5,-55962
FITEM,5,55972
FITEM,5,-55973
FITEM,5,55983
FITEM,5,-55984
FITEM,5,55994
FITEM,5,-55995
FITEM,5,56005
FITEM,5,-56006
FITEM,5,56016
FITEM,5,-56017
FITEM,5,56027
FITEM,5,-56028
FITEM,5,56038
FITEM,5,-56039
FITEM,5,56049
FITEM,5,-56050
FITEM,5,56060
FITEM,5,-56061
FITEM,5,56071
FITEM,5,-56072
FITEM,5,56082
FITEM,5,-56083
FITEM,5,56093
FITEM,5,-56094
FITEM,5,56104
FITEM,5,-56105
FITEM,5,56115
FITEM,5,-56116
FITEM,5,56126
FITEM,5,-56127
FITEM,5,56137
FITEM,5,-56138
FITEM,5,56148
FITEM,5,-56149
FITEM,5,56159
FITEM,5,-56160

```
FITEM,5,56170
FITEM,5,-56171
FITEM,5,56181
FITEM,5,-56182
FITEM,5,56192
FITEM,5,-56193
FITEM,5,56203
FITEM,5,-56204
FITEM,5,56214
FITEM,5,-56215
FITEM,5,56225
FITEM,5,-56226
FITEM,5,56236
FITEM,5,-56237
FITEM,5,56247
FITEM,5,-56248
FITEM,5,56258
FITEM,5,-56259
FITEM,5,56269
FITEM,5,-56270
FITEM,5,56280
FITEM,5,-56281
FITEM,5,56291
FITEM,5,-56292
FITEM,5,56302
FITEM,5,-56303
FITEM,5,56313
FITEM,5,-56314
FITEM,5,56324
FITEM,5,-56325
FITEM,5,56335
FITEM,5,-56336
FITEM,5,56346
FITEM,5,-56347
FITEM,5,56357
FITEM,5,-56358
FITEM,5,56368
FITEM,5,-56369
FITEM,5,56379
FITEM,5,-56380
FITEM,5,56390
FITEM,5,-56391
FITEM,5,56401
FITEM,5,-56402
FITEM,5,56412
FITEM,5,-56413
FITEM,5,56423
FITEM,5,-56424
NSEL,R, , ,P51X
CM,contact,NODE
CMSEL,A,contact
/MREP,EPLOT
ALLSEL,ALL
VPLOT

! comments: creating contact pair

/COM, CONTACT PAIR CREATION - START
CM,_NODECM,NODE
CM,_ELEMCM,ELEM
CM,_KPCM,KP
CM,_LINECM,LINE
CM,_AREACM,AREA
CM,_VOLUCM,VOLU
/GSAV,cwz,gsav,,temp
MP,MU,1,0.2                    ! coefficient of friction
```

```
MAT,1
MP,EMIS,1,7.88860905221e-031
R,3
REAL,3
ET,4,170
ET,5,175
R,3,,,1.0,0.1,0,
RMORE,,,1.0E20,0.0,1.0,
RMORE,0.0,0,1.0,,1.0,0.5
RMORE,0,1.0,1.0,0.0,,1.0
RMORE,10.0
KEYOPT,5,4,0
KEYOPT,5,5,3
KEYOPT,5,7,0
KEYOPT,5,8,0
KEYOPT,5,9,1
KEYOPT,5,10,2
KEYOPT,5,11,0
KEYOPT,5,12,0
KEYOPT,5,2,0
KEYOPT,4,5,0
! Generate the target surface
NSEL,S,,,TARGET
CM,_TARGET,NODE
TYPE,4
ESLN,S,0
ESURF
CMSEL,S,_ELEMCM
! Generate the contact surface
NSEL,S,,,CONTACT
CM,_CONTACT,NODE
TYPE,5
ESLN,S,0
ESURF
ALLSEL
ESEL,ALL
ESEL,S,TYPE,,4
ESEL,A,TYPE,,5
ESEL,R,REAL,,3
/PSYMB,ESYS,1
/PNUM,TYPE,1
/NUM,1
EPLOT
ESEL,ALL
ESEL,S,TYPE,,4
ESEL,A,TYPE,,5
ESEL,R,REAL,,3
CMSEL,A,_NODECM
CMDEL,_NODECM
CMSEL,A,_ELEMCM
CMDEL,_ELEMCM
CMSEL,S,_KPCM
CMDEL,_KPCM
CMSEL,S,_LINECM
CMDEL,_LINECM
CMSEL,S,_AREACM
CMDEL,_AREACM
CMSEL,S,_VOLUCM
CMDEL,_VOLUCM
/GRES,cwz,gsav
CMDEL,_TARGET
CMDEL,_CONTACT
/COM, CONTACT PAIR CREATION - END
/MREP,EPLOT
ALLSEL,ALL
VPLOT
```

```
VSEL,R, , ,       7

! comments: defining major volumes and area for viewing results

CM,indenter,VOLU
CMSEL,A,indenter
VSEL,R, , ,       2
CM,keyvolume,VOLU
CMSEL,A,keyvolume

ASEL,R, , ,       7
CM,intarea,AREA
CMSEL,A,intarea
ASEL,R, , ,       5
CM,extarea,AREA
CMSEL,A,extarea
/MREP,EPLOT
ALLSEL,ALL
VPLOT
FINISH
CMDELE,EXTAREA
CMDELE,KEYVOLUME
VSEL,R, , ,       2
CM,keyvolume,VOLU
CMSEL,A,keyvolume
ASEL,R, , ,       5
CM,extarea,AREA
CMSEL,A,extarea
/MREP,EPLOT
ALLSEL,ALL
VPLOT

! comments: Applying boundary conditions and loading

/SOL
FLST,2,10,5,ORDE,10
FITEM,2,1
FITEM,2,-2
FITEM,2,4
FITEM,2,9
FITEM,2,14
FITEM,2,19
FITEM,2,24
FITEM,2,29
FITEM,2,33
FITEM,2,35
DA,P51X,SYMM
FLST,2,3,4,ORDE,3
FITEM,2,36
FITEM,2,44
FITEM,2,52
!*
/GO
DL,P51X, ,UY,0
/VIEW,  1, -0.285897591914    ,  0.560463916543E-01, -0.956619761933
/ANG,   1,  -8.35318777249
/REPLO
FLST,2,2,5,ORDE,2
FITEM,2,13
FITEM,2,42
!*
/GO
DA,P51X,UZ,0
FLST,2,1,5,ORDE,1
FITEM,2,40
!*
```

```
/GO
DA,P51X,UX,0
FLST,2,1,5,ORDE,1
FITEM,2,40
!*
/GO
DA,P51X,UZ,0
FLST,2,1,5,ORDE,1
FITEM,2,40
!*
/GO
DA,P51X,UY,-11                          ! initial dent depth before removal of indenter
LSWRITE,1,                              ! Defining load steps
/DIST,1,0.924021086472,1
/REP,FAST
FLST,2,1,5,ORDE,1
FITEM,2,40
!*
/GO
DA,P51X,ALL,0                           ! removing indenter
LSWRITE,2,

/SOL
FLST,2,6,5,ORDE,6
FITEM,2,7
FITEM,2,12
FITEM,2,17
FITEM,2,23
FITEM,2,30
FITEM,2,44
/GO
!*
SFA,P51X,1,PRES,19.6                    ! applying pressure
LSWRITE,3,
/DIST,1,1.08222638492,1
/REP,FAST
FLST,2,6,5,ORDE,6
FITEM,2,7
FITEM,2,12
FITEM,2,17
FITEM,2,23
FITEM,2,30
FITEM,2,44
/GO
!*
SFA,P51X,1,PRES,24.5
LSWRITE,4,
/DIST,1,1.08222638492,1
/REP,FAST
FLST,2,6,5,ORDE,6
FITEM,2,7
FITEM,2,12
FITEM,2,17
FITEM,2,23
FITEM,2,30
FITEM,2,44
/GO
!*
SFA,P51X,1,PRES,17
LSWRITE,5,
FLST,2,6,5,ORDE,6
FITEM,2,7
FITEM,2,12
FITEM,2,17
FITEM,2,23
FITEM,2,30
```

```
FITEM,2,44
/GO
!*
SFA,P51X,1,PRES,0
LSWRITE,6,
/DIST,1,1.08222638492,1
/REP,FAST
FLST,2,6,5,ORDE,6
FITEM,2,7
FITEM,2,12
FITEM,2,17
FITEM,2,23
FITEM,2,30
FITEM,2,44
/GO
!*
SFA,P51X,1,PRES,17
LSWRITE,7,
/DIST,1,1.08222638492,1
/REP,FAST
FLST,2,6,5,ORDE,6
FITEM,2,7
FITEM,2,12
FITEM,2,17
FITEM,2,23
FITEM,2,30
FITEM,2,44
/GO
!*
SFA,P51X,1,PRES,24.5
LSWRITE,8,
FLST,2,6,5,ORDE,6
FITEM,2,7
FITEM,2,12
FITEM,2,17
FITEM,2,23
FITEM,2,30
FITEM,2,44
/GO
!*
SFA,P51X,1,PRES,0
LSWRITE,9,
/DIST,1,1.08222638492,1
/REP,FAST
FLST,2,6,5,ORDE,6
FITEM,2,7
FITEM,2,12
FITEM,2,17
FITEM,2,23
FITEM,2,30
FITEM,2,44
/GO
!*
SFA,P51X,1,PRES,17
LSWRITE,10,
/DIST,1,1.08222638492,1
/REP,FAST
FLST,2,6,5,ORDE,6
FITEM,2,7
FITEM,2,12
FITEM,2,17
FITEM,2,23
FITEM,2,30
FITEM,2,44
/GO
!*
```

```
SFA,P51X,1,PRES,24.5
LSWRITE,11,
FLST,2,6,5,ORDE,6
FITEM,2,7
FITEM,2,12
FITEM,2,17
FITEM,2,23
FITEM,2,30
FITEM,2,44
/GO
!*
SFA,P51X,1,PRES,0                    ! removing pressure
LSWRITE,12,

! comments: defining non-linear settings

ANTYPE,0
NLGEOM,1
NSUBST,100,1000,10                   ! defining sub-steps
OUTRES,ERASE
OUTRES,ALL,1
AUTOTS,1
LNSRCH,1
TIME,1
/nerr,10000,10000,off

! comments: Solving by load steps

LSSOLVE,1,12,1,
FINISH

! comments: post processing phase

/POST1
/SHOW,WIN32C
SET,FIRST
/PLOPTS,INFO,3
/CONTOUR,ALL,18
/PNUM,MAT,1
/NUMBER,1
/REPLOT,RESIZE
PLNSOL,S,1
SET,,,,,,,30
PLNSOL,S,1
SET,,,,,,,150
PLNSOL,S,1

SET,,,,,,,165
PLNSOL,S,EQV
/VIEW,  1, -0.848432968233    ,  0.470218480067    , -0.243014566269
/ANG,   1,  -2.45095216813
/REPLO
PLNSOL,S,1
PLESOL,S,1
SET,,,,,,,150
PLESOL,S,1
SET,,,,,,,180
PLESOL,S,1
SET,,,,,,,30
PLNSOL,EPTO,X
PLNSOL,EPTO,X
/VIEW,  1, -0.997442935461    , -0.629260703159E-01, -0.338806755116E-01
/ANG,   1,  0.221807311586
/REPLO
PLNSOL,EPTO,Z
PLNSOL,EPTO,EQV
```

```
/VIEW,  1, -0.851533959070    ,  0.501761475551    , -0.152070175258
/ANG,   1,  -3.18384292738
/REPLO
SET,,,,,,,150
PLNSOL,EPTO,EQV
PLNSOL,EPTO,Z
PLNSOL,EPTO,X
SET,,,,,,,165
PLNSOL,EPTO,X
PLNSOL,EPTO,X
PLNSOL,EPTO,Z
PLNSOL,EPTO,EQV
SET,,,,,,,30
PLNSOL,EPTO,EQV
PLNSOL,EPTO,1
PLNSOL,EPTO,2
PLNSOL,EPTO,3
PLNSOL,EPTO,2
! /UIS,ABORT,1
/SHOW,WIN32
/REPLOT,RESIZE
FINISH
! /EXIT,
```